TECHNISCHE UNIVERSITÄT MÜNCHEN

TUM School of Natural Sciences

On the Effects of PCE Superplasticizers in Low-carbon "Green" Cements Based on Calcined Clay and Slag

Ran Li

Vollständiger Abdruck der von der TUM School of Natural Sciences der Technischen Universität München zur Erlangung des akademischen Grades einer

Doktorin der Naturwissenschaften (Dr. rer. nat.)

genehmigten Dissertation.

Vorsitz:	Prof. Dr-Ing. Kai-Olaf Martin Hinrichsen
Prüfer der Dissertation:	1. Prof. Dr. Johann Peter Plank
	2. Prof. Dr. Thomas Brück
	3. Prof. Dr-Ing. Karl-Christian Thienel, Universität der Bundeswehr München

Die Dissertation wurde am 11.07.2022 bei der Technischen Universität München eingereicht und durch die TUM School of Natural Sciences am 08.12.2022 angenommen

Per aspera ad astra

循此苦旅，以达星辰

Acknowledgements

During my doctoral period, what I have gained is not only the academic acheivements, but also the people I have met and the experiences I have obtained during this journey. I would like to acknowledge all those who contributed to this work and accompanied and supported me along the way.

First and foremost, I would like to express my deep gratitude to my supervisor,

Prof. Dr. Johann Plank

who has provided me the great opportunity to conduct my doctoral study at the Chair for Construction Chemistry, Technische Universität München, on this challenging and interesting research subject. Moreover, his insightful feedback pushed me to sharpen my thinking and brought my work to a higher level.

A special thanks goes to my supervisor and mentor **Dr. Lei Lei** who always gives me valuable guidance, generous help and warm encouragement throughout my studies. Without her input my PhD career would not be so successful. She has set a great model for me.

I would like to thank **China Scholarship Council** for providing me a scholarship to finance my research and stay at TU München.

Moreover, I want to thank all my current and former colleagues at the chair: **Christopher Schiefer, My Linh Vo, Yue Zhang, Na Miao, Xinyue Wang,**

Jiaxin Chen, Yuexin Zhang, Hsien-Keng Chan, Zitao Qu, Dr. Haijing Yang, Dr. Manuel Ilg, Dr. Stefanie Gruber, Johann Mekulanetsch, Matthias Werani, Marlene Schmid, Dr. Johannes Stecher, Dr. Matthias Theobald, Dr. Florian Hartmann, Dominik Staude, Timon Echt, and our excellent secretary team members: **Jingnv Liu** and **Xiaoshan Hu**.

In addition, I would like to thank my boyfriend, **Yingshuai Wang**. He always encourages me when I feel upset and confused. In the past few years, he has soothed my Chinese stomach and eased my homesickness with his excellent cooking skills.

Last but not least, my thanks would go to my families, my parents **Zhaoji Li** and **Faqin Liu**, and my brother **Yongxu Li** for their endless love, support and encouragement over the years.

List of papers:

This thesis is based on a total of 10 papers which are listed in the following:

Peer reviewed SCI journal papers

1. **R. Li**, L. Lei, T. Sui, J. Plank.

   “Effectiveness of PCE superplasticizers in calcined clay blended cements”

   Cement and Concrete Research, 141 (2021) 106334

   https://doi.org/10.1016/j.cemconres.2020.106334

2. **R. Li**, L. Lei, T. Sui, J. Plank.

   “Approaches to achieve fluidity retention in low-carbon calcined clay blended cements”

   Journal of Cleaner Production, 311 (2021) 127770

   https://doi.org/10.1016/j.jclepro.2021.127770

3. **R. Li**, L. Lei, J. Plank.

   “Impact of meta kaolin content and fineness on the behavior of calcined clay blended cements admixed with PCE superplasticizer”

   Cement and Concrete Composites, 133 (2022) 104654

   https://doi.org/10.1016/j.cemconcomp.2022.104654

4. **R. Li**, W. Eisenreich, L. Lei, J. Plank.

   “Low Carbon Alkali Activated Slag Binder and its interaction with Polycarboxylate Superplasticizers (PCE): Importance of Microstructural Design of the PCEs”

ACS Sustainable Chemistry & Engineering, Publication date 14.12.2022.

https://doi.org/10.1021/acssuschemeng.2c05430

Peer reviewed data in brief

5. L. Zhang, **R. Li**, L. Lei and J. Plank.

   "Characterization data of reference industrial polycarboxylate superplasticizer VP 2020/15.2 used for Priority Program DFG SPP 2005 "Opus Fluidum Futurum-Rheology of reactive, multiscale, multiphase construction materials"" Data in Brief, 39 (2021) 107657

   https://doi.org/10.1016/j.dib.2021.107657

Peer reviewed conference papers

6. **R. Li**, M. Schmid, T. Sui, J. Plank.

   "Influence of calcined clays on workability of low carbon composite cements" International Conference series on Geotechnics, Civil Engineering and Structures (CIGOS), October 28-29, 2021, Ha Long (Vietnam). Emerging Technologies and Applications for Green Infrastructure, Springer, Singapore, 2022. 677-685.

   https://doi.org/10.1007/978-981-16-7160-9_68

7. **R. Li**, L. Lei, J. Plank.

   "Influence of calcined clay types on the performance of polycarboxylate superplasticizers"

   8th National Conference on Polycarboxylate Superplasticizer and Application Technology, November 21- 23, 2022, Xiamen (China), Proceedings, 70-74.

8. **R. Li**, M. Schmid, T. Sui, J. Plank.

   “Superplasticizers for calcined clay blended cements”

   15th International Conference on Recent Advances in Concrete Technology and Sustainability Issues (CANMET/ACI), July 13-15, 2022, Milan (Italy), SP - 355 - 7.

Peer reviewed SCI journal papers on other topics

9. L. Lei, **R. Li**, A. Fuddin.

   “Influence of maltodextrin retarder on the hydration kinetics and mechanical properties of Portland cement”

   Cement and Concrete Composites, 114 (2020) 103774.

   https://doi.org/10.1016/j.cemconcomp.2020.103774

10. L. Lei, Y. Zhang, **R. Li**

    “Specific molecular design of polycarboxylate polymers exhibiting optimal compatibility with clay contaminants in concrete”

    Cement and Concrete Research, 147 (2021) 106504.

    https://doi.org/10.1016/j.cemconres.2021.106504

List of abbreviations:

Common cement chemistry notation:

Notation	Chemical formula	Mineral name
A	Al_2O_3	Aluminium oxide
C	CaO	Calcium oxide
F	Fe_2O_3	Iron oxide
H	H_2O	Water
S	SiO_2	Silicon dioxide
$\overline{S}$	SO_3	Sulfur trioxide
C_3A	$Ca_9Al_6O_{18}$	Tricalcium aluminate
C_2S	$Ca_2(SiO_4)$	Dicalcium silicate
C_3S	$Ca_3O(SiO_4)$	Tricalcium oxy silicate
C_4AF	$Ca_2(Al_xFe_{1-x})_2O_5$	Tetracalcium alumino ferrite
CH	$Ca(OH)_2$	Calcium hydroxide
$C_3AS_3H_{32}$/ AF_t	$[Ca_3Al(OH)_6]_2(SO_4)_3 \cdot 26H_2O$	Ettringite
C_3ASH_{12}/ AF_m	$[Ca_2Al(OH)_6]_2(SO_4) \cdot 6H_2O$	Monosulfate
C-S-H	-	Calcium silicate hydrate

General abbreviations:

Abbreviation	Description
AA	Acrylic acid
AAS	Alkali-activated slag
ALT	Adsorbed layer thickness
BET	Brunauer–Emmett–Teller, method for determining the specific surface area of solid particles
bwob	By weight of binders
bwoc	By weight of cement
bwos	By weight of solids
°C	Degree Celsius
CC	Calcined clay

cm	Centimeter
CEM I	Portland cement (after DIN EN 197-1)
$d_{10/50/90}$	Unit of the grain size distribution (mass-averaged particle diameter)
GGBS	Ground granulated blast-furnace slag
g/L	Gram per litre
GPC	Gel permeation chromatography
h	Hour
HPEG	α-methallyl-ω-methoxy or -ω-hydroxy poly(ethylene glycol) ether
IPEG	Isoprenyl oxy poly(ethylene glycol) ether
J	Joule
kDa	Kilodaltons, 1 kDa = 10^3 Da
Kg	Kilogram
L	Litre
LC^3	Limestone calcined clay cement
LDH	Layered double hydroxide
M	Molar (mol per litre)
MA	Methacrylic acid
mg	Milligram
mL	Mililitre
Min	Minute
M_n	Number average molecular weight
M_w	Weight average molecular weight
MPEG	ω-Methoxy-poly(ethylene glycol) methacrylate ester
nm	Nanometer
OPC	Ordinary Portland cement
PCE	Polycarboxylate ether/ ester
PDI	Polydispersity index
Q-XRD	Quantitative x-ray diffraction
R^3	Rapid, relevant and reliable test method to determine pozzolanic reactivity
RI	Refractive index
rpm	Rotations per minute
SEM	Scanning electron microscope
SCPS	Synthetic cement pore solution
TEM	Transmission electron microscopy
TOC	Total organic carbon
µm	Micrometer
wt. %	Weight percent
w/b ratio	Water-to-binder ratio
w/c ratio	Water-to-cement ratio
w/s ratio	Water-to-solid ratio
XRD	X-ray diffraction

Contents

1. Introduction

Global warming and climate change caused by CO_2 emission are currently among the most important and urgent issues in the world. The EU and the US have committed to reach net-zero emissions by 2050 [1, 2] while China plans to achieve carbon neutrality by 2060 [3]. Reducing CO_2 emissions has become a common goal for all of humanity.

As an important part of the industry, cement manufactures have attracted increasing attention regarding the issue of energy-saving and emission reduction. Cement is reported to account for about 8 % of the total global anthropogenic CO_2 emissions [4]. Approximate 825 kg of carbon dioxide are released into the atmosphere from the production of 1 ton of cement clinker. This CO_2 mainly comes from decomposition of raw materials ($CaCO_3$) and the consumption of fuel resources and the grinding which account for 60 - 70 % and 30 - 40 % of direct CO_2 emissions from cement clinkerization, respectively [5]. In view of the continued growth of urban population, the demand for large infrastructure construction has increased significantly. In the foreseeable future, cement and concrete materials will still maintain their dominant position in the construction field. Consequently, an increasing demand for cement clinker can be predicted.

In this case, alternative binders, i.e. low-carbon cements, need to be developed to meet the requirements. A common approach to achieve this goal is to allow partial substitution of Portland cement clinker with binders exhibiting a low-

carbon footprint. Supplementary cementitious materials (SCMs) including silica fume, fly ash, Ground Granulated Blast-furnace Slag (GGBS) and calcined clays are prominent examples thereof [6-8].

This thesis mainly focusses on two kinds of low-carbon cements, namely calcined clay blended composite cement and alkali-activated slag (AAS) composite cement.

Calcined clays have currently become the focus of research as a SCM. Compared to the clinker calcination process for OPC cement, it can save a significant amount of CO_2 due to the much lower calcination temperature (600 to 800 °C) [9, 10] and the absence of decarbonization of the raw material ($CaCO_3$). It is reported that by applying Limestone Calcined Clay blended Cement (LC^3) around 30 % of CO_2 emission can be saved [11] without compromising the compressive strength [9, 12, 13]. This is attributed to the high pozzolanic reactivity of calcined clay which contains significant amounts of meta kaolin (in LC^3 > 45 wt.%). In addition, another advantage of using calcined clay as SCM is the global availability of its raw materials, common clay.

On the other hand, slag is a waste product originating from the production of different types of metals. Most of the slag used as an alkali-activated material in construction comes from the iron and steel industry [14]. It is known as blast-furnace slag, which consists of alumina, silicates, calcium and magnesium oxides. Its use in construction is beneficial to the environment, not only by saving energy and natural resources which reduces the carbon dioxide

emissions, but also by improving waste management [15, 16].

However, despite the great environmental benefits of low-carbon cements, issues relating to their poor workability much limits their widespread application. Calcined clays possess extremely high specific surface areas which greatly increases the water demand and further compromises the fluidity of the composite cements. Similarly, AAS composite cements are known for their poor workability.

To tackle the poor workability of low-carbon cements, concrete admixtures present the key. Among all the superplasticizers, polycarboxylates (PCEs) are the most important one due to their superior performance [17-19] and flexible designability of the molecular structure [20-28].

This study addresses the problem of poor workability of low-carbon composite cements containing calcined clay or AAS. Through systematic variation of PCE molecular structures, superplasticizers which are effective in those binder systems were identified, synthesized and tested with respect to the engineering properties of mortar samples admixed with them. Moreover, mechanistic studies on the interaction between PCE superplasticizer and those low carbon binders have been performed in an effort to elucidate the reason behind the differences in effectiveness of various PCE molecules. From the results it was hoped to gain more insight into the interplay between low-carbon binders and PCE superplasticizers and thus facilitate their more widespread practical application.

2. Aims and scope

This PhD work deals with the effect of PCE superplasticizers in two low-carbon binders, namely calcined clay blended cements as well as alkali-activated slag composite cements.

2.1 Effectiveness of PCEs in calcined clay blended cements

The study on the behavior of PCE superplasticizers in calcined clay blended cements addresses the following 3 aspects:

1) Initial fluidity of a calcined clay blended cement rich in meta kaolin

This study presents an investigation on the dispersing performance of superplasticizers in blended cements which contain a calcined clay rich in metakaolin supplied by Sinoma/ China. It is found that calcined clay increases the water demand of such blended cements significantly and therefore decreases their fluidity. The general effectiveness of a PCE superplasticizer in OPC/CC blends can be assessed from its performance in neat OPC. This means that PCEs which fluidize ordinary Portland cement well also perform well in calcined clay blended cements. Among all PCE polymers tested, an HPEG PCE and a zwitterionic MPEG PCE polymer showed optimal dispersing ability in those cements. Furthermore, the results suggest that while in the cement pore solution the initial surface charge of the calcined clay is negative, it

changed to neutral through the uptake of huge amounts of Ca^{2+} from the pore solution. Accordingly, a layer of adsorbed Ca^{2+} ions facilitates the adsorption of PCE superplasticizers on CC.

2) Slump retention of a calcined clay blended cement rich in meta kaolin

This study focused on the slump retention performance of conventional PCEs and a novel admixture in calcined clay blended cements (source of calcined clay: China). The results indicate that it is difficult to achieve slump retention in meta kaolin rich calcined clay blended cements, opposite to OPC. However, sufficient fluidity retention presents a key requirement for ready-mix concrete.

It was found that in such calcined clay blended cements, conventional ready-mix type PCEs based on hydrolyzing esters and their combination with a retarder (sodium gluconate) exhibit only limited effectiveness with respect to slump retention. The negative effect of the calcined clay can be attributed to its high uptake/adsorption of PCE. On the other hand, a novel admixture in the form of a PCE-LDH nanocomposite in which the PCE is chemically trapped between $[Ca_2Al(OH)_6]^+$ main layers demonstrated much improved slump retention in those cements when combined with a common water-reducing type of PCE. Moreover, pore solution analysis revealed that the PCE-LDH admixture achieves fluidity retention via a gradual release of the superplasticizer from the PCE-LDH through anion exchange with sulfate anions. This way, extended workability times can be achieved from those cements.

The purpose of this study was to stimulate more work on calcined clay blended

composite cements and promote a broader actual application of those “green” cements.

3) Impact of meta kaolin content and fineness on the fluidity of calcined clay blended cement

This study presents an investigation on the impact of the meta kaolin content and its fineness on the fluidity and early strength of such composite cements. Three calcined common clays exhibiting 23, 51 and 86 wt.% meta kaolin were selected for comparing their pozzolanic reactivity and fluidity behavior in composite cements. Moreover, a series of composite cements with stepwise increasing meta kaolin contents were prepared, and their water demand and PCE dosage requirement as a function of their meta kaolin content was determined.

It was found that higher meta kaolin contents improve their pozzolanic reactivity and thus promote early strength development, however, it also greatly increases PCE dosages. It is concluded that the fineness of the calcined clay mainly affects the water demand, while the meta kaolin content plays a dominant role with respect to early strength development and PCE requirements. Furthermore, the high PCE dosages of calcined clays rich in meta kaolin result from the pronounced negative surface charge of meta kaolin. This general trend was confirmed for meta kaolin samples from different industrial sources.

The aim of this study was to offer a better understanding of the role of meta

kaolin in calcined clay composite cements and to further promote the application of such low-carbon cements.

2.2 Impact of PCEs on the fluidity of AAS composite cements

Alkali activated slag is known as an environmentally friendly supplementary cementitious material and as a potential substitute for cement clinker. However, AAS exhibits inferior rheological properties as compared to ordinary Portland cement. Therefore, superplasticizers present the key to solve this problem. This study focused on the effect of the microstructure and molar mass of PCE polymers on the fluidity of the AAS system. PCEs possessing different macromonomers; different molar ratios of acid: side chain and macromonomers varying in molecular weights (chain length) were synthesized and their dispersing performance was determined.

The results suggest that the molar mass of a PCE affects its adsorption conformation which further impacts the dispersing performance. Besides, the correlation between the microstructure of PCE polymers and their interaction mode was also developed by employing ^{13}C NMR spectroscopy to uncover the microstructure of PCE polymers. It revealed that the dispersing power and enhanced adsorption behavior of PCEs on slag particles correlates with their anionicity and specific motifs in the microstructure.

This research was intended to help designing novel PCE geometries with extraordinary dispersing effectiveness in AAS system.

3. Theoretical background and state of the art

3.1 Polycarboxylate superplasticizers

Chemical admixtures play an important role in modern advanced concrete technologies such as Ultra-High Performance Concrete (UHPC) [29-31], 3D printing technology [32, 33] as well as the new concept of low-carbon binders [34-41]. Representing the third generation of superplasticizers, polycarboxylate superplasticizers (PCEs) emerged as one of the most important chemical admixtures for concrete due to their superior performance [17-19]. Resulting from the flexible designability of the molecular structure of PCEs, a wide range of concrete properties can be accomplished [20-28].

3.1.1 Structures and classification of polycarboxylates (PCEs)

PCE polymers consist of polyethylene oxide (PEO) side chains and backbones in a comb-like structure [17, 19]. Conventional PCEs possess anionic backbones made of methacrylic acid, acrylic acid, maleic acid or maleic anhydride which enables the adsorption of PCEs onto positively charged clinker phases or early hydrates [42]. In addition, there are also cationic and zwitterionic (amphoteric) PCEs have been proposed which exhibit positive or both charges. The positive charge can be provided by cationic monomers like diallyl dimethylammonium chloride (DADMAC) [43], 2-trimethylammonium ethyl methacrylate chloride (TMAEMC) [26, 44], and 3-trimethylammonium propyl

methacrylamide chloride (MAPTAC) [45]. The chemical structures of common anionic and cationic monomers are shown in **Figure 1**.

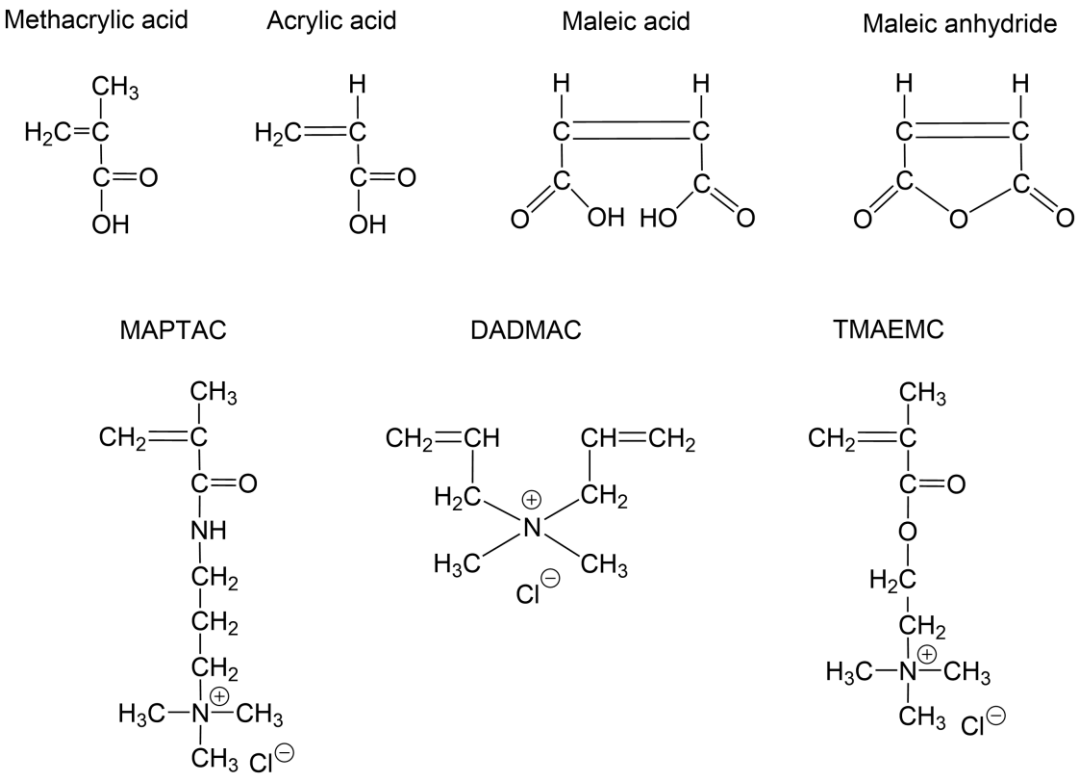

Figure 1. Chemical structures of anionic and cationic monomers commonly contained in PCEs.

(1) Conventional anionic PCEs

According to the different PEG macromonomer types, PCEs can also be classified into MPEG, APEG, VPEG, HPEG and IPEG based PCEs [46, 47]. The chemical structures of all those macromonomers listed here are shown in **Figure 2**.

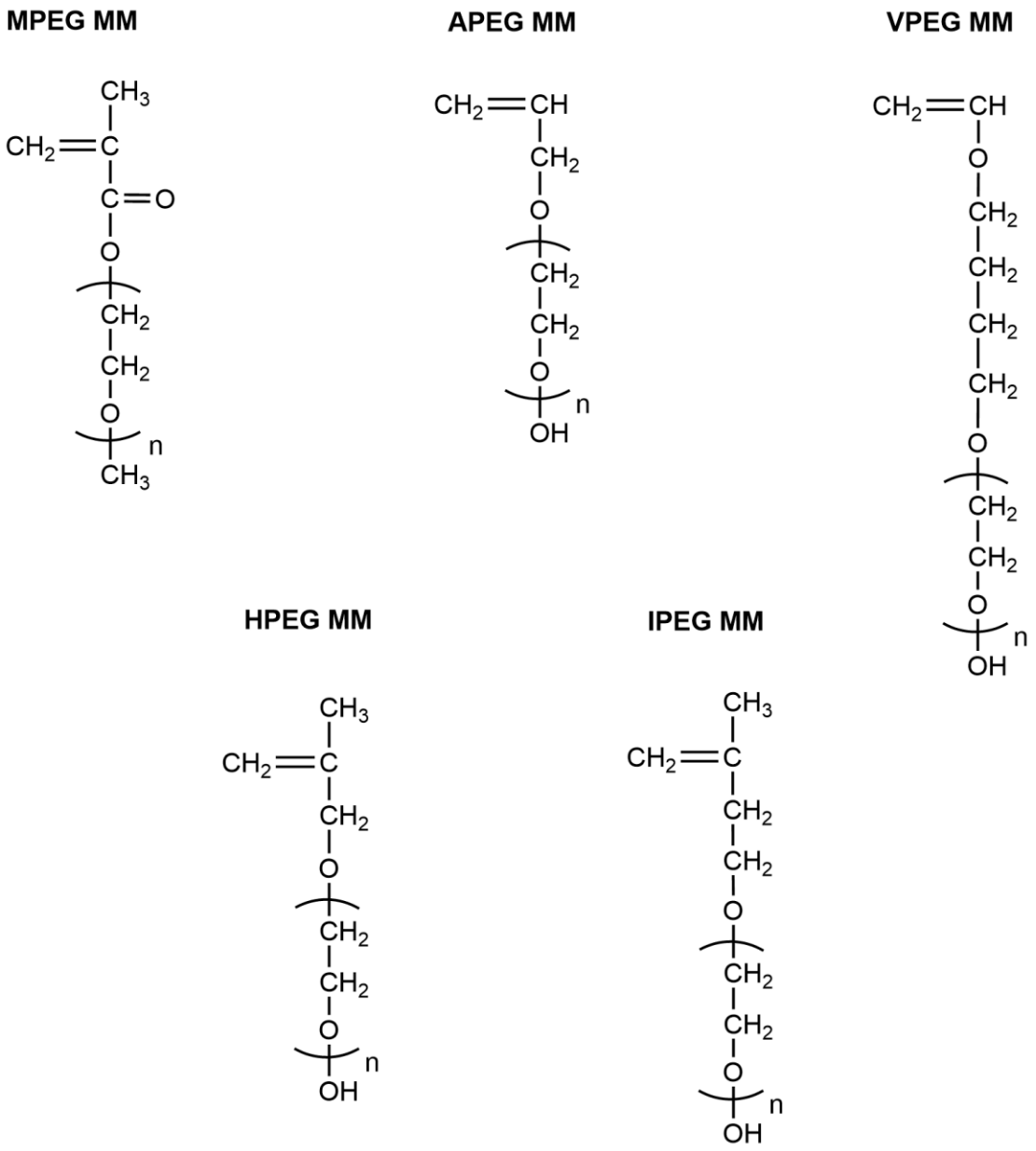

Figure 2. Chemical structures of the different macromonomers mainly used by the PCE industry.

MPEG PCEs were the first polycarboxylates introduced in 1986. They consist of ω-methoxy poly(ethylene glycol) methacrylate ester macromonomer and a methacrylic acid backbone [48]. The advantage of MPEG PCEs is that they make the concrete more cohesive, thus prevent concrete from bleeding [49].

However, with respect to dosage effectiveness, MPEG PCEs are considered to be less efficient than current HPEG or IPEG PCEs [47].

APEG PCEs can be synthesized from ω-hydroxy-α-allyl poly(ethylene glycol) macromonomer and maleic anhydride or acrylic acid. At first, APEG PCEs consisted of ω-hydroxy-α-allyl poly(ethylene glycol) macromonomer and maleic anhydride (MAH) [50]. This polymer is characterized as a “star polymer”, the shape of which provides excellent dispersing performance [47]. However, due to the fixed molar ratio between maleic anhydride (MAH) and the allyl ether owed to the resonance stabilization of the allyl radical, only A-B-A-B copolymers that exhibit a strict regular sequence can be obtained. Recently, a new copolymerization method for APEG macromonomers with acrylic acid has been introduced which could prevent this drawback, thus considerably broadening the scope for designing APEG PCEs with various anionicity [51].

VPEG PCEs are vinyl ether-based PCEs which consist of maleic anhydride, vinyl ether and acrylic acid [52]. The advantage of the vinyl over the allyl ether technology is that vinyl ethers are more reactive, thus a wider range of molecular compositions can be achieved in a low temperature synthesis [47]. In addition, both water-reducing and slump-retaining PCEs can be obtained. Recently, two new subclasses of vinyl ether PCEs base on novel vinyl ethers have been introduced, they are called **EPEG PCEs** [53] and **GPEG PCEs** [54].

HPEG PCEs were synthesized using α-methallyl-ω-methoxy or ω- hydroxy

poly(ethylene glycol) ether as side chain and acrylic acid as backbones. Compared to the APEG macromonomer, the HPEG macromonomer possesses a much higher reactivity which makes the synthesis of HPEG PCEs easier [47]. Moreover, they can be produced in an energy saving process including a room temperature synthesis [55].

IPEG (or TPEG) PCEs are made from isoprenyl oxy poly(ethylene glycol) macromonomers and acrylic acid. IPEG PCEs are becoming increasingly popular due to their ease of preparation and high effectiveness in concrete [56]. In addition, such PCEs are considered to be more effective than HPEG PCEs in maintaining the fluidity of concrete over longer time periods [47].

(2) Cationic and zwitterionic PCEs

Typically, most PCEs are ionic polymers with the anionicity provided by methacrylic acid, acrylic acid or maleic anhydride. However, in some cases polymers possessing different charges are applied [57], such as concrete containing montmorillonite with a heterogeneous surface charge [58] as well as composite cements containing calcined clays [59].

Zwitterionic PCEs incorporate negatively charged groups (e.g. carboxylates) as well as positively charged (cationic) functional groups. Recently, this kind of PCEs were found to have excellent performance in calcined clay blended composite cements [60-62].

Cationic PCEs are PCEs possessing cationic monomers in the backbone [59].

However, this kind of PCE normally are more expensive due to the cationic monomer, and they require higher dosages than their anionic counterparts.

3.1.2 Working mechanisms of PCE superplasticizers

The dispersing effectiveness of PCE superplasticizers in cement is considered to result from the combined influence of electrostatic repulsion and steric stabilization [42, 46]. In addition, the adsorption conformation also plays an important role on the rheology performance [46].

Electrostatic repulsion and steric hindrance

Conventional polycarboxylate superplasticizers are based on negatively charged backbones containing methacrylic acid, acrylic acid and maleic anhydride which can adsorb onto the positively charged surfaces of cement hydrates (C_3A, ettringite, monosulfoaluminate) [63, 64]. Consequently, electrostatic repulsion occurs, which contributes to the dispersing effectiveness [42]. According to previous experiments, PCEs possessing higher charge density adsorb in a larger amount than others. In this way, the dispersing performance is improved [65, 66]. In addition, a steric hindrance effect is created by the hydrophilic pendant chains which freely protrude into the pore space and contribute to the stabilizing force in the system. Thus, the steric hindrance between cement particles or early hydrates enhances the dispersing effect.

The combined hybrid effect of electrostatic repulsion and steric hindrance from polycarboxylates are shown in **Figure 3** [67].

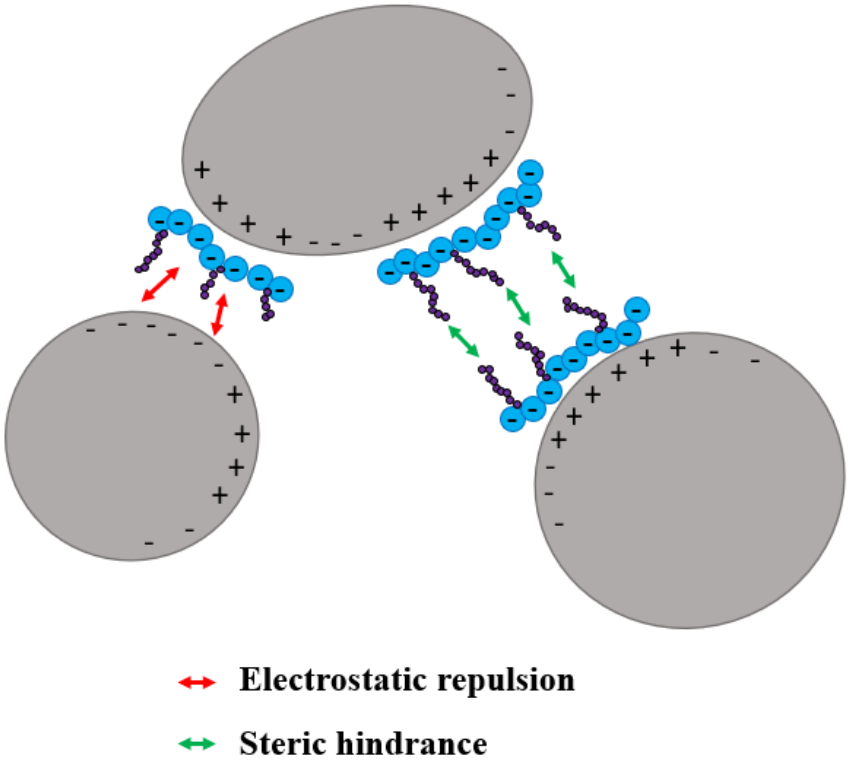

Figure 3. Combined effect of electrostatic repulsion and steric hindrance of polycarboxylate superplasticizers on cement [67].

Adsorption conformation

In addition to the electrostatic repulsion and steric hindrance, also the adsorbed conformation of a PCE superplasticizer has a significantly influence on its dispersing performance in cementitious materials. Generally, PCE polymers can exhibit three distinct conformations when adsorbed onto binder particles, namely train, loop and tail (see **Figure 4**). According to *Lei et al.* [34], PCE polymers possessing higher M_w are more likely to adsorb a “loop” than in a “train” conformation which results in a thicker adsorbed layer around the slag

particles. Consequently, a stronger dispersing effect was observed. When M_w of the PCE was as high as 400,000 Da, an even thicker adsorbed layer signifying “tail” adsorption conformation can be observed. As a result, much enhanced dispersion was achieved.

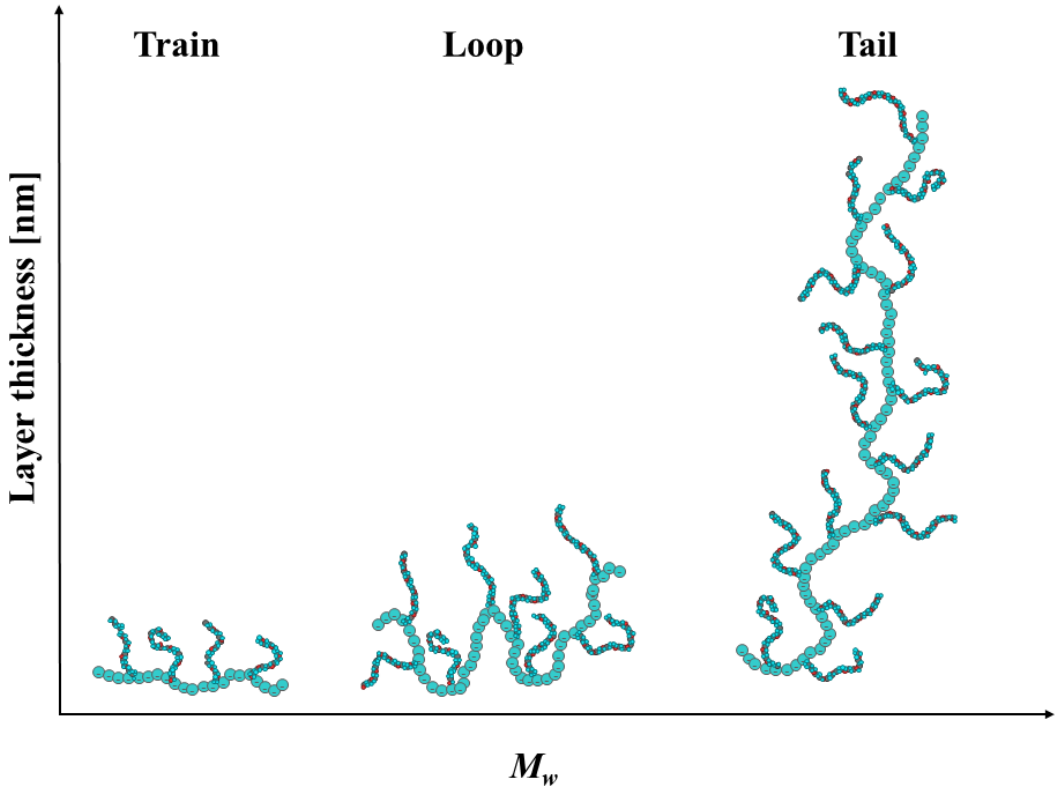

Figure 4. Potential adsorbed conformations of PCE superplasticizers on cement surfaces.

Overall, a great number of PCEs can be designed and synthesized by adjusting critical parameters such as side chain length (repeating EO numbers in PEG), backbone type, molar ratio between the monomers and alternative functional groups. In this study, a broad range of polycarboxylate superplasticizers

including commercial benchmark PCEs and self-synthesized anionic PCEs as well as amphoteric (zwitterionic) PCEs were investigated to elucidate the interaction between polycarboxylate superplasticizers and low-carbon composite cements. Also, a mechanistic study on the interaction between PCEs and pristine calcined clays, pure meta clays, calcined clay blended cements and pristine alkali-activated slag was launched to uncover the interaction between PCE superplasticizers and such low carbon binders.

3.2 Calcined clays

3.2.1 Structure of raw clays

Clay minerals are characterized by layered structural units consisting of a tetrahedral silica sheet and an aluminate octahedral sheet. The tetrahedral sheet has the net composition of $Si_2O_6(OH)_4$. Each silicate unit consists of a central silicon atom which is coordinated to four oxygen atoms, and they are connected to the adjacent tetrahedral sheet by shared corners forming a two-dimensional hexagonal mesh pattern. On the other hand, an octahedral sheet possess the net composition of $Al_2(OH)_6$, whereby each unit is surrounded by six oxygen or hydroxyl atoms [68-70]. The connection between two octahedral units is a shared edge. The presence of Al atoms renders two-thirds of the positions occupied and the remaining position empty. Clay minerals can be classified into 1:1 and 2:1 phyllosilicates based on their crystal structure, especially the number of tetrahedral and octahedral sheets that constitute the main layer. In the following, the structures of several major clay minerals are listed and discussed.

- **Kaolinite**

Kaolinite exhibits the general composition of $Al_2Si_2O_5(OH)_4$. Its structure is characterized by a 1:1 phyllosilicate which contains one SiO_4 tetrahedral sheet and one octahedral alumina layer (**Figure 5**). The Si tetrahedral sheet and Al octahedral layer share two-third of O atoms between the Si and Al central atoms.

The rest of O atoms exist as hydroxyl groups in the octahedral sheet, and are attached to the Al central atoms. Al^{3+} ions occupy around two-thirds of the sites available in the octahedral layer, leaving the rest of the sites empty. The presence of hydroxyl groups above and below two Al central atoms renders a central hexagonal distribution in one plane within the octahedral layer. Kaolinite generally has a neutral net surface charge. However, slight negative charges may develop at the broken edges of the structure [71]. As a result, kaolinite typically exhibits a stable crystalline (non-swelling) structure which is ascribed to hydrogen bonds and van der Waals forces between successive layers [72].

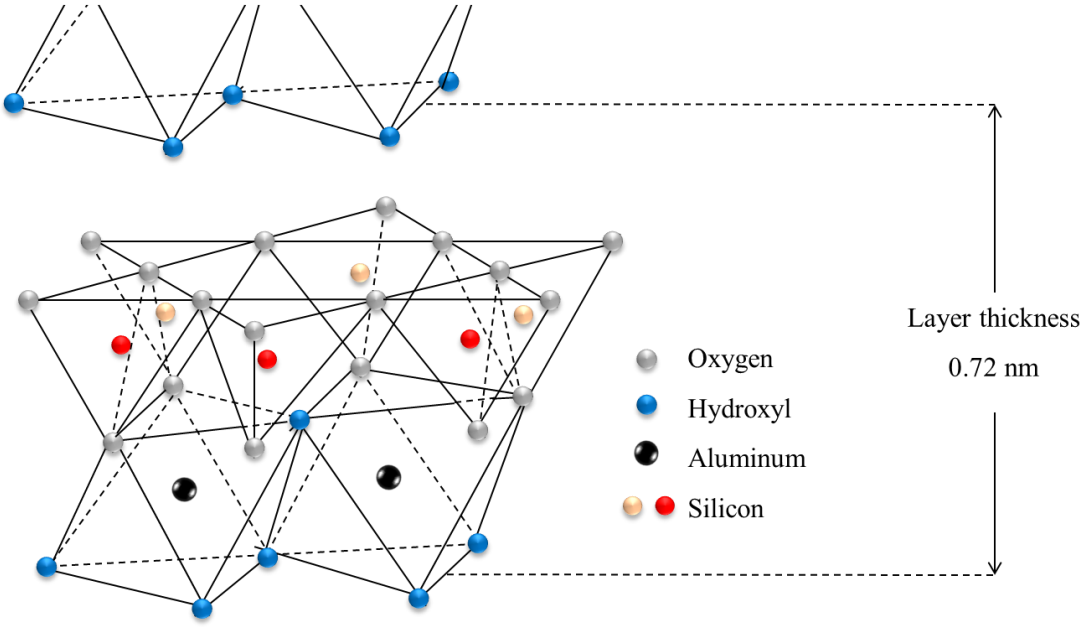

Figure 5. Structure of kaolinite, modified after Grim [73].

- **Montmorillonite**

Montmorillonite is chemically represented as $(Na,Ca)_{0,3}(Al,Mg)_2Si_4O_{10}(OH)_2$

nH_2O [71]. Different to kaolinite, its structure consists of three layers (2:1 type), with an octahedral aluminate layer in the middle and two tetrahedral silicate layers surrounding it (see **Figure 6**). In the actual structure, defects exist such as Si^{4+} central atoms in the tetrahedral layer are easily substituted by Al^{3+}, while Al^{3+} in the octahedral sheet can be replaced by Mg^{2+}. Consequently, a net negative charge is registered on montmorillonite which is balanced by interlayer exchangeable cations like Na^{+} and Ca^{2+} [74]. In addition, montmorillonite presents a typical expanded or expandable (swelling) 2:1 clay mineral due to lattice expansion caused by polar molecules such as water entering between the layers [69]. The interlayer spacing is influenced by the cations occurring between the silicate sheets.

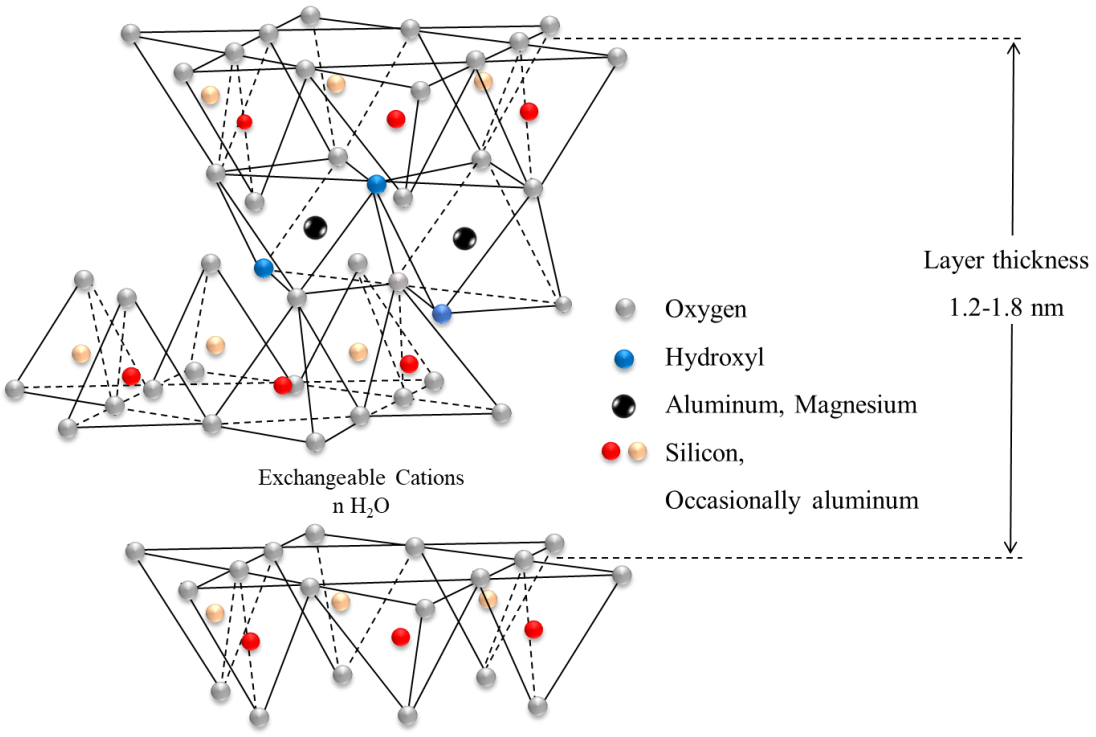

Figure 6. Structure of montmorillonite, modified after Grim [73].

- **Illite**

The chemical composition of illite can be presented as $(K,H_3O)Al_2(Si_3Al)O_{10}(H_2O,OH)_2$ [71] (structure see **Figure 7**). Illite belongs to the group of 2:1 phyllosilicate which consists of two tetrahedral silicate layers and a central octahedral aluminate layer possessing a similar unit as in montmorillonite. In the structure, around two-thirds of the sites available in the octahedral layer are occupied by Al^{3+} ions, while the rest of the sites are empty. Compared to montmorillonite, the isomorphic substitution tendency in illite appears to be lower, with an average only one-sixth of all silicon atoms substituted. Mostly, K^+ ions are the interlayer cations which balance the negative charge. In some cases, K^+ ions can be replaced by other exchangeable cations such as H^+, Ca^{2+} and Mg^{2+} [71, 75-77].

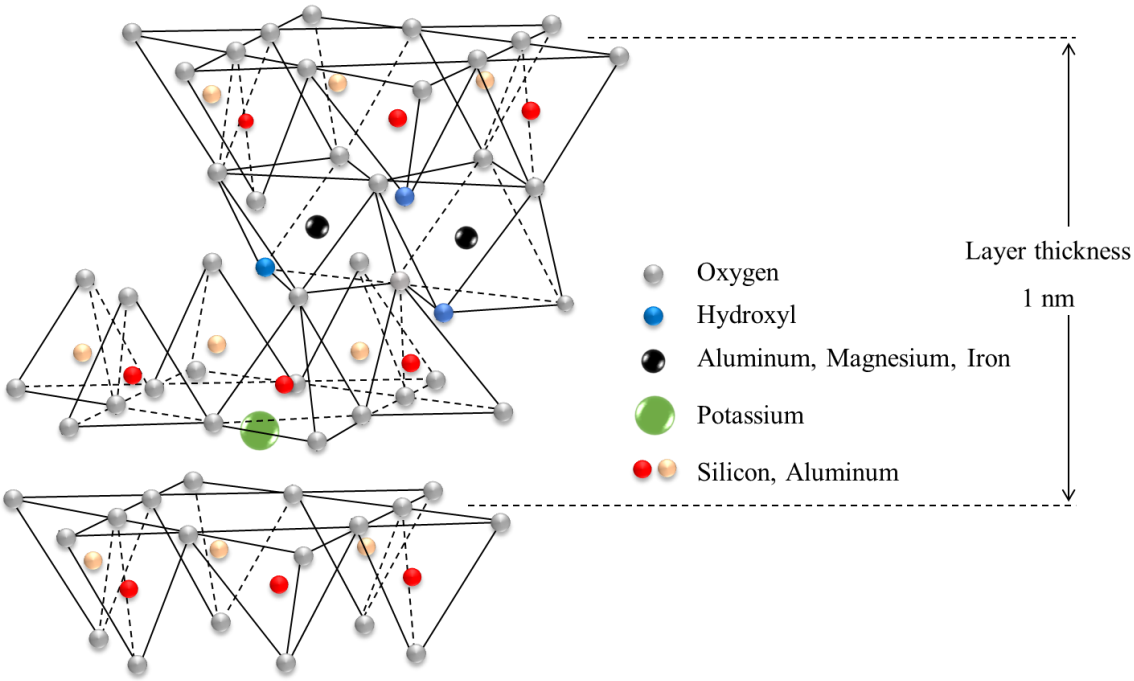

Figure 7. Structure of illite, modified after Grim [73].

- **Muscovite**

Muscovite (see **Figure 8**) is chemically represented as $KAl_2(AlSi_3O_{10})(OH)_2$. Closely resembled by illite, its crystal structure consists of two tetrahedral silicate layers and one octahedral aluminate layer. The difference between muscovite and illite is the different layer charge. The layer charge of muscovite is slightly more negative than that of illite.

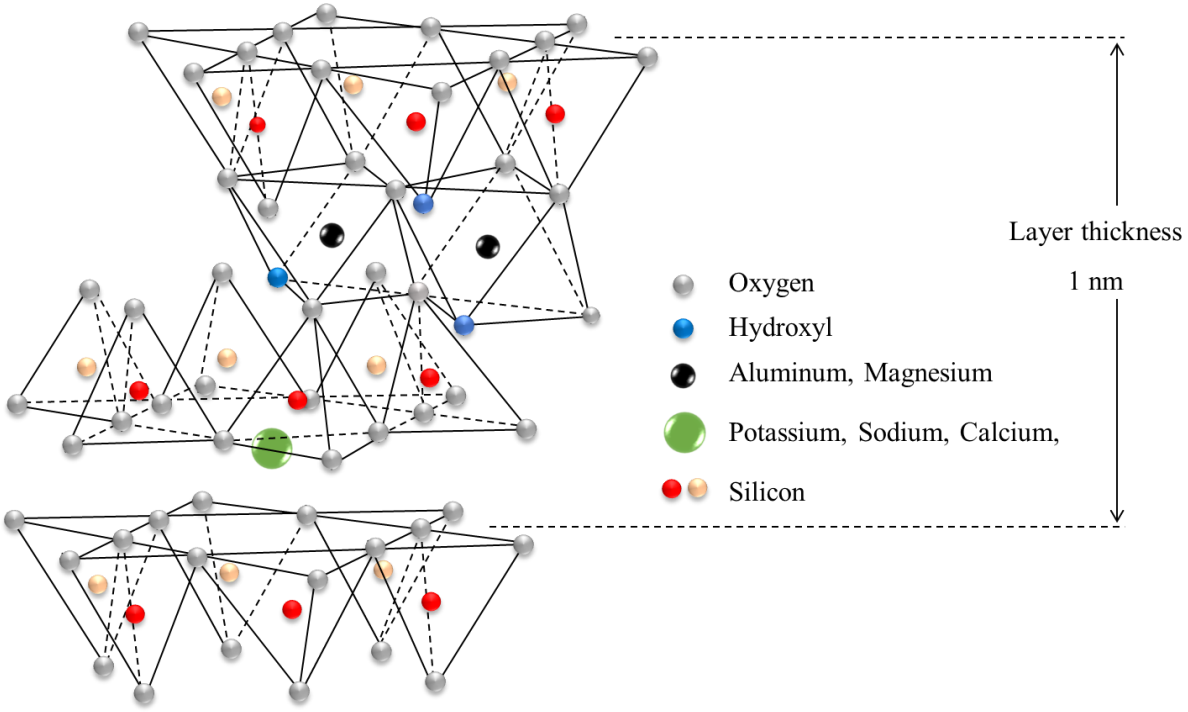

Figure 8. Structure of muscovite, modified after Grim [73].

3.2.2 Calcination process

The structure and composition of clay minerals are changed by heating, and the accompanying change in properties enables clays to be utilized as SCMs in cement. Depending on the significant changes occurring in the structures of

clay, the processes occurring during calcination can be divided into three principal temperature stages, named dehydration, dehydroxylation, and recrystallization processes [78]. Dehydration typically occurs at temperatures below 200 °C, where the clays release adsorbed and hydration water. When the temperature continues to rise, dehydroxylation proceeds resulting in a breakdown of the clay structure. This process occurs primarily at temperatures between 400 and 800 °C. However, the actual temperature at which dehydroxylation occurs varies with the specific mineral, structural stacking order, morphology, and heating conditions. As exemplified in **Figure 9**, the 2:1 clays possess different dehydroxylation temperatures in comparison to a kaolinite sample, measured using both TGA and oven [79].

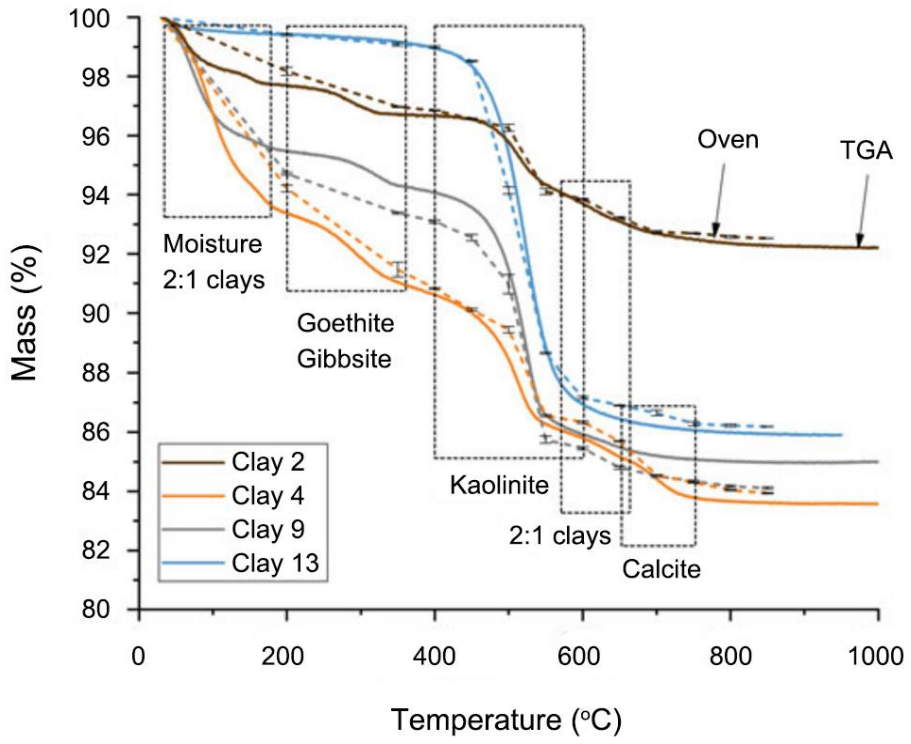

Figure 9. Mass loss of clay samples with increasing temperature (measured by TGA and oven) [79].

Calcination conditions such as temperature, exposure time and process (rotary kiln vs. flash calciner) can affect the pozzolanic reactivity of the calcined clay product. For example, the products produced in the flash calciner system are superior to those from rotary kiln systems [80]. This conclusion was reached by Canut *et al*. after comparing the performance of numerous clays from global sources calcined in the calciner system (flash calcination) and a rotary kiln system (soak calcination). **Figure 10** illustrates the degree of reaction with calcium hydroxide (CH) produced by clays calcined using different processes. It indicates that the clay calcined in a flash gas suspension calciner is more reactive than from soak calcination (kiln).

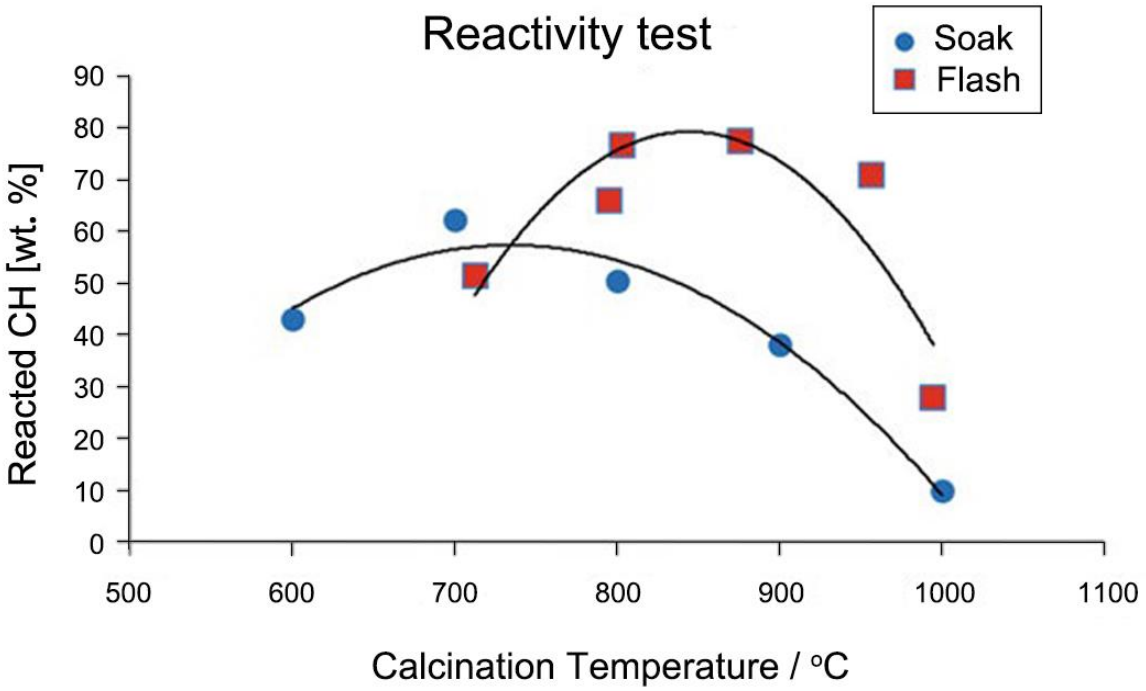

Figure 10. Reactivity of calcined clays depending on the specific calcination process [80].

The relationship between the calcination conditions, including calcination process, and the pozzolanic reactivity of the calcined clays will be discussed in detail in the next section.

3.2.3 Pozzolanic reactivity of calcined clays

Definition and reaction mechanism

Pozzolans are defined as silico-aluminous materials which react chemically with calcium hydroxide (CH) in the presence of water to form compounds with cementitious properties [81]. The pozzolanic reaction is a slow reaction which improves the mechanical properties of the cementing system. Several materials are used as supplementary cementitious materials because of their pozzolanic reactivity, including fly ash, silica fume, calcined clay etc.

According to DIN EN 197-1 [82], calcined clay is a naturally tempered pozzolan that can be used in concrete. Its highly reactive component is recognized as an intermediate transitional phase formed by the thermal activation of the clay minerals at high temperatures through dehydroxylation. This transitional phase (amorphous aluminosilicate phases, AS_2, AS_4) reacts with CH in the presence of water to produce cement hydrates like C–S–H and the alumina bearing phase C-A-S-H [83, 84]. The proposed reactions [85] are summarized in **Equation (1)** and **(2)**:

$$AS_2 + 3CH + 6H \rightarrow C\text{-}S\text{-}H + C_2ASH_8 \qquad \boldsymbol{Equation\ (1)}$$

$$AS_4 + 5CH + 6H \rightarrow 3C\text{-}S\text{-}H + C_2ASH_8 \qquad \boldsymbol{Equation\ (2)}$$

Depending on the AS_2/CH ratio and the reaction temperature, the reaction products vary, such as C_2ASH_8, C_4AH_{13} and C_3AH_6.

Origin of the pozzolanic activity of calcined clays

Although calcined clays have been shown to have good pozzolanic reactivity and their potential beneficial usage in concrete has been demonstrated, the origin of their pozzolanic reactivity is still a subject of ongoing research. Currently the consensus is that the pozzolanic reactivity of calcined clays is closely related to the dehydroxylation occurring during calcination. More specifically, activation of the calcined clay is achieved upon dehydroxylation of the octahedral sheet. According to Rocha and Klinowski [86, 87], the high reactivity of metakaolin is attributed to the transition of octahedrally coordinated Al (Al^{VI}) to 5-fold coordination (Al^{V}) as was evidenced by ^{27}Al nuclear magnetic resonance (NMR) spectroscopy. The same trend has been reported on the thermal behavior of other clay minerals such as illite [88] and montmorillonite [89].

In a recent study, Fernandez *et al*. [12] compared the ^{27}Al NMR spectra of three clay minerals (kaolinite, montmorillonite and illite) calcined at different temperatures (shown in **Figure 11**) and related their decomposition process to the pozzolanic reactivity of each sample. It was found that the pozzolanic activity was closely related to the appearance of 5-coordinated aluminum (Al^{V}). Moreover, they recognized that kaolinite undergoes a different decomposition process as compared to illite or montmorillonite, resulting from the amount and

location of OH groups in its structure. This difference leads to an important loss of crystallinity. Therefore, kaolinite exhibits superior pozzolanic reactivity in comparison to other clays.

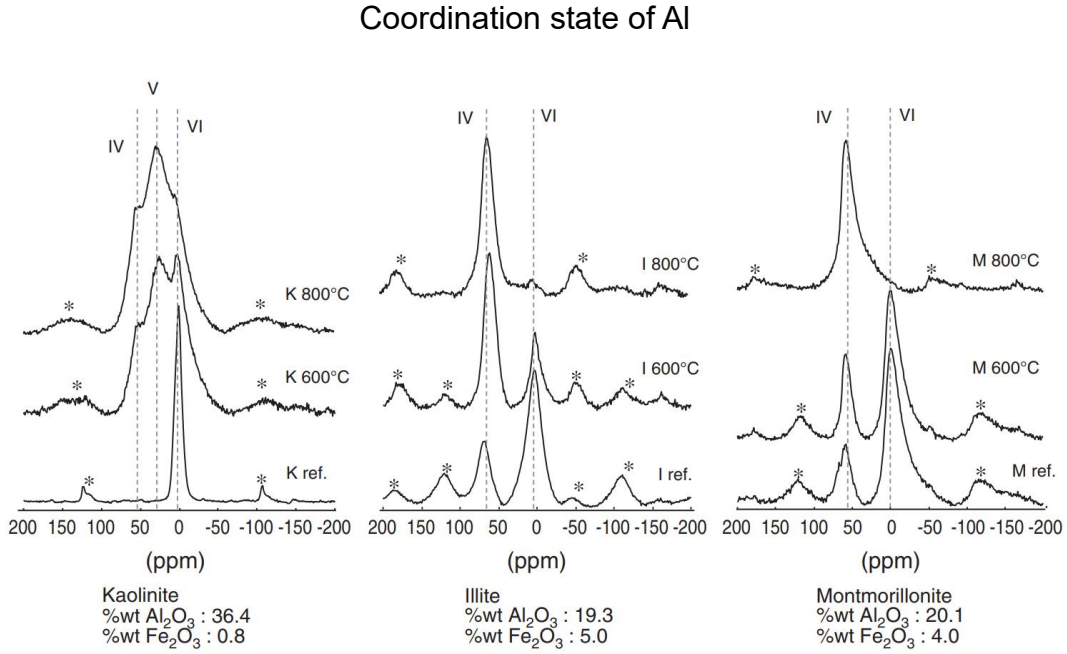

Figure 11. ^{27}Al NMR spectra of kaolinite, illite and montmorillonite and the changes in Al coordination resulting from the calcination process [12].

Factors influencing the pozzolanic reactivity of calcined clays

Calcined clays are known to exhibit substantial pozzolanic reactivity. However, natural clay deposits contain various clay minerals such as kaolinite, montmorillonite, muscovite, chlorite and illite. In addition, a large percentage of non-clay mineral impurities such as quartz, calcite, feldspar, mica, anatase and

sulfide can be present in natural clay samples [90]. Therefore, the reactivity of calcined clays can vary substantially from sample to sample.

Several factors can affect their pozzolanic reactivity, including the type and amount of individual clay minerals, the nature and content of impurities, the method of thermal treatment and the specific surface area obtained after the calcination [85, 91].

- **Reactivity of different clay minerals**

Back in 1995, He *et al*. [92] tried to relate the mineral composition of six calcined clays to their pozzolanic reactivity. However, in their case, they failed to exclude the effect of the particle size of the calcined clay samples. Therefore, they did not find a correlation between the mineral composition of the calcined clays and their pozzolanic reactivity. They concluded that kaolin and some montmorillonites had the highest pozzolanic activity, while the rest of the clay minerals could be assigned low pozzolanic activity. Later Fernandez *et al*. [12] systematically compared the pozzolanic reactivity of calcined clays prepared from kaolinite, montmorillonite and illite and also discussed the origin of the pozzolanic reactivity. They showed that meta kaolin possesses the highest pozzolanic reactivity, followed by meta montmorillonite and meta illite. A similar conclusion was reached by Hollanders *et al*. [9] who reported that calcined smectite had higher pozzolanic reactivity than calcined illite, but was still inferior to that of calcined kaolinite. In addition, the pozzolanic activity of meta kaolin is closely associated with the crystallinity of the raw clay. Well-ordered kaolinite

tends to transform into meta kaolin of relatively low reactivity [93].

As for the impurities present in calcined natural clay, they were reported to dilute the reactivity of the calcined clay [94].

Also, the fine particles present in a calcined clay promote its pozzolanic reactivity resulting from the high specific surface area [95].

- **Calcination conditions**

Apart from the mineral composition of the clay, the condition during thermal treatment is also one of the important factors affecting the pozzolanic reactivity of calcined clays. The relationship between the thermal treatment conditions (temperature, residence time and cooling) and the degree of pozzolanic reactivity of the calcined products has been extensively studied for different clays to derive optimal heat treatment conditions. In general, for the production of calcined clay the calcination temperature is between 600 – 800 °C. When the clay is heated at higher calcination temperatures, a liquid phase is formed which solidifies into an amorphous glass phase upon cooling which is undesirable.

Shvarzman *et al*. [96] investigated the effect of thermal treatment parameters on the dehydroxylation of kaolinites. They found that at calcination temperatures lower than 450°C, kaolinite exhibited a relatively low degree of dehydroxylation which is around 0.18. Thereafter, the degree of dehydroxylation rises with increasing calcination temperature. It increases to 0.98 in the temperature range of 450 - 570 °C, with kaolinite becoming fully dehydroxylated between 570 and 700 °C. To some extent the dehydroxylation

was accompanied by kaolinite amorphization which affected the activity of the calcined kaolinite.

With respect to the reactivity, the optimum activation temperature varies for different clay minerals and deposits. Ambroise *et al*. [97] determined the optimum temperature for kaolinite as 700 ºC by evaluating the compressive strength of mortars. Ferreiro *et al*. [98] concluded that a calcination temperature up to 850°C and a finer particle size distribution of a 2:1 raw clay resulted in a higher degree of dehydroxylation which enhanced the strength development of mortar. Hollanders *et al*. [9] compared the effect of the calcination temperature on the pozzolanic reactivity of three clay mineral phases. The results show that kaolinite samples possess high reactivity after calcination from a broad temperature range of 500 to 900 °C, while smectitic clays and illite clearly exhibit optimal calcination temperatures of 800 and 900 °C, respectively.

Clays are usually calcined in a conventional rotary kiln or a flash calciner. A rotary kiln takes hours to produce calcined clay, while the calcining time can be reduced to seconds by applying flash calcination [99, 100]. In addition, the calcined clays prepared by using flash calcination exhibit higher reactivity as compared to rotary kiln [100]. This can be attributed to the flame physics in a conventional rotary kiln which produces a wide temperature distribution. In spite of the relatively long residence time in the rotary kiln (**Figure 12**), the clay is only partially heated up completely when the optimum activation temperature is reached, leading to partial recrystallization effects and loss of activity [101].

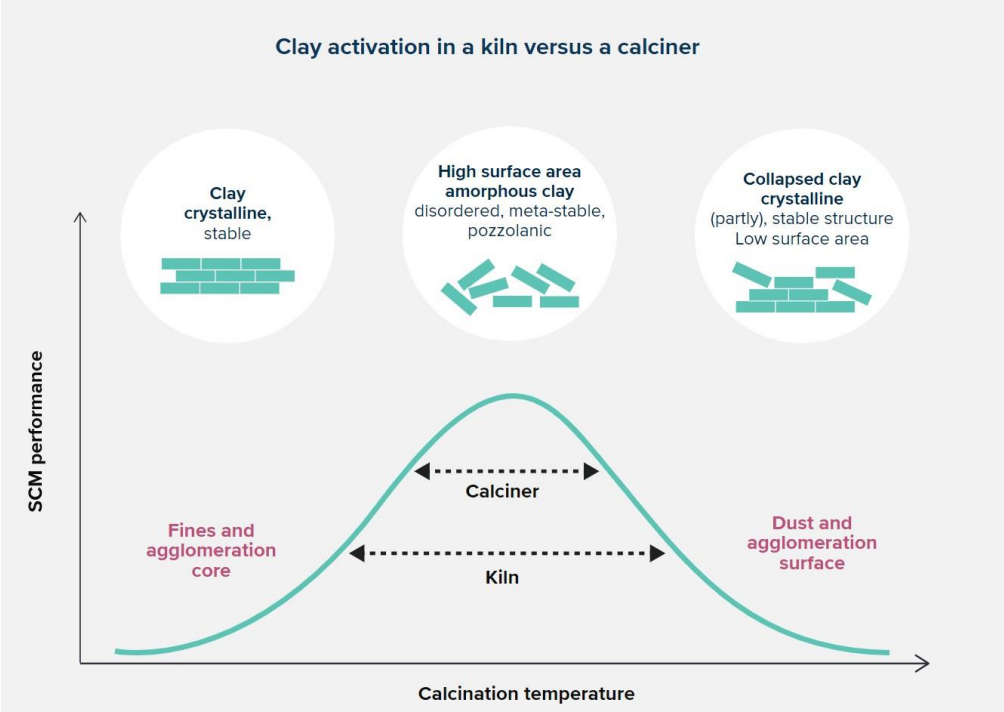

Figure 12. Clay activation in a rotary kiln versus a flash calciner [102].

3.2.4 Application of calcined clays in cement

Resulting from their excellent pozzolanic reactivity, calcined clays have been studied for application in cement and concrete for a long time [92, 94, 100, 103, 104]. In recent years, a ternary blended cement characterized by a high clinker substitution rate known as “Limestone calcined clay cement (LC^3)” has received more attention in order to reduce the CO_2 emission originating from cement clinker production [11, 105-111]. With a base composition of 50 % clinker, 30 % of calcined clay, 15 % limestone powder and 5 % gypsum the LC^3 cement achieves a cement clinker substitution ratio of 50 % which qualifies it as a low carbon cement.

Hydration of calcined clay blended cement

Calcined clay blended in combination with limestone into Portland cement was first reported in 2012 [105]. The alumina present in calcined clays can react with the carbonate phases in limestone to produce carbonate aluminate phases that are hard and crystalline and contribute to the development of strength. It was reported that C-A-S-H has been formed from this combination and comparable performance as from Portland cement was observed [11]. This comparable performance is considered to result from similar densities of C-A-S-H and C-S-H [112, 113]. Avet *et al*. employed ^{1}H NMR spectroscopy to investigate the density of C-A-S-H produced by calcined clay blended cements exhibiting different meta kaolin contents [112]. They found that all systems display similar bulk densities which are close to 2.0 g/cm^3 and around 2.8 g/cm^3 for the solid density.

Mechanical properties

Calcined clay blended cements are often designed to achieve a clinker substitution rate as high as 30 – 50 wt.% without compromising the mechanical performance [9, 12, 13]. Considerable literatures have focused on this key parameter of compressive strength for the LC^3 cement. Dhandapani *et al*. discussed the mechanical properties of concretes prepared using LC^3 [108]. They found that the 3 day strength of LC^3 concrete is slightly lower than that of OPC. However, other authors reported the 7 and 28 days strengths of LC^3 to be similar to or higher than that of OPC [13].

The extent of strength increase can be controlled by the meta kaolin present in a calcined clay. Meta kaolin provides additional alumina which reacts with $CaCO_3$ to form more carbon aluminates, while consuming portlandite in the early hydration of the cement to produce C-A-S-H [112]. However, a high meta kaolin content present in a calcined clay causes a negative effect with respect to the workability of this cement. As a consequence, much higher superplasticizer dosages are required for effective dispersion of such blended cements [39, 114].

Workability

Although calcined clay blended cement is an environmentally friendly low carbon cement with excellent mechanical strength properties, its poor workability (initial fluidity and slump retention) cannot be ignored in real practical applications.

Calcined clays exhibit high specific surface areas and considerable internal porosity which causes the poor workability of their blended cements [39, 40, 61, 98, 115-122]. Consequently, with ascending substitution of the cement clinker by calcined clay a significant increase in PCE dosage is required to achieve a higher spread flow [39, 121, 123, 124]. This negative influence on the fluidity of calcined clays greatly depends on their individual mineral compositions. A study on the interaction of PCEs with individual meta clay minerals revealed that meta muscovite constitutes the most easily dispersed meta phase, followed by meta montmorillonite and meta kaolin, while meta illite presented the most difficult

one [122]. Therefore, the specific mineral composition of calcined clays must be taken into account when discussing the workability of blended cements.

In conclusion, calcined clay presents a most promising substitution material for cement clinker due to its environmentally friendly characteristics, beneficial mechanical properties and the global availability of clays. However, more studies need to be done to fully understand the rheological behavior of calcined clay blended cements as well as the interaction between PCE superplasticizers and calcined clays to facilitate their routine use in the construction industry.

3.3 Slump retention of concrete

Ready-mix concrete which is pre-prepared and delivered to the construction site plays a significant role in the modern concrete market. For ready-mix concrete, in order to maintain the sufficient workability, extended slump retention over 2 hours is required or sometimes even longer in large cities. There are many ways to achieve slump retention in concrete. In this section, conventional methods and a novel method are discussed.

3.3.1 Conventional methods to achieve slump retention in concrete

Several technologies are applied to achieve the fluidity retention in Portland cement-based concretes, and are listed as follows:

Combing superplasticizer and retarder

The first concept to improve concrete slump retention was to combine polycondensate superplasticizers with retarders, such as sodium gluconate, molasse, anhydro glucose or lignosulfonates containing sugars etc. [125-129]. Interestingly, sugar was first found to have a retarding effect on concrete when it was observed that cement stored in old sugar sacks failed to set properly [130]. Later, it became particularly popular in combination with polycondensate-based superplasticizers such as BNS or melamine sulfonate [131]. Through this combination, fluidity retention was achieved via hydration retardation (especially ettringite formation) [125, 132]. Depending on the retarding efficacy

of the individual admixture, the prolonged setting time can vary from several hours to several days [133]. However, the disadvantage of this approach involving retarders was decreased early strength. Also, the setting time is quite sensitive to the dosage of set retarder. Sometimes, excessively high dosages of retarders can lead to a surprisingly quick set of the concrete [134].

PCE superplasticizers with optimized side chain density

It is well established that the molecular structure of PCE superplasticizers influences the rheological properties of concrete. Already in the 1990s, it was reported that PCE superplasticizers which were characterized by high side chain density and low amount of carboxylate functionalities in the backbone (low anionicity) adsorb slowly onto the cement particle surface, thus achieving extended slump retention [20]. Such extended workability times result from successive gradual adsorption onto the cement particles, without a negative effect on the early strength development. However, they demand higher PCE dosages. Additionally, Mardani-Aghabaglou *et al*. reported that the slump retaining effect of PCE superplasticizers is improved when the amount of carboxylic acid group is low [135].

Incorporation of hydrolyzing esters into the PCE structure

In addition to changing the side chain density of PCEs, the incorporation of hydrolyzing esters into the molecular structure was found to present another route to achieve high slump retention from PCEs. Common examples of such

esters include hydroxyethyl acrylate (HEA) [136, 137], hydroxypropyl acrylate (HPA) [136], 2-hydroxyethyl methacrylate (HEMA) [138, 139], 3-hydroxypropyl methacrylate (HPMA) [140], 4-hydroxybutyl methacrylate (HBMA) [140] and monomethyl maleate (MMM) [141, 142]. These esters produce additional carboxylate groups during their hydrolysis in the highly alkaline pore solution of cement and thus continuously PCE molecules are formed which now are able to adsorb onto cement and provide dispersion [143, 144].

Applying delayed addition of PCE to concrete

A more simple approach comprises the delayed addition of polycarboxylate superplasticizer which prevents the formation of early nanoscale ettringite and immediately consumes the entire dosage of the PCE polymer via instantaneous adsorption [145]. This approach can effectively compensate for the loss of cement workability. However, the disadvantages of this approach are the cost and operational complexity [146].

PCE encapsulation

Finally, encapsulation of the dry superplasticizer powder particles via polyvinyl alcohol (PVA) coating or packaging of the admixture in water-soluble PVA bags [147] which are added to the rotating container of the concrete truck were proposed and are commercially applied, e.g. in the U.S.

The above methods are commonly used in practical applications to enhance the fluidity retention time of concrete prepared by OPC. However, in actual

application it has been observed that fluidity retention is much more difficult to achieve when calcined clays are present in the cement as compared to OPC. Conventional methods for achieving sufficient slump in OPC do not meet the requirements in calcined clay blended cements. Therefore, new technologies need to be developed. In the following a new concept to achieve slump retention in concrete is introduced.

3.3.2 Novel method to achieve slump retention in calcined clay blended cements

Inspired from the encapsulation and delayed addition methods mentioned above, the intercalation (“chemical packaging”) of PCE superplasticizers into layered double hydroxides (LDHs) was considered as a promising new approach to improve fluidity retention in calcined clay blended cements.

LDHs are referred to as anionic clays, due to their high anion exchange properties [78]. In Portland cement, the hydration of tricalcium aluminate (C_3A) and tetracalcium aluminoferrite (C_4AF) can produce layered double hydroxides [148] which have the ability to intercalate inorganic as well as organic anions in between their $[Ca_2Al(OH)_6]^+$ main layers. Various intercalations of organic anions (anionic polymers) have been reported, such as poly(ethylene oxide) derivatives [149], poly(acrylic acid) [150], poly(styrene sulfonic acid) [150], and poly(amino acids) [151].

The first combination of LDH material with comb-like PCE polymers was proposed by Plank *et al* [152]. The structure of a PCE-LDH nanocomposite is

illustrated in **Figure 13** [63]. PCE-LDH hybrid materials are successully synthesized using e.g. rehydration of pure C_3A in the presence of comb-like PCE polymers based on methacrylic acid-co-ω-methoxy poly(ethylene glycol) methacrylate.

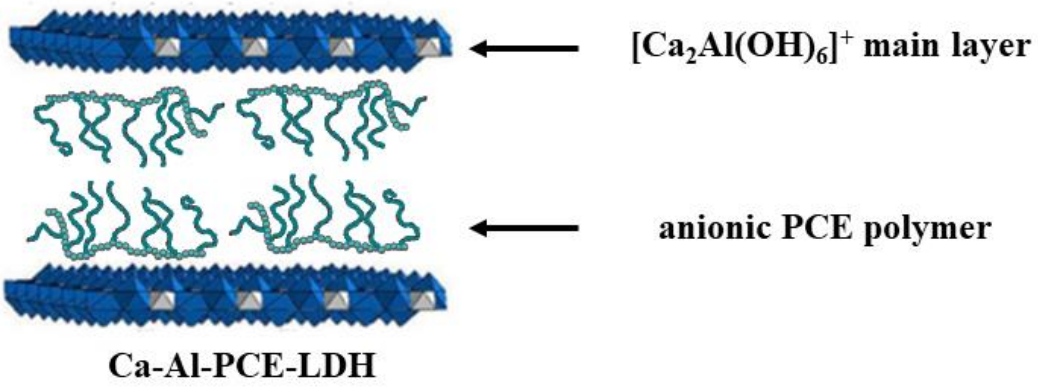

Figure 13. Schematic illustration of the structure of a PCE-Ca–Al–LDH intercalation compound, redrawn after [63].

Furthermore, in another study [63] these authors reported that the interaction between C_3A and PCE is quite complex, while their intercalation potential is greatly determined by the amount of sulfate present in cement pore solution. Anion exchange experiments presented in their study confirm that PCE cannot replace and exchange against sulfate, while sulfate can gradually replace the PCE in PCE-LDH nanocomposites (see **Figure 14**).

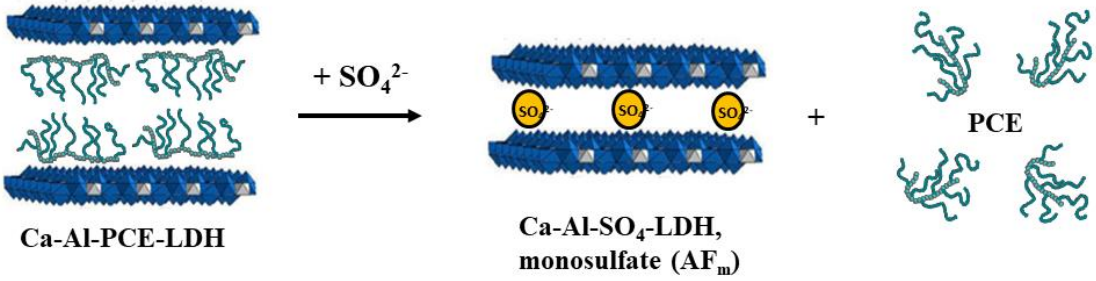

Figure 14. Illustration of the anion exchange process in Ca-Al-PCE-LDH whereby sulfate releases PCE; redrawn after [63].

Based on the idea of a gradual replacement of PCE with sulfate in PCE-LDH nanocomposites, it can provide slump retention by a continuous release of PCE molecules over time. This concept seems to be a promising solution to achieve slump retention also in calcined clay blended cements.

Therefore, in this study PCE-LDH nanocomposites were synthesized via hydration of tricalcium aluminate (C_3A) in the presence of PCEs, thus forming ($[CaAl(OH)_6]^+$ (PCE) • nH_2O) nanocomposites. It was hoped to achieve fluidity retention through this mechanism, and their effectiveness was compared with that of slump retaining PCEs commonly used in ready-mix concrete.

3.4 Alkali-activated slag composite cement

Ground granulated blast furnace slag (GGBFS) is a byproduct of the steel industry. The main components in slag are alumina, silicates, calcium and magnesium oxides. Its application in construction is beneficial to the environment, not only by saving energy and natural materials which reduces carbon dioxide emissions, but also by improving waste management [15, 16]. Recently, alkali-activated slag (AAS) and composite cements containing AAS are attracting more and more attention as an environmentally friendly low carbon material which can replace OPC [14, 153, 154].

3.4.1 Activators used to stimulate AAS hydration

Due to the latent hydraulic property of slag, activation is required to achieve or accelerate the hydration process. Many activators have been used in the AAS system [14] which include: sodium hydroxide (NaOH) [34, 155, 156], sodium silicate (Na_2SiO_3), sodium sulfate (Na_2SO_4), sodium carbonate (Na_2CO_3) [155], potassium hydroxide (KOH), potassium silicate (K_2SiO_3), calcium oxide (CaO) [157], calcium hydroxide ($Ca(OH)_2$) [158] and magnesium oxide (MgO) [159]. The activator can be used alone or in combination with one or more activators [14, 154].

The types and concentration of activators significantly affects the performance of the AAS system, including mechanical and workability properties. According to Fernández-Jiménez *et al*. [160] and Wang *et al*. [161], the mechanical strength of slag activated by various activators proceeds in the following order:

Na_2SiO_3 > Na_2CO_3 > Na_2SO_4 > NaOH. Moreover, Fernandez and Palomo reported that the combination of NaOH and waterglass as activator promotes the strength more than twice as much as when the system was activated by NaOH alone [162, 163].

3.4.2 Hydration of AAS system

Alkali activation of slag is known as “a complex process of structural disruption of slag and polycondensation of hydrate products” [164]. It is well established that the activation of slag begins with the breakage of the covalent bonds (i.e. Si–O–Si, Al–O–Si) and is accompanied by the formation of compact structures [165-167]. According to Glukhovsky *et al*. and Krivenko, the possible hydration process of AAS can be described by the following equations [168, 169]:

$$= Si - O^- + M^+ \longrightarrow = Si - O - M \qquad \textbf{Equation (3)}$$

$$= Si - O - M + OH^- \longrightarrow = Si - O - M - OH^- \qquad \textbf{Equation (4)}$$

$$= Si - O - M - OH^- + Ca^{2+} \longrightarrow = Si - O - Ca - OH + M^+ \qquad \textbf{Equation (5)}$$

Here, M^+ presents the alkali cation which accelerates the entire process as a catalyst. It is obvious from the equations that the activator fasters the hydration process of AAS which explains the huge differences in strength of AAS treated with different activators. Therefore, the hydration process of AAS system greatly depends on the activators. For example, it has been reported that with NaOH as the activator an immediate induction period after the dissolution of slag was

observed, while in the water glass activated slag system at first a polycondensation reaction appears rather than an induction period [170].

3.4.3 Workability of AAS composite cements

Despite the many advantages of AAS – such as a lower heat of hydration [171], improved mechanical properties [160], favorable environmental properties as well as the enhanced chemical resistance [172-174] – the poor rheological properties have so far limited its application on large scale [175]. The rheology of alkali-activated slag systems is influenced by several parameters which include the nature and concentration of the alkaline activator [176-178], the amount of water and chemical admixtures present etc. [36]. Palacios *et al*. [179] reported that the rheology of alkali-activated slag strongly depends on the type of the alkali activator being used. Sodium hydroxide activated slag was reported exhibiting much better fluidity as compared to that activated by sodium silicate [180]. Atiş *et al*. found that Na_2CO_3 activated slag exhibited better flexural tensile strength as compared to those activated by NaOH and Na_2SiO_3 [181]. Although the various activators have different influences on the fluidity, in general the AAS system possesses poor workability.

For this reason, chemical admixtures become an indispensable component in AAS systems to meet the operational requirements in application. Many studies have focused on the behavior of various superplasticizers in AAS. Palacios *et al*. [182] found that the naphthalene-based polycondensate exerts a better effect in improving the rheology of AAS systems as compared to a melamine-

based superplasticizer as well as a vinyl copolymer, possibly due to its higher chemical stability in such an extremely alkaline medium. In a separate study, Jang [183] claimed that polycarboxylate-based superplasticizers exhibited improved workability as compared to that of a naphthalene-based superplasticizer. Furthermore, Conte *et al*. [37] demonstrated that an α-allyl-ω-hydroxy poly (ethylene glycol)-based PCE possessing short PEG side chains produced superior dispersing effectiveness in an NaOH activated slag system owed to its good solubility in NaOH solution. They also found that the dispersing power of such APEG PCEs is greatly enhanced when its molecular weight increases above 30,000 g/mol, though the reason behind the high M_w required is not specified. In a recent study, Lei *et al*. [34] compared the dispersing performance in AAS of a series of HPEG PCE polymers of different molecular geometry. It was concluded that the key parameters determining the PCE dispersing efficiency in slag is presented by the anionicity, while the pendant chain length impacts to a lesser extent.

However, overall the available literature remains insufficient for understanding how PCE superplasticizers influence AAS composite cement systems. Therefore, this study aimed to gain more insights into the interaction between PCE superplasticizers and alkali-activated slag composite cements.

4. Materials and methods

In this section, the key steps in the experimental parts for interaction between PCE superplasticizers and two low carbon cements, i.e. a calcined clay blended composite cement and an alkali-activated slag composite cement, are summarized.

4.1 Part I

PCEs in calcined clay blended cements

In this part, effectiveness and interaction between PCEs and calcined clay blended cements is investigated based on the following 3 main topics: initial fluidity, slump retention and the influence of the mineral composition in the calcined clay (see **Figure 15**).

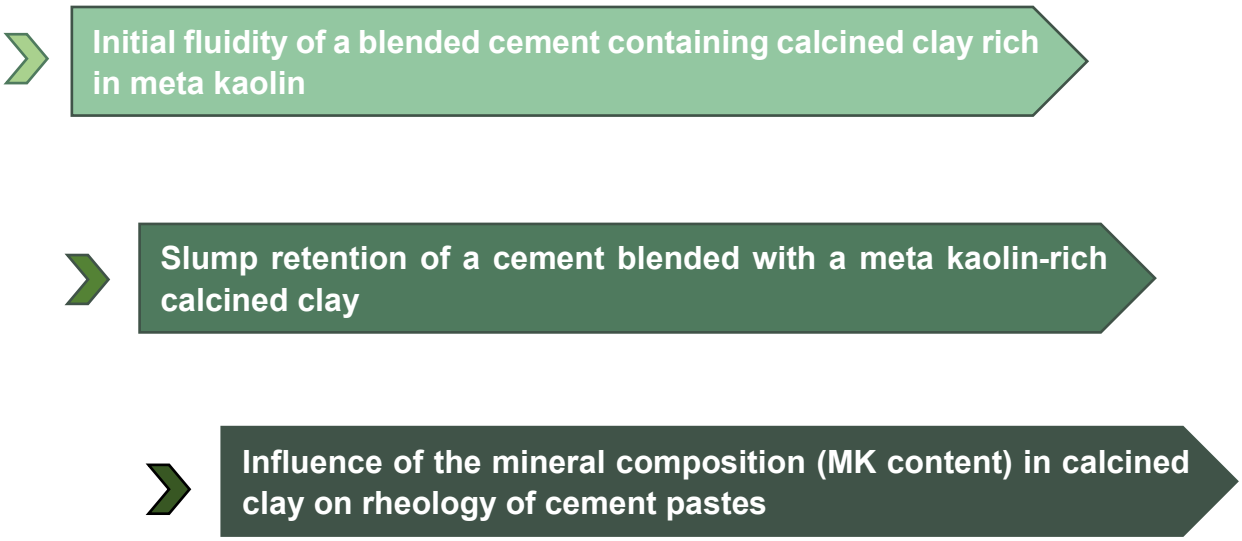

Figure 15. The three main research topics regarding the effects of PCEs in calcined clay blended composite cements.

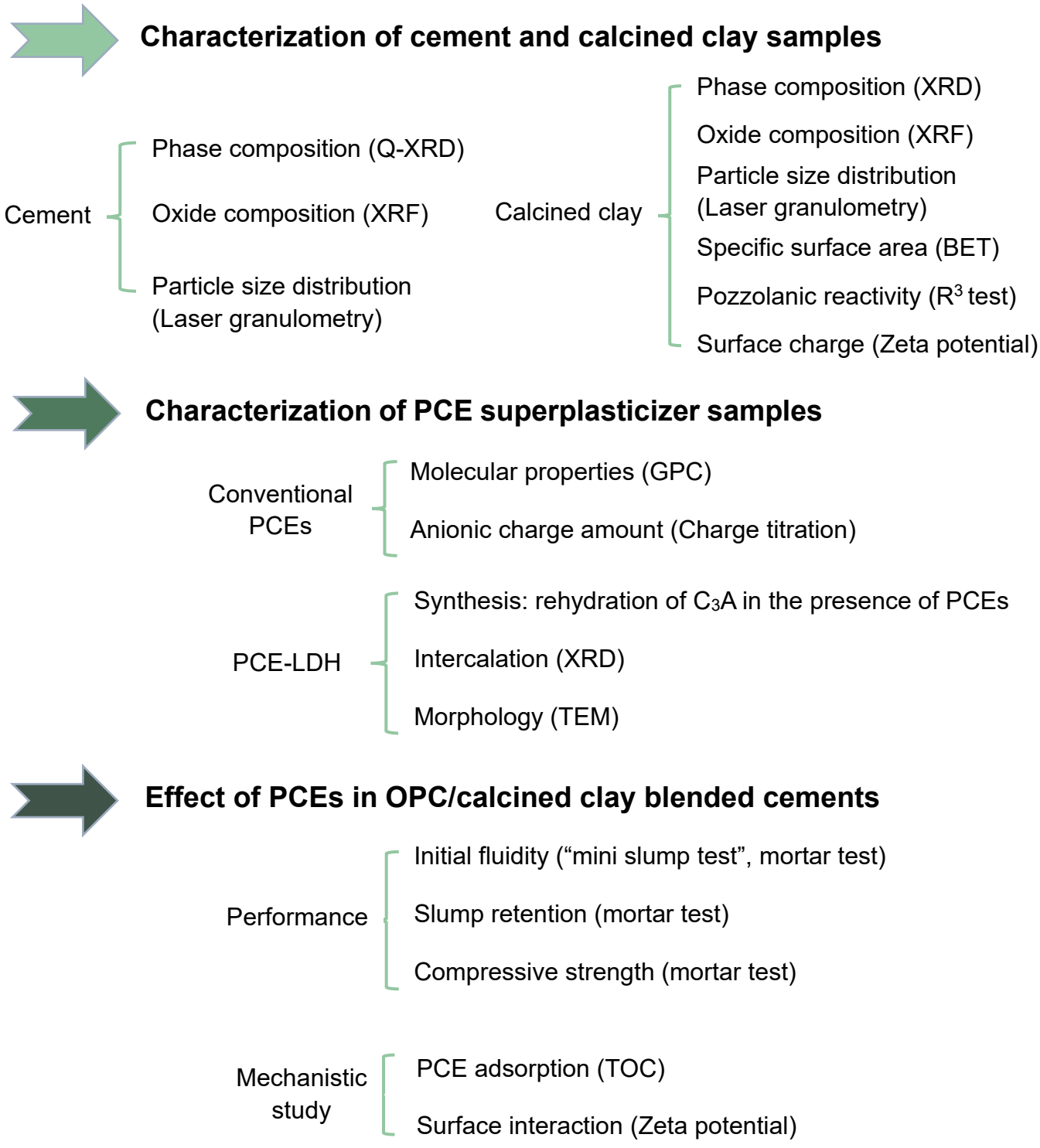

Figure 16. Experimental approach taken in Part I of the study regarding the effects of PCE superplasticizers in calcined clay blended composite cements.

4.2 Part II

Impact of PCEs on the fluidity of AAS composite cements

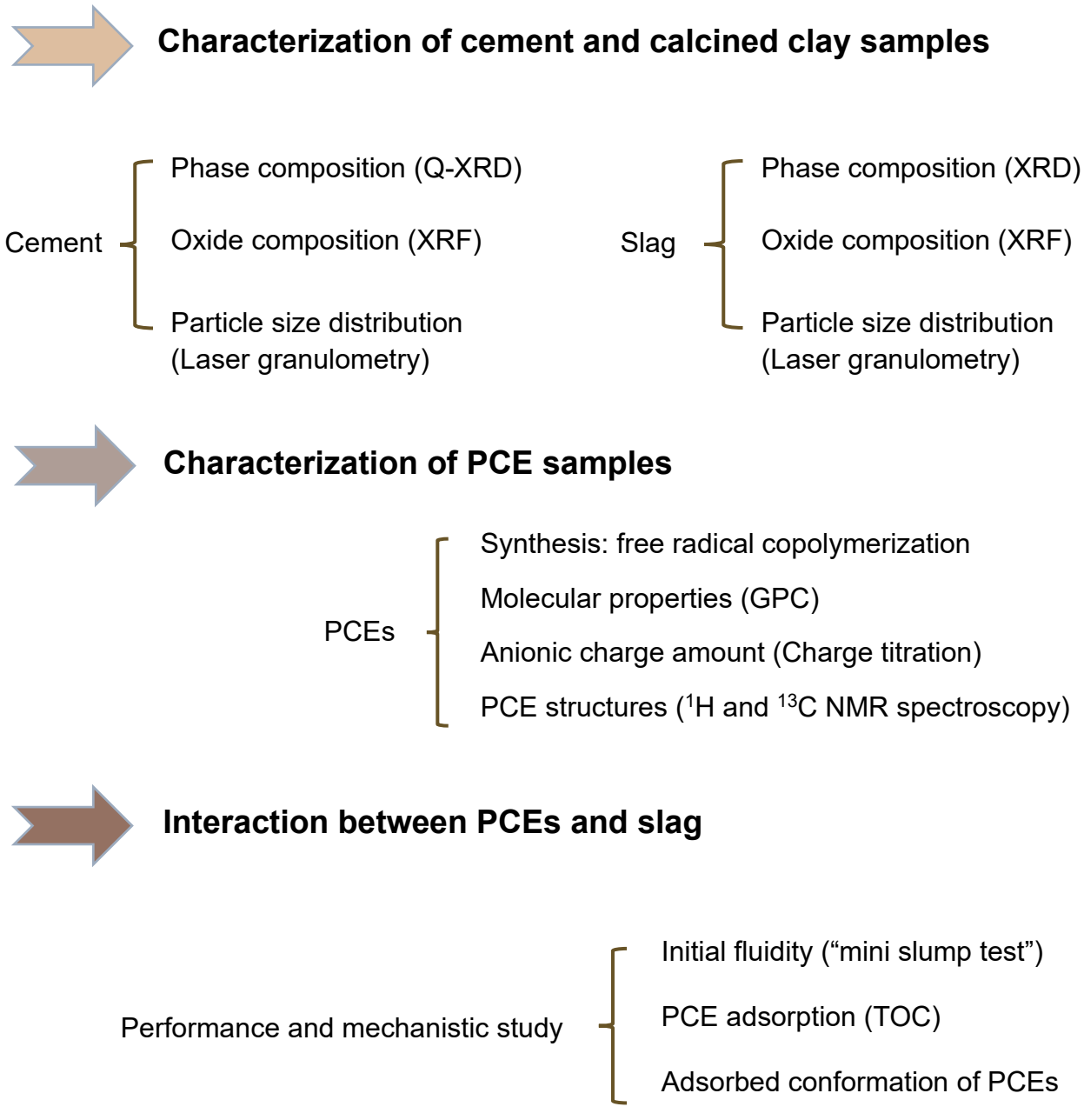

Figure 17. Experimental approach applied in Part II of this study relating to the effects of PCE superplasticizers in alkali-activated slag systems.

5. Results and discussion

This chapter includes 8 publications on two kinds of low-carbon cement systems:

Part I: calcined clay blended cements

Part II: alkali-activated slag composite cements.

Part I: Calcined clay blended cements

1) 3 Peer reviewed journal papers

5.1 Paper # 1:

"Effectiveness of PCE superplasticizers in calcined clay blended cements"

5.2 Paper # 2:

"Approaches to achieve fluidity retention in low-carbon calcined clay blended cements"

5.3 Paper # 3:

"Impact of meta kaolin content and fineness on the behavior of calcined clay blended cements admixed with PCE superplasticizer"

2) Peer reviewed conference papers

5.4 Paper # 4:

"Superplasticizers for calcined clay blended cements"

5.5 Paper #5:

"Influence of calcined clays on workability of low-carbon composite cements"

5.6 Paper # 6:

"Effect of calcined clay types on the performance of polycarboxylate superplasticizers"

3) Peer reviewed Data in Brief

5.7 Paper # 7:

"Characterization data of reference industrial polycarboxylate superplasticizer VP 2020/15.2 used for Priority Program DFG SPP 2005 "Opus Fluidum Futurum-Rheology of reactive, multiscale, multiphase construction materials""

Part II: Alkali-activated slag composite cements

1) Peer reviewed journal papers

5.8 Paper # 8:

"Low Carbon Alkali Activated Slag Binder and its interaction with Polycarboxylate Superplasticizers (PCE): Importance of Microstructural Design of the PCEs"

Section 5.1

Publication # 1

Effectiveness of PCE superplasticizers in calcined clay blended cements

R. Li, L. Lei, T. Sui, J. Plank

Cement and Concrete Research (IF = 12.0)

141 (2021) 106334

DOI: 10.1016/j.cemconres.2020.106334

This paper presents our first study on the effect of PCEs in calcined clay blended cements. The purpose of this study was to investigate the **effectiveness of different PCE structures** on the composite cements containing calcined clays.

The calcined clay sample used was rich in meta kaolin (~50 %) and was obtained from China. To obtain the composite cements, an ordinary Portland cement (OPC) was mixed with this calcined clay at different weight ratios ranging from 90:10 to 60:40. Additionally, five PCE superplasticizers were selected from the group of methacrylate esters (MPEG) and methallyl ethers (HPEG). At first, the water demand of the blended cements and the dispersing performance of the PCEs were determined using mini slump test in paste. It was found that the **water and PCE dosage demand** of the composite cements **increased with ascending calcined clay contents**. Among all the tested PCE structures, the **methallyl ether (HPEG) PCE** polymer showed the **best dispersing performance**, in both neat calcined clay and composite cement.

A mechanistic study via zeta potential analysis revealed that this calcined clay sample initially exhibits a highly negative surface charge which upon uptake of huge amounts of Ca^{2+} ions present in the cement pore solution becomes neutral. This layer of **adsorbed Ca^{2+} ions facilitates** the **adsorption of the PCE superplasticizers**. Furthermore, TOC adsorption measurements revealed that on calcined clay the adsorbed amount of PCEs is much higher than on OPC. This result signifies that the negative effect of **calcined clay** on cement rheology (workability) is owed to its **higher affinity to PCE as compared to OPC**.

Cement and Concrete Research 141 (2021) 106334

Contents lists available at ScienceDirect

Cement and Concrete Research

journal homepage: www.elsevier.com/locate/cemconres

Effectiveness of PCE superplasticizers in calcined clay blended cements

Ran Li [a], Lei Lei [a], Tongbo Sui [b], Johann Plank [a,*]

[a] Technische Universität Müncheen, Chair for Construction Chemistry, 85747 Garching, Lichtenbergstraße 4, Germany
[b] Sinoma Research Institute, Sinoma International Engineering Co., Ltd, No. 16 Wangjing North Road, Chaoyang District, Beijing 100102, China

ARTICLE INFO

Keywords:
Natural clay minerals
Calcined clay
Blended cement (D)
Workability (A)
Polycarboxylate (PCE) Superplasticizer

ABSTRACT

The impact of a calcined clay (CC) rich in meta kaolin (~50 wt%) present in composite cements at 0–40% substitution rate for the clinker was studied relative to the dispersing force of different PCE superplasticizers. It was found that CC increases the water demand of the blended cements considerably (+85% for the 60:40 blend vs. neat OPC). Furthermore, PCEs which fluidize OPC best also provide optimal performance in CC blended cements, but require much higher dosages (in OPC/CC 60:40, 4–6 times as compared to neat OPC). In all systems, HPEG-PCE produced superior dispersing performance over anionic MPEG-PCEs. A mechanistic study involving zeta potential measurements revealed that the initially negatively charged calcined clay surface adsorbs huge amounts of Ca^{2+} ions from the pore solution, thus facilitating adsorption of anionic PCE superplasticizers. The results signify that commercially available PCE products can effectively fluidize OPC/CC blended cements.

1. Introduction

Global warming and climate change issues caused by carbon dioxide emissions are becoming more and more important and urgent in the world [1]. For instance, an impact of global warming on the recent Australian bushfire cannot be ruled out. In particular, with the sustained growth of the urban population, the demand for large infrastructure construction is much increased as well. As of today, concrete and cement present the most widely used man-made materials and will remain much in the foreseeable future. However, cement clinker production presents one major source of CO_2 emission [2,3]. It has been reported that the carbon dioxide emissions originating from cement production account for ~8% of total global anthropogenic CO_2 release [4]. In the clinkerization process, CO_2 mainly originates from raw material decomposition ($CaCO_3$) and - to a lesser extent - from fuel burning. Both processes contribute 60–70% and 30–40%, respectively to the direct CO_2 emission from clinkerization [5].

For this reason, alternative materials which allow partial replacement of Portland cement clinker and exhibit a low carbon footprint have attracted increasing interest and have been discussed executively [6]. These include alkali-activated binders [7,8], Belite-Ye'elimite-Ferrite (BYF) clinker [9] and carbonate binder [10,11]. Moreover, supplementary cementitious materials (SCMs) such as silica fume, fly ash or blast furnace slag also offer a huge potential to reduce CO_2 emission from cement production [12,13]. However, the limited supply of these industrial by-products restricts a wider use in many countries as their availability relies on the degree of economic development [1]. On the other hand, natural pozzolans such as volcanic ashes are available only in certain regions according to local geological conditions [14]. Thus, calcined clays attract growing interest as SCM because of the global abundance of natural clays. In addition, significantly less CO_2 is released during their calcination as compared to clinker, because they do not require the decarbonation of $CaCO_3$. Moreover, according to a recent study calcined kaolinite (meta kaolin) is particularly suitable for co-substitution with limestone because of its high alumina content which leads to the formation of carboaluminate [15]. Furthermore, meta kaolin presents superior pozzolanic reactivity which results in accelerated early strength development [16,17]. To summarise, calcined clay offers a tremendous potential as supplementary cementitious material which can partially replace cement clinker.

However, relative to practical use, their specific surface properties and the internal porosity of individual calcined clays can lead to an increased water demand resulting in poor workability. Furthermore, the mineral phase composition of calcined clays is highly dependent on the natural deposit, and this can cause significant variations in reactivity and dispersing performance. Thus identification of effective superplasticizers presents a key element to achieve a more widespread use of calcined clay blended cements.

So far, only few studies have investigated the impact of superplasticizers on the properties of calcined clay or calcined clay blended

* Corresponding author.
E-mail address: sekretariat@bauchemie.ch.tum.de (J. Plank).

https://doi.org/10.1016/j.cemconres.2020.106334
Received 10 February 2020; Received in revised form 23 October 2020; Accepted 9 December 2020
Available online 24 December 2020

cements. Akbulut et al. [18] focused on the modification of polycarboxylate ether-based superplasticizers in a ternary OPC calcined clay-limestone blend (LC^3 cement). They reported that a *co*-monomer which introduced sulfonic acid groups into the acrylic acid backbone of MPEG PCEs possessing a low polyethylene glycol grafting density enhances its dispersing performance even at high clinker substitution rates, but requires high dosages [18]. In addition, Schmid et al. [19] compared the dispersing power of zwitterionic superplasticizers with that of conventional PCEs. They found that the amphoteric comb polymers show slight superiority over strictly carboxylated PCEs relative to the dispersion of calcined clays or calcined clay blended cements.

In this study, a calcined clay from China which is rich in meta kaolin (~50%) was investigated with respect to the dispersing performance of five PCE superplasticizers selected from the groups of methacrylate esters (MPEG) and methallyl ethers (HPEG). Additionally, a zwitterionic MPEG PCE was included into the study. The purpose of this investigation was to identify specific PCE structures which work best in a composite cement which contains a particularly high content of meta kaolin. As cements, blends of an ordinary Portland cement (OPC) and the calcined clay at ratios of 90:10, 80:20, 70:30 and 60:40 were probed. First, the water demand of the blended cements was determined to assess their overall requirement for superplasticizer dosages. The dispersing performance of the PCEs in these cements and the neat OPC and calcined clay respectively were evaluated via "mini slump" tests. From this, it was hoped to obtain an understanding of which PCE structure is most suitable to disperse CC blended cements. Furthermore, the interaction of the different PCE polymers with the composite cements was assessed via zeta potential and adsorption measurements, and a mechanism for the dispersion of CCs by PCE polymers is proposed.

2. Materials and methods

2.1. Cement

An ordinary Portland cement (CEM I 42.5R) from Schwenk cement company (Ulm, Germany) exhibiting a density of 3.13 $g \cdot cm^{-3}$ (Helium pycnometry) and a d_{50} value of 18.13 μm (laser granulometer, Cilas 1064, Cilas Company, Marseille, France) was used in this work. The phase composition of the cement sample was determined via Q-XRD including *Rietveld* refinement and is shown in Table 1.

2.2. Calcined clay

Natural clay deposits can exhibit significantly diverging compositions. For this reason, as a first step, the mineralogical composition of the raw clay and the calcined clay sample were determined via quantitative XRD analysis including *Rietveld* refinement. Measurements were performed on a PANalytical instrument (Empyrean, Profex BGMN software) using an external Si-standard to distinguish between crystalline and amorphous content. The respective diffractograms are exhibited in Fig. 1, and the results from the quantification are listed in Table 2.

Table 1
Phase composition of the cement sample CEM I 42.5 R.

Phase	wt%
C_3S, monoclinic	54.52
C_2S, monoclinic	18.41
C_4AF, orthorhombic	10.85
C_3A, cubic	5.23
C_3A, orthorhombic	0.88
Anhydrite ($CaSO_4$)	0.94
Dihydrate ($CaSO_4 \bullet 2H_2O$)	3.61
Hemihydrate ($CaSO_4 \bullet 0.5H_2O$)	0.33
Calcite ($CaCO_3$)	3.04
Dolomite ($CaMg(CO_3)_2$)	1.13
Quartz (SiO_2)	0.91
Free lime (*Franke*)	0.14
Total	100.00

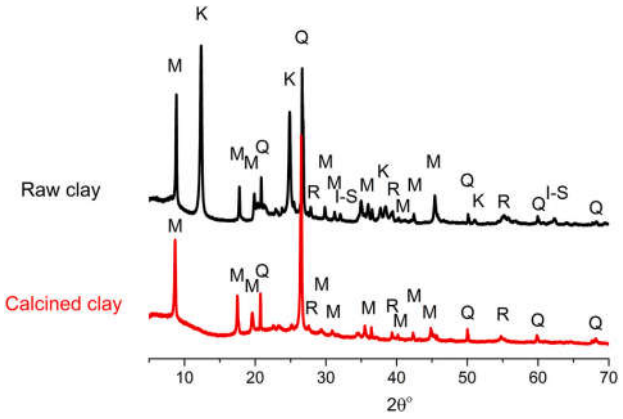

Fig. 1. XRD patterns of the raw and the calcined clay samples (K: kaolinite, M: muscovite, I-S: illite-smectite, Q: quartz, R: rutile).

According to this analysis, the main component of the raw clay is kaolinite which makes up ~51.3 wt%. Besides, the raw clay also contains significant quantities of muscovite (~18.1 wt%) and illite-smectite (~19.7 wt%) which is an interstratified mixed layer clay [20].

The calcined clay used in this study exhibited a bulk density of 2.63 $g \cdot cm^{-3}$ and was provided by Sinoma International Engineering Co., Ltd., Beijing, China. Its particle sizes (d_{10}, d_{50}, d_{90} values) measured via laser granulometry were found at 2.18 μm (d_{10}), 10.42 μm (d_{50}) and 26.16 μm (d_{90}), respectively. Calcination was performed in a rotary kiln by heating to a temperature of 800 °C for 1 h. At such temperature, the structural water is removed from the clay minerals resulting in dehydroxylation. For example, the kaolinite phase was completely converted to very fine amorphous meta kaolin which exhibits high pozzolanic reactivity [21]. According to the data, the calcined clay sample investigated in this work was particularly rich in meta kaolin. It was a particular aim of this study to elucidate how specific PCE polymers interact with composite cements containing significant amounts of meta kaolin.

2.3. Cement and calcined clay mixtures

In this study, the properties of OPC, of composite cements (OPC:CC wt. ratios of 90:10, 80:20, 70:30 and 60:40) and of the neat calcined clay sample were investigated. The bulk density and specific surface area of each mixtures were measured, as listed in Table 3.

It has been established before that at very high clinker substitution rates by calcined clays, addition of more gypsum is advantageous to improve the long-term mechanical properties of such cement [15]. Here, however, such addition was not performed because the dispersing ability of the PCE samples was not affected by additional gypsum, as was proven by comparative experiments, and because at low substitution rates (e.g. 10% or 20%) no such sulfate addition is necessary.

Table 2
Mineralogical composition of the raw and the calcined clay samples, as determined by XRD including *Rietveld* refinement.

Mineral phase	Raw clay (wt%)	Calcined clay (wt%)
Kaolinite	51.3	–
Illite – smectite	19.7	–
Muscovite	18.1	2.3
Muscovite HT[a]	–	15.5
Quartz	10.3	13.8
Rutile	0.5	0.3
Amorphous content	–	68.2
Total	99.9	100.1

[a] Muscovite HT presents a well-defined high-temperature modification characterized by expansion of the K interlayer region [20].

Table 3
Density and specific surface area of the neat and composite cements and of the neat calcined clay.

Samples	Density (g/cm^3)	*Blaine* value (cm^2/g)	BET SSA (m^2/g)
OPC	3.13	3041	1.0
OPC-CC 90:10	3.09	4507	2.2
OPC-CC 80:20	3.04	5900	3.4
OPC-CC 70:30	3.00	7339	4.7
OPC-CC 60:40	2.95	9137	5.9
Calcined clay	2.63	–	13.2

2.4. Superplasticizers

2.4.1. PCE samples

All MPEG-based polycarboxylate superplasticizers and the amphoteric superplasticizer were self-synthesized using aqueous free radical copolymerization. The specific polymer compositions, the molar ratios and the anionic charge density of the products are exhibited in Table 4, and the chemical structures of the superplasticizer samples tested in this study are presented in Fig. 2.

The carboxylated MPEG PCE samples (23MPEG6, 45MPEG6 and 114MPEG6) were prepared at the same methacrylic acid (MAA) to macromonomer ratio of 6:1, but from ω-methoxy poly(ethylene glycol) methacrylate ester macromonomers holding different numbers of ethylene oxide (EO) units (23, 45 or 114), thus yielding comb polymers with increasing side chain length. The amphoteric polymer designated as MAA-114MPEG-MAPTAC (molar ratios 6:1:0.5) contained 3-trimethylammonium propyl methacrylamide chloride (MAPTAC) as an additional cationic monomer, yielding a zwitterionic polymer with both anionic and cationic groups present in the same molecule. The copolymerization process followed exactly the description on MPEG PCE preparation applying the high temperature synthesis method as presented in [22]. The amounts of initiator (sodium persulfate) and chain transfer agent (sodium methallyl sulfonate) were the same as described in this literature. The final PCE solutions had a solids content of ~30 wt % and were neutralized with 30% NaOH solution.

Additionally, an industrial commercial PCE polymer based on HPEG macromonomer provided from JILIN Chemical Industrial (Jilin, China) was incorporated into these tests. This polymer is characterized by a relatively low anionicity (medium content of acrylic acid to ω-hydroxy polyethylene glycol methallylether macromonomer) and a medium long side chain. The polymer was prepared according to the room temperature synthesis method. GPC analysis confirmed this PCE sample to be non-formulated with other admixtures, and impurities were <2%. This product is commonly applied in precast concrete.

2.4.2. Characterization of PCE polymers

Gel permeation chromatography was used to determine the molecular properties (M_w, M_n, PDI) of the polymers on a *Waters 2695* separation module equipped with three Ultrahydrogel™ columns (120, 250, 500) and an Ultrahydrogel™ guard column (all from Waters, Eschborn, Germany). 0.1 N $NaNO_3$ (pH = 12) was used as eluent at a flow rate of 1.0 mL min^{-1}.

The molecular weights (M_n, M_w), polydispersity index (PDI) and conversion of the polymer samples are listed in Table 5. According to the results, all PCE samples exhibit low PDI values (1.8–2.4) and high rates for macromonomer conversion (91–97%) which are characteristic for high quality PCE polymers. The only exception is 114MPEG6, the reason being that for such long-chain macromonomer the kinetics of the copolymerization shifts in favor of MAA homopolymerization and thus a less homogeneous copolymer is achieved.

In Fig. 3, the GPC spectra of all PCE polymers tested are displayed. For the anionic polymer samples, a large peak signifying the PCE polymer as well as two minor peaks representing residual macromonomer (MM) and the solvent can be observed. On the other hand, the GPC spectrum of amphoteric polymer MAA-114MPEG-MAPTAC is more complicated. There, the main polymer peak appears at 17–23 min elution time. Also, a very small amount (~0.002 wt%) of polymethacrylic acid is detected at short elution times (15–17 min) followed by a low molecular weight peak at ~23–24 min elution time. Furthermore, nonreacted macromonomer (M_w of 4700–5400 g mol^{-1}) and an oligomer (M_w ~ 1300–1500 g mol^{-1}) are also detected, thus suggesting formation of a less homogeneous polymer as compared to the other samples.

Table 4
Composition of the different PCE polymer samples synthesized for the study.

PCE sample designation	Molar ratio of monomers MAA:MPEG-mm[a]:MAPTAC	Side chain n (EO)
23MPEG6	6:1:0	23
45MPEG6	6:1:0	45
114MPEG6	6:1:0	114
MAA-114MPEG-MAPTAC	6:1:0.5	114

[a] mm = macromonomer.

2.5. Zeta potential

To gain more insight into the surface properties of the calcined clay and cement samples, zeta potential measurements of slurries were performed on a *Model DT-1200 Electroacoustic Spectrometer* (Dispersion Technology, Inc., NY, USA). The cement sample was prepared at a water-to-cement ratio of 0.5 whereas the calcined clay sample was suspended in synthetic cement pore solution (hereafter abbreviated as SCPS) at a higher water-to-binder ratio of 1.2, to account for its higher water demand. The SCPS used in this work was prepared according to a description published in [23]. It contained 1.72 g of $CaSO_4{\cdot}2H_2O$, 6.959 g of Na_2SO_4, 4.757 g of K_2SO_4 and 7.12 g of KOH dissolved in 1 L of deionized water (pH = 13.2).

The uptake of Ca^{2+} by the calcined clay sample was also determined via zeta potential. There, a 0.01 mol $Ca(NO_3)_2$ solution was titrated in 50 steps to the calcined clay slurry until saturated adsorption of Ca^{2+} had been achieved. During the $Ca(NO_3)_2$ titration, the pH value was kept constant at ~12.4 (initial pH value) by minor additions of 30 wt% aqueous NaOH.

2.6. Dispersing effectiveness of PCEs

Fluidity (workability) of OPC, of the composite cements (OPC:CC ratios of 90:10, 80:20, 70:30 and 60:40) and of the neat calcined clay sample were assessed via a modified "mini slump" test according to DIN 1015 [24]. The water-to-binder (w/b) ratio was fixed at 0.5 for OPC and OPC/CC binders, while it was 1.2 for the neat calcined clay.

The procedure was as follows: 300 g of binder were added to the mixing water contained in a porcelain cup and were vigorously stirred manually for 10 s with a spoon. Then the superplasticizer solution was added to the mixture and stirred for 50 s. Thereafter, the suspension was allowed to rest for 1 min and was then mixed again for an additional 1 min. The water content of the PCE solution was subtracted from the total amount of mixing water to perform all experiments at the same w/b ratio. The freshly prepared paste was immediately poured into a Vicat cone with the dimensions of 40 mm (height), 70 mm (top diameter) and 80 mm (bottom diameter) which was placed on a glass plate. After the cone was lifted vertically, the resulting spread of the cement paste was measured twice, and the average was taken as the final result. Applying this procedure, the dosages of polymers to reach a spread flow of 26 ± 0.5 cm were determined.

The solid volume fractions of the pastes vary as Portland cement is increasingly substituted by calcined clay and the water-to-binder ratio is kept constant at 0.5. Therefore, the solid volume fractions of the different mixtures were calculated and are listed in Table 6.

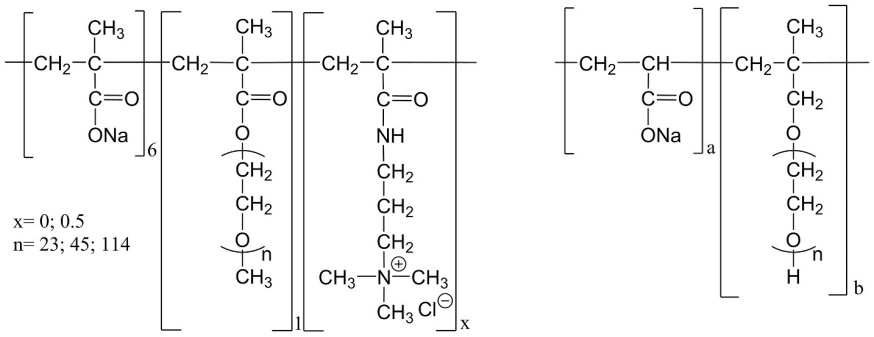

Fig. 2. Chemical structures of the kinds of PCE superplasticizers used in this study.

Table 5
Molecular properties of the PCE polymers studied in this work.

Polymer sample	M_w [Da]	M_n [Da]	PDI	Macromonomer conversion	Anionic charge density[a] [μeq/g]
23MPEG6	22,510	11,730	1.92	90.7%	3739
45MPEG6	25,180	10,610	2.37	95.1%	2417
114MPEG6	81,880	27,870	2.94	96.8%	1143
MAA-114MPEG-MAPTAC	38,350	16,850	2.28	93.0%	1024
Commercial HPEG PCE	35,340	19,490	1.81	91.8%	1805

[a] Measured in aqueous 0.1 M NaOH solution.

2.7. Polymer adsorption

Polymer adsorption on neat cement and calcined clay were determined according to the depletion method based on total organic carbon (TOC) analysis. At each polymer concentration, the amount of polymer remaining in the interstitial pore solution at the equilibrium condition before and after contact with cement or calcined clay was detected. In a typical experiment, 16 g of cement were dispersed in 8 mL of DI water (w/c ratio of 0.5) or 7 g of calcined clay in 8.4 mL of SCPS (w/b ratio of 1.2), homogenized and then separated via centrifugation at 8500 rpm for 10 min. A detailed description of the method can be found in [25]. A LiquiTOC analyzer (Elementar, Hanau, Germany) was utilized to determine the organic carbon content in the supernatant collected from centrifugation. The amount of polymer adsorbed was then calculated from the carbon content present in the filtrate and the carbon content which was introduced with the respective polymer dosage initially dissolved in the mixing water. Each sample was measured twice and the values obtained were averaged.

3. Results and discussion

3.1. Surface charge of calcined clay

It is well established that the surface charge of e.g. cement particles or early cement hydrates controls the adsorption and hence the dispersing performance of superplasticizers [26]. Thus, it is most critical to understand the surface charge of the calcined clay sample (CC) in cement. For this reason, zeta potential measurements were performed with the aim of uncovering the development of the electrical double layer on the surface of CC which actually hosts the adsorbed PCEs.

As is shown in Table 7, the cement sample developed a positive surface charge of around +5 mV, while the calcined clay dispersed in SCPS exhibited a highly negative value of around −30 mV, thus signifying quite the opposite behavior as compared to cement. This result provokes several consequences: first, common cement superplasticizers which usually are negatively charged will not adsorb on such CC particles; second, according to the DLVO theory developed by Derjaguin, Landau, Verwey and Overbeek [27,28], colloidal particles possessing such high charges repel each other via strong electrostatic repulsion and therefore would not require a dispersant to achieve workability. However, a simple test by dispersing the CC sample in SCPS demonstrated that the CC particles were poorly dispersed, as indicated by a relatively high slurry viscosity. Thus, it was assumed that the CC would interact strongly with ions present in the SCPS, such as e.g. Ca^{2+} and that the zeta potential measured here might not be representative for the actual situation in cement where Ca^{2+} adsorbed by CC will immediately be replenished in the pore solution by continued dissolution from the clinker phases. Opposite to this, in SCPS the concentration of Ca^{2+} ions is limited and is not replenished once an uptake of Ca^{2+} by CC has occurred. Hence, it was speculated whether the calcined clay sample would adsorb a significant quantity of Ca^{2+} ions from the pore solution.

In order to find out, the uptake capacity for Ca^{2+} by the calcined clay sample was validated via zeta potential measurements. The experiment was performed by stepwise titrating a $Ca(NO_3)_2$ solution to a suspension of the CC in SCPS and recording the zeta potential at increasing Ca^{2+} addition while the pH was maintained at ~12.4. In this way, it was hoped to gain insight into the actual surface charge of the calcined clay present in a cement. The result is shown in Fig. 4.

As is obvious from there, addition of increased amounts of Ca^{2+} shifts the zeta potential to much less negative values until a plateau is reached at the isoelectric point. Hence it is confirmed that the surface of CC is densely occupied by Ca^{2+} ions which can facilitate the adsorption of negatively charged PCE polymers and then achieve dispersion and workability. This experiment demonstrates that the dynamic condition occurring in cement pore solution needs to be taken into consideration to develop a realistic view of the surface chemistry of CC particles present in cementitious suspensions.

3.2. Water demand of calcined clay blended cements

In the following experiments, the water demand of composite cements containing 0–40 wt% of calcined clay and its impact on cement workability was assessed and compared with that of the neat OPC.

At first, the fluidity of the pastes was measured at a constant water-to-binder ratio of 0.5 and compared. It was found that increased additions of CC significantly affect paste fluidity. For example, already at a clinker substitution rate of 30% the paste flow had decreased from ~19 cm to 8 cm (Fig. 5) which signifies a complete loss of fluidity since the diameter of the Vicat cone is 8 cm. We attribute this effect to the much increased specific surface area of the composite cements as presented in

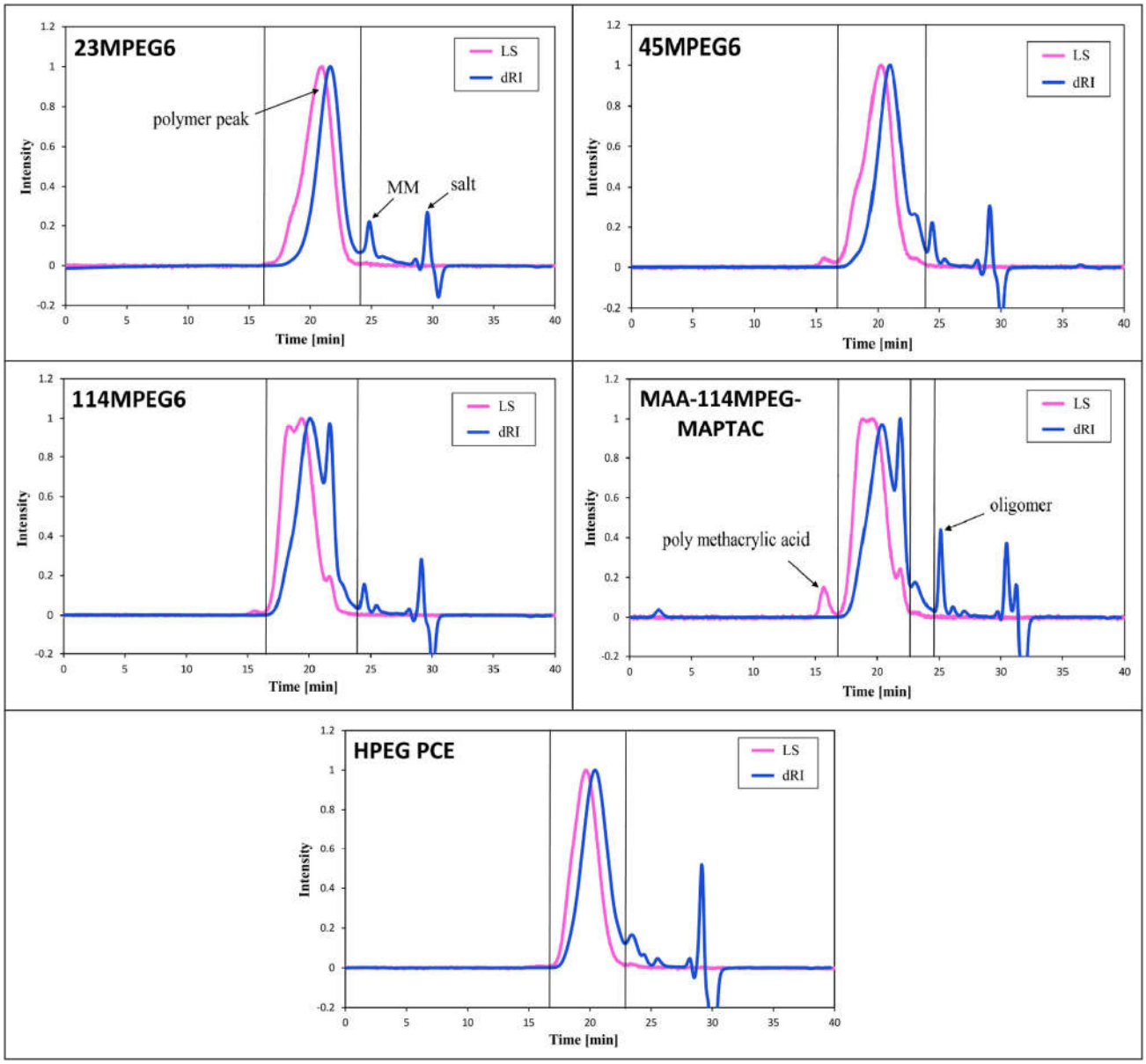

Fig. 3. GPC spectra of all PCE samples tested in this study; eluent: 0.1 M $NaNO_3$.

Table 6
Solid volume fractions of pastes from neat cement, OPC/CC composites and neat CC; w/s ratio constant at 0.5.

Samples	Solid volume fraction (%)
OPC	38.99
OPC-CC 90:10	39.29
OPC-CC 80:20	39.68
OPC-CC 70:30	40.00
OPC-CC 60:40	40.04
Calcined clay	24.06

Table 7
Zeta potential of the cement and calcined clay samples dispersed in DI water and SCPS, respectively.

Samples	Cement (w/c = 0.5)	Calcined clay (w/b = 1.2)
Zeta potential [mV]	+5	−37

Table 3. It is in line with findings from Mantellato et al. who reported that the yield stress of a cement paste increases exponentially with the increase of the specific surface area [29]. Furthermore, also the solid volume fraction of the composites will influence the yield stress of the cement paste [30]. Here, as we kept the water-to-binder ratio constant at 0.5, the solid volume fraction in OPC and the OPC-CC blends varied from 38.99% (for the neat OPC) to 40.04% (for the 60:40 OPC/CC composite) (see Table 6). However, such an increase is relatively minor and therefore of limited impact on workability.

Our results suggest that the water demand of CC is much higher than of OPC. To confirm, the water demand of the different OPC/CC blends was determined.

In this series of tests, the w/b ratios at which a paste spread flow of 18 ± 0.5 cm was obtained for different OPC/CC blends were determined. The results are displayed in Fig. 6. There it can be seen that the amount

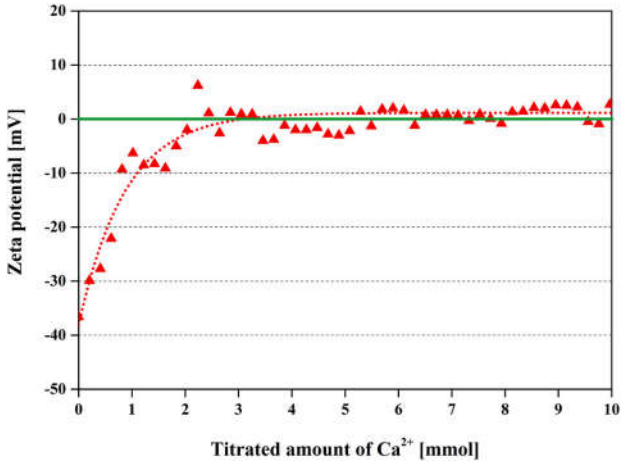

Fig. 4. Zeta potential of the calcined clay sample suspended in SCPS as a function of $Ca(NO_3)_2$ solution added.

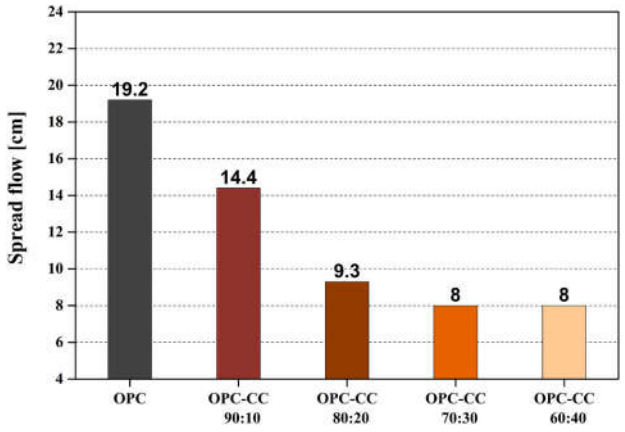

Fig. 5. Spread flow of OPC/CC blended cements representing different substitution rates for the clinker, w/b ratio = 0.5, no PCE polymer added.

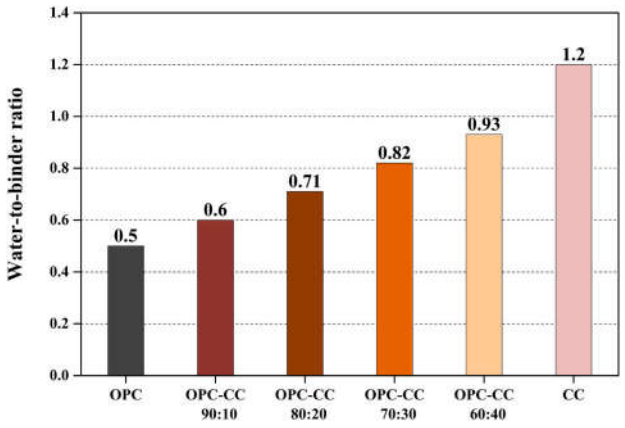

Fig. 6. Water demand of composite cements containing OPC and CC at different substitution rates; no PCE polymer added.

of water required increases linearly with ascending substitution rate for the cement clinker. For example, at 40% replacement of cement clinker by CC (OPC:CC 60:40), the water demand had almost doubled from 0.5 for neat OPC to 0.93 for the 60:40 blend. For the neat calcined clay sample, the water demand raised to an even much higher value of 1.2 to achieve the targeted spread flow. This indicates that the water demand of the CC sample investigated here is particularly high, presumably resulting from the high content of fine meta kaolin, as was presented before (see Table 2).

To summarise, the results relative to the water demand of the CC sample clearly suggest that in actual application of such blended cements the addition of effective superplasticizers is indispensable to achieve acceptable workability and strength.

3.3. Dispersing performance of PCEs in OPC

At first, the dispersing performance of the superplasticizer polymers was evaluated in neat OPC via "mini slump" test. There, the PCE dosage required to achieve a cement paste spread flow of 26 ± 0.5 cm at a water-to-cement ratio of 0.5 was determined.

As is displayed in Fig. 7, the dosages required from all five superplasticizers were quite comparable (0.04–0.06%), with the commercial HPEG product performing slightly better and the short chain MPEG sample 23MPEG6 dispersing slightly less. It is also interesting to note that the zwitterionic PCE sample MAA-114MPEG-MAPTAC dispersed as well as the strictly anionic polycarboxylates. Unfortunately, the drawback of the zwitterionic PCE is its higher cost and slight toxicity as compared to strictly anionic PCEs.

3.4. Dispersing performance of PCEs in calcined clay

Next, the dispersing capacity of the five polymers in neat calcined clay suspensions prepared in SCPS was assessed by measuring the dosage dependent paste spread flow (see Fig. 8). Again all PCE samples performed quite comparably, with the exception of the commercial HPEG polymer which was vastly superior over the other PCEs. Most importantly, by adding this polymer it was possible to achieve a very high fluidity as expressed by a spread flow of 26 cm, whereas all MPEG copolymers leveled out at a spread flow of ~21 cm, and even much higher dosages could not enact the excellent fluidity which was advisable from the HPEG sample (see Fig. 8). This result signifies that calcined clays can be very selective to PCE superplasticizers with respect to their specific chemical composition.

3.5. Dispersing performance of PCEs in calcined clay blended cements

In the next step, the dispersing ability of the five PCE samples in the OPC/CC composite cements was assessed via mini slump tests. The results are exhibited in Fig. 9.

First, it is observed that increasing substitution rates of clinker by CC

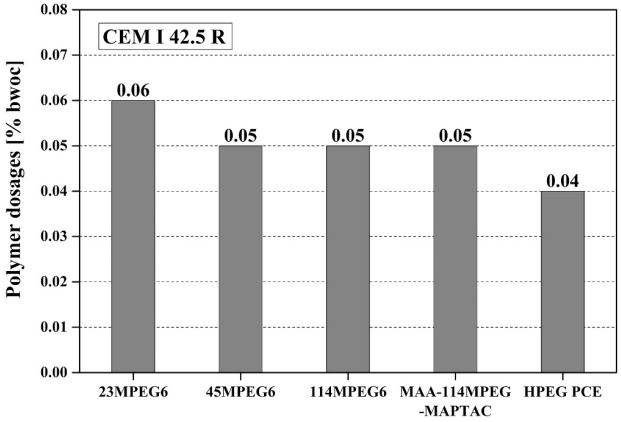

Fig. 7. Dosages of PCE superplasticizers required to obtain a cement paste spread flow of 26 ± 0.5 cm; w/c ratio = 0.5.

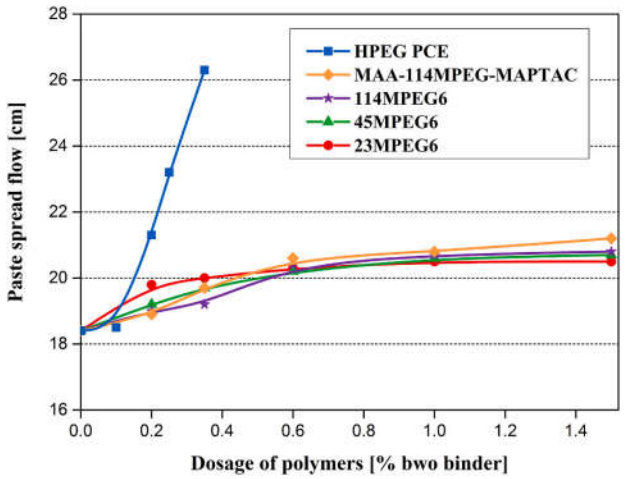

Fig. 8. Spread flow of calcined clay pastes prepared at a w/b ratio of 1.2 with increasing dosages of polymers.

results in a sharp increase in PCE dosages. This negative impact of CC on dosage is comparable for all PCE polymers and generally leads to a roughly sixfold increase in addition rate for the 60:40 blend as compared to the neat OPC. The difference between individual polymers only arises from the initial effectiveness in OPC: PCEs which are most effective in OPC such as the HPEG or the zwitterionic PCE also fluidize the blends at comparatively lower dosages while other polymers generally require higher dosages, independent of whether CC is present or not.

Interestingly, in neat calcined clay all MPEG-based PCEs could not provide any fluidity at all whereas the HPEG sample still reached the targeted spread flow of 26 cm at a dosage of 0.35% bwob. These results again confirm the superior performance of HPEG over MPEG chemistry in these systems.

In order to gain more insight into the effect of increased calcined clay contents on the dispersing power of the PCEs, their dosages were plotted against the ascending CC content present in the blended cements and then linearly fitted, as is displayed in Fig. 10. From the slopes it becomes evident that the HPEG PCE and the zwitterionic MPEG polymer present the most dosage-effective PCEs in comparision to the other copolymers because their dosages remain at the lowest with ascending CC content. Whereas, from the point of robustness against increasing CC contents, the polymers 23MPEG6 and the zwitterionic PCE encounter the least percentual increase in dosage when the CC content increases. It is also noteworthy that the zwitterionic MPEG PCE outperforms its strictly anionic counterpart. We attribute the superiority of this amphoteric polymer to its ability to adsorb on to positively as well as negatively charged surfaces which allows to achieve a more complete coverage of the particle surfaces.

The results suggest that the HPEG and the zwitterionic polymer present the most effective superplasticizers in composite cements containing calcined clays. Furthermore, it is also demonstrated that the incorporation of a cationic monomer such as MAPTAC can greatly improve the performance of MPEG PCEs in such systems.

3.6. Adsorption of PCEs on OPC and CC

Generally, the dispersing performance of superplasticizers among other is correlated to their amount adsorbed onto the binder particles [31]. To investigate the mechanism behind the different performance of the PCE samples studied in the workability tests (see Section 3.6), adsorption isotherms were developed for the individual polymers on neat OPC and CC at a w/b ratio of 0.5 or w/b ratio of 1.2, respectively. Here and in the following, PCE sample 114MPEG6 was omitted because of its lower homogeneity as compared to its short-chain counterparts, which might influence the results. The results for adsorption on OPC are plotted in Fig. 11.

First, all polymers produced a *Langmuir*-type adsorption isotherm which is characterized by a steep increase in adsorbed amount at low PCE dosages until it levels out at a plateau which represents the point of complete surface coverage (=saturated adsorption). Significantly higher adsorbed amounts were reached for the anionic MPEG polymers as compared to the zwitterionic and the HPEG PCE. More specific, 23MPEG6 and 45MPEG6 reached the saturated adsorption at ~3.0 mg/g cement, while the MAA-114MPEG-MPTAC and HPEG samples attained their plateau at 2.0 and 1.8 mg/g cement, respectively. However, in order to assess the dispersing behavior of the PCEs in this cement, their

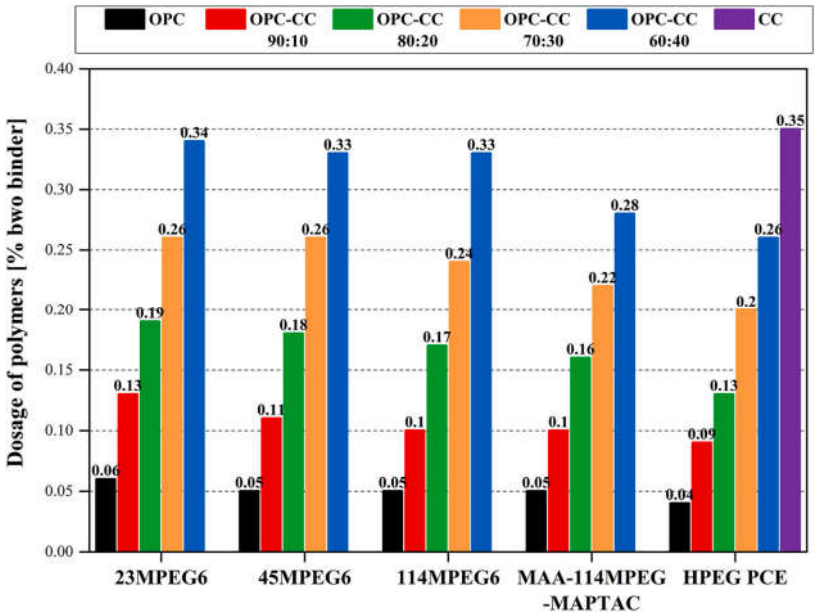

Fig. 9. PCE dosages required to achieve a spread flow of 26 ± 0.5 cm, measured in neat OPC, CC and OPC/CC blended systems; w/b ratio = 0.5 for cements or 1.2 for neat CC.

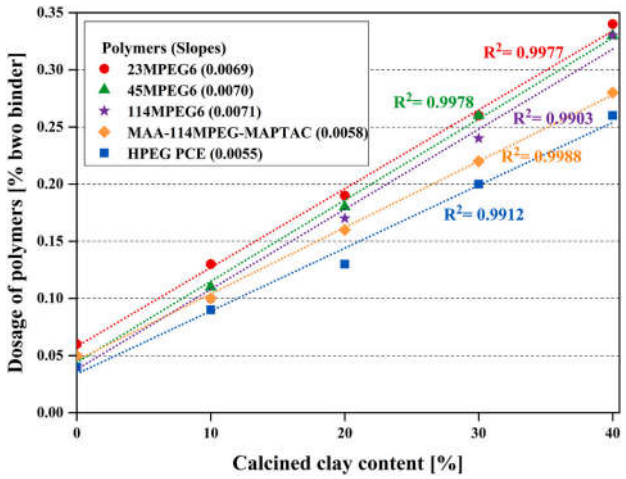

Fig. 10. Relationship between PCE dosages required and calcined clay content in the OPC/CC blended cements.

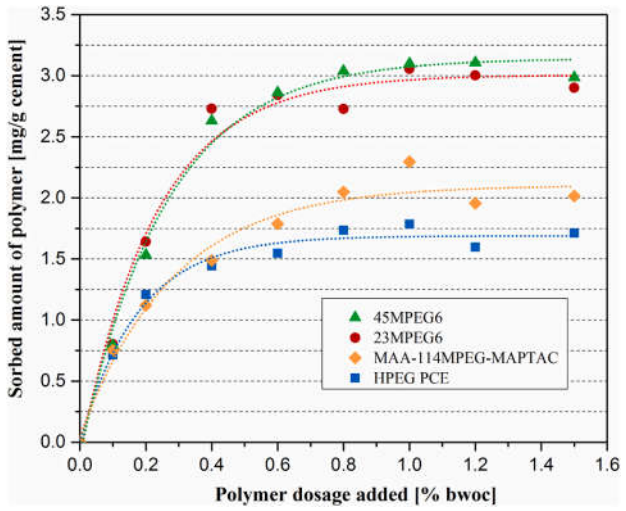

Fig. 11. Adsorption isotherms for PCE polymers on OPC (w/c = 0.5).

adsorption at the actually applied dosages needs to be looked at. These values are tabulated in Table 8.

There, it can be seen that the adsorbed amounts of all PCE polymers are very similar and increased with the dosage added, as would be expected. This explains why all samples disperse cement equally, as was displayed before in Fig. 7. The only exception from this is the zwitterionic polymer MAA-114MPEG-MPTAC which consistently exhibits slightly lower adsorbed amounts. It is assumed that the cationic charge present in its backbone somehow reduces its adsorption, because of its overall lower anionic charge amount of the molecule (see Table 5).

Table 8
Adsorbed amounts of the PCE superplasticizers on OPC at the dosages used in the spread flow experiments displayed in Fig. 7.

Polymer	Adsorbed amount [mg/m^2 cement][a]			
Dosage [% bwoc]	23MPEG6	45MPEG6	MAA-114MPEG-MAPTAC	HPEG PCE
0.04	0.27	0.26	0.23	0.28
0.05	0.36	0.36	0.32	0.37
0.06	0.46	0.46	0.37	0.46

[a] Based on BET SSA of 1.0 m^2/g cement.

Next, the adsorbed amounts on neat calcined clay were determined and are listed in Table 9. At first, it was noticed that for CC suspensions, much lower adsorbed amounts than for OPC are recorded which can be attributed to the different surface chemistry of the calcined clay. Second, inspite of its initially highly negative surface charge as recorded in the zeta potential measurements (see Fig. 4), this calcined clay still can sorb very significant amounts of PCEs. This ability either derives from the uptake of Ca^{2+} ions as was demonstrated in Fig. 4 or from charge heterogeneity which is known to exist in non-calcined clays such as e.g. in bentonite [32]. Moreover, when considering to the PCE structure, a longer side chain results in higher polymer adsorption, as the mass per molecule increases. Interestingly, the HPEG polymer consistently records the highest adsorbed amounts while the anionic MPEG PCE samples exhibit lower sorption on CC. This could explain why these polymers perform significantly less with CC, as has been demonstrated in Fig. 8. Thus it becomes obvious that in order to disperse CC, high surface occupancy is critical.

4. Conclusion

In this study, composite cements containing a calcined clay that is rich in meta kaolin were investigated. Furthermore, their water demand and their behavior towards structurally different PCE polymers were assessed to understand how increased amounts of CC would impact the workability of these cements. Finally, the purpose of this study was to determine whether OPC or calcined clay has a greater impact on PCE performance, and whether specific PCE superplasticizer structures exist which are more tolerant towards increased calcined clay contents.

From the results obtained, the following conclusions can be drawn:

1. The effectiveness of a PCE superplasticizer in OPC/CC blends can be derived from its performance in neat OPC. PCEs which fluidize OPC well will also work well in calcined clay blended cements.
2. Calcined clay initially exhibits a highly negative surface charge which through the uptake of huge amounts of Ca^{2+} ions from the pore solution then becomes almost neutral. This layer of adsorbed Ca^{2+} ions facilitates the adsorption of PCE superplasticizers.
3. Of all PCE structures tested, the methallyl ether (HPEG) polymer produced superior dispersing performance compared to the MPEG-based superplasticizers, in both neat calcined clay and calcined clay blended cements.
4. Introduction of a cationic group into an MPEG PCE improved its performance as compared to conventional anionic MPEG polymers. It suggests that the presence of the positive charge in the backbone of the polymer promotes its interaction with the surface of cement.

In future studies, the interaction of individual calcined clay minerals (e.g. meta kaolin, meta montmorillonite, meta muscovite, etc.) with different PCE molecules should be studied to gain more insight into which meta clay mostly controls the workability property of a mixed calcined clay. From this information, it might be possible to develop a matrix which allows to roughly predict the water demand of this binder and the dispersing performance of a PCE at any mix proportion of these meta clays with cement clinker.

Table 9
Adsorbed amounts of the superplasticizers on neat calcined clay at the dosages used in the spread flow experiments displayed in Fig. 8.

Polymer	Adsorbed amount [mg/m^2 calcined clay][a]			
Dosage [% bwob]	23MPEG6	45MPEG6	MAA-114MPEG-MAPTAC	HPEG PCE
0.10	0.07	0.08	0.08	0.09
0.20	0.10	0.13	0.13	0.14
0.35	0.14	0.15	0.17	0.19
0.60	0.15	0.17	0.19	0.20
1.00	0.16	0.16	0.20	0.22
1.50	0.16	0.16	0.20	0.22

[a] Based on values for BET SSA as shown in Table 3.

CRediT authorship contribution statement

Ran Li: Methodology, Data Curation, Investigation.
Lei Lei: Formal analysis, Visualization, Validation.
TongBo Sui: Recources.
Johann Plank: Conceptualization, Supervision, Writing - Review & Editing.

Declaration of competing interest

The authors declare that they have no known competing financial interests or personal relationships that could have appeared to influence the work reported in this paper.

Acknowledgements

Ran Li wants to show her gratitude to China Scholarship Council (CSC) for financial support of her Ph.D. study at TU München. The authors like to thank Prof. Thienel had his team from the Institute for Construction Materials of Universität der Bundeswehr München (Germany) for the mineralogical quantification of the raw and calcined clays.

References

[1] M. Schneider, M. Romer, M. Tschudin, H. Bolio, Sustainable cement production—present and future, Cem. Concr. Res. 41 (2011) 642–650.
[2] E. Benhelal, G. Zahedi, E. Shamsaei, A. Bahadori, Global strategies and potentials to curb CO_2 emissions in cement industry, J. Clean. Prod. 51 (2013) 142–161.
[3] S.A. Miller, V.M. John, S.A. Pacca, A. Horvath, Carbon dioxide reduction potential in the global cement industry by 2050, Cem. Concr. Res. 114 (2018) 115–124.
[4] S.A. Miller, A. Horvath, P.J.M. Monteiro, Readily implementable techniques can cut annual CO2 emissions from the production of concrete by over 20%, Environmental Research Letters 11 (2016).
[5] International Energy Agency and The Cement Sustainability Initiative, Technology Roadmap: Low-Carbon Transition in the Cement Industry, Paris, 2018, p. 61.
[6] E. Gartner, T. Sui, Alternative cement clinkers, Cem. Concr. Res. 114 (2018) 27–39.
[7] J.L. Provis, Alkali-activated materials, Cem. Concr. Res. 114 (2018) 40–48.
[8] M.H. Samarakoon, P.G. Ranjith, T.D. Rathnaweera, M.S.A. Perera, Recent advances in alkaline cement binders: a review, J. Clean. Prod. 227 (2019) 70–87.
[9] T. Link, F. Bellmann, H.M. Ludwig, M. Ben Haha, Reactivity and phase composition of Ca_2SiO_4 binders made by annealing of alpha-dicalcium silicate hydrate, Cem. Concr. Res. 67 (2015) 131–137.
[10] M. Zajac, J. Skibsted, P. Durdzinski, F. Bullerjahn, J. Skocek, M. Ben Haha, Kinetics of enforced carbonation of cement paste, Cem. Concr. Res. 131 (2020) 106013.
[11] M. Zajac, J. Skibsted, J. Skocek, P. Durdzinski, F. Bullerjahn, M. Ben Haha, Phase assemblage and microstructure of cement paste subjected to enforced, wet carbonation, Cem. Concr. Res. 130 (2020) 105990.
[12] P. Suraneni, A. Hajibabaee, S. Ramanathan, Y. Wang, J. Weiss, New insights from reactivity testing of supplementary cementitious materials, Cem. Concr. Compos. 103 (2019) 331–338.
[13] S. Samad, A. Shah, Role of binary cement in production of environmentally sustainable concrete: a critical review, Int. J. Sustain. Built Environ. 6 (2017) 663–674.
[14] R.E. Rodríguez-Camacho, R. Uribe-Afif, Importance of using the natural pozzolans on concrete durability, Cement and Concrete Research 32 (2002) 1851–1858.
[15] K. Scrivener, F. Martirena, S. Bishnoi, S. Maity, Calcined clay limestone cements (LC^3), Cem. Concr. Res. 114 (2018) 49–56.
[16] R. Fernandez, F. Martirena, K. Scrivener, The origin of the pozzolanic activity of calcined clay minerals: a comparison between kaolinite, illite and montmorillonite, Cem. Concr. Res. 41 (2011) 113–122.
[17] S. Hollanders, R. Adriaens, J. Skibsted, Ö. Cizer, J. Elsen, Pozzolanic reactivity of pure calcined clays, Appl. Clay Sci. 132-133 (2016) 552–560.
[18] O. Akhlaghi, T. Aytas, B. Tatli, D. Sezer, A. Hodaei, A. Favier, K. Scrivener, Y. Z. Menceloglu, O. Akbulut, Modified poly(carboxylate ether)-based superplasticizer for enhanced flowability of calcined clay-limestone-gypsum blended Portland cement, Cem. Concr. Res. 101 (2017) 114–122.
[19] M. Schmid, N. Beuntner, K.C. Thienel, J. Plank, Amphoteric Superplasticizers for Cements Blended with a Calcined Clay, ACI Symposium Publication 12th International Conference on Superplasticizers and Other Chemical Admixtures in Concrete, American Concrete Institute, Beijing, China, 2018, pp. 41–54.
[20] M. Catti, G. Ferraris, G. Ivaldi, Thermal strain analysis in the crystal structure of muscovite at 700 °C, Eur. J. Mineral. 1 (1989) 625–632.
[21] J.A.F. Gamelas, E. Ferraz, F. Rocha, An insight into the surface properties of calcined kaolinitic clays: the grinding effect, Colloids Surf. A Physicochem. Eng. Asp. 455 (2014) 49–57.
[22] J. Plank, K. Pöllmann, N. Zouaoui, P.R. Andres, C. Schaefer, Synthesis and performance of methacrylic ester based polycarboxylate superplasticizers possessing hydroxy terminated poly(ethylene glycol) side chains, Cem. Concr. Res. 38 (2008) 1210–1216.
[23] A. Habbaba, J. Plank, Surface chemistry of ground granulated blast furnace slag in cement pore solution and its impact on the effectiveness of polycarboxylate superplasticizers, J. Am. Ceram. Soc. 95 (2012) 768–775.
[24] DIN EN 1015-3:2007-5, Methods of Test for Mortar for Masonry -Part 3: Determination of Consistence of Fresh Mortar, DIN, Berlin/Germany, 2007.
[25] L. Lei, J. Plank, A study on the impact of different clay minerals on the dispersing force of conventional and modified vinyl ether based polycarboxylate superplasticizers, Cem. Concr. Res. 60 (2014) 1–10.
[26] J. Plank, C. Hirsch, Impact of zeta potential of early cement hydration phases on superplasticizer adsorption, Cem. Concr. Res. 37 (2007) 537–542.
[27] B. Derjaguin, L. Landau, Theory of the stability of strongly charged lyophobic sols and of the adhesion of strongly charged particles in solutions of electrolytes, Prog. Surf. Sci. 43 (1993) 30–59.
[28] E. Verwey, T. Overbeek, Theory of the stability of lyophobic colloids, The Journal of Physical and Colloid Chemistry 51 (1947) 631–636.
[29] S. Mantellato, M. Palacios, R.J. Flatt, Relating early hydration, specific surface and flow loss of cement pastes, Mater. Struct. 52 (2019) 5.
[30] S. Mantellato, R.J. Flatt, Shifting factor-a new paradigm for studying the rheology of cementitious suspensions, J. Am. Ceram. Soc. 103 (2020) 3562–3574.
[31] A. Lange, J. Plank, Contribution of non-adsorbing polymers to cement dispersion, Cem. Concr. Res. 79 (2016) 131–136.
[32] J. Bujdák, Effect of the layer charge of clay minerals on optical properties of organic dyes. A review, Appl. Clay Sci. 34 (2006) 58–73.

Section 5.2

Publication # 2

Approaches to achieve fluidity retention in low-carbon calcined clay blended cements

R. Li, L. Lei, T. Sui, J. Plank

Journal of Cleaner Production (IF = 11.1)

311 (2021) 127770

DOI: 10.1016/j.jclepro.2021.127770

In publication # 1, the initial fluidity of PCE superplasticizers in calcined clay blended cements was discussed. In real application, however, the slump retention behavior of concrete presents a most critical property for the ready-mix concrete industry. Therefore, in the next step (**publication # 2**) the study was focused on improving the **slump retention behavior in calcined clay blended cements**.

Again, a calcined clay sample provided from Sinoma/China with a meta kaolin content of 51 % was applied. Several approaches to achieve slump retention in mortars prepared from composite cements holding 20 – 40 wt.% of the calcined clay were investigated. First, a common industrial ready-mix type HPEG PCE was employed. The tests revealed that the addition of **calcined clay increases the PCE dosages** and significantly **deteriorates fluidity retention**. Furthermore, a combination of the ready-mix HPEG PCE and a retarder (sodium gluconate) which is commonly applied in the concrete industry was investigated. It was found that also this combination does not work well in improving fluidity retention in such composite cements. The results highlight the **difficulty of achieving slump retention for such low carbon binders**. To solve this problem, a new admixture formulation combining the precast type HPEG PCE and a **novel PCE-LDH** nanocomposite was developed and tested. Mortar tests confirmed that this combination **produces long fluidity retention** in such calcined clay blended cements.

A pore solution analysis revealed that the PCE-LDH nanocomposite releases

the PCE superplasticizer gradually via progressive anion exchange with sulfate anions present in the pore solution. This way, an extended workability time was achieved in the mortar.

The anion exchange process which presents the working mechanism of the LDH-PCE is illustrated in **Figure 18**.

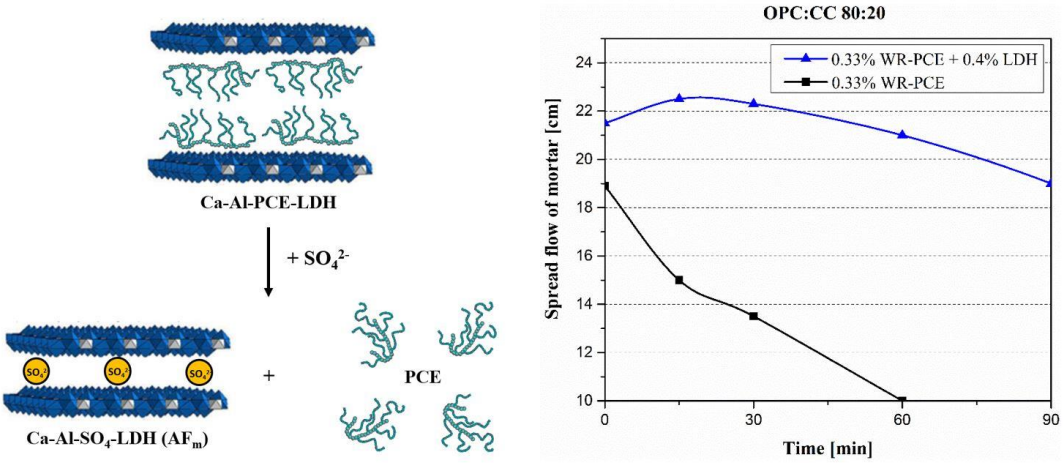

Figure 18. Illustration of the working mechanism of the newly designed LDH-PCE nanocomposite in calcined clay blended cement.

Journal of Cleaner Production 311 (2021) 127770

Contents lists available at ScienceDirect

Journal of Cleaner Production

journal homepage: www.elsevier.com/locate/jclepro

Approaches to achieve fluidity retention in low-carbon calcined clay blended cements

Ran Li [a], Lei Lei [a], Tongbo Sui [b], Johann Plank [a,*]

[a] Technische Universität München, Chair for Construction Chemistry, 85747, Garching, Lichtenbergstraße 4, Germany
[b] Sinoma Research Institute, Sinoma International Engineering Co., Ltd, No. 16 Wangjing North Road, Chaoyang District, Beijing, 100102, China

ARTICLE INFO

Handling editor: Zhen Leng

Keywords:
Low carbon cement
Calcined clay
Polycarboxylate (PCE)
Superplasticizer
Fluidity retention
LDH nanocomposite

ABSTRACT

High meta kaolin content (e.g. 50 wt%) present in a calcined clay blended into a composite cement is positive with respect to early strength development, but significantly decreases the dispersing effectiveness of PCE superplasticizers. Moreover, it has been observed that for such cements, slump retention is much more difficult to achieve than in OPC or other composite cements. In this study, several approaches to achieve extended workability times in mortars prepared from composite cements holding 20–40 wt % of a calcined clay were investigated. First, it was found that the slump retaining performance of a common industrial ready-mix type HPEG PCE rapidly decreased when the portion of calcined clay was increased in the blended cement. Furthermore, a combination of the ready-mix HPEG PCE and a retarder (sodium gluconate) which is commonly applied in ready-mix concrete also could not much improve fluidity retention, thus highlighting the difficulty of slump retention for such cements. To solve this problem, a new admixture formulation is introduced based on a combination of a precast type HPEG PCE and a novel PCE-LDH nanocomposite. This approach to improve slump retention was tested on composite cements holding 20–40 wt % of a calcined clay high in meta kaolin content. Mortar tests revealed that the high water-reducing (precast) type HPEG PCE and the PCE-LDH nanocomposite work synergistically and can achieve a significant improvement in fluidity retention of such calcined clay blended cements. A mechanistic investigation revealed that the PCE which was intercalated in between the $[Ca_2Al(OH)_6]^+$ main layers of the PCE-LDH nanocomposite is released gradually from the mixed metal hydroxide via anionic exchange with sulfate anions present in the pore solution. This way, an extended workability time was achieved in the mortar.

1. Introduction

Green construction materials are drawing an increasing attention because of global warming and climate change which is attributed to anthropogenic carbon dioxide (CO_2) emissions. It is reported that the cement industry contributes ~8% of the total global man-made CO_2 release (Andrew, 2018). In the production of Portland cement, around 65% of the CO_2 liberated results from the decomposition of $CaCO_3$ while the remainder originates from energy consumption in the clinkerization and milling processes (OECD/IEA and CSI, 2018). Thus, supplementary cementitious materials (SCMs) (Gartner and Sui, 2018) and alternative binders (Samarakoon et al., 2019; Shi et al., 2019) are receiving more interest to achieve greener cements and a more sustainable concrete production. Currently, in real applications, the most widely used SCMs include limestone, fly ash and slag (Scrivener et al., 2018). However, global availability of fly ash and slag is limited and therefore cannot solve the problem of excessive CO_2 emission from cement production.

Nowadays, calcined clay is attracting growing attention as an alternative SCM due to the global abundance of clay. The temperatures required for the calcination of raw clays range from 600 to 900 °C (Hollanders et al., 2016) which is much lower than in Portland cement production which occurs at ~ 1450 °C. Therefore, the production of calcined clay liberates much less CO_2, also because it does not include the decomposition of significant amounts of limestone.

The dehydroxylation process occurring in the thermal treatment of the clay minerals results in a partial collapse of their crystal lattice structure, forming a mostly amorphous transition phase of high pozzolanic reactivity (Sabir et al., 2001). Meta kaolin in particular possesses a superior pozzolanic reactivity which is highly beneficial for early strength development (Fernandez et al., 2011). It is owed to a chemical

* Corresponding author.
E-mail address: sekretariat@bauchemie.ch.tum.de (J. Plank).

https://doi.org/10.1016/j.jclepro.2021.127770
Received 18 December 2020; Received in revised form 22 April 2021; Accepted 30 May 2021
Available online 2 June 2021

reaction between the amorphous meta kaolin (Al_2O_3•$2SiO_2$) and calcium hydroxide resulting in a C-A-S-H gel (Antoni et al., 2012). Moreover, it has been reported that a specifically composed meta kaolin blended cement can produce an even higher compressive strength than an ordinary Portland cement sample at all ages (Tironi et al., 2014).

Unfortunately, the high specific surface area and the considerable internal porosity of individual calcined clays can lead to poor workability. As a consequence, much higher superplasticizer dosages are required for initial dispersion when increased contents of calcined clay are present in blended cements (Li et al., 2021; Schmid and Plank, 2020). This negative effect is most pronounced when the calcined clay incorporates a high meta kaolin content. Moreover, in actual application it has been observed that fluidity retention which presents a key requirement for ready-mix concrete is much more difficult to achieve in calcined clay blended cements than in OPC.

At present, several technologies are employed to achieve fluidity retention in Portland cement-based concretes: (1) Historically, the first concept included a combination of the superplasticizer with a retarder, e. g. sodium gluconate, molasse, anhydro glucose or lignosulfonates containing sugars etc (Bishop and Barron, 2006; Huang et al., 2020; Juenger and Jennings, 2002; Nalet and Nonat, 2016; Rixom et al., 1999). This concept became particularly popular when polycondensate-based superplasticizers such as BNS or melamine sulfonate were used (Li et al., 2012). Through this combination, fluidity retention was achieved via hydration retardation (especially ettringite formation) (Bishop and Barron, 2006; Cheung et al., 2011). However, the disadvantage of this approach was decreased early strength. (2) In the 1990s, the concept of slump retention achieved via slowly adsorbing PCE superplasticizers characterized by high side chain density and low amount of carboxylate functionalities in the backbone was introduced (Yamada et al., 2000). They achieve extended workability times via gradual adsorption onto the cement particles, without negative effect on the early strength development. (3) This concept was further improved by the incorporation of hydrolyzing esters into the structure of such PCEs. Common examples of such esters include hydroxyethyl acrylate (HEA), hydroxypropyl acrylate (HPA), 2-hydroxyethyl methacrylate (HEMA), 3-hydroxypropyl methacrylate (HPMA), 4-hydroxybutyl methacrylate (HBMA) and monomethyl maleate (MMM). These esters produce additional carboxylate groups during their hydrolysis in the highly alkaline pore solution of cement and thus continuously produce PCE molecules which now are able to adsorb onto cement and provide dispersion (Tahara et al., 1995; Tanaka et al., 2001). (4) A more simple approach comprises delayed addition of polycarboxylate. It prevents the formation of early nanoscale ettringite which immediately consumes the entire dosage of the PCE polymer via instantaneous adsorption (Lange et al., 2015). (5) Finally, encapsulation of the dry superplasticizer powder particles via polyvinyl alcohol (PVA) coating or packaging of the admixture in water-soluble PVA bags (Laramay and Lavene, 2012) which are added to the rotating container of the concrete truck were proposed and are commercially applied, e.g. in the U.S.

Inspired from the encapsulation and delayed addition methods mentioned above, the intercalation (“chemical packaging”) of PCE superplasticizers into layered double hydroxides (LDHs) was considered as a promising new approach to improve fluidity retention in calcined clay blended cements. For this purpose, PCE-LDH nanocomposites were synthesized via hydration of tricalcium aluminate (C_3A) in the presence of PCEs. The resulting nanocomposites ($[CaAl(OH)_6]^+$ (PCE) • nH_2O) were then tested with respect to their post-release property of the PCE molecules via anion exchange with the sulfate from the pore solution. It was hoped to achieve fluidity retention through this mechanism, and their effectiveness was compared with that of common slump retaining PCEs used in ready-mix concrete.

For the experiments, a low-carbon calcined clay blended cement (clinker factor 0.6–1.0) was utilized. The calcined clay sample incorporated a high meta kaolin content (~50 wt %) which rendered the cement to become rather difficult to disperse. In order to probe into slump retention, at first the effect of a conventional industrial ready-mix type PCE known for its superior workability retention in OPC was tested individually and in combination with a retarder (sodium gluconate). The tests were performed in mortars based on neat OPC or an OPC:CC 70:30 blend. In the next step, the combination of a commercial precast type PCE and the novel PCE-LDH nanocomposite which was designed such as to provide slump retention was tested in composite cements holding 20–40 wt % of the calcined clay. By including such commercial PCEs into our study we hoped to gain insight into how common industrial admixtures will behave in such low-carbon calcined clay blended cements. Moreover, the PCE-LDH nanocomposite was studied to elucidate whether it could solve the urgent problem of inadequate slump retention in calcined clay blended cements. Finally, the mechanism of fluidity retention achieved by the HPEG PCE and the novel PCE-LDH nanocomposite was examined via adsorption measurements.

2. Materials and methods

2.1. Cement and calcined clay samples

The ordinary Portland cement sample (CEM I 42.5R) was provided by Schwenk cement company (Allmendingen plant, Germany). Its phase composition as determined via Q-XRD including *Rietveld* refinement is shown in Table 1.

This cement exhibits a density of 3.13 g cm^{-3} (Helium pycnometry) and a d_{50} value of 18.13 μm (laser granulometer, Cilas 1064, Cilas Company, Marseille, France). Moreover, its oxide composition is listed in Table 2.

The calcined clay used in this investigation was obtained from Sinoma International Engineering Co., Beijing, China. It was produced via calcination in an industrial-scale rotary kiln at 800 °C (exposure time 1 h) and possesses a relatively high specific surface area (BET method, N_2) of 13.2 m^2/g, as compared to ~ 1 m^2/g only for the cement sample. Its mineralogical composition as determined by quantitative XRD measurements is shown in Table 3. The sample is characterized by a high amorphous content of ~62 wt %, and a high content of meta kaolin (~50 wt %), as is suggested by the kaolinite content present in the raw clay. Furthermore, an appreciable amount of the high temperature modification of muscovite, ~18 wt % were detected.

2.2. Admixtures

2.2.1. Superplasticizers

A commercial ready-mix type HPEG-based PCE from JILIN Chemical Industrial, Jilin, China which contains a mixture of hydrolyzing hydroxyethyl and hydroxyl propyl acrylate ester was employed

Table 1
Phase composition of the cement sample CEM I 42.5 R used in the study.

Phase	wt. %
C_3S, monoclinic	59.55
C_2S, monoclinic	11.08
C_4AF, orthorhombic	10.07
C_3A, cubic	4.88
C_3A, orthorhombic	2.06
Anhydrite ($CaSO_4$)	2.59
Dihydrate ($CaSO_4$• $2H_2O$)	3.09
Hemihydrate ($CaSO_4$• $0.5H_2O$)	0.10
Calcite ($CaCO_3$)	2.34
Dolomite ($CaMg(CO_3)_2$)	0.97
Periclase (MgO)	0.53
Portlandite ($Ca(OH)_2$)	0.78
Arcanite (K_2SO_4)	0.22
Quartz (SiO_2)	0.42
Free lime (*Franke*)	1.32
Total	100.00

Table 2
Oxide composition of the CEM I 42.5 R sample as determined by XRF.

Oxide	wt. %
SiO_2	20.12
Al_2O_3	5.34
Fe_2O_3	2.98
CaO	61.38
MgO	1.70
SO_3	3.65
K_2O	0.73
Na_2O	0.11
TiO_2	0.37
P_2O_6	0.41
MnO	˂ 0.1
SrO	˂ 0.1
ZnO	˂ 0.1
BaO	0.17
Total	97.83

Table 3
Mineralogical composition of the raw and the calcined clay samples, as determined by XRD including *Rietveld* refinement.

Mineral phase	Raw clay (wt. %)	Calcined clay (wt. %)
Kaolinite	51.3	–
Illite - Smectite	19.7	–
Muscovite	18.1	5.2
Quartz	10.3	13.8
Rutile	0.5	0.3
Muscovite HT [a]	–	18.6
Amorphous	–	62.2
Total	99.9	100.1

[a] Muscovite HT presents a well-defined high-temperature modification characterized by an expanded K interlayer region (Catti et al., 1989).

representing an industry standard among slump retaining PCEs. Its chemical formula is presented in Fig. 1. This polymer exhibits a specific anionic charge amount of 915 μeq/g which is relatively low, thus signifying a high ester content.

Additionally, an industrial precast-type HPEG PCE (also supplied by JILIN Chemical Industrial, Jilin, China) which is designed such as to provide high initial fluidity (the so-called "high water-reducing" type, WR PCE) was used. Its specific anionic charge amount in 0.1 M NaOH was found at 1805 μeq/g, thus signifying a particularly high anionicity as is characteristic for precast type PCEs.

Furthermore, in the synthesis of the PCE-LDH nanocomposite (see Section 2.4.1) a methacrylic ester (MPEG) type PCE comprised of methacrylic acid and ω-methoxy polyethylene glycol methacrylate ester macromonomer (n_{EO} = 45) at a molar ratio of 6: 1 was utilized. Its preparation is described in detail in (Plank and Pöllmann, 2008). This polymer (henceforth designated as "45PC6") was self-synthesized and its characteristics is high water-reducing ability which classifies it as a typical PCE admixture for precast concrete.

2.2.2. Retarder

As retarder, sodium gluconate (>99% purity) supplied by China Academy of Building Research (CABR, Beijing) was applied.

2.3. Ca–Al-LDH nanocomposite

2.3.1. Synthesis of Ca–Al-PCE-LDH nanocomposite

The Ca–Al-PCE-LDH nanocomposite was prepared via rehydration of C_3A as described in (Plank et al., 2010). Tricalcium aluminate was obtained via a sol–gel process followed by calcination for 14 h at 1260 °C, with two intermediate grinding steps (Plank and Dai, 2008; Stephan and Wilhelm, 2004). In synthesis, the self-prepared methacrylate ester (MPEG) PCE 45PC6 was dissolved at a concentration of 2.5 wt % in 500 mL of deionized water. Then, 12.5 g of C_3A were added and the suspension was stirred at room temperature for 70 h under a nitrogen flow to avoid carbonation. After an aging time of 1 day, the PCE-LDH nanocomposite was separated via centrifugation at 8500 rpm for 10 min and washed 3 times with deionized water to remove residual, non-intercalated PCE polymer. Finally, the solid was freeze dried for 24 h and applied as such in the tests. For comparison, a Ca–Al–OH-LDH sample was prepared by the reaction of C_3A in deionized water following the same steps as for the PCE-LDH sample except that no PCE was present.

2.3.2. Characterization of Ca–Al-A^--LDH nanocomposites

Characterization of the synthesized Ca–Al-A^--LDH samples (A^- = PCE or OH^-) was performed via X-ray powder diffraction using a Bruker AXS D8 Advance diffractometer (Bruker, Karlsruhe, Germany). The structural build-up of the PCE-LDH nanocomposite was observed via transmission electron microscopy (TEM), with images captured on a JEOL JEM 2011 (JEOL, Japan) microscope equipped with a LaB6 cathode. In preparation, the LDH sample was dissolved in isopropanol and then sonicated for 2 min before being dropped on a plasma surface-treated 300 mesh Cu grid with carbon support films (Quantifoil Micro Tools GmbH, Germany).

2.4. Mortar testing

The time-dependent dispersing performance of the admixtures was ascertained via mortar tests following DIN EN 196-1 standard. For all mortar samples, the water-to-binder ratio (w/b) and the binder-to-sand ratio were fixed at 0.4 and 3:1, respectively. The mixing procedure was

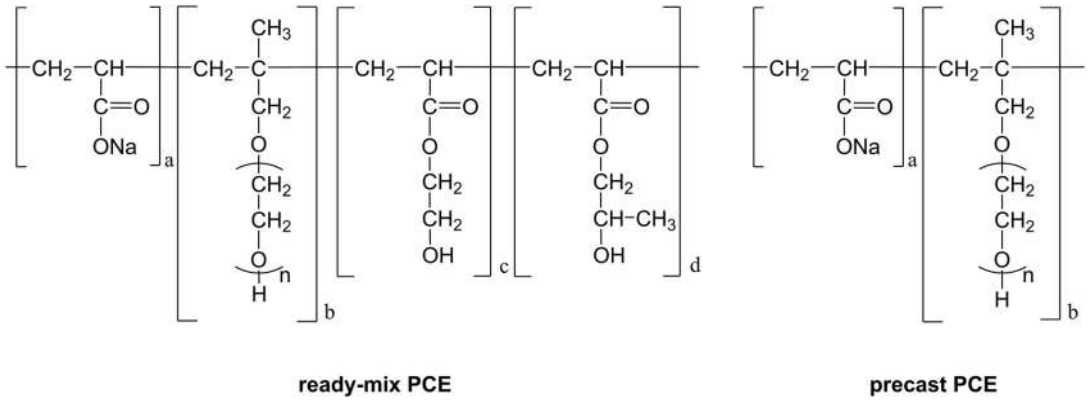

Fig. 1. Chemical structures of the HPEG PCE superplasticizer samples used in the study.

as follows: First, 450 g of OPC (or OPC/CC composite binder) were added to a mixing bowl containing 180 g of DI water holding different dosages of dissolved PCE or PCE/retarder combinations. In tests involving the PCE-LDH nanocomposite, this admixture was dry-blended with the binder first. Additionally, 1 drop of a defoamer (Surfynol MD-20, Air Products, the Netherlands) was added to prevent any air entrainment by the PCE. Immediately after the binder had been added, the mixer (Toni Technik, Berlin, Germany) was started for 30 s at a mixing speed of 140 rpm. Next, norm sand according to DIN EN 196-1 was dropped in to the mixture within 30 s while stirring at the same speed. When addition was complete, the mortar was mixed at 285 rpm for another 30 s. During a 90 s pause, a spoon was used to scrape the mortar from the bowl edges to ensure homogeneity. Then the mixing was continued at 285 rpm for another 60 s. When the mixing process was finished, the mortar was filled into a Hägermann cone (height 60 mm, top diameter 70 mm, bottom diameter 100 mm) which was placed on a spread flow table (FORM + TEST, Riedlingen, Germany). Followed by 15 shocks the spread flow was measured vertically twice using a caliper and the averaged value was taken as the final result. Time-dependent spread flow measurements were taken every 15 min (Fig. 8) or 30 min all other tests after mixing. After each measurement, the mortar was transferred back to the mixing bowl and covered with a wet towel to avoid desiccation. Prior to each spread flow test, the cement mortar was stirred for 2 min at a speed of 285 rpm.

2.5. Adsorption measurements

Superplasticizer adsorption on neat cement and neat calcined clay were determined according to the depletion method based on total organic carbon (TOC) analysis. At each polymer concentration, the amount of polymer remaining in the fluid phase (water or the pore solution) at equilibrium condition before and after contact with cement or calcined clay was captured. In a typical experiment, 16 g of solids were dispersed in water or cement pore solution at a certain water-to-binder ratio (see Table 4) which in the mini slump test produced a paste spread flow value of ~18 ± 0.5 cm. Next, the mixture was homogenized using a wobbler (VWR Inter-national, Darmstadt, Germany) for 2 min at 2400 rpm and then separated by a centrifuge (Primo R, Thermo Scientific Heraeus, Germany) for 10 min at 8500 rpm. A LiquiTOC analyzer (Elementar, Hanau, Germany) was utilized to determine the organic carbon content in the supernatant collected from centrifugation. The amount of polymer adsorbed was then calculated from the carbon content present in the filtrate and the carbon content introduced by the respective polymer which initially was dissolved in the mixing water. Each sample was measured twice.

In the tests capturing the time-dependent adsorption of PCE released from the PCE-LDH nanocomposite, the water-to-binder ratio for the OPC:CC 70:30 blend was settled as 0.82 (see Table 4). Here, 0.6 g of the PCE-LDH nanocomposites were added to 123 g of synthetic cement pore solution (hereafter abbreviated as SCPS) which contained 1.72 g of $CaSO_4{\cdot}2H_2O$, 6.959 g of Na_2SO_4, 4.757 g of K_2SO_4 and 7.12 g of KOH dissolved in 1 L of deionized water. The PCE-LDH suspension in SCPS was stirred, and after 2, 15, 30, 45, 60, 90, 120 and 150 min 12 mL were pulled from the suspension and filtered through a 0.2 μm polyethersulfone syringe filter. From 1 g of each filtered solution the carbon amount released from the PCE-LDH nanocomposite was quantified and calculated as amount of PCE liberated over time. Furthermore, 10 g of the OPC:CC 70:30 blend were suspended in 8.2 g of the filtered solution and shaken in a wobbler. After centrifugation at 8500 rpm for 10 min, the supernatant was collected and the carbon content present in the filtrate of the binder suspension was measured via TOC as a function of time. From the difference between the amount of PCE liberated from the PCE-LDH at a given time and the amount of PCE which had not adsorbed on the cement, the amount of PCE released from the LDH which sorbed by the composite cements could be calculated.

Table 4
Water-to-binder ratios as determined via mini slump test to achieve a paste spread flow of 18 ± 0.5 cm.

	OPC	Calcined clay	OPC:CC 70:30
Water/SCPS-to-binder ratio	0.5 (water)	1.2 (SCPS)	0.82 (water)

2.6. Isothermal heat flow calorimetry

In order to investigate the effect of the PCE-LDH nanocomposite on the hydration of calcined clay blended cements, heat flow calorimetric measurements were carried out using a TAM Air Calorimeter (TA Instruments, Järfälla, Sweden). For the measurements, 4 g of OPC:CC 70:30 binder with and without 0.4% bwob of PCE-LDH were weighed into 20 mL glass ampoules and mixed with DI water at a water-to-binder ratio of 0.82. Next, the ampoules were capped, homogenized in a wobbler for 2 min and then placed in the calorimeter. Measurements were carried out until the release of heat from the hydration reaction subsided completely.

2.7. Environmental assessment of admixtures

To evaluate the impact of PCE and PCE-LDH on the environment, their CO_2 footprints were determined. For the PCE, a value of 0.0052 kg CO_2 –eq/L as published in (Flower and Sanjayan, 2007) for a standard industrial PCE superplasticizer was taken. Using this number, the CO_2 footprint of PCE-LDH was calculated following the method of (Ügdüler et al., 2020) based on the preparation process as described in section 2.4.1.

3. Results

The investigation was started by assessing the slump retaining effect of a commercial benchmark ready-mix type HPEG PCE with proven workability extension ability in OPC. This admixture was tested on a stand-alone basis and in combination with sodium gluconate, a common auxiliary retarding admixture to prolong workability time. The mortars were prepared either from neat OPC or a low-carbon blended cement holding 20–40 wt % of calcined clay.

3.1. Slump retaining ability of conventional ready-mix PCE

In order to investigate the negative impact of calcined clay on the time-dependent fluidity of mortars admixed with the ready-mix type PCE, its performance in cements holding increasing contents of calcined clay was tested. For this purpose, composite cements blended with up to 40 wt % of calcined clay were probed, and the evolution of mortar fluidity over time was measured.

As is shown in Fig. 2, in neat OPC the ready-mix HPEG PCE produced excellent slump retention over a period of ~90 min, and then fluidity gradually decreased over a period of 2 h until it reached the spread flow value of the non-treated mortar. The mechanism behind the slump retaining effect of this PCE relies on continuously produced carboxylate groups as a result of ester hydrolysis occurring under the highly alkaline conditions of the cement pore solution (Liu et al., 2012).

However, with increasing content of calcined clay in the composite cement, the slump retaining ability of this ready-mix PCE deteriorated steadily. For example, at 20 wt % substitution rate (clinker factor 0.8), fluidity retention lasted only for 60 min as compared to 90 min for the neat OPC sample. Moreover, for the 30 and 40 wt % calcined clay blended cements, workability could be retained for 45 and 30 min only, respectively, thus signifying an extremely negative effect of the calcined clay on fluidity retention. In the 60: 40 OPC/CC blend, even an increase in the dosage of PCE to 0.8% could not remedy the problem. The results signify that when a threshold value of ~20 wt % of this calcined clay in the binder is exceeded, then slump retention becomes a serious issue for

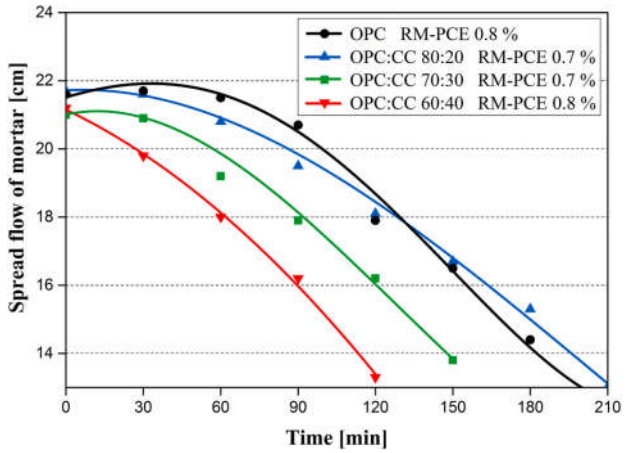

Fig. 2. Fluidity retention of mortars prepared from neat OPC or OPC/CC blends admixed with different dosages of a commercial benchmark ready-mix HPEG PCE (w/b ratio = 0.4).

such concretes, and conventional PCE admixtures fail to solve this problem.

3.2. Slump retention from PCE/sodium gluconate combination

Next, slump retention of a combination of the commercial ready-mix type PCE and sodium gluconate retarder was tested. The results are displayed in Fig. 3. As is shown there, in neat OPC at a dosage of 0.7% of this PCE a spread flow of 19 cm is reached and initial fluidity is maintained for around 60 min. Dosing in of additional 0.03% of sodium gluconate (such addition rate is commonly used in practice) prolonged the fluidity retention time from 60 to ~ 100 min, thus demonstrating the well-known synergistic effect between the PCE and this retarder. Such slump retaining effect of sodium gluconate has been studied extensively before and was found to rely on postponed ettringite formation (Cheung et al., 2011).

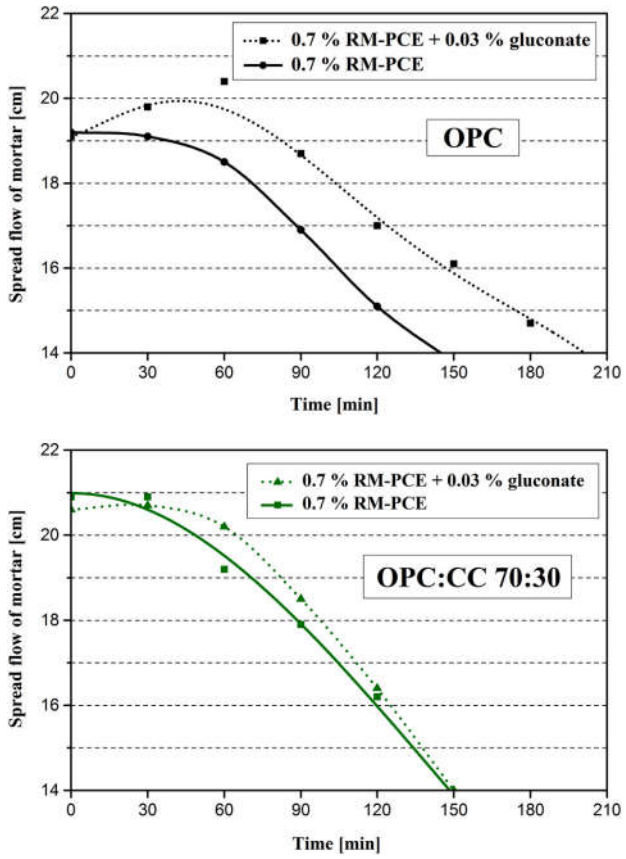

Fig. 3. Fluidity retention of mortars prepared from neat OPC or OPC:CC 70:30 blend admixed with an industrial benchmark ready-mix PCE (RM-PCE), with or without sodium gluconate (w/b ratio = 0.4).

Following those experiments on OPC, the same combination of the ready-mix PCE with sodium gluconate was utilized on the composite cement holding 30 wt % of calcined clay (see Fig. 3). As is evident from there, the presence of calcined clay severely impedes slump retention, for the system based on the individual PCE as well as for the PCE/gluconate combination. Moreover, the effect of sodium gluconate as auxiliary slump retaining admixture is almost completely lost.

The results signify that in calcined clay blended cements fluidity retention is difficult to achieve when using the conventional concepts established on OPC. However, a solution to this problem is crucial to enable a more widespread use of calcined clay blended cements in the future.

3.3. Mechanistic study via adsorption measurements

In order to understand the reason behind the negative impact of calcined clay, adsorption of the ready-mix PCE on neat OPC and neat calcined clay was quantified and compared. Individual adsorption isotherms were developed for both systems prepared at a water-to-cement ratio of 0.5 for OPC and a SCPS-to-solid ratio of 1.2 for the CC. These ratios were chosen because in the mini slump tests they produce a comparable paste spread flow of 18 ± 0.5 cm.

In both suspensions the ready-mix PCE produces *Langmuir* type adsorption isotherms as is displayed in Fig. 4. Significantly higher adsorbed amounts were found for the calcined clay. To be specific, on calcined clay the PCE polymer reached saturated adsorption at 2.6 mg/g binder while it was 1.5 mg/g only on the neat OPC. This finding suggests that the calcined clay sorbs considerably more superplasticizer than OPC. A similar observation has been made for another CC blended cement (Li et al., 2021).

However, as the ready-mix PCE continuously produces carboxylate groups via hydrolysis, it was considered that the time-dependent adsorption of the superplasticizer might be important when evaluating

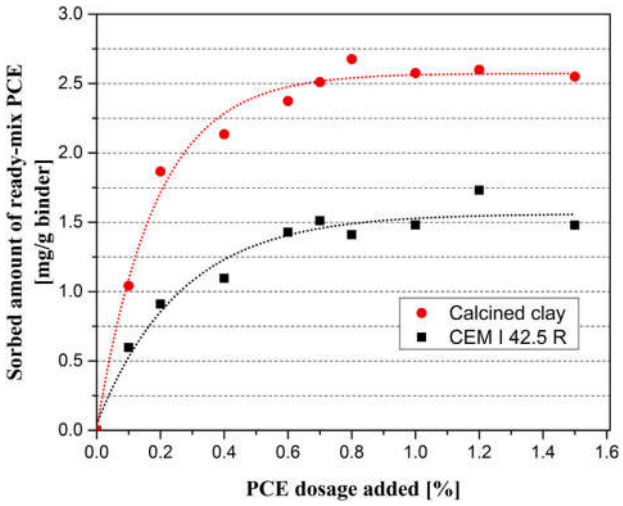

Fig. 4. Adsorption isotherms for the ready-mix HPEG PCE in pastes prepared from neat OPC (w/c = 0.5) and neat calcined clay (SCPS/b = 1.2); values taken 10 min after end of mixing.

slump retention. Consequently, this behavior was measured and the results are displayed in Fig. 5.

Interestingly, in the OPC suspension the adsorbed amount of the PCE increased steadily over time, from ~1.5 to ~3 mg/g after 90 min. This behavior can be attributed to ester hydrolysis of this PCE polymer (see Fig. 1) which occurs in the highly alkaline pore solution. This effect continuously feeds anionic polymer as adsorbate into the system. Apparently, initially a considerable amount of PCE remains dissolved in the pore solution instead of being adsorbed onto the cement grains' surface. Yet, adsorption progresses as more carboxylate groups are produced. Unfortunately, this mechanism only occurs in OPC suspension and not in the calcined clay system. As is shown in Fig. 5, throughout the 2 h test period the amount of HPEG PCE adsorbed on calcined clay remained constant at ~2.5 mg/g which presents the saturated amount adsorbed on calcined clay, as was shown before in Fig. 4.

The findings suggest that the calcined clay immediately takes up all PCE available. It proposes that the PCE exhibits a higher affinity to the surfaces of the calcined clay particles than to those of OPC which explains the higher dosages often required in CC blended cements, especially when high meta kaolin contents are present. This result correlates well with the findings for slump retention as displayed in Fig. 2.

To summarize, the concept of hydrolyzing esters in PCE to achieve slump retention does not work well for binders holding appreciable amounts of calcined clay with high meta kaolin content. It explains why mortar workability decreases with increased contents of this calcined clay.

3.4. Performance of LDH-PCE slump retainer in calcined clay blended cement

According to an earlier study, the hydration of tricalcium aluminate produces layered double hydroxides which have the ability to intercalate anionic superplasticizers in between their $[Ca_2Al(OH)_6]^+$ main layers (Plank and Dai, 2008). In the following, the use of Ca–Al-PCE-LDH hybrid materials is introduced as a new type of slump retainer which captures the PCE in the interlayer region and gradually releases the polymer during cement hydration via anionic exchange with sulfate anions.

3.4.1. Characterization of the synthesized Ca–Al-PCE-LDH nanocomposite

When pure C_3A is hydrated in water, then a mixture of a Ca–Al–OH-LDH (C_4AH_{13}), cubic katoite and a minor amount of monocarbo aluminate $[Ca_4Al_2(OH)_{12}](CO_3)\cdot 8H_2O$ (another LDH compound formed from the uptake of carbon dioxide during hydration) can be identified, as is evidenced in the X-ray diffraction patterns of freshly rehydrated C_3A (Fig. 6).

Whereas, the Ca–Al-PCE-LDH synthesized from an MPEG PCE (45PC6) and C_3A is characterized by a strong reflection occurring at low 2θ angle (~2.7°) which signifies successful formation of the PCE-LDH, with an interlayer distance of ~3.0 nm (Plank and Dai, 2008). Additionally, C_4AH_{13} was recorded as a minor by-product. Furthermore, a shoulder is observed at ~4.8° 2θ which represents an intercalation product exhibiting a *d* value of 1.8 nm. Presumably, this reflection can be attributed to impurities such as polymethacrylate present in the PCE polymer (Plank et al., 2010).

The layered structure of the synthesized Ca–Al-PCE-LDH intercalation compound was verified by TEM, as is shown on the image displayed in Fig. 7. Clearly stacked layers are observed, whereby the dark layers represent the skeleton of the inorganic $[Ca_2Al(OH)_6]^+$ main layer while the light areas correspond to the organic interlayer harboring the PCE. Thus, analysis confirmed successful formation of the organic-inorganic hybrid material.

3.4.2. Fluidity retention performance of the PCE-LDH nanocomposite

In the following, the fluidity retaining ability of the PCE-LDH nanocomposite was assessed via mortar testing. As the PCE-LDH cannot provide instant fluidity, a high water reducing type PCE was combined with this admixture to generate the initial dispersion. More specific, a commercially available precast type HPEG PCE was applied to provide this effect. For this purpose, mortars prepared from neat OPC and three different composite cements (OPC:CC 80:20, 70:30 and 60:40 wt/wt. %) were fluidized with the respective dosage of the HPEG water-reducing admixture to ensure an initial spread flow of 19 ± 0.5 cm.

Time-dependent recording of mortar fluidity revealed that, as expected, this kind of PCE provided high initial fluidity at low dosage (0.28% in OPC), but was unable to maintain sufficient workability over time (see Fig. 8). This negative trend became even worse at increased contents of calcined clay, as is evident from Fig. 8. Thus, in order to improve slump retention, the mortars holding the WR PCE were additionally treated with 0.4% of the PCE-LDH nanocomposite, and the time-dependent fluidity was recorded every half hour. The result is displayed in Fig. 9.

From a comparison of Figs. 8 and 9 it is evident that a combination of the WR PCE and the PCE-LDH nanocomposite substantially improves fluidity retention across all systems. Apparently, the PCE-LDH hybrid admixture can effectively prolong workability times.

A closer analysis of the data presented in Fig. 9 reveals that – much

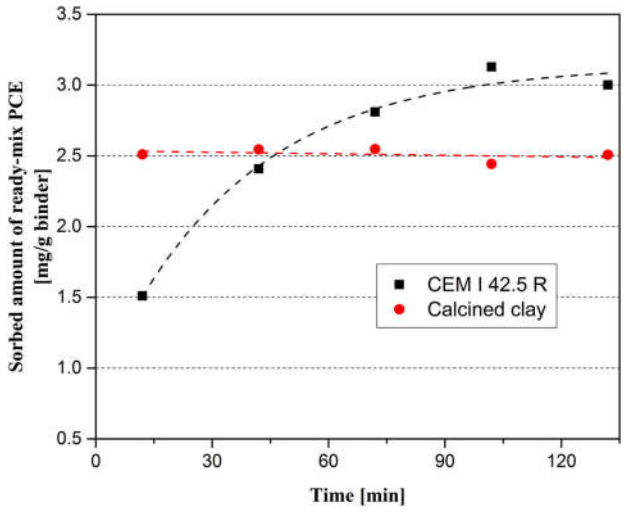

Fig. 5. Time-dependent adsorption behavior of the ready-mix HPEG PCE (0.7% dosage) on neat OPC (w/c = 0.5) or neat calcined clay (SCPS/b = 1.2), values taken 10 min after end of mixing.

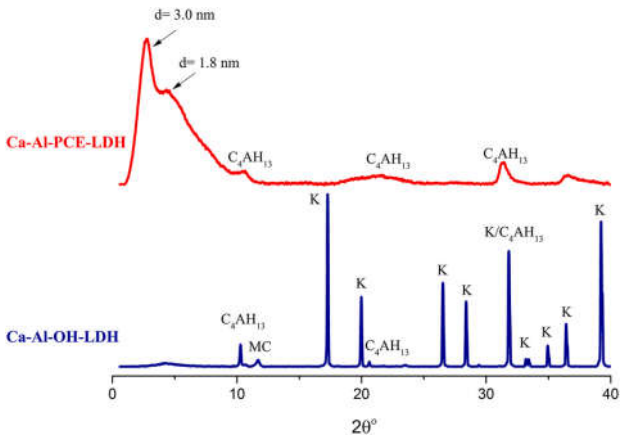

Fig. 6. X-ray diffraction patterns for the rehydrated C_3A (Ca–Al–OH-LDH) and the synthesized Ca–Al-PCE-LDH nanocomposite (K = katoite, MC = monocalcium aluminate).

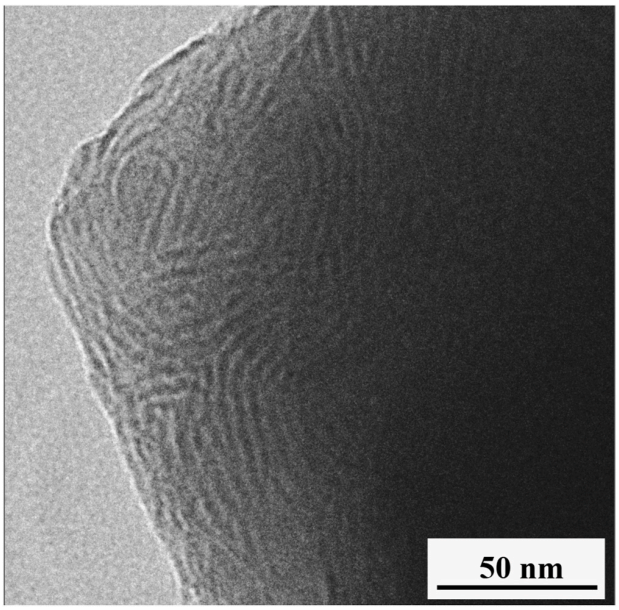

Fig. 7. TEM image of the synthesized Ca–Al-PCE-LDH nanocomposite.

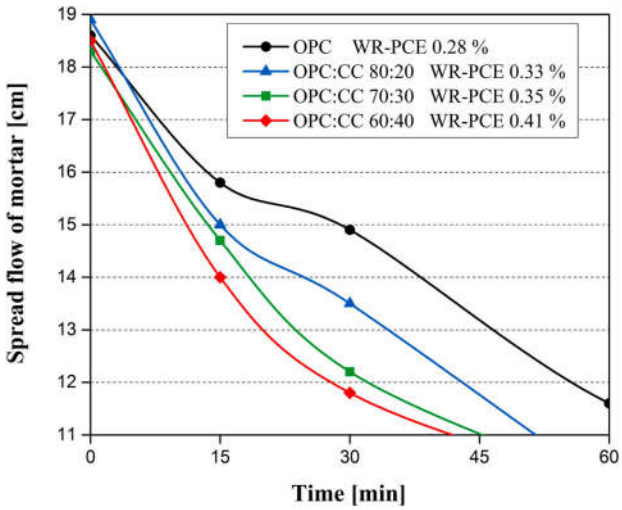

Fig. 8. Time-dependent fluidity of mortars prepared from neat OPC and OPC/CC blended cements, admixed with different dosages of the water-reducing PCE (WR-PCE).

surprisingly– addition of the PCE-LDH slump retainer to the 80:20 cement blend allows to achieve comparable slump retention as in the OPC mortar. At increased clinker substitution rates, effectiveness of the PCE-LDH admixture gradually diminishes. However, at the lowest clinker factor studied of 0.6, workability is still retained for ~45 min which is far superior over the performance of a standard commercial ready-mix type PCE (see Fig. 10). Moreover, an increased dosage of PCE-LDH (0.9%) allows to extend the workability time even for this demanding 60:40 system to ~ 90 min. Thus, it is demonstrated that the nanocomposite enables to reach slump retention times which are much superior over those achieved with conventional industrial products representing the current state-of-art.

The results signify that the combination of a WR-type HPEG PCE and a PCE-LDH nanocomposite can successfully overcome the fluidity retention problem caused by the addition of calcined clay to cement.

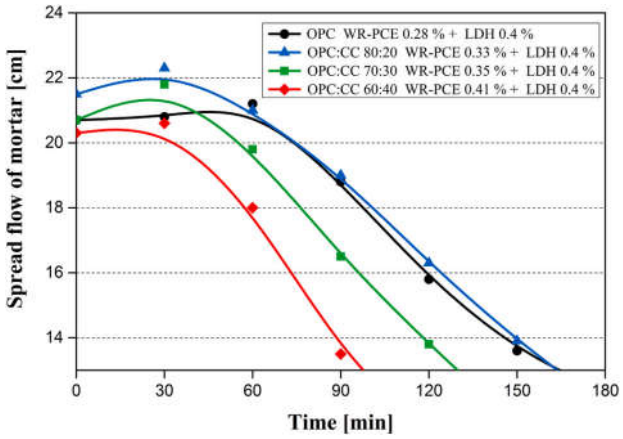

Fig. 9. Fluidity retention of mortars prepared from neat OPC or OPC/CC blends admixed with a WR-PCE and Ca–Al-PCE-LDH nanocomposite; w/b ratio = 0.4.

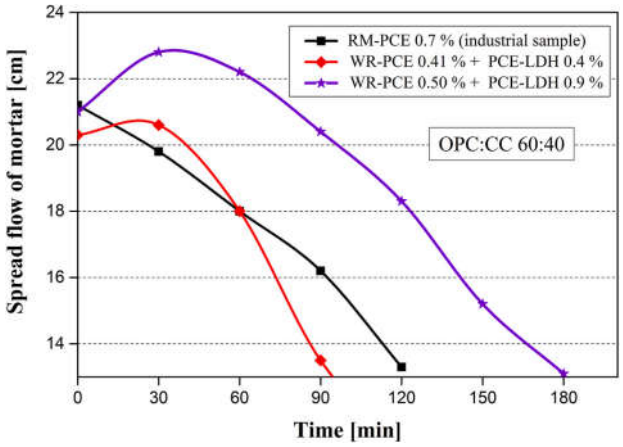

Fig. 10. Fluidity retention of mortars (w/b ratio = 0.4) achieved in the OPC:CC 60:40 blend when admixed with different PCE products.

3.4.3. *Working mechanism of the PCE-LDH slump retainer*

To obtain more insight into the working mechanism of the PCE-LDH nanocomposite, the amount of free dissolved PCE released from the LDH into the pore solution was captured via total organic carbon (TOC) analysis. For this purpose, the synthesized PCE-LDH sample was suspended in cement pore solution, from there samples were pulled at 2–150 min intervals after initial mixing, and the amount of PCE released from the nanocomposite over time was determined. The results are displayed in Fig. 11.

There, a gradually rising carbon content signifies continuous release of PCE over time, as is displayed in Fig. 11. The release ceased after ~120 min, as is demonstrated by a plateau. The result suggests that the PCE captured in between the inorganic layers of the Ca–Al-LDH is slowly released over time into the pore solution and is replaced by sulfate anions which then occupy the interlayer space. This anion exchange process is driven by the higher specific negative charge of sulfate as compared to that of the PCE (Plank et al., 2010). In this process, sulfate gradually replaces the PCE in the LDH and thus initiates its slow release.

To investigate how much of the PCE released from the LDH nanocomposite adsorbs on the OPC:CC 70:30 blend, an adsorption isotherm was developed over time. Here, the water-to-binder ratio was 0.82 at which a flow value of 18 cm is achieved.

The PCE released from the PCE-LDH nanocomposite which adsorbs on the composite cement produces a *Langmuir* adsorption isotherm and

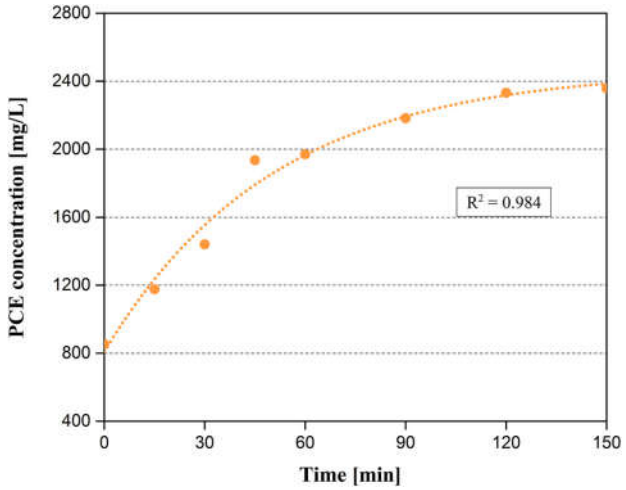

Fig. 11. Time-dependent release of the PCE superplasticizer from the PCE-LDH nanocomposite in SCPS (SCPS/LDH = 205:1), captured via total organic carbon analysis of the pore solution.

reaches a plateau at around 2 mg of polymer/g binder (Fig. 12). This data confirms progressive adsorption of the PCE released from the nanocomposite onto the calcined clay blended composite cement. It manifests that the working mechanism of the PCE-LDH admixture occurs via anion exchange, this way producing the fluidity retention as displayed in Fig. 9.

3.4.4. Effect of PCE-LDH on cement hydration

Next, the impact of the PCE-LDH nanocomposite on the hydration of the calcined clay blended cement was investigated via isothermal heat flow calorimetry. The time-dependent heat release from cement substituted with 30 wt % of calcined clay (w/b ratio = 0.82) is illustrated in Fig. 13.

According to this measurement, hydration curves which are typical for calcined clay blended cements are observed. They include two distinct peaks whereby the first (weaker) peak signifies the hydration of the silicate phases (primarily C_3S) whereas the second (stronger) peak is associated with the dissolution of aluminates from the calcined clay.

As is evidenced in Fig. 13, addition of 0.4% of PCE-LDH retards hydration for ~6 h which is common for highly anionic PCE polymers such as the one present in the LDH nanocomposite. It should be noted here that in actual concrete, the retardation inflicted by the PCEs is much less than observed in pastes which are shown here. Hence, the retardation on cement hydration registered here will not severely impact the actual field use of PCE-LDH.

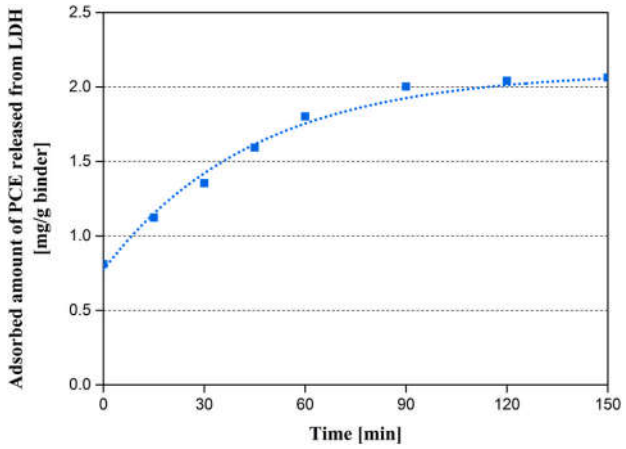

Fig. 12. Time-dependent adsorption of the PCE released from the PCE-LDH nanocomposite on OPC:CC 70:30 composite cement (w/b ratio = 0.82).

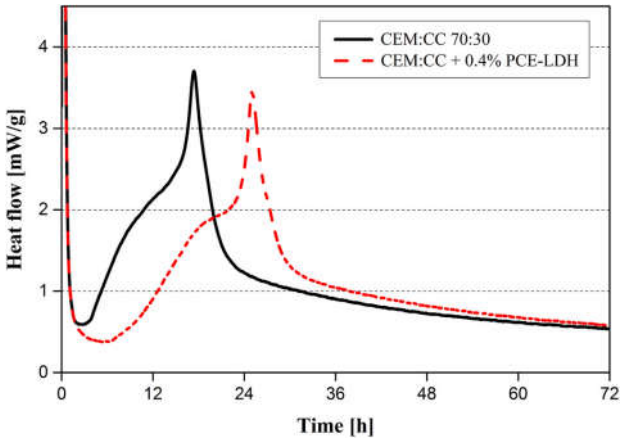

Fig. 13. Time-dependent evolution of the hydration heat released from pastes of the OPC:CC 70:30 blend admixed with and without 0.4% of PCE-LDH (w/b = 0.82).

3.5. Environmental impact of PCE-LDH nanocomposite

The practical implementation of calcined clay blended cements is justified only if the reduction in CO_2 emission achieved from clinker substitution is not compensated by the CO_2 footprint of the PCE and/or PCE-LDH admixture. To probe into this, the CO_2 emissions resulting from PCE and PCE-LDH nanocomposite were determined following the protocol as described in section 2.8. Additionally, the amounts of water used for PCE and PCE-LDH production were assessed from our preparation process and are listed in Table 5.

Accordingly, the PCE superplasticizer exhibits a carbon footprint of 0.0052 kg CO_2-eq/L only as compared to 0.0805 kg CO_2-eq/L for the PCE-LDH nanocomposite. Additionally, approximately 3.5 L of water are consumed in the preparation of 1 L PCE and 20 L/L of PCE-LDH. Apparently, the carbon footprint of both PCE and PCE-LDH is very minor in comparison to cement clinker which is about 0.82 kg CO_2-eq/kg. As such, these admixtures do not much impact the environmental balance sheet of calcined clay blended cements. E.g. based on a clinker substitution rate of 30%, a savings of ~250 kg CO_2/ton of cement is achieved. At the same time, addition of 0.4 wt % of the PCE-LDH imposes an additional ~1.07 kg CO_2/ton of cement only. Thus, it is apparent that the use of such admixture has no significant impact on the overall attractive environmental properties of the calcined clay blended cement.

4. Conclusion

In this study, the fluidity retention behavior of different admixtures in a new type of low-carbon cement (calcined clay blended composite cement) was investigated. A comparison between a commercial slump retaining HPEG PCE commonly used in ready-mix concrete as a benchmark product and the new PCE-LDH nanocomposite was performed in composite cements holding different amounts of calcined clay

Table 5
CO_2 emission and water used for the production of PCE or PCE-LDH.

Environmental parameter	PCE	PCE-LDH
CO_2 emission [kg CO_2-eq/L]	0.0052	0.0805
Water used [L/L]	3.5	20

(20–40 wt %).

First, it was found that the addition of calcined clay holding a high content of meta kaolin to OPC clinker makes it extremely difficult to achieve proper fluidity retention. In such cements, conventional ready-mix HPEG PCEs based on hydrolyzing esters and their combination with sodium gluconate exhibit only limited effectiveness on slump retention. This effect is owned to the high uptake/adsorption of PCE by the calcined clay. In contrast, the novel PCE-LDH admixture allows to achieve extended slump retention times as required in practical field applications. A pore solution analysis revealed that the PCE-LDH nanocomposite releases the superplasticizer gradually via progressive anion exchange with sulfate anions present in the pore solution, thus producing an extended workability time alongside with continuous dispersion.

Our findings first suggest that calcined clay blended composite cements require some adjustment with respect to the chemical admixtures to be used in order to achieve the properties demanded in actual use in concrete; and second, that such cements still present an environmentally highly attractive alternative to OPC, although the CO_2 footprint of the admixture cannot be ignored. It is safe to assume that a more widespread use of calcined clay blended cements will trigger the development of improved new technologies.

CRediT authorship contribution statement

Ran Li: Methodology, Data curation, Investigation, Writing – original draft, Writing – review & editing. **Lei Lei:** Formal analysis, Visualization, Validation. **Tongbo Sui:** Resources. **Johann Plank:** Conceptualization, Supervision, Writing – review & editing.

Declaration of competing interest

The authors declare that they have no known competing financial interests or personal relationships that could have appeared to influence the work reported in this paper.

Acknowledgements

Ran Li wants to show her gratitude to China Scholarship Council (CSC) for financial support of her Ph.D. study at TU München. The authors also thank Jilin Zhongxin Chemical Group Co. Ltd. for providing the HPEG PCEs, and Schwenk Cement Co. for supplying the CEM I 42.5 R sample. Appreciation also goes to Prof. Thienel and his team (University of the Federal Army, Munich/Germany) for analysis of the raw and the calcined clay.

References

Andrew, R.M., 2018. Global CO_2 emissions from cement production. Earth Syst. Sci. Data 10 (1), 195–217. https://doi.org/10.5194/essd-10-195-2018.

Antoni, M., Rossen, J., Martirena, F., Scrivener, K., 2012. Cement substitution by a combination of metakaolin and limestone. Cement Concr. Res. 42 (12), 1579–1589. https://doi.org/10.1016/j.cemconres.2012.09.006.

Bishop, M., Barron, A.R., 2006. Cement hydration inhibition with sucrose, tartaric acid, and Lignosulfonate: analytical and spectroscopic study. Ind. Eng. Chem. Res. 45 (21), 7042–7049. https://doi.org/10.1021/ie060806t.

Catti, M., Ferraris, G., Ivaldi, G., 1989. Thermal strain analysis in the crystal structure of muscovite at 700 °C. Eur. J. Mineral 1 (5), 625–632. https://doi.org/10.1127/ejm/1/5/0625.

Cheung, J., Jeknavorian, A., Roberts, L., Silva, D., 2011. Impact of admixtures on the hydration kinetics of Portland cement. Cement Concr. Res. 41 (12), 1289–1309. https://doi.org/10.1016/j.cemconres.2011.03.005.

DIN EN 196-1:2016. Methods of Testing Cement – Part 1: Determination of Strength.

Fernandez, R., Martirena, F., Scrivener, K., 2011. The origin of the pozzolanic activity of calcined clay minerals: a comparison between kaolinite, illite and montmorillonite. Cement Concr. Res. 41 (1), 113–122. https://doi.org/10.1016/j.cemconres.2010.09.013.

Flower, D.J.M., Sanjayan, J.G., 2007. Green house gas emissions due to concrete manufacture. Int. J. Life Cycle Assess. 12 (5), 282–288. https://doi.org/10.1065/lca2007.05.327.

Gartner, E., Sui, T., 2018. Alternative cement clinkers. Cement Concr. Res. 114, 27–39. https://doi.org/10.1016/j.cemconres.2017.02.002.

Hollanders, S., Adriaens, R., Skibsted, J., Cizer, Ö., Elsen, J., 2016. Pozzolanic reactivity of pure calcined clays. Appl. Clay Sci. 132–133, 552–560. https://doi.org/10.1016/j.clay.2016.08.003.

Huang, G., Pudasainee, D., Gupta, R., Liu, W.V., 2020. Utilization and performance evaluation of molasses as a retarder and plasticizer for calcium sulfoaluminate cement-based mortar. Construct. Build. Mater. 243 https://doi.org/10.1016/j.conbuildmat.2020.118201.

Juenger, M.C.G., Jennings, H.M., 2002. New insights into the effects of sugar on the hydration and microstructure of cement pastes. Cement Concr. Res. 32 (3), 393–399. https://doi.org/10.1016/S0008-8846(01)00689-5.

Lange, A., Lei, L., Plank, J., 2015. Cement compatibility of PCE superplasticizers. In: Shi, C., Yao, Y. (Eds.), 14th International Congress on the Chemistry of Cement. Admixtures, Beijing, China, p. 380. Section 4.

Laramay, S.B., Lavene, J.J., 2012. Encapsulated Compositions, US Patent 8273426B1.

Li, G., He, T., Hu, D., Huang, R., Shi, C., 2012. Effects of retarders on the fluidity of pastes containing β-naphthalenesulfonic acid-based superplasticiser. Adv. Cement Res. 24 (4), 203–210. https://doi.org/10.1680/adcr.11.00006.

Li, R., Lei, L., Sui, T., Plank, J., 2021. Effectiveness of PCE superplasticizers in calcined clay blended cements. Cement Concr. Res. 141, 106334. https://doi.org/10.1016/j.cemconres.2020.106334.

Liu, X., Wang, Z.M., Li, H.Q., Li, T., 2012. Mechanism and application performance of slow-release polycarboxylate superplasticizer. Adv. Mater. Res. 560, 574–579. https://doi.org/10.4028/www.scientific.net/AMR.560-561.574.

Nalet, C., Nonat, A., 2016. Ionic complexation and adsorption of small organic molecules on calcium silicate hydrate: relation with their retarding effect on the hydration of C_3S. Cement Concr. Res. 89, 97–108. https://doi.org/10.1016/j.cemconres.2016.08.012.

OECD/IEA, CSI, 2018. Low-carbon Transition in the Cement Industry: Technology Roadmap. International Energy Agency, Paris. Available at: https://webstore.iea.org/technology-roadmap-low-carbontransition-in-the-cement-industry.

Plank, J., Dai, Z., 2008. Novel hybrid materials obtained by intercalation of organic comb polymers into Ca–Al–LDH. J. Phys. Chem. Solid. 69 (5–6), 1048–1051. https://doi.org/10.1016/j.jpcs.2007.10.042.

Plank, J., Pöllmann, K., 2008. Synthesis and performance of methacrylic ester based polycarboxylate superplasticizers possessing hydroxy terminated poly(ethylene glycol) side chains. Cement Concr. Res. 38 (10), 1210–1216. https://doi.org/10.1016/j.cemconres.2008.01.007.

Plank, J., Zhimin, D., Keller, H., Hössle, F.v., Seidl, W., . Fundamental mechanisms for polycarboxylate intercalation into C3A hydrate phases and the role of sulfate present in cement. Cement Concr. Res. 40 (1), 45–57. https://doi.org/10.1016/j.cemconres.2009.08.013.

Rixom, R., Mailvaganam, N., Manson, D.P., Gonzales, C., 1999. Chemical Admixtures for Concrete, third ed. CRC Press, London. https://doi.org/10.4324/9780203017241.

Sabir, B.B., Wild, S., Bai, J., 2001. Metakaolin and calcined clays as pozzolans for concrete: a review. Cement Concr. Compos. 23, 441–454. https://doi.org/10.1016/S0958-9465(00)00092-5.

Samarakoon, M.H., Ranjith, P.G., Rathnaweera, T.D., Perera, M.S.A., 2019. Recent advances in alkaline cement binders: a review. J. Clean. Prod. 227, 70–87. https://doi.org/10.1016/j.jclepro.2019.04.103.

Schmid, M., Plank, J., 2020. Dispersing performance of different kinds of polycarboxylate (PCE) superplasticizers in cement blended with a calcined clay. Construct. Build. Mater. 258 https://doi.org/10.1016/j.conbuildmat.2020.119576.

Scrivener, K., Martirena, F., Bishnoi, S., Maity, S., 2018. Calcined clay limestone cements (LC^3). Cement Concr. Res. 114, 49–56. https://doi.org/10.1016/j.cemconres.2017.08.017.

Shi, C., Qu, B., Provis, J.L., 2019. Recent progress in low-carbon binders. Cement Concr. Res. 122, 227–250. https://doi.org/10.1016/j.cemconres.2019.05.009.

Stephan, D., Wilhelm, P., 2004. Synthesis of pure cementitious phases by sol-gel process as precursor. Z. Anorg. Allg. Chem. 630 (10), 1477–1483. https://doi.org/10.1002/zaac.200400090.

Tahara, H., Ito, H., Mori, Y., Mizushima, M., 1995. Cement Additive, Method for Producing the Same, and Cement Composition. US patent 5476885.

Tanaka, Y., Ohta, A., Hirata, T., Uno, T., Yuasa, T., Tahara, H., 2001. Cement composition using the dispersant of (meth) acrylic esters,(metha) acrylic acids polymers. US Patent 6187841B1.

Tironi, A., Trezza, M.A., Scian, A.N., Irassar, E.F., 2014. Potential use of Argentine kaolinitic clays as pozzolanic material. Appl. Clay Sci. 101, 468–476. https://doi.org/10.1016/j.clay.2014.09.009.

Ügdüler, S., Van Geem, K.M., Denolf, R., Roosen, M., Mys, N., Ragaert, K., De Meester, S., 2020. Towards closed-loop recycling of multilayer and coloured PET plastic waste by alkaline hydrolysis. Green Chem. 22 (16), 5376–5394. https://doi.org/10.1039/d0gc00894j.

Yamada, K., Takahashi, T., Hanehara, S., Matsuhisa, M., 2000. Effects of the chemical structure on the properties of polycarboxylate-type superplasticizer. Cement Concr. Res. 30 (2), 197–207. https://doi.org/10.1016/S0008-8846(99)00230-6.

Section 5.3

Publication # 3

Impact of meta kaolin content and fineness on the behavior of calcined clay blended cements admixed with PCE superplasticizer

R. Li, L. Lei, J. Plank

Cement and Concrete Composites (IF = 9.9)

133 (2022) 104654

DOI: 10.1016/j.cemconcomp.2022.104654

In the previous sections, the study mainly focused on the workability of a calcined clay sample rich in meta kaolin (~ 50 wt.%) and with high pozzolanic reactivity. However, from our observation the water demand of such calcined clay was strongly related to its high meta kaolin content. Therefore, in the following study (**publication # 3**) the **impact of the meta kaolin content** and its **fineness** on the **early strength and fluidity** of composite cements was investigated.

For this purpose, calcined clay samples exhibiting different meta kaolin contents (from 23 to 86 wt.%) were selected to compare their fluidity behavior in composite cements prepared at a clinker substitution ratio of 30 %. First, the water demand and PCE dosage requirement of those calcined clay composite cements were determined and correlated with their meta kaolin content. It was found that **higher meta kaolin contents** improve the pozzolanic reactivity and further **promote early compressive strength**, however, they **also greatly increase PCE dosages**. More interestingly, it was evidenced that the **fineness of the calcined clay** mainly **affects the water demand** while the **meta kaolin content** plays a **dominant** role with respect to **early strength development** and **PCE requirements**. Additionally, this general trend was also confirmed on different meta kaolin samples obtained from different industrial sources.

Cement and Concrete Composites 133 (2022) 104654

Contents lists available at ScienceDirect

Cement and Concrete Composites

journal homepage: www.elsevier.com/locate/cemconcomp

Impact of metakaolin content and fineness on the behavior of calcined clay blended cements admixed with HPEG PCE superplasticizer

Ran Li, Lei Lei **, Johann Plank *

Technische Universität München, Chair for Construction Chemistry, 85747 Garching, Lichtenbergstraße 4, Germany

ARTICLE INFO

Keywords:
Calcined clay composite cements
Metakaolin content
Workability
Pozzolanic reactivity
Superplasticizer
Polycarboxylate

ABSTRACT

In this study, three calcined clays (CCs) possessing different metakaolin contents (23; 51 and 86 wt%) were investigated with respect to their pozzolanic reactivity, water demand and workability in the presence of an HPEG PCE superplasticizer. Furthermore, mixed CC samples were prepared by blending a specific CC of low metakaolin content (23 wt%) with pure metakaolin to achieve metakaolin contents of 30, 40 and 51 wt% in the final CC. Results on pozzolanic reactivity from the R^3 test evidenced that increased metakaolin contents result in higher pozzolanic reactivity and improve 1d compressive strength. Whereas, higher metakaolin contents increased water demand significantly. Moreover, PCE dosages of up to 12 times were recorded. Furthermore, it was found that also fineness of the CC influences workability. Fineness mainly affects the water demand, while the metakaolin content plays a dominant role regarding PCE dosage. A mechanistic investigation revealed that in cement pore solution calcined clays initially exhibit a negative surface charge, but then sorb huge quantities of Ca^{2+} which enables PCE to adsorb onto the surfaces of CCs, as was evidenced by zeta potential measurements and from adsorption isotherms.

1. Introduction

Calcined clay blended cements are drawing more and more attention as a new concept for low-carbon cements [1–5]. In the production of calcined clay, a temperature range of 600–800 °C is required [6,7] which is much lower than that of ordinary Portland cement (OPC) at ~ 1450 °C. As a result, the carbon dioxide released from fuel combustion is reduced. More important, an even much higher CO_2 emission resulting from the main source in OPC production, the decarbonization of $CaCO_3$, is prevented [8]. It has been reported that by applying Limestone Calcined Clay blended Cement (LC^3), CO_2 emission can be reduced by around 30% [1]. Interestingly, at a cement substitution rate as high as 50%, no major influence on the final compressive strength of concrete has been observed [6,9,10]. Dhandapani et al. discussed the mechanical properties of concretes prepared using LC^3 [11]. They found that the 3 day strength of LC^3 concrete is slightly lower than that of OPC. Moreover, the 7 and 28 day strengths of LC^3 have been reported to be similar to or higher than that of on OPC [10]. This favorable strength development can be attributed to the high pozzolanic reactivity of a calcined clay which carries a significant amount of amorphous alumina that reacts with limestone to produce carbo-aluminate hydrates. In fact, the pozzolanic reactivity of calcined clays greatly depends on their specific mineral phase composition. Fernandez et al. [9] studied the pozzolanic reactivity of individual calcined pure clay phases. They found that metakaolin possesses by far the highest pozzolanic reactivity, followed by meta montmorillonite and meta muscovite. Consequently, the metakaolin content presents an important parameter with respect to the compressive strength development of a calcined clay blended cement.

On the other hand, it is known that the higher surface area of calcined clays as compared to OPC commonly induces poor workability into such calcined clay blended cements [2,12–16]. Moreover, in addition to the high specific surface area, also the specific mineral composition of the common natural clay can also much impact the rheology of the composite cement. Recent work suggests that compared to OPC, approximately twice the amount of a polycarboxylate (PCE) superplasticizer can be required in calcined clay blended cement (40% cement substitution with calcined clay) [17]. In another case, even 500% more PCE had to be dosed to a calcined clay blended cement of the same cement substitution ratio where the calcined clay contained ~51 wt% metakaolin [12]. These preliminary studies suggest that the metakaolin

* Corresponding author.
** Corresponding author.
E-mail addresses: lei.lei@bauchemie.ch.tum.de (L. Lei), sekretariat@bauchemie.ch.tum.de (J. Plank).

https://doi.org/10.1016/j.cemconcomp.2022.104654
Received 21 January 2022; Received in revised form 10 June 2022; Accepted 28 June 2022
Available online 1 July 2022

Table 1
Phase composition of the cement sample CEM I 42.5 R used in the study.

Phase	[wt.%]
C_3S, monoclinic	59.72
C_2S, monoclinic	11.53
C_4AF, orthorhombic	10.25
C_3A, cubic	4.42
C_3A, orthorhombic	2.54
Anhydrite ($CaSO_4$)	2.08
Dihydrate ($CaSO_4 \bullet 2H_2O$)	2.13
Hemihydrate ($CaSO_4 \bullet 0.5H_2O$)	0.79
Calcite ($CaCO_3$)	2.54
Dolomite ($CaMg(CO_3)_2$)	1.27
Quartz (SiO_2)	0.48
Portlandite (CH)	0.27
Arcanite (K_2SO_4)	0.41
Periclase (MgO)	0.76
Free lime (*Rietveld*)	0.44
Free lime (*Franke*)	0.35
Total	100.00

content of a calcined clay sample might play a significant role with respect to workability and PCE dosage requirements of such composite cements.

The specific interaction of calcined clays with anionic superplasticizers is vastly unknown. In a first study, Schmidt et al. investigated the interaction of PCE superplasticizers with individual pure meta clays [18]. They found that in synthetic cement pore solution, metakaolin exhibits the most negative surface charge, followed by meta montmorillonite, meta illite and meta muscovite. Obviously, such different surface charges of the meta clays can greatly impact the interaction with PCE and hence workability of the calcined clay blended cement.

To summarize, the metakaolin content present in a calcined clay appears to generally exercise a positive effect on the early strength development of such composite cements while it negatively affects workability. However, the impact of different kinds and concentrations of metakaolin in calcined clay samples is yet unknown. Thus, it is necessary to better understand the role of metakaolin in calcined clay composite cements in terms of water demand, PCE dosage requirement, early strength development and its surface chemistry in the cement pore solution. For this reason, in this study the impact of the metakaolin contents present in different calcined clay samples was investigated with respect to workability and strength development. Three calcined clay samples possessing increasing metakaolin contents were selected: CT-07 (23 wt%), CCC (51 wt%) and a relatively pure metakaolin, MK (86 wt%). In the first step, the pozzolanic reactivity of the three calcined clay samples was assessed via the R^3 method. Second, calcined clay samples holding stepwise increased metakaolin contents of 30, 40 and 51 wt% were prepared by mixing the respective amounts of MK into CT-07 to achieve such stepwise increases in the metakaolin content. From these experiments it was hoped to elucidate the effects of an increasing metakaolin content present in the cement. As superplasticizer, a benchmark commercial HPEG PCE was selected to investigate the impact of metakaolin on the workability of such cements. Also, the 1 day compressive strengths of mortars prepared from composite cements holding calcined clays of increasing metakaolin content (Portland cement substitution ratio 30 wt%) were compared under two different conditions: (1) applying the same PCE dosage; and (2) adjusting comparable mortar fluidity by using different PCE additions. Furthermore, water demand and PCE dosage requirement of all composite cements were determined via mini slump tests in order to get a comprehensive understanding of the influence of the fineness and the content of metakaolin present in calcined clay on the properties of a composite cement. Moreover, zeta potential and Total Organic Carbon (TOC) measurements were utilized to uncover the mechanism underlying the negative effect of metakaolin

Table 2
Metakaolin contents of the calcined clay samples used in this study.

Sample	Metakaolin content [wt.%]
CT-07	23
CCC	51
MK	86
CT-MK 30	30
CT-MK 40	40
CT-MK 51	51
MK-40	55
M1000	65
M1200s	78
Meta Star®	95

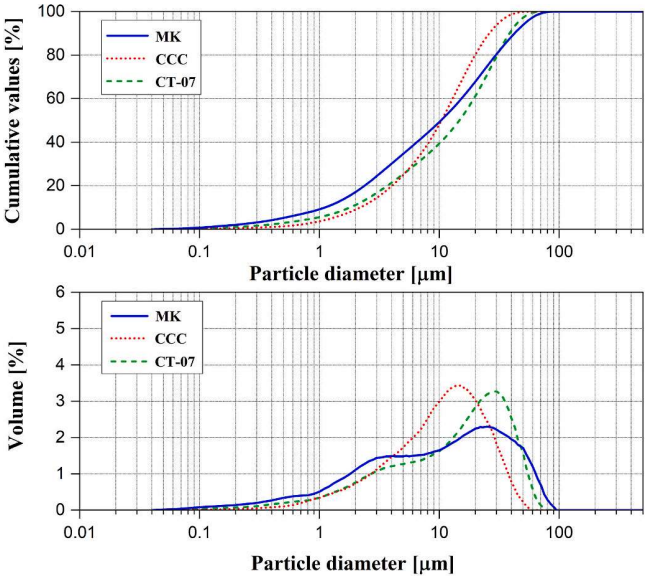

Fig. 1. Particle size distribution of the pristine calcined clay samples, as determined via laser granulometry.

on the workability of those composite cements. The overall aim of this study was to gain more knowledge about the relevance of the metakaolin content regarding workability and compressive strength development of low carbon calcined clay composite cements.

2. Materials and methods

2.1. Cement

The cement used in this study was an ordinary Portland cement (CEM I 42.5 R) provided by Schwenk cement company (Ulm, Germany). Its phase composition was determined by quantitative XRD analysis involving *Rietveld* refinement (Table 1). Its average particle size (d_{50} value) was found at 18.52 μm (laser granulometer, Cilas 1064, Cilas, Marseille) and a density of 3.15 g/cm^3 (Helium pycnometry) was recorded.

2.2. Calcined clay samples

Several calcined clay samples exhibiting different metakaolin contents were utilized in this study (Table 2). Sample CT-07 was produced in an industrial rotary kiln by exposure to a calcination temperature of 750 °C for about 30 min. It was provided by Universität der Bundeswehr, Munich, Germany. It contains ~23 wt% metakaolin. Sample CCC presents a calcined clay sample from Sinoma International Engineering Co., Ltd., Beijing. Its metakaolin content was determined at ~51 wt%.

Table 3
Particle size and specific surface area of the OPC and calcined clay samples investigated.

Samples	d_{10}	d_{50}	d_{90}	BET value [m^2/g]
OPC	1.36	18.52	51.78	1.77
CT-07	1.79	14.68	38.57	3.89
CCC	2.18	10.42	26.16	12.43
MK	1.11	10.32	42.44	20.82
CT-MK30	1.57	14.76	40.23	5.86
CT-MK40	1.21	13.48	40.07	8.51
CT-MK51	1.33	12.88	38.46	11.44
MK-40	0.91	9.35	45.73	16.75
M-1000	2.01	11.7	49.53	20.05
M1200s	0.34	5.79	26.89	23.52
Meta Star® 501	0.81	4.70	24.38	37.92

Table 4
Packing density and water film thickness of OPC and composite cement samples.

Samples	Packing density	Water film thickness [μm] at W/CM ratio by volume = 1
OPC	0.593	0.177
OPC: CT-07	0.553	0.077
OPC: CCC	0.540	0.028
OPC: MK	0.514	0.012
OPC: CT-MK30	0.551	0.057
OPC: CT-MK40	0.556	0.050
OPC: CT-MK51	0.508	0.006
OPC: M1000	0.490	0.005
OPC:M1200s	0.418	0.004
OPC:MK-40	0.548	0.002
OPC:Meta Star® 501	0.483	0.004

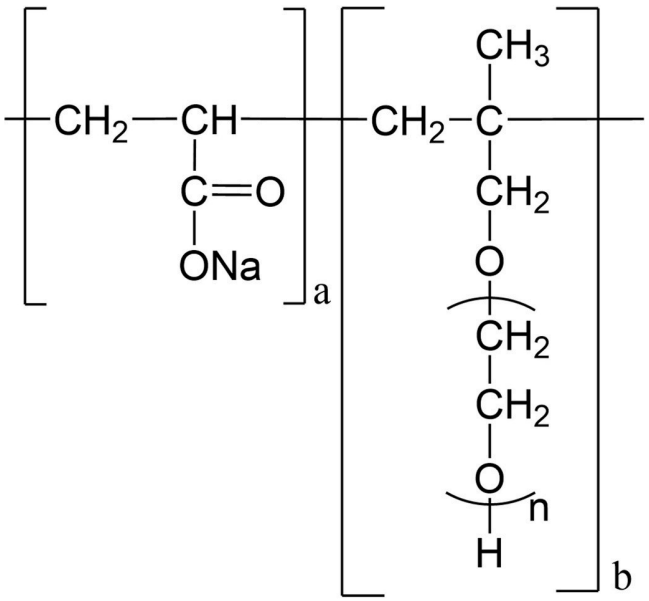

Fig. 2. Chemical structure of the HPEG PCE sample used in the study.

Sample MK presents a relatively pure metakaolin which was prepared industrially via flash calcination between 550° and 650 °C from a natural clay mineral containing 86.3 wt% kaolin (sample provided by Universität der Bundeswehr, Munich).

Moreover, mixtures exhibiting stepwise ascending metakaolin contents were prepared by blending CT-07 with MK at different weight proportions to achieve increasing total metakaolin contents of 30; 40 and 51 wt%. These calcined clay samples were named CT-MK 30, CT-MK 40 and CT-MK 51, respectively.

Additionally, four more industrial metakaolin samples provided by Imerys S.A. (Paris, France) were investigated in the second part of this study. Their metakaolin contents were specified by the suppliers as ~55 wt% (MK 40), ~65 wt% (M1000), ~78 wt% (M1200s) and ~95 wt% (MetaStar®).

In addition to the metakaolin content, these calcined clay samples also differ with respect to their particle size distribution. Fig. 1 displays the particle size distribution of CT-07, CCC and MK samples as captured via laser granulometry (Cilas, Marseille/France). Apparently, sample CCC exhibits a relatively narrow particle size distribution while CT-07 and MK possess a comparably broad distribution.

More specifically, Table 3 lists the d_{10}, d_{50} and d_{90} values and the specific surface areas (BET values) of these three calcined clays as well as of the blended calcined clay samples CT-MK 30, CT-MK 40 and CT-MK 51. Of all samples, the pure metakaolin (MK) exhibits the highest specific surface area, followed by CCC and CT-07 which is in line with their metakaolin contents. As for the blends of calcined clays, their specific surface area increases as more MK was incorporated.

2.3. PCE superplasticizer

The HPEG precast PCE superplasticizer sample was obtained from JILIN Chemical Industrial Co. (Jilin, China). This polymer presents a commercial benchmark PCE which exhibits a M_w of 35, 000 Da and an excellent macromonomer conversion rate of ~92%. Fig. 2 shows its chemical structure. It is characterized by medium molar ratio of acrylic acid to ω-hydroxy polyethylene glycol methallylether macromonomer and a long side chain which is commonly used in precast concrete.

2.4. Packing density and water film thickness of cementitious materials

The packing density of the OPC and calcined clay blended composite cements at OPC: CC by mass ratio of 70:30 was measured using the wet packing method [19,20]. And the water film thickness (WFT) was calculated at a fixed w/cm ratio of 1 (by volume) according to the equations published in Ref. [21].

2.5. Pozzolanic reactivity of calcined clay samples

In order to assess the pozzolanic reactivity of the calcined clay samples, the rapid, relevant and reliable (R^3) method was applied [22]. The cumulative heat of reaction was measured in an isothermal calorimeter (TAMAir Instrument, Thermometric AB, Sweden) at 40 °C for over 72 h. In sample preparation, the calcined clays were mixed with portlandite at a wt. ratio of 1:3 and a water-to-solid ratio of 1.2 was applied. In addition, soluble alkalis and sulfate were added to reproduce the conditions (pH etc.) present in cement pore solution and to accelerate the pozzolanic reaction. An SO_3/calcined clay ratio of 0.06 and a K_2O/calcined clay ratio of 0.08 were used. These ratios were identified in early works by Avet et al. to ensure high pozzolanic reactivity [22]. Potassium hydroxide (88.2% purity) from VWR (Radnor, USA) and potassium sulfate (99% purity) from Merck (Darmstadt, Germany) were dissolved in DI water to adjust those parameters.

2.6. Dispersing performance

A Vicat cone was applied for spread flow measurement to determine fluidity of OPC and the composite cements prepared from different calcined clays at an OPC:CC ratio of 70:30 wt/wt. %. The water-to-binder ratio was fixed at 0.5.

In the experiment, 300 g of OPC or composite cement were added to 150 mL of water placed in a porcelain cup and stirred manually for 10 s with a spoon. Then the PCE solution which was pre-weighted was added to the mixture and stirring was continued for another 50 s. After resting for 1 min, the suspension was mixed for an additional 1 min. The water

Table 5
SCPS-to-solid ratios of calcined clay samples to achieve a paste spread flow of 18 ± 0.5 cm as determined via mini slump test.

Calcined clay sample	CT-07	CCC	MK
SCPS-to-solid ratio	0.77	1.2	1.14

present in the PCE solution was subtracted from the total amount of mixing water to perform all experiments at exactly the same w/b ratio. Then the paste was immediately poured into a Vicat cone (height 40 mm, top diameter 70 mm, bottom diameter 80 mm) which was placed on a glass plate. After the cone was lifted vertically, the resulting spread of the cement paste was measured twice, in two perpendicular direction. The dosages of PCE required for each composite cements to reach a final spread flow of 26 ± 0.5 cm were recorded.

When the water demand was determined, no superplasticizer was added and the water-to-binder ratio to achieve a spread flow of 18 ± 0.5 cm (= base consistency) was measured. As mixing water, a synthetic cement pore solution (SCPS) [23] was used to mimic the ionic environment present in cement. Table 5 shows the water requirement of each neat calcined clay sample at a spread flow of 18 ± 0.5 cm.

2.7. Zeta potential

The surface charge of selected calcined clays was determined via zeta potential measurement on a Model DT-1200 Electroacoustic Spectrometer (Dispersion Technology, Inc., NY, USA). The calcined clay samples were suspended in synthetic cement pore solution (SCPS; for its ionic composition refer to Ref. [23]) at various SCPS/solid ratios.

In measurement, 30 mL of a 0.6 M $Ca(NO_3)_2$ solution were titrated in 60 steps to the calcined clay slurry until saturated adsorption of Ca^{2+} was achieved. During the $Ca(NO_3)_2$ titration, the pH value was kept constant at the initial pH value by minor additions of 30 wt% aqueous NaOH.

2.8. PCE adsorption

Polymer adsorption on calcined clays was investigated based on the depletion method using TOC analysis. In the experiments, all calcined clay samples were dispersed in SCPS at the different w/s ratios as shown in Table 5.

In measurement, at first different concentrations of HPEG PCE solutions (0.1; 0.2; 0.4; 0.6; 0.8; 1.0; 1.2; and 1.5% by weight of calcined clay) were prepared in SCPS. After mixing the calcined clay sample and the PCE solutions, the slurries were homogenized on a wobbler for 2 min and then separated via centrifugation at 8500 rpm for 10 min. Next, the supernatant was extracted with a syringe and filtered through a 0.2 μm polyethersulfone syringe filter. Then the filtrate was diluted with DI water and 10 drops of 1 M HCl. The TOC measurement was conducted on a LiquiTOC analyzer (Elementar, Hanau, Germany). Each sample was measured twice and the average value was taken as the final result.

2.9. Compressive strength

Compressive strength of cement mortar specimens prepared from OPC or OPC:CC 70:30 composite cements was tested after 24 h of hydration following DIN EN 196-1 standard [24]. From each mix, three sets of mortar prisms (40 × 40 × 160 mm dimension) were prepared. After 24 h, the specimens were demolded and stored in a climate chamber at 20 ± 1 °C and a relative humidity of ~90%. For 28 d sample, the specimens were cured under water in the climate chamber. Then compressive strengths were measured on a test apparatus provided by ToniTechnik (Berlin, Germany).

Since the water demand of each calcined clay sample was significantly different, the amount of PCE required for each mortar sample was also different. Therefore, in order to exclude the influence of different PCE dosages on strength development, the compressive strengths of the different composite cements were compared under two scenarios: 1) at the same PCE dosage, but at different fluidity; 2) at the same fluidity (spread flow of 22 cm), but with different PCE additions to achieve the same fluidity.

To all the mortar samples, few drops of defoamer (SURFYNOL MD 40 from Air Products, Utrecht/Netherlands) were applied to achieve exactly comparative mortar density.

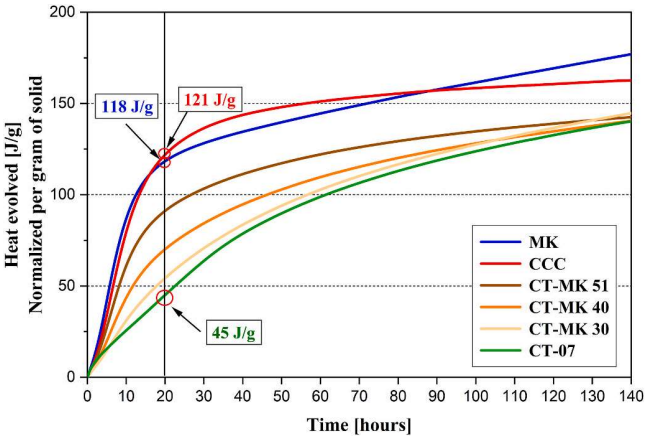

Fig. 3. Heat release from different calcined clay-portlandite samples at 40 °C, according to the R^3 method [22].

3. Results

3.1. Pozzolanic reactivity of the calcined clay samples

It is well established that metakaolin possesses higher pozzolanic reactivity than other meta clays such as meta montmorillonite and meta illite [9]. Consequently, the content of metakaolin in a calcined clay presents one of the most important parameters influencing the property of the composite cement. Its high pozzolanic reactivity promotes the early strength of a calcined clay composite cement.

Therefore, firstly the pozzolanic reactivity of all calcined clay samples was determined via the R^3 method, and the results are displayed in Fig. 3. It was found that, generally, calcined clay samples possessing high metakaolin content exhibit higher pozzolanic reactivity. After 140 h, CT-07 produced the lowest total heat release of 140 J/g while the heat release from CCC and MK samples were much higher (162 and 177 J/g, respectively). Interestingly, a high metakaolin content actually accelerates the speed of heat release at the beginning of the reaction. For example, at 20 h only 45 J/g heat were released from CT-07 while a much higher heat release was recorded for MK (118 J/g) and CCC (121 J/g) samples resulting from their higher metakaolin contents. As for the blended calcined clay samples CT-MK 30; 40 and 51, their heat release at 20 h increased gradually from 54 J/g to 90 J/g as the metakaolin content ascended from 30 to 51 wt%.

This trend can be explained by the different pozzolanic reactivity of the meta minerals. Apart from 23 wt% metakaolin, CT-07 sample contains ~27 wt% meta illite-smectite phase which has a lower pozzolanic reactivity than metakaolin. This explains the slow heat release from CT-07 and its mixtures.

According to the data from the R^3 method, samples MK and CCC possess highest and almost comparable pozzolanic reactivity, while CT-07 sample attains a much lower value. In CT-MK 30, CT-MK 40 and CT-MK 51, the pozzolanic reactivity increases with ascending metakaolin content and lies between that of CT-07 and MK.

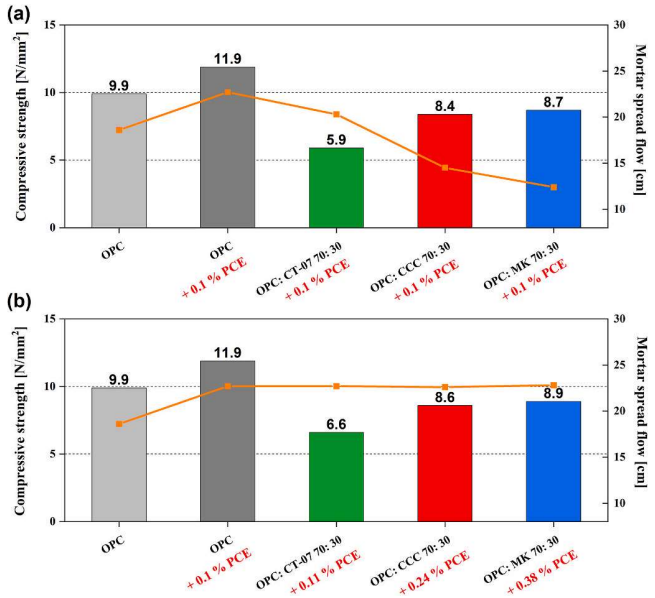

Fig. 4. 1 d compressive strength of mortar specimens prepared from OPC and OPC:CC 70:30 composite cements: (a) at the same dosage of HPEG PCE; (b) at the same mortar fluidity adjusted by different HPEG PCE additions.

Table 6
Raw mortar densities (fresh mortar densities) of the composite cement mortar samples.

Samples	Raw mortar density [g/cm^3]
OPC	2.282
OPC + 0.10% HPEG PCE	2.308
OPC: CT-07 + 0.10% HPEG PCE	2.263
OPC: CCC + 0.10% HPEG PCE	2.259
OPC: MK + 0.10% HPEG PCE	2.248
OPC: CT-07 + 0.11% HPEG PCE	2.302
OPC: CCC + 0.24% HPEG PCE	2.268
OPC: MK + 0.38% HPEG PCE	2.254

3.2. Strength development

In the next step, the 1 d and 28 d compressive strengths of composite cements containing 30 wt% of the calcined clays were tested and compared to that of OPC. To exclude the effect of different PCE dosages on the strength development, the mortars were compared for two cases: 1) at the same PCE dosage of 0.10% bwob which results in different fluidity; 2) at the same fluidity of 22 cm spread flow, but using different PCE additions, as shown in Fig. 4. All mortar samples were adjusted to comparable raw mortar densities by using a defoamer (see Table 6).

As is shown in Fig. 4 (a), all samples prepared from the composite cements exhibit significantly lower 1d strengths as compared to OPC. For example, the specimen holding CT-07 possessing the lowest metakaolin content develops only ~50% of the compressive strength of OPC. While at increasing metakaolin contents, a gain in early strength is observed. Albeit, as is also evidenced from Fig. 4 (a), the presence of metakaolin generally reduces workability, and the higher the metakaolin content the stronger is the decrease in fluidity. The results signify that while a higher metakaolin content in the calcined clay boosts early strength development, it is highly disadvantageous with respect to workability.

Interestingly, when mortars adjusted to the same fluidity by admixing different PCE dosages were compared, then almost similar strength values as recorded in Fig. 4 (a) at constant PCE addition of 0.1% bwob were found (Fig. 4 (b)). This signifies that the impact of PCE on the early strength development of OPC:CC composite cements essentially is

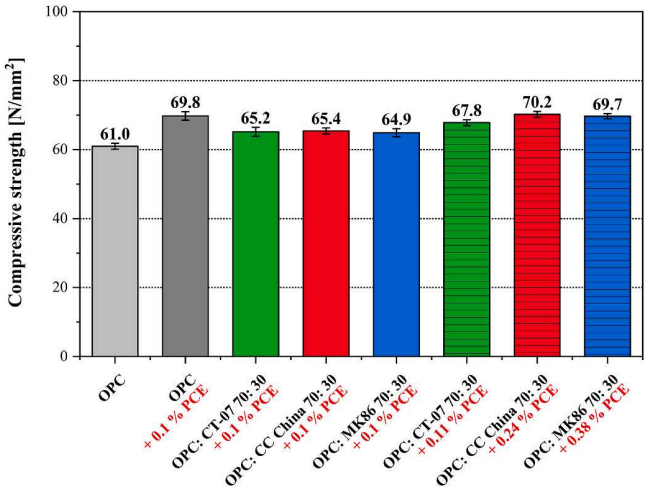

Fig. 5. 28 d compressive strength of mortar samples prepared from OPC and OPC:CC 70:30 composite cements.

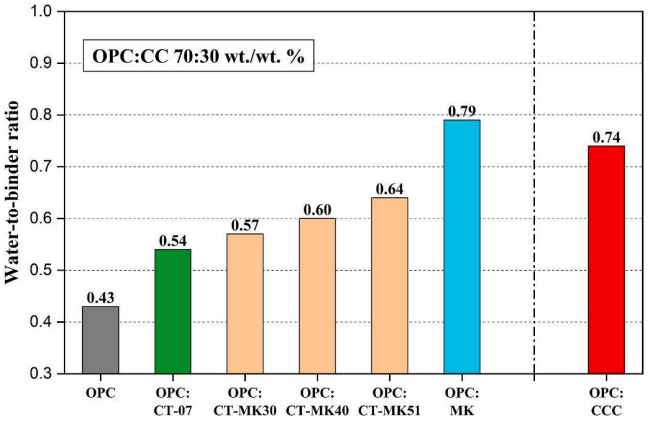

Fig. 6. Water demand of different calcined clay blended cements formulated at an OPC:CC ratio of 70:30; no PCE added.

negligible as compared to that of the metakaolin content. It also suggests that achieving high workability in calcined clay blended cements does not necessarily come at the price of decreased early strength.

Fig. 5 displays the 28 d compressive strength results of OPC and OPC: CC 70:30 composite cements containing different amount of PCEs. It can be seen from the results that all mortar samples show similar compressive strengths after 28 days of curing. In particular, there is no significant difference in compressive strength for composite cements possessing different calcined clays. This implies that the high metakaolin content in calcined clay is more favorable for early strength, e.g. 1 day, rather than 28 days.

In addition, a slightly increase in strength can be observed due to the higher PCE addition. This result is in line with the early strength development of OPC at 1 day. It should be noted that the results shown here relate to this specific precast type HPEG polymer which possesses a relatively long side chain and might differ for other PCE products.

3.3. Water demand of calcined clay blended cements

In order to uncover the effects of fineness and metakaolin content of calcined clay samples on the workability of blended cement, the water demand of composite cements containing 30 wt% of different calcined clay samples with varying metakaolin contents were compared to that of neat OPC. For this purpose, the water-to-binder ratios required to

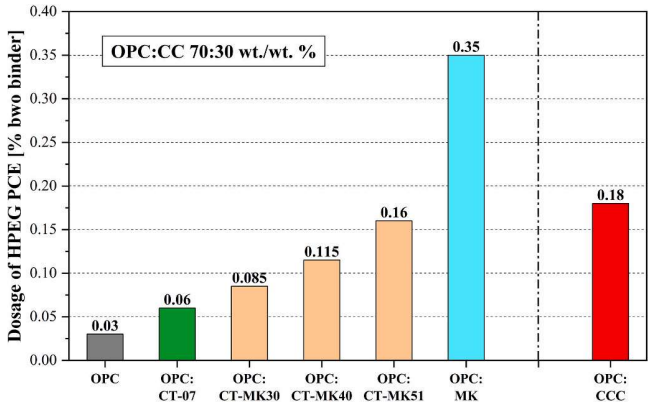

Fig. 7. HPEG PCE dosages required for different calcined clay blended cements containing OPC:CC at a wt. ratio of 70:30 to achieve the same paste spread flow of 26 cm; w/c ratio = 0.5.

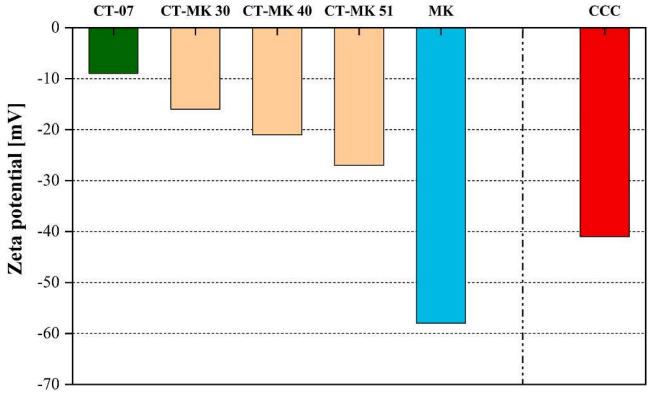

Fig. 8. Zeta potential values of the calcined clay samples suspended in SCPS, measured after 4 min.

achieve a spread flow of 18 ± 0.5 cm were determined. The results are displayed in Fig. 6.

The results signify that all composite cements exhibit a higher water demand than for OPC which was found at 0.43. This effect can be attributed to the higher water requirement of calcined clay in general, and in particular to increased metakaolin contents [12]. As such, the OPC:MK 70:30 sample possessing the highest metakaolin content also records the highest water demand of 0.79. This is owed to the fact that MK exhibits the highest specific surface area of 20.82 m^2/g (see Table 3). Moreover, the water demand of the composite cements increases linearly from 0.54 to 0.64 with ascending metakaolin content in the calcined clay sample. This increase may originate from the finer particles when more metakaolin is incorporated.

It is worth noting that the blends OPC:CT-MK 51 and OPC:CCC show quite a different water demand (0.64 versus 0.74), although both CT-MK 51 and CCC exhibit the same metakaolin content of 51 wt%. This difference can be attributed to the different specific surface areas of those two samples. As was displayed in Table 3, CCC exhibits a higher BET value of 12.43 m^2/g as compared to 11.44 m^2/g for CT-MK51. Apparently, the higher particle fineness in CCC explains the higher water demand. It is in line with findings from Mantellato et al. [25] who reported that the yield stress of a cement paste increases exponentially with the increase of the specific surface area.

3.4. Dispersing performance of HPEG PCE in CC blended cements

In the following, the dispersing performance of the HPEG PCE sample in composite cements containing 30 wt% of different calcined clays with varying metakaolin contents was assessed using the "mini slump" test. There, the PCE dosage required to achieve a cement paste spread flow of 26 ± 0.5 cm at a water-to-binder ratio of 0.5 is determined. The results are exhibited in Fig. 7.

As displayed in Fig. 7, the dosage of HPEG PCE required to reach the targeted spread flow of 26 cm increases steadily with ascending metakaolin content present in the composite cements. For example, the PCE demand doubles from 0.03% to 0.06% bwob just when 30% of the OPC are substituted with CT-07. For blends containing CCC and pure MK, the PCE dosages even increase by a factor of 6 to 0.18% (for CCC) and 12 times to 0.35% (for MK). Again, the CT-MK mixtures which require PCE dosage of 0.085%–0.16% bwob are situated in between the dosages of their educts CT-07 and MK blended with OPC.

As was expected from the results shown before for the water demand (see Fig. 6), PCE dosages increase with ascending metakaolin content in the calcined clay sample, however at a much steeper pace as compared to the water demand. It suggests that such low carbon cements are characterized by a generally higher PCE dosage requirement.

Interestingly, the difference between CT-MK51 and CCC with respect to the PCE dosage is smaller here than in the water demand. For example, the water demand of CT-MK 51 and CCC composite cements which possess the same metakaolin content differed noticeably at 0.64 and 0.74, while the PCE dosages were almost comparable at 0.16% and 0.18% bwob, respectively. This minor difference can be attribute to the higher specific surface area of CCC as compared to CT-MK 51 (see Table 3). It signifies that in a calcined clay the metakaolin content plays a more dominant role for the dispersing effectiveness of PCEs, while the specific surface area exercises a more pronounced effect on the water demand.

In addition, the results for packing density and water film thickness are corelated with the results for HPEG PCE polymers on dispersion properties. As listed in Table 4, OPC sample possessing the highest packing density of 0.593 and highest WFT value of 0.177. When the calcined clay samples were added into the system, the packing density and water film thickness for all samples decreased. Addition of CT-07 decreases the values the least while MK sample decreases the most. And CCC, MK30, MK40 and MK51 samples are in between. In theory, a higher the packing density of the cementitious material particle leads to a better workability [19,21,26]. In this study, these results are consistent with the dispersing performance of HPEG PCE that the composite cement contains MK presents the most difficult one for dispersing, while CT-07 is the easiest with MK30, MK40 and MK51 in between.

It is worth to notice that the addition of metakaolin does not always decrease the packing density of the samples. Marchetti et al. [21] found that the addition of metakaolin increased the packing density of the composite cement. However, the better fluidity can be directly related to water film thickness, with higher values of WFT being associated with a better fluidity of the composite cement.

To summarize, the metakaolin content of composite cements strongly affects the dispersing performance of polycarboxylate superplasticizers. The higher the content of metakaolin in the calcined clay, the higher is the amount of PCE required to achieve sufficient workability. To understand the reason behind this, the mechanism controlling the influence of metakaolin on PCE performance and workability was investigated.

3.5. Mechanistic study

It is well established that – among other parameters - the surface charge of cement particles much determines the adsorption and thus the dispersing performance of PCEs [27]. Therefore, it is desirable to understand the surface charge developed by calcined clays in cementitious systems. For that reason, zeta potential measurements were performed in the following.

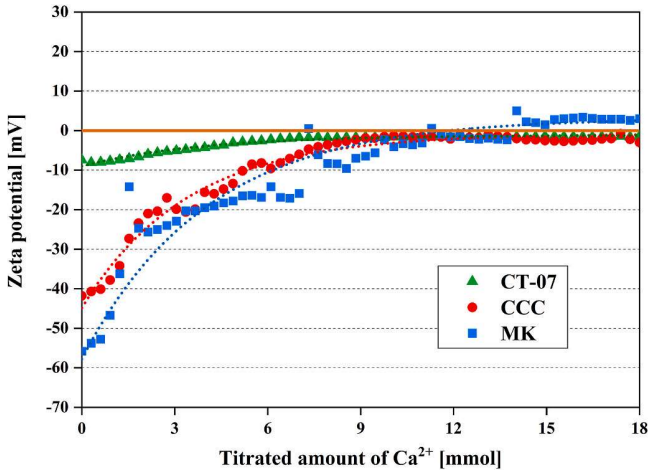

Fig. 9. Zeta potentials of calcined clay samples suspended in SCPS as a function of the volume of $Ca(NO_3)_2$ solution added; SCPS/s ratios: CT-07 = 0.77; CCC = 1.2; MK = 1.14.

3.5.1. Zeta potential measurements

To account for the different water demands of the calcined clay samples, all zeta potential measurements were performed at w/s ratios achieving a suspension spread flow of 18 ± 0.5 cm in SCPS.

As displayed in Fig. 8, all calcined clay samples develop a negative surface charge covering a broad range from – 9 mV (for CT-07) to – 58 mV (for MK). For the blends of CT-07 and MK, the surface charges increase steadily from −16 mV to −27 mV as the metakaolin content increases. This result correlates well with the PCE dosage requirements as shown in Fig. 7. Moreover, the pure MK sample stands out owed to its most pronounced negative surface charge of −48 mV as compared to the other calcined clays. This finding corroborates that the metakaolin content much impacts the negative surface charge of a cement sample, which directly affects the PCE demand of such composite cements.

The result from above is surprising because negatively charged PCE polymers are not supposed to adsorb on negatively charged surfaces of calcined clays, assuming that the clay surfaces are homogeneously charged. Hence, supposedly another effect comes into play here. Generally, it needs to be considered that zeta potential measurement of calcined clay samples in SCPS are not fully representative for the actual situation in cement where Ca^{2+} adsorbed by the calcined clay will be replenished immediately by continuous dissolution from the clinker phases into the pore solution [12]. Whereas in SCPS, the concentration of Ca^{2+} ions is limited and is not replenished in case of an uptake by the calcined clay. Hence, in the next step it was investigated whether the calcined clays would adsorb significant quantities of Ca^{2+} ions from the pore solution.

For that reason, zeta potential measurements on suspension of the calcined clay samples in SCPS were repeated while titrating a Ca^{2+} solution to the system to mimic the replenishment of Ca^{2+} by cement. Here, CT-07, CCC and the pure MK sample were measured to gain an insight into the actual surface charge of the calcined clays in cement.

As displayed in Fig. 9, at step-wise addition of Ca^{2+} the zeta potentials of all three calcined clays shifted gradually to less negative values until a plateau around the isoelectric point was reached. This finding confirms that the surfaces of the calcined clays are densely occupied by Ca^{2+} ions which can easily facilitate the adsorption of negatively charged PCE polymers by docking onto those surface Ca^{2+} ions.

Interestingly, the three calcined clay samples bind different amounts of Ca^{2+} ions to reach the point of saturated adsorption. As an example, for CT-07 a constant zeta potential signifying saturated adsorption is reached after the addition of approximately 7.5 mmol Ca^{2+} ions, while it requires 10 mmol and 15 mmol Ca^{2+} for CCC and MK, respectively. These observations are in line with the initial zeta potentials of the clays which is as expected since a more negative surface charge will demand a higher number of Ca^{2+} ions to reach charge neutralization.

It can be speculated that surfaces packed more densely with Ca^{2+} ions should adsorb more PCE which could explain the sharp increase in PCE dosages for composite cements containing calcined clays, especially of high metakaolin content. To elucidate, in the next section PCE adsorption on these three calcined clay samples was quantified.

3.5.2. PCE adsorption on calcined clay

Adsorption of the HPEG PCE polymer on three calcined clay samples CT-07, CCC and MK in SCPS was investigated at the different water-to-solid ratios listed in Table 5.

First, as is shown in Fig. 10, *Langmuir*-type adsorption isotherms were detected for all calcined clay samples. They are characterized by a steep increase in the adsorbed amount at low PCE dosages until the uptake levels out at a plateau which represents the point of saturated adsorption. In accordance with the high sorption of Ca^{2+} ions as demonstrated before (see Fig. 9), all three calcined clay samples adsorbed significant amounts of the anionic PCEs.

Significantly higher adsorbed amounts were observed for the MK sample as compared to CT-07 and CCC. More specifically, MK reached the point of saturated adsorption at ~5.0 mg PCE/g calcined clay, while CT-07 and CCC attained their plateau at ~2.0 and ~3.0 mg PCE/g calcined clay, respectively. These results confirm the conclusion derived from the different uptake of Ca^{2+} as evidenced in the zeta potential measurements (see Fig. 9) and also are in accordance with the results on the PCE dosage requirement (Fig. 7). With rising metakaolin content, the zeta potential in SCPS becomes more negative which attracts more Ca^{2+} ions and prompts higher PCE dosages as is evidenced by higher PCE adsorption on the calcined clay particles. Consequently, in calcined clays which are rich in metakaolin higher PCE dosages can be expected to achieve sufficient workability.

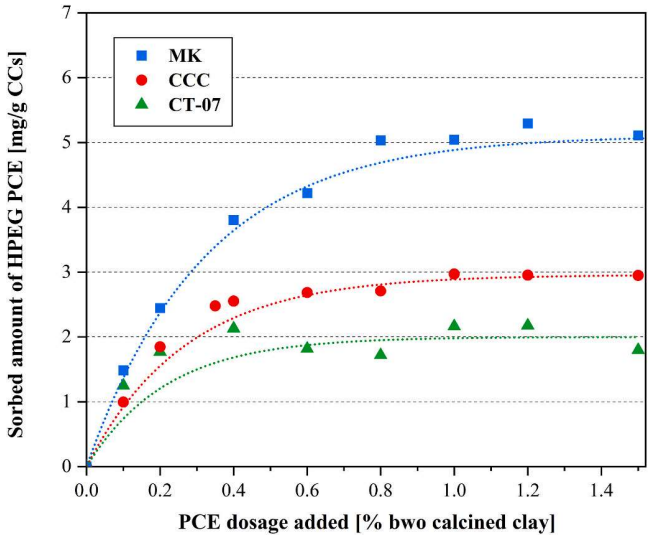

Fig. 10. Adsorbed amounts of the HPEG PCE on the neat calcined clay samples; SCPS/s ratios: CT-07 = 0.77; CCC = 1.2; MK86 = 1.14.

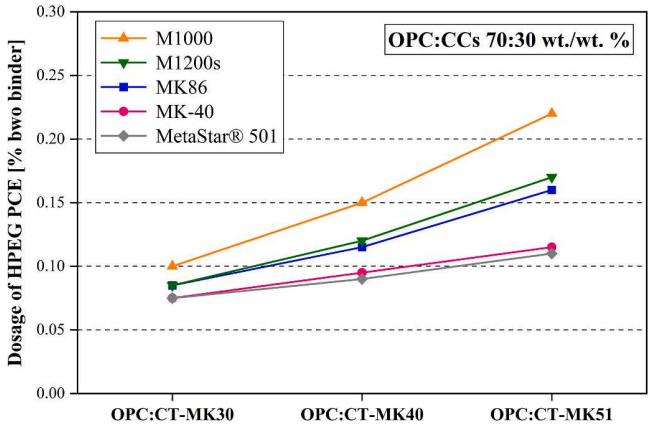

Fig. 11. PCE dosages required for composite cements containing OPC and a blend of CT-07 with different industrial metakaolin products to achieve a paste spread flow of 26 cm (OPC:CCs 70:30, w/c ratio = 0.5).

3.6. Impact of different metakaolin samples on workability

To check on the results obtained so far with one specific metakaolin sample (MK), more products from several sources possessing different mineral composition, particle size distribution, surface charge and degree of calcination were tested. Their metakaolin contents varied between 55 wt% and 95 wt%, as is displayed in Table 2. Their PCE dosage requirement was compared with that of the MK sample. The aim of this analysis was to confirm the concept that high metakaolin content in a calcined clay will always prompt higher PCE dosages.

In the experiments, all metakaolin samples were blended with CT-07 to achieve metakaolin contents of 30, 40 or 51% by weight of the calcined clay. Then the dispersing performance of the HPEG PCE in those composite cements containing 30 wt% of the calcined clay blends was tested using the "mini slump" test, and the PCE dosages required to achieve a paste spread flow of 26 ± 0.5 cm at a water-to-binder ratio of 0.5 was recorded.

As displayed in Fig. 11, all composite cements show a higher PCE demand at increased metakaolin contents. This is in line with the observations made before. Here the highest PCE demand was detected for cements blended with M1000 metakaolin sample characterized by a medium specific surface area (22.05 m^2/g) which is much less than that of the MetaStar® sample (37.92 m^2/g) which however demands less PCE (see Fig. 11). However, this result also signifies that the metakaolin content and particle size of calcined clay are not the only parameters which determines the PCE demand. The calcined clay blended composite cements clearly present complex systems, hence their fluidity can be influenced by multiple factors including, but not limited to, particle fineness, packing densities, water film thickness, mineral phase composition, calcination temperature and conditions (flash vs. rotary kiln) etc.

4. Conclusion

In this study, composite cements containing different calcined clays with varying metakaolin contents were investigated to evaluate the impact of the metakaolin content and fineness of the calcined clays on the fluidity of composite cements. In order to do that, three calcined clay samples holding 23% (CT-07); 51% (CCC) and 86% (MK) metakaolin and mixtures of a base calcined clay sample (CT-07) of relatively low metakaolin content (~23 wt%) with a relatively pure metakaolin sample (86 wt%) to achieve increasing metakaolin contents (30; 40 and 51 wt %) in the blended were studied. Pozzolanic reactivity, water demand, PCE dosage requirement and compressive strength of the blended cements were determined at an OPC substitution ratio of 70:30.

From the results obtained, the following conclusions can be drawn:

1. Increased metakaolin content in a calcined clay sample fosters its pozzolanic reactivity and early strength, however, there is no significant influence on 28 d strength. Also, it increases the water demand and prompts higher superplasticizer dosages.
2. Water demand and PCE dosage of such composite cements are closely related to the metakaolin content and particle fineness. While fineness mainly affects the water demand, the metakaolin content plays a dominant role with respect to PCE dosage.
3. A direct correlation exists between PCE dosage and the metakaolin content present in a calcined clay. This can be explained by the more negative surface charge of metakaolin-rich samples which sorb increased amounts of Ca^{2+} from the pore solution and then allow more PCE superplasticizer to adsorb onto their surfaces.
4. This behavior was confirmed for several commercial metakaolin samples from different sources. PCE dosages generally increase with ascending metakaolin contents in the calcined clay blended cement.

In the future, new technologies for chemical admixtures which can integrate both diverging properties of high fluidity and at the same time sufficient early strength need to be developed.

Declaration of competing interest

The authors declare that they have no known competing financial interests or personal relationships that could have appeared to influence the work reported in this paper.

Acknowledgment

The authors greatly acknowledge Deutsche Forschungsgemeinschaft (DFG, German Research Foundation) for financial support of this project [grant number PL 472/15–1] "Shear-dependent rheological behavior of ecologically improved cements containing calcined clays as clinker substitute". Also, thanks to Jilin Zhongxin Chemical Group Co. Ltd. for providing the HPEG PCE product, and Schwenk Cement Co. for supplying the CEM I 42.5 R sample. Appreciation also goes to Prof. Thienel and his group at Universität der Bundeswehr, München for providing and analyzing the calcined clays. Furthermore, our thanks go to Dr. Kwasny from Imerys company for providing the industrial metakaolin samples. Moreover, Ran Li likes to express her gratitude to China Scholarship Council (CSC) for financial support of her Ph.D. study at TU München.

References

[1] K. Scrivener, F. Martirena, S. Bishnoi, S. Maity, Calcined clay limestone cements (LC^3), Cement Concr. Res. 114 (2018) 49–56.
[2] R. Sposito, N. Beuntner, K.-C. Thienel, Characteristics of components in calcined clays and their influence on the efficiency of superplasticizers, Cem. Concr. Compos. 110 (2020).
[3] T.R. Muzenda, P. Hou, S. Kawashima, T. Sui, X. Cheng, The role of limestone and calcined clay on the rheological properties of LC^3, Cem. Concr. Compos. 107 (2020), 103516.
[4] S. Krishnan, S. Bishnoi, A numerical approach for designing composite cements with calcined clay and limestone, Cement Concr. Res. 138 (2020), 106232.
[5] M. Sharma, S. Bishnoi, F. Martirena, K. Scrivener, Limestone calcined clay cement and concrete: a state-of-the-art review, Cement Concr. Res. 149 (2021).
[6] S. Hollanders, R. Adriaens, J. Skibsted, Ö. Cizer, J. Elsen, Pozzolanic reactivity of pure calcined clays, Appl. Clay Sci. 132–133 (2016) 552–560.
[7] M. Izadifar, P. Thissen, A. Steudel, R. Kleeberg, S. Kaufhold, J. Kaltenbach, R. Schuhmann, F. Dehn, K. Emmerich, Comprehensive examination of dehydroxylation of kaolinite, disordered kaolinite, and dickite: experimental studies and density functional theory, Clay Clay Miner. 68 (4) (2020) 319–333.
[8] International Energy Agency and The Cement Sustainability Initiative, Technology Roadmap: Low-Carbon Transition in the Cement Industry, 2018, p. 61. Paris.
[9] R. Fernandez, F. Martirena, K. Scrivener, The origin of the pozzolanic activity of calcined clay minerals: a comparison between kaolinite, illite and montmorillonite, Cement Concr. Res. 41 (1) (2011) 113–122.

[10] S. Krishnan, A.C. Emmanuel, S. Bishnoi, Hydration and phase assemblage of ternary cements with calcined clay and limestone, Construct. Build. Mater. 222 (2019) 64–72.
[11] Y. Dhandapani, T. Sakthivel, M. Santhanam, R. Gettu, R.G. Pillai, Mechanical properties and durability performance of concretes with limestone calcined clay cement (LC^3), Cement Concr. Res. 107 (2018) 136–151.
[12] R. Li, L. Lei, T. Sui, J. Plank, Effectiveness of PCE superplasticizers in calcined clay blended cements, Cement Concr. Res. 141 (2021), 106334.
[13] M. Schmid, J. Plank, Dispersing performance of different kinds of polycarboxylate (PCE) superplasticizers in cement blended with a calcined clay, Construct. Build. Mater. 258 (2020).
[14] M. Schmid, R. Sposito, C. Thienel, J. Plank, Novel Zwitterionic Superplasticizers for Cements Blended with Calcined Clays, 2018.
[15] M. Schmid, N. Beuntner, K.-C. Thienel, J. Plank, Amphoteric superplasticizers for cements blended with a calcined clay, in: ACI Symposium Publication 12th International Conference on Superplasticizers and Other Chemical Admixtures in Concrete, American Concrete Institute, Beijing, China, 2018, pp. 41–54.
[16] F. Nazário Santos, S. Raquel Gomes de Sousa, A. José Faria Bombard, S. Lopes Vieira, Rheological study of cement paste with metakaolin and/or limestone filler using Mixture Design of Experiments, Construct. Build. Mater. 143 (2017) 92–103.
[17] M. Schmid, J. Plank, Dispersing performance of different kinds of polycarboxylate (PCE) superplasticizers in cement blended with a calcined clay, Construct. Build. Mater. 258 (2020), 119576.
[18] M. Schmid, J. Plank, Interaction of individual meta clays with polycarboxylate (PCE) superplasticizers in cement investigated via dispersion, zeta potential and sorption measurements, Appl. Clay Sci. 207 (2021).
[19] H.H.C. Wong, A.K.H. Kwan, Packing density of cementitious materials: part 1—measurement using a wet packing method, Mater. Struct. 41 (4) (2008) 689–701.
[20] A. Kwan, H. Wong, Packing density of cementitious materials: Part 2-packing and flow of OPC + PFA + CSF, Mater. Struct. Materiaux et Construct. 41 (2008) 773–784.
[21] G. Marchetti, V.F. Rahhal, E.F. Irassar, Influence of packing density and water film thickness on early-age properties of cement pasteswith limestone filler and metakaolin, Mater. Struct. 50 (2) (2016).
[22] F. Avet, R. Snellings, A. Alujas Diaz, M. Ben Haha, K. Scrivener, Development of a new rapid, relevant and reliable (R^3) test method to evaluate the pozzolanic reactivity of calcined kaolinitic clays, Cement Concr. Res. 85 (2016) 1–11.
[23] A. Habbaba, J. Plank, Surface chemistry of ground granulated blast furnace slag in cement pore solution and its impact on the effectiveness of polycarboxylate superplasticizers, J. Am. Ceram. Soc. 95 (2) (2012) 768–775.
[24] DIN EN 196-1, Methods of Testing Cement – Part 1: Determination of Strength, 2016.
[25] S. Mantellato, R.J. Flatt, Shifting factor—a new paradigm for studying the rheology of cementitious suspensions, J. Am. Ceram. Soc. 103 (6) (2020) 3562–3574.
[26] L.G. Li, A.K.H. Kwan, Effects of superplasticizer type on packing density, water film thickness and flowability of cementitious paste, Construct. Build. Mater. 86 (2015) 113–119.
[27] J. Plank, C. Hirsch, Impact of zeta potential of early cement hydration phases on superplasticizer adsorption, Cement Concr. Res. 37 (4) (2007) 537–542.

Section 5.4

Publication # 4

Superplasticizers for calcined clay blended cements

R. Li, M. Schmid, T. Sui, J. Plank

15th International Conference on Recent Advances in Concrete Technology

and Sustainability Issues (CANMET/ACI)

July 13-15, 2022, Milan (Italy)

SP – 355 – 7.

In **publication # 4** (a conference paper), the influence of a meta kaolin rich calcined clay from China on conventional precast and ready-mix type PCEs in those composite cements was investigated.

At first, a series of precast-type PCEs was selected from the groups of MPEG, HPEG and IPEG polymers. Their dispersing effectiveness was tested in calcined clay composite cements with clinker substitution rates of 0 – 50 wt.%. It was found that the presence of **this calcined clay prompts significantly higher PCE dosages** (up to 800 % more for the 50:50 OPC/CC blend). Moreover, the **HPEG PCE performed best** in these composite cements, followed by the IPEG and the MPEG PCEs. Furthermore, the slump retention behavior of these composite cement was studied and compared with that of OPC. An industrial ready-mix type HPEG PCE and its combination with sodium gluconate was applied to achieve an appropriate slump retention time. Albeit, the results signify that in those calcined clay composite cements slump retention is more difficult to achieve than in OPC. In addition, also **the water demand** of four **pure calcined clays** were determined, and the order found was as follows: **meta muscovite ≫ meta illite ≫ meta kaolin > meta montmorillonite**.

This study concludes that a **calcined clay blended low-carbon cement requires** extremely **high PCE dosages** while providing ecological benefits. The extend of the negative **effect** on workability greatly **depends on the mineral phase composition in the raw clay**.

SP – 043 – 1

Superplasticizers for Calcined Clay Blended Cements

Ran Li, Marlene Schmid, Tongbo Sui, Johann Plank

Synopsis: In this study, the behavior of a calcined mixed clay (CMC) exhibiting a particularly high metakaolin content (~51 %) in composite cements (substitution rates 0–50 wt. %) was studied. It was found that CMC much decreases workability and substantially increases the water demand due to its higher fineness as compared to OPC. Furthermore, the water demand of pure calcined clays was investigated, and the order as follows was established: meta muscovite ≫ meta illite ≫ metakaolin > meta montmorillonite. Additionally, the dispersing effectiveness of a series of precast-type PCEs selected from the groups of MPEG, HPEG and IPEG polymers was tested in blended cements holding 0–50 wt. % of the CMC. According to this, the HPEG PCE disperses these composite cements best, followed by the IPEG and the MPEG PCEs. Generally, the presence of CMC prompts significantly higher PCE dosages (up to 800 % more for the 50:50 OPC/CC blend). Furthermore, it was found that in OPC/CMC blended cements slump retention is much more difficult to achieve than in OPC. As such, an industrial ready-mix type HPEG PCE or its combination with sodium gluconate failed to provide flowability retention times which are commonly required by the ready-mix industry. Our study concludes that while such low carbon calcined mixed clay blended cements offer significant ecological advantages, they demand higher superplasticizer dosages which negatively affects their cost effectiveness and at the same time poses significant technical challenges, particularly in ready-mix concrete applications. It should be mentioned that the problems pointed out here will be less severe for CMCs of lower metakaolin content.

Keywords: Polycarboxylate; superplasticizer; composite cement; calcined clay; metakaolin; workability; slump retention

INTRODUCTION

A noticeable CO_2 emission originates from the cement clinker production process which liberates approximately 8 % of all anthropogenic CO_2 [1]. Meanwhile, the worldwide demand for cement only keeps increasing every year. To solve this problem, researchers are focusing on supplementary cementitious materials (SCMs) exhibiting pozzolanic reactivity which could partially replace cement clinker [2-4] including micro silica, fly ash, blast furnace slag (GGBFS), limestone, burnt oil shale or calcined clay. Among all SCMs, calcined clay is drawing more and more attention due to its global ubiquitous availability and its high pozzolanic reactivity [5]. Generally, the thermal activation of clay is carried out at temperatures ranging from 600 to 900 °C. In the process of calcination, dehydroxylation of the clay associated with structural changes occurs resulting in partially amorphous phases exhibiting pozzolanic reactivity. According to those studies [6, 7], metakaolin (calcined kaolinite) possesses much superior pozzolanic reactivity as compared to meta montmorillonite or meta illite. Its high pozzolanic reactivity is attributed to the higher content of hydroxyl groups and their specific location in the structure of the clay [5]. In cement, metakaolin reacts with calcium hydroxide and produces alumina-containing hydrate phases including C_4AH_{13}, C_3AH_6 and C_2ASH_8. Thus, metakaolin presents a valuable component in calcined clays used in composite cements as it provides higher early strength [8]. Besides, metakaolin can also improve other concrete properties such as chloride [9] and corrosion resistance [10] and shrinkage reduction at early ages [11]. Unfortunately, a high metakaolin content present in the composite cement results in decreased workability, as was reported in some previous publications [12, 13].

In this study, at first the impact of a calcined mixed clay sample particularly rich in metakaolin (~ 51 wt. %) on workability and water demand of composite cements holding 0 – 50 wt. % of this calcined mixed clay was investigated. Moreover, the water demand of pure meta clay samples obtained from kaolinite, montmorillonite, illite and muscovite was determined to assess their individual impact on cement workability. Finally, the dispersing effectiveness of the common precast type PCEs based on HPEG, IPEG, and MPEG chemistry were evaluated and the slump retention behavior of a common ready-mix type PCE and its combination with a retarder (sodium gluconate) in these composite cements were evaluated. From the results the PCE admixtures which work particularly well in calcined clay blended cements was established.

RESEARCH SIGNIFICANCE

Calcined clay blended composite cements exhibit poor workability and high water demand as compared to OPC. Moreover, it has been noticed that slump retention is difficult to achieve for such cements. This study aimed to provide more insight into the impact of a metakaolin rich calcined mixed clay on workability and to uncover the dispersing effectiveness of differently composed PCE superplasticizers in composite cement prepared holding this calcined mixed clay. Based on these results a better understanding of the specific properties of calcined clay blended cements was sought to facilitate their widespread successful application in the future.

EXPERIMENTAL PROCEDURES

Materials

Cement sample

The cement used in this study was an ordinary Portland cement CEM I 42.5 R provided by Schwenk company (Allmendingen plant, Germany). This is a rapid set (R) cement resulting in > 42.5 N/mm² final compressive strength. Its phase composition as determined by quantitative X-ray diffraction (Q-XRD) including *Rietveld* refinement is shown in **Table 1**. Its *Blaine* value was 3,130 cm^2/g. Moreover, its particle size distribution was determined via laser granulometer (see **Figure 1)** and its d_{50} value was 18.13 µm.

Table 1–Phase composition of the cement sample CEM I 42.5 R

Phase/ Constituent	wt. %
C_3S, monoclinic	54.52
C_2S, monoclinic	18.41
C_4AF, orthorhombic	10.85
C_3A, cubic	5.23
C_3A, orthorhombic	0.88
Anhydrite ($CaSO_4$)	0.94

Dihydrate ($CaSO_4 \cdot 2H_2O$)	3.61
Hemihydrate ($2CaSO_4 \cdot H_2O$)	0.33
Calcite ($CaCO_3$)	3.04
Dolomite ($CaMg(CO_3)_2$)	1.13
Quartz (SiO_2)	0.91
Free lime (*Franke*)	0.14
Total	100.00

Calcined mixed clay sample

The calcined mixed clay used in this study was provided by Sinoma International Engineering Co., Beijing, China. It was produced in an industrial-scale rotary kiln at 800 °C. The chemical and mineralogical composition of the raw and the calcined clay as determined via Q-XRD is shown in **Table 2**.

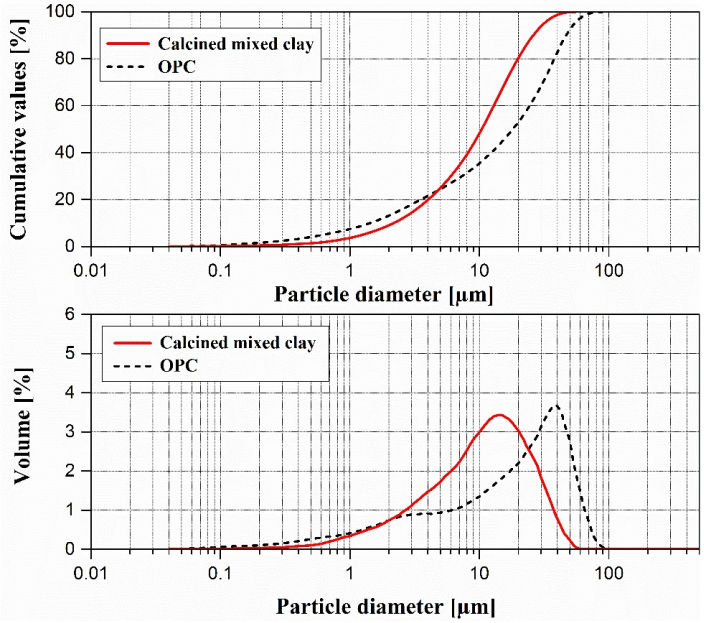

Fig. 1 – Particle size distribution of the OPC and calcined mixed clay samples used in the investigation.

This calcined mixed clay sample is characterized by a high metakaolin content (~ 51 wt. %) and a high amorphous content of ~ 68.2 wt. %. Its specific surface area (BET method) was 132,000 cm^2/g which is significantly higher than that of the OPC sample. **Figure 1** displays the particle size distribution of the calcined mixed clay which exhibits a d_{50} value of 10.42 µm. According to this, the calcined mixed clay sample used in this study exhibits a more narrow size distribution and generally is finer than the OPC sample.

Table 2–Mineralogical composition of the raw and the calcined mixed clay samples, as determined by XRD including Rietveld refinement.

Mineral phase	Raw clay (wt. %)	Calcined clay (wt. %)
Kaolinite	51.3	-
Illite – Smectite	19.7	-
Muscovite	18.1	2.3
Muscovite HT	-	15.5
Quartz	10.3	13.8
Rutile	0.5	0.3
Amorphous content	-	68.2
Total	99.9	100.1

Calcined pure clays

The first three meta clays are obtained from the group of Prof. Thienel at Universität der Bundeswehr München, Germany. Metakaolin was prepared industrially from > 73 wt. % pure kaolin via flash calcination between 550-650°C while meta illite and meta muscovite were obtained via 1 hour calcination at 770 °C and 800 °C, respectively. Meta montmorillonite was self-prepared applying a 2 hours calcination treatment in a lab-scale muffle furnace at 800 °C. Their specific surface area and d values are listed in **Table 3**.

Table 3–Properties if the calcined clay samples

Parameter	Meta muscovite	Meta kaolinite	Meta montmorillonite	Meta illite
Specific surface area [m^2/g]	11.8	17.8	34.8	94.6
Bulk density [g/cm^3]	2.79	2.61	2.59	2.72
d_{10} [µm]	9.3	3.0	6.5	2.7
d_{50} [µm]	19.2	14.8	39.1	6.8
d_{90} [µm]	45.7	76.2	107.0	61.9

[a] Values from [14]

PCE samples

A series of chemically diverse PCEs prepared from ω-methoxy poly(ethylene glycol) methacrylate ester (MPEG), methallyl poly(ethylene glycol) ether (HPEG) and isoprenyl oxy poly(ethylene glycol) ether (IPEG) macromonomer were utilized.

First, two precast type PCEs (designated as "45MPEG6" and "52IPEG6") characterized by high anionicity and relatively long PEG side chains were synthesized via free radical copolymerization at molar ratios of 6:1 ((meth)acrylic acid: macromonomer) following common literature descriptions [15, 16]. Additionally, an industrial high-range water-reducing type of PCE (denominated as "HPEG precast") and a commercial ready-mix, slump retaining type PCE (designated as "HPEG ready-mix") were also used in this study. Both industrial products were provided by JILIN Zhongxin Chemical Group Co. (Jilin, China). The chemical structures of all superplasticizer samples are displayed in **Figure 2**.

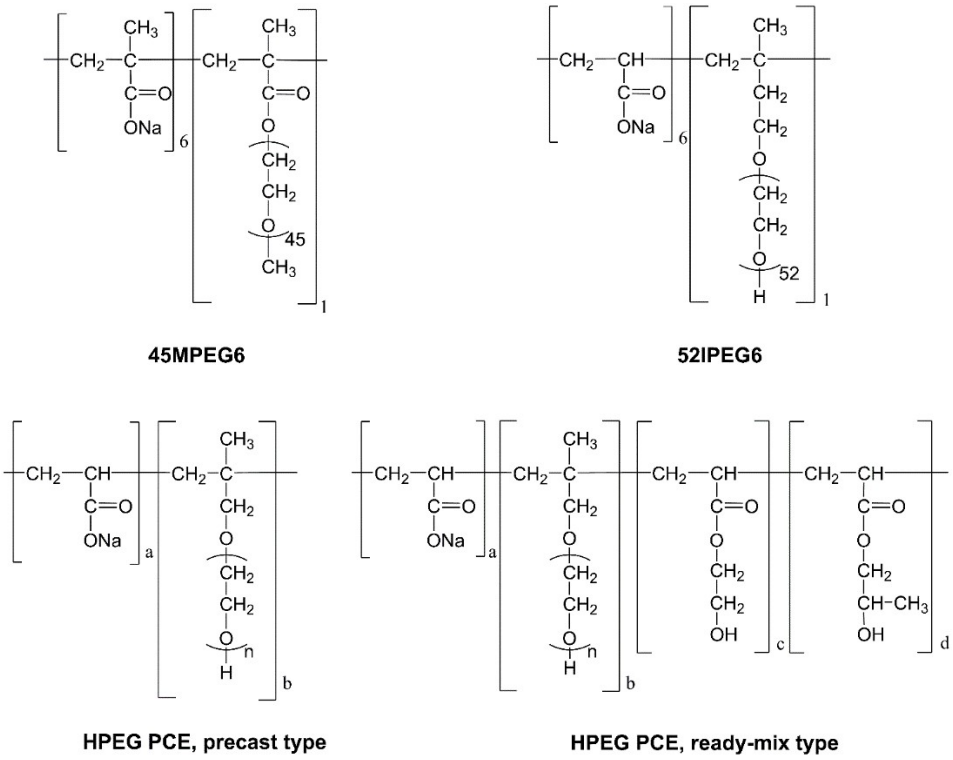

Fig. 2 – Chemical structures of the PCE samples used in the study.

Retarder
Sodium gluconate (> 99 % purity) supplied by China Academy of Building Research (CABR, Beijing) was applied as retarder.

Methods
Polymer analysis
The PCE samples were deployed to gel permeation chromatography (GPC) in order to determine their molecular properties (M_w, M_n, PDI). The measurements were performed on a *Waters 2695* separation module equipped with three Ultrahydrogel™ columns (120, 250, 500) and an Ultrahydrogel™ guard column (all from Waters, Eschborn, Germany). 0.1 M $NaNO_3$, 0.2 g/L NaN_3 (pH=12) was used as eluent at a flow rate of 1.0 mL min^{-1}.

Dispersing performance
A modified "mini slump" test according to DIN EN 1015 [17] was utilized to determine the spread flow of OPC and composite cement pastes. OPC:CC ratios of 90:10; 80:20; 70:30; 60:40 and 50:50 (by weight percent) were evaluated. A fixed water-to-binder ratio of 0.5 which corresponded to an OPC spread flow value of 18 ± 0.5 cm was used in all tests. The amount of water contained in the PCE solution was subtracted from the total amount of mixing water to maintain a constant w/b ratio. For instance, 0.45 mL of water was subtracted from total water for a PCE sample with solid content of 40 % at the dosage of 0.1 % bwob. At this w/b ratio, the dosages of the superplasticizer samples required to reach a spread flow of 26 ± 0.5 cm were determined. The "mini slump" test was carried out as follows: 300 g of binder were added to 150 mL of deionized water contained in a porcelain cup and stirred manually for 10 s with a spoon. Then PCE solution was added to the mixture and homogenized for 50 s. After 1 min of rest the suspension was mixed again for another 1 min. After stirring was finished, the freshly prepared paste was immediately filled into *Vicat* cone (height 40 mm, top diameter 70 mm and bottom diameter 80 mm) to the rim and then was quickly lifted upwards. The diameter of the cement paste which had spread out was measured at two perpendicular axes and averaged to obtain the final result.
The solid volume fractions of the different mixtures are listed in **Table 4**.

Table 4–Mineralogical composition of the raw and the calcined mixed clay samples, as determined by XRD including Rietveld refinement.

Samples	Solid volume fraction [%]
OPC	39.0
OPC:CC 90:10	39.3
OPC:CC 80:20	39.7
OPC:CC 70:30	40.0
OPC:CC 60:40	40.1

Slump retention
To investigate the slump retaining behavior of mortars admixed with the ready-mix type HPEG PCE and its combination with sodium gluconate retarder, the procedure following DIN EN 196-1 [18] was employed. In this experiment, a fixed water-to-binder ratio of 0.4 and a binder-to-sand ratio of 1:3 (wt./wt.) were utilized. The procedure was as follows: firstly, 450 g of OPC (or OPC:CC 70:30 binder) were added into a mixing bowl which contained 180 g of DI water holding the respective amount of PCE or PCE/retarder combination. The amount of water contained in the PCE solution was subtracted from the total amount of mixing water to maintain a constant water-to-binder ratio. Additionally, 1 drop of defoamer (Surfynol MD-20, Air Products, the Netherlands) was added to prevent any air entrainment by the PCE. Then, after a 4 min mixing schedule as specified by DIN EN 196-1 standard the spread flow was measured. For the time-dependent spread flow measurements individual values were taken every 30 min after the mortar had been prepared. Following each measurement, the mortar was transferred back to the mixing bowl and covered with a wet towel to avoid desiccation. Prior to each spread flow test, the mortar was re-stirred for 2 min at a speed of 285 rpm.

EXPERIMENTAL RESULTS AND DISCUSSION

Molecular properties of PCE samples

The PCE samples used in this study were characterized by GPC. The respective spectra are shown in **Figure 3**, while **Table 5** lists their molecular properties.

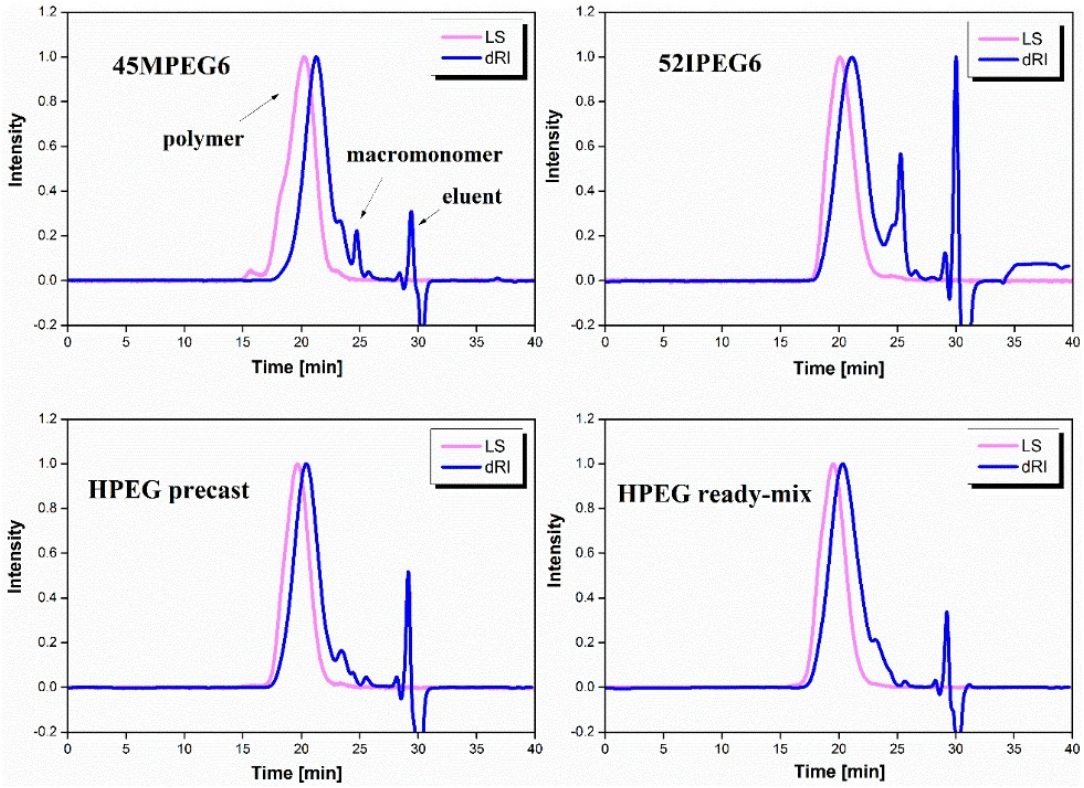

Fig. 3 – GPC spectra of all PCE samples tested in this study; eluent: 0.1 M $NaNO_3$ (LS: light scattering; dRI: differential refractometer)

According to these data, all PCE samples exhibit properties which are characteristic for high quality PCE polymers, especially low PDI values (1.8- 2.4) and high rates for macromonomer conversion (90 - 97 %). This signifies that all polymers used in this study meet highest quality standards.

Table–5 Molecular properties of the superplasticizer samples used in this study

PCE sample	M_w [Da]	M_n [Da]	PDI (M_w/M_n)	Conversion [%]
45MPEG6	25,180	10,610	2.4	95.1
52IPEG6	38,110	20,100	1.9	89.7
HPEG precast	35,340	19,490	1.8	91.8
HPEG ready-mix	40,170	18,900	2.1	92.0

Influence of calcined mixed clay on cement workability

At first, the impact of the calcined mixed clay on cement workability was studied. For this purpose, the spread flow values of pastes holding 0 – 50 wt. % of the calcined mixed clay were determined at a fixed water-to-binder ratio of 0.5, and the results are shown in **Figure 4**.

The results signify that addition of even a very minor amount (10 wt. %) of this calcined mixed clay significantly reduces the flowability of the cement paste. Furthermore, incorporating 20 wt. % of the calcined mixed clay results in a complete loss of flowability which declines from 19.2 cm to 9.3 cm. At even higher clinker replacement rates, a solid lump is obtained. Apparently, this calcined mixed clay affects cement workability extremely strong which is attributed to its high specific surface area as compared to that of the OPC sample.

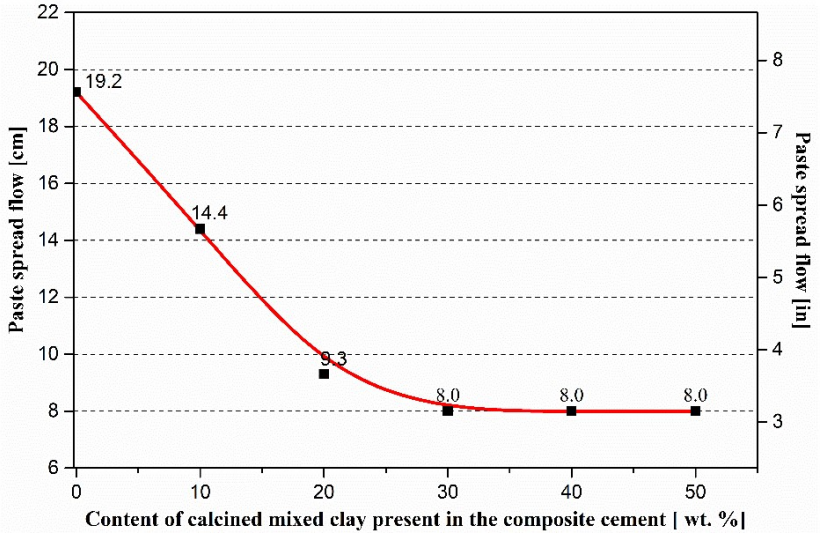

Fig. 4 – Impact of the calcined mixed clay sample on the workability of composite cements holding increasing amounts of this calcined mixed clay

Impact of calcined mixed clay sample on water demand

In the next step, for each composite cement the water-to-binder ratio required to achieve a spread flow value of 18 ± 0.5 cm was determined. The results are displayed in **Figure 5**.

As can be seen there, the water demand of the individual composite cements increases linearly with ascending calcined mixed clay content. For example, the water-to-binder ratio rises linearly from 0.5 (for neat OPC) to 0.98 at a clinker substitution rate of 50 wt. %. This result corroborates that the calcined mixed clay used in this study exhibits a particularly high water demand which is a consequence of its fine particles. Moreover, it has been reported that metakaolin – which commonly constitutes a fine powder obtained from the calcination process – strongly affects the water demand of calcined mixed clay samples [19]. In order to elucidate this aspect in more detail, the water demand of four pure calcined clay samples (meta muscovite, meta montmorillonite, meta illite and metakaolin) was determined and compared.

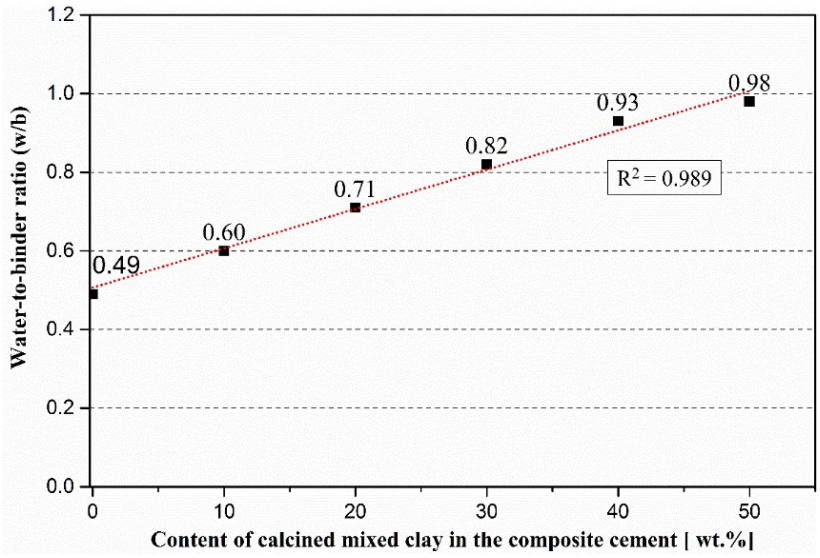

Fig. 5 – Water demand of composite cements containing 0 - 50 wt. % of the calcined mixed clay; amount of water required to reach a paste spread flow of 18 ± 0.5 cm; no PCE polymer added.

Water demand of pure calcined clay samples

Four meta clays (metakaolin, meta montmorillonite, meta illite and meta muscovite) were prepared via calcination of the pure clay samples, and their water demand was determined in the same manner as before for the composite cements. All meta clays were suspended in synthetic cement pore solution to simulate the environment in cement.

As is shown in **Figure 6**, all meta clay samples develop a significantly higher water demand than the OPC sample, and different meta clays exhibit significantly different water demands. The highest water demand was recorded for meta muscovite which achieves the target spread flow of 18 cm) at a water-to-solid ratio as high as 2.7. This is explained by the high specific surface area and the internal porosity of the meta muscovite particles. On the other hand, meta montmorillonite exhibits the lowest water demand because of its relatively coarse particles. From our previous work the calcined clay possessing high meta kaolin content always requires higher water demand due to the high specific surface area [13]. However, an even higher water demand value was registered for meta illite as compared to metakaolin.

The data presented in **Figure 6** signify that all meta clay samples cause a higher water demand than the Portland cement sample. This characteristics inevitably increases the water demand of composite cements when calcined clay is blended into these binders. Consequently, it has to be expected that the presence of calcined clay in a composite cement will prompt higher PCE dosages which was investigated in the following.

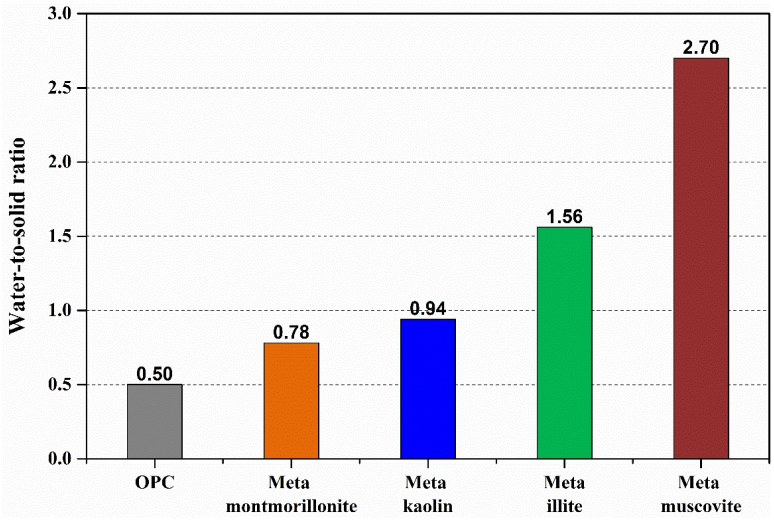

Fig. 6 – Water demand of the pure calcined clay samples suspended in synthetic cement pore solution; no PCE polymer added

Effectiveness of PCEs in composite cements holding calcined mixed clay

The dispersing ability of three PCE samples commonly used in precast concrete (high-range water-reducing type) in pastes prepared from neat OPC and OPC/CC composites at clinker substitution rates of 0 - 50 wt. % was assessed. In this experiment, the PCE dosages required to achieve a flow spread value of 26 cm were determined at a fixed water-to-binder ratio of 0.5.

According to the results presented in **Figure 7** it becomes clear that addition of this calcined mixed clay generally prompts higher PCE dosages, with a staggering increase of ~ 800 % for the 50:50 blend as compared to the OPC sample. On the other hand, different PCEs exhibit different dispersing effectiveness. The HPEG precast type PCE provides the best dispersing ability, in both OPC and calcined clay composite cement systems, and is followed by the IPEG PCE while the MPEG PCE consistently requires the highest dosages. Thus, the effectiveness of a PCE superplasticizer in calcined mixed clay cements can be derived from its performance in neat OPC.

It suggests that PCEs which work well in neat OPC will also exhibit a good performance in calcined clay composite cements.

The data from **Figure 7** also signify that it is quite difficult to achieve high flowability in composite cements holding substantial (e.g. ≥ 30 wt. %) cements of a calcined mixed clay which is rich in metakaolin.

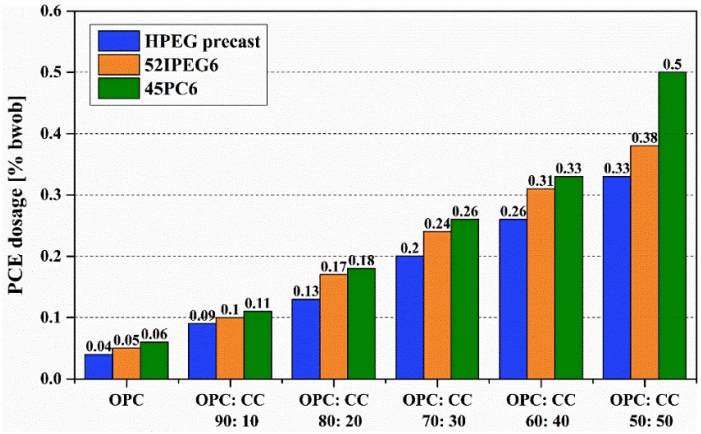

Fig. 7 – PCE dosages required in pastes from neat OPC and OPC/CC blends to achieve a spread flow of 26 ± 0.5 cm, w/b ratio = 0.5.

Slump retention of PCEs in calcined mixed clay blended cements

In ready-mix concrete, extended workability over e.g. 1 – 2 hours is commonly required to account for longer delivery times. For this purpose, specifically designed slump retaining PCE polymers [20] and/or PCE combinations with retarders [21] are used.

At first, an industrial ready-mix type HPEG PCE was utilized which provides long lasting flowability resulting from continuous hydrolysis of ester units into carboxylate groups which then facilitate adsorption of the PCE and hence a dispersing effect. The time – dependent flowability of mortars prepared from neat OPC and OPC/CC cements holding up to 40 wt.% of the calcined mixed clay was tested by recording the flowability of the mortars every half hour over a period of ~ 3 h until workability was completely was lost.

As is shown in **Figure 8**, in neat OPC the ready-mix HPEG PCE provides excellent slump retention over ~ 90 min before mortar flowability gradually declines. However, increasing substitution rates for the clinker seriously affect slump retention of the composite cements. Already at the substitution rate of 20 %, mortar flowability could be maintained for 60 min only and then declined steadily. At even higher contents of calcined mixed clay, workability decreased even more rapidly. For example, the 70:30 blended cement maintains its initial flowability for 30 min only, and for the 60:40 blend no slump retention at all was observed.

These results signify when using calcined clay blended cements slump retention presents a great challenge because conventional slump retaining PCEs do not perform to satisfaction.

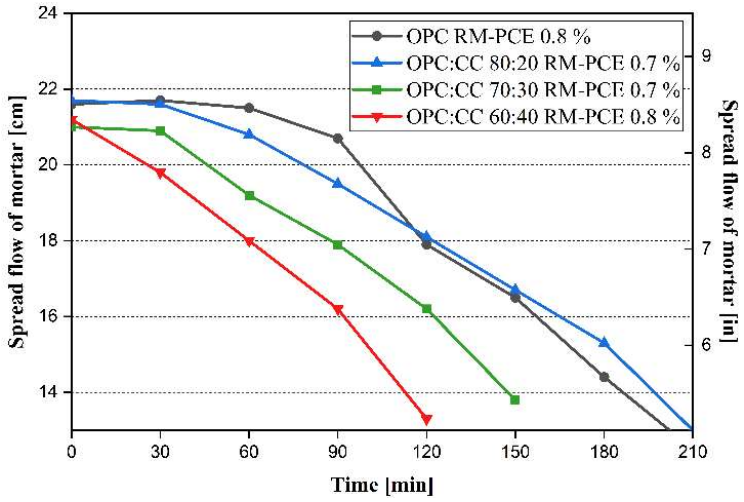

Fig. 8 – Flowability retention of mortars prepared from neat OPC or OPC/calcined mixed clay (CMC) blends admixed with different dosages of a commercial ready-mix HPEG PCE (RM-PCE), w/b ratio = 0.4

Slump retention of PCE/retarder combinations in composite cements

As was mentioned before, improved slump retention is also achieved by admixing retarders to cement and, more specifically, by combining slump retaining PCEs with retarders to improve their economics. Common retarders for this purpose include sodium gluconate or melasse (sugar syrup) [21]. In view of the relatively disappointing performance of the ready-mix HPEG PCE on its own, in the following a combination of the ready-mix PCE with sodium gluconate was tested to assess its effect on slump retention in neat OPC and OPC:CC 70:30 cement based mortars.

As is displayed in **Figure 9**, in the neat OPC system addition of 0.03 wt. % of sodium gluconate (such dosage is commonly used in practice) extended workability of the mortar admixed with the ready-mix HPEG PCE noticeably to ~100 min. This can be attributed to a synergistic effect between the PCE and the retarder as is well established for CEM I/II/III cements. The effect of sodium gluconate on OPC is based on retardation of the hydration process by inhibiting the hydration of C_3S at the early hydration period which increased the duration of induction period [22, 23].

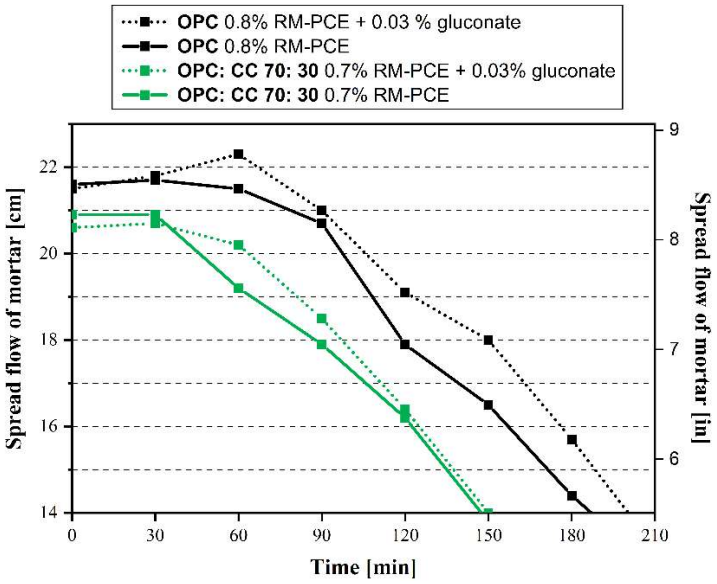

Fig. 9 – Flowability retention of mortars prepared from neat OPC or an OPC:CC 70:30 blend, admixed with ready-mix HPEG PCE (RM-PCE), with or without sodium gluconate; w/b ratio = 0.4.

However, when tested in a mortar prepared from a composite cement holding 30 wt. % of the calcined mixed clay, this combination of ready-mix HPEG PCE and sodium gluconate was unable to provide a sufficiently long workability time (see **Figure 9**). Still some improvement was observed, but the extension gained in no way satisfies the need of the ready-mix concrete industry in actual applications. It should be noted here that higher gluconate dosages did not produce any improvement.

To summarize, when using blended cements containing significant portions of calcined mixed clay flowability retention presents a serious problem because currently existing technology which was established based on OPC systems fails to perform well in those systems.

CONCLUSIONS

Based on the results of this experimental investigation, the following conclusions can be drawn:

1. Substitution of clinker with a calcined mixed clay decreases the workability of the composite cement, and this negative effect becomes even more severe at increasing calcined clay contents.
2. Cements holding calcined mixed clay exhibit a significantly increased water demand and, correspondingly, prompt higher PCE dosages to achieve the same flowability as the OPC base. This effect if owed to the high specific surface area of the calcined clay.
3. High content of metakaolin present in the calcined mixed clay affects water demand, workability and PCE dosages most severely.

4. Pure meta clays generally exhibit a higher water demand as compared to OPC. This property is most pronounced for meta muscovite (450 % increase in water demand vs. OPC) and less for meta illite (+ 200 %), metakaolin (+ 90 %) and meta montmorillonite (+ 55 %).
5. From the group of MPEG, IPEG and HPEG pecast-type PCEs the latter produced superior dispersing performance in calcined mixed clay blended composite cements.
6. The presence of a calcined mixed clay in a composite cement makes it extremely difficult to achieve proper slump retention. Because commonly practiced technology does not work well for those cements. Substantial research and innovation are needed to solve this problem which could be directly linked to the high metakaolin content of this calcined mixed clay sample used in this study.

Our findings suggest that although a high metakaolin content in a calcined mixed clay is very advantageous with respect to the early strength development of such cements, it brings about significant negative effects on workability and flowability retention which may hamper its widespread application especially in the ready-mix concrete industry.

ACKNOWLEDGMENTS

Ran Li wants to show her gratitude to China Scholarship Council (CSC) for financial support of her Ph.D. study at TU München. The authors also thank Jilin Zhongxin Chemical Group Co. Ltd. for providing the HPEG PCEs and Schwenk Cement Co. for supplying the CEM I 42.5 R sample. Moreover, the authors would like to thank Prof. Thienel and his team for supporting this work by providing samples of metakaolin, meta illite, meta muscovite and the analysis shown in Table 2. Finally, Deutsche Forschungsgemeinschaft (DFG) is thanked for providing funding for Marlene Schmid's research.

REFERENCES

1. Andrew, R. M., Global CO2 emissions from cement production. *Earth System Science Data* **2018,** *10* (1), 195-217.
2. Samarakoon, M. H.; Ranjith, P. G.; Rathnaweera, T. D.; Perera, M. S. A., Recent advances in alkaline cement binders: A review. *Journal of Cleaner Production* **2019,** *227*, 70-87.
3. Shi, C.; Qu, B.; Provis, J. L., Recent progress in low-carbon binders. *Cement and Concrete Research* **2019,** *122*, 227-250.
4. Scrivener, K.; Martirena, F.; Bishnoi, S.; Maity, S., Calcined clay limestone cements (LC3). *Cement and Concrete Research* **2018,** *114*, 49-56.
5. Siddique, R.; Klaus, J., Influence of metakaolin on the properties of mortar and concrete: A review. *Applied Clay Science* **2009,** *43* (3-4), 392-400.
6. Fernandez, R.; Martirena, F.; Scrivener, K., The origin of the pozzolanic activity of calcined clay minerals: A comparison between kaolinite, illite and montmorillonite. *Cement and Concrete Research* **2011,** *41* (1), 113-122.
7. Hollanders, S.; Adriaens, R.; Skibsted, J.; Cizer, Ö.; Elsen, J., Pozzolanic reactivity of pure calcined clays. *Applied Clay Science* **2016,** *132-133*, 552-560.
8. Tironi, A.; Trezza, M. A.; Scian, A. N.; Irassar, E. F., Potential use of Argentine kaolinitic clays as pozzolanic material. *Applied Clay Science* **2014,** *101*, 468-476.
9. Poon, C. S.; Kou, S. C.; Lam, L., Compressive strength, chloride diffusivity and pore structure of high performance metakaolin and silica fume concrete. *Construction and Building Materials* **2006,** *20* (10), 858-865.
10. Batis, G.; Pantazopoulou, P.; Tsivilis, S.; Badogiannis, E., The effect of metakaolin on the corrosion behavior of cement mortars. *Cement and Concrete Composites* **2005,** *27* (1), 125-130.
11. Brooks, J. J.; Megat Johari, M. A., Effect of metakaolin on creep and shrinkage of concrete. *Cement and Concrete Composites* **2001,** *23* (6), 495-502.
12. Schmid, M.; Plank, J., Dispersing performance of different kinds of polycarboxylate (PCE) superplasticizers in cement blended with a calcined clay. *Construction and Building Materials* **2020,** *258*.
13. Li, R.; Lei, L.; Sui, T.; Plank, J., Effectiveness of PCE superplasticizers in calcined clay blended cements. *Cement and Concrete Research* **2021,** *141*, 106334.
14. Sposito, R.; Beuntner, N.; Thienel, K.-C., Characteristics of components in calcined clays and

their influence on the efficiency of superplasticizers. *Cement and Concrete Composites* **2020,** *110*.
15. Plank, J.; Li, H.; Ilg, M.; Pickelmann, J.; Eisenreich, W.; Yao, Y.; Wang, Z., A microstructural analysis of isoprenol ether-based polycarboxylates and the impact of structural motifs on the dispersing effectiveness. *Cement and Concrete Research* **2016,** *84*, 20-29.
16. Plank, J.; Pöllmann, K.; Zouaoui, N.; Andres, P. R.; Schaefer, C., Synthesis and performance of methacrylic ester based polycarboxylate superplasticizers possessing hydroxy terminated poly(ethylene glycol) side chains. *Cement and Concrete Research* **2008,** *38* (10), 1210-1216.
17. DIN EN 1015-3: 2007-5. In *Methods of test for mortar for masonry –Part 3: Determination of consistence of fresh mortar (by flow table)*.
18. Lahalle, H.; Cau Dit Coumes, C.; Mercier, C.; Lambertin, D.; Cannes, C.; Delpech, S.; Gauffinet, S., Influence of the w/c ratio on the hydration process of a magnesium phosphate cement and on its retardation by boric acid. *Cement and Concrete Research* **2018,** *109*, 159-174.
19. Gmür, R.; Thienel, K.-C.; Beuntner, N., Influence of aging conditions upon the properties of calcined clay and its performance as supplementary cementitious material. *Cement and Concrete Composites* **2016,** *72*, 114-124.
20. Liu, X.; Wang, Z. M.; Li, H. Q.; Li, T., Mechanism and Application Performance of Slow-Release Polycarboxylate Superplasticizer. *Advanced Materials Research* **2012,** *560*, 574-579.
21. Cheung, J.; Jeknavorian, A.; Roberts, L.; Silva, D., Impact of admixtures on the hydration kinetics of Portland cement. *Cement and Concrete Research* **2011,** *41* (12), 1289-1309.
22. Lv, X.; Li, J.; Lu, C.; Liu, Z.; Tan, Y.; Liu, C.; Li, B.; Wang, R., The Effect of Sodium Gluconate on Pastes' Performance and Hydration Behavior of Ordinary Portland Cement. *Advances in Materials Science and Engineering* **2020,** *2020*, 9231504.
23. Ma, S.; Li, W.; Zhang, S.; Ge, D.; Yu, J.; Shen, X., Influence of sodium gluconate on the performance and hydration of Portland cement. *Construction and Building Materials* **2015,** *91*, 138-144.

BIOGRAPHY

Ran Li studied materials and science engineering. She holds a B.Sc. degree from Qingdao University of Technology and a M.Sc. degree from University of Jinan, China. Since 2018 she is a Ph.D. candidate at the Chair for Construction Chemistry (Prof. Plank) at Technical University of Munich (TUM), Germany. Her research focuses on the interaction between calcined clays and PCE superplasticizers and rheological aspects of calcined clay blended low carbon cements.
Marlene Schmid studied chemistry at Technical University of Munich (TUM), Germany and received her B.Sc. and M.Sc. from there. From 2017- 2020, she was a Ph.D. student at the Chair for Construction Chemistry (Prof. Plank) at TUM. Her research focused on the synthesis and performance of novel superplasticizers for cements containing calcined clays as supplementary cementitious material (SCM).
Tongbo Sui is vice president at Sinoma International Engineering Co., Ltd., China. As a professor, he focuses on the R&D of low energy and low CO_2 emission advanced cement based materials. He received various awards including that of a national expert on cement based materials, the 2nd class national prize for technological invention on low energy and low emission high belite cement, and for his outstanding contributions to the technology of cement and concrete.
Johann Plank is full Professor for Construction Chemistry at Technische Universität München, Germany. His research interests include cement chemistry, chemistry of low-carbon binders, chemical admixtures, organic-inorganic composites and nano materials, latex dispersions, concrete, dry-mix mortars and oil well cementing. Prof. Plank authored 450 scientific papers, holds 40 patents and in 2015 received the prestigious Alois Aignesberger award from CANMET/ACI in honor of his profound work and inventions in the field of superplasticizers and other admixtures.

Section 5.5

Publication # 5

Influence of calcined clays on workability of low-carbon composite cements

R. Li, M. Schmid, T. Sui, J. Plank

International Conference series on Geotechnics, Civil Engineering and Structures (CIGOS), October 28-29, 2021, Ha Long (Vietnam).

Emerging Technologies and Applications for Green Infrastructure

Springer, Singapore, 2022. 677-685.

DOI: 10.1007/978-981-16-7160-9_68

As is known, the deposits of clays are non-homogeneous with respect to mineral type, crystallinity and particle size etc. which significantly affects the properties of calcined clay samples. Therefore, it is necessary to investigate the **impact of different clay minerals on the workability**.

This work in this **publication # 5** was carried out in cooperation with another Ph. D. candidate, Marlene Schmid. **Four pure meta phases** obtained via calcination of natural **kaolin, montmorillonite, illite and muscovite were investigated** with respect to their water demand. It was found that the negative effect in workability depends on the **chemical composition** of the native clay and **the fineness and internal porosity of the calcined clay**. Moreover, three industrial calcined clay samples originating from natural deposits in Germany, India and China were investigated regarding to the water demand of composite cements formulated from them. The results instigate that the increase in **water demand correlates with the particle size**, the **amorphous part** and the **meta kaolin content** of the calcined clays.

The study concludes that although calcined clays offer the potential of significant CO_2 reduction in cement manufacture, higher superplasticizer dosages need to be used. This signifies that new improved admixture technology needs to be developed to make the application of such new green cements more attractive.

INFLUENCE OF CALCINED CLAYS ON WORKABILITY OF LOW CARBON COMPOSITE CEMENTS

Ran Li[1], Marlene Schmid[1], Tongbo Sui[2] and Johann Plank[1]

[1] Technische Universität München, Department of Chemistry, Chair for Construction Chemistry, Lichtenbergstrasse 4, 85747 Garching
[2] Sinoma Int'l & Sinoma Research Institute, No. 16 North Wangjing Road, Chaoyang District Beijing, 100102 China

Abstract. This work highlights that the CO_2 footprint of cement can be reduced significantly by blending Portland cement clinker with thermally activated (calcined) clay (CC). Investigations on pure meta phases obtained *via* calcination of native kaolin, montmorillonite, illite and muscovite reveal that they noticeably increase the water demand and decrease workability of the cement. The effect depends on the fineness and internal porosity of the calcined clay and the chemical composition of the native clay. A comparison of three industrial calcined samples of mixed layer clays originating from natural deposits in Germany, India and China confirmed the increased water demand of composite cements holding up to 40 wt. % of these calcined clays. The increase in water demand correlates with the amorphous part and the meta kaolin content. Also, the particle size and morphology of the calcined clay impact water demand. For one sample holding ~ 50 % meta kaolin, an increase in superplasticizer dosage of ~ 400 % as compared to neat OPC was recorded. Whereas, a high content of meta kaolin proved to be favorable with respect to rapid early strength development as a result of its high pozzolanic reactivity. It can be concluded that calcined clays offer the potential of significant CO_2 reduction in cement manufacture, however higher superplasticizer dosages need to be used. Still, because of the low CO_2 footprint of superplasticizers a substantial savings in CO_2 emission can be realized, and the cement industry can progress into an era of more eco-friendly binders.

Keywords: Cement, CO_2 footprint, Clay minerals, Calcined clay, Admixtures, Superplasticizers, Workability.

2

1 Introduction

The production of Ordinary Portland Cement (OPC) comes with a significant environmental impact because per ton of OPC, no less than 850 kg of the greenhouse gas CO_2 are emitted [1]. This means that at the current volume of global cement production of about 4.4 billion tons, over 3 billion tons of CO_2 are released. This represents roughly 7 % of total anthropogenic CO_2 emission and even exceeds that from the global air traffic. Consequently, there is a dire need to reduce the environmental footprint of cement.

Recently, a new concept for the partial substitution of cement clinker by thermally activated (calcined) clays has been introduced, with the most prominent example being the so-called LC^3 cement [2]. Its clinker content is reduced to 50 %, with the remainder being calcined clay (30 %), limestone powder (15 %) and gypsum (5 %) [3]. The main advantages of LC^3 lie in the worldwide availability of huge clay deposits and the relatively low calcination temperature for the clay (~ 650 – 850 °C vs. 1450 °C for Portland cement).

In this paper, at first the characteristic properties of four different pure calcined clays – meta kaolin, meta montmorillonite, meta illite and meta muscovite – will be presented and their particle size, water demand and behavior towards a common industrial polycarboxylate (PCE) superplasticizer will be compared in order to understand the specifics of each pure calcined clay. Thereafter, three industrially produced calcined mixed layer clays obtained from different clay deposits were blended with a Portland cement CEM I 42.5 R at a clinker substitution rate of 30 wt. % and their behavior in cement with respect to water demand, response to superplasticizer and strength development was analyzed. The overall goal of the study was to develop a more fundamental understanding of the behavior of thermally activated clays blended into cement and to assess their general usefulness in practical applications.

2 Materials and Methods

Cement. An ordinary Portland cement (OPC) CEM I 42.5 R (Schwenk Zement KG, Allmendingen plant, Germany) was used in the study. Its phase composition is shown in **Table 1**. The average particle size (d_{50} value) measured by laser granulometry was 19.8 µm. A density of 3.15 g/cm^3 was determined by helium pycnometry and for the specific surface area (*Blaine* fineness) a value of 3,020 cm^2/g was obtained.

Table 1 - Phase composition of the CEM I 42.5 R sample as determined by Q-XRD using *Rietveld* refinement (left); mineralogical analysis of the calcined mixed layer clay samples used in the study (right).

Phase	**[wt. %]**
C_3S, m	57.4
C_2S, m	15.2
C_3A, c	5.7
C_3A, o	1.8
C_4AF, o	9.5
Free lime (*Franke*)	0.8
Periclase	0.6
Anhydrite	2.3
Hemihydrate*	2.3
Gypsum*	0.3
Calcite	2.6
Quartz	0.4
Dolomite	1.1
Total	100.0

*Determined *via* thermogravimetry.

Phase	**Mineral content [wt. %]**		
	German CC	**Chinese CC**	**Indian CC**
Illite-Smectite	4.6	-	-
Muscovite	2.2	5.2	-
Muscovite HT	-	18.6	-
Kaolinite	-	-	5.5
Mullite	-	-	8.8
Cristobalite	-	-	2.2
Chlorite	0.4	-	-
Quartz	16.2	13.8	1.0
Feldspars	6.0	-	
Calcite	0.6	-	0.6
Sulfates	1.6	-	-
Silicates	6.3	-	-
Hematite	0.6	-	0.8
Pyrite	1.1	-	-
Anatase	-	-	1.6
Rutile	-	0.3	0.7
Amorphous content	**60.8**	**62.2**	**78.9**

Pure calcined clay samples. Meta kaolin was prepared industrially from > 73 wt. % pure kaolin *via* flash calcination between 550 ° and 650 °C. Meta montmorillonite was self-prepared *via* 2 hours calcination in a lab-scale muffle furnace at 800 °C. In the same furnace, meta illite and meta muscovite were prepared *via* 1 hour calcination at 770 °C and 800 °C, respectively.

Calcined mixed layer clay samples. Three mixed layer clay samples were subject to calcination at 750 °C (German CC) and 800 °C (Indian and Chinese CC). The mineralogical analysis of these three samples is presented in **Table 1**.

PCE superplasticizer. As superplasticizer, a commercial industrially produced acrylic acid-co-methallyl polyethylene glycol polycarboxylate (HPEG PCE) was used. This kind of PCE is most popular in the Asian market. Owed to its high anionic charge density, this type is mostly applied in precast concrete.

4

3 Results and Discussion

Pure Calcined Clay Samples

As a first, the pure calcined clay samples were characterized.

XRD analysis revealed the **mineralogical compositions**. According to this data it is evident that meta kaolin contains the highest content of amorphous phase (93 wt. %) while meta montmorillonite exhibited the lowest (10 wt. %). Generally, the amorphous content presents the dehydroxylated phases which are responsible for the pozzolanic activity of a calcined clay [4]. Hence, the data suggest that meta kaolin exhibits the highest reactivity (thus producing a particularly high early strength) while meta montmorillonite and meta illite will hydrate slower in cement and meta muscovite can be expected to present the least reactive of the four clinker phases.

It is well established that the pozzolanic reactivity of thermally activated clays is also much impacted by the fineness of the CC sample. To elucidate further, a **particle size analysis** was performed for the four meta clay samples. It revealed that meta illite consisted of particularly fine particles whereas meta montmorillonite presented a relatively coarse material. Relative to their d_{50} values, the order as follows could be established: Mmo≫ Mmu > Mka ≫ Mil.

In the next step, the **specific water demand** of each meta clay sample was determined. The "water demand" is defined as the amount of water which is required to achieve a specific spread flow (e.g. 18 ± 0.5 cm) from a suspension of the meta clay in synthetic cement pore solution. According to this experiment, different meta clays exhibited significantly different water demands, as is evident from Figure 2. By far the highest water demand was recorded for meta muscovite (w/b ratio = 2.70) as a consequence of its high surface area and the internal porosity of the particles. As expected, the lowest water demand was observed for the relatively coarse meta montmorillonite, and medium water demand values could be assigned to meta kaolin and meta illite.

The data presented in **Figure 1** signify that all meta clay samples cause a higher water demand than the Portland cement sample. This allows to predict that when such calcined clay materials are blended with cement clinker, then the water demand of the resulting composite cement will increase as compared to the neat OPC. The increase will be less when the raw clay used in the calcination predominantly contains montmorillonite, but will be most pronounced when the calcined clay is rich in meta illite or meta muscovite. The consequence of this behavior is that cements blended with meta muscovite require particularly high dosages of superplasticizers to reduce the water content to practical values which typically lie around 0.5 to achieve acceptable strength values whereas meta kaolin and meta montmorillonite are more benign and require less superplasticizer to reach the required water-to-binder ratio of ~ 0.5.

In order to elaborate more on the **dispersing behavior** of the different meta clay phases when treated with the HPEG PCE superplasticizer, the spread flow of pastes

prepared from the calcined clay samples in synthetic cement pore solution and admixed with the acrylic acid-co-methallyl polyethylene glycol polycarboxylate (HPEG PCE) superplasticizer was examined. There, the water-to-binder ratios exhibited in **Figure 1** which produce a spread flow value of 18 cm were used for each CC sample. The results are exhibited in **Figure 2**.

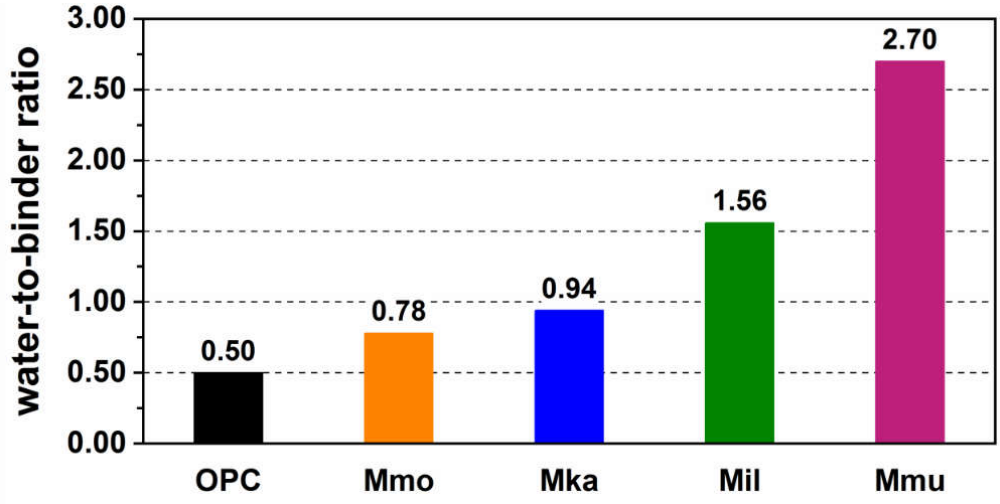

Figure 1 - Specific water demand for the pure calcined clay samples and the CEM I 42.5 R sample used in the study.

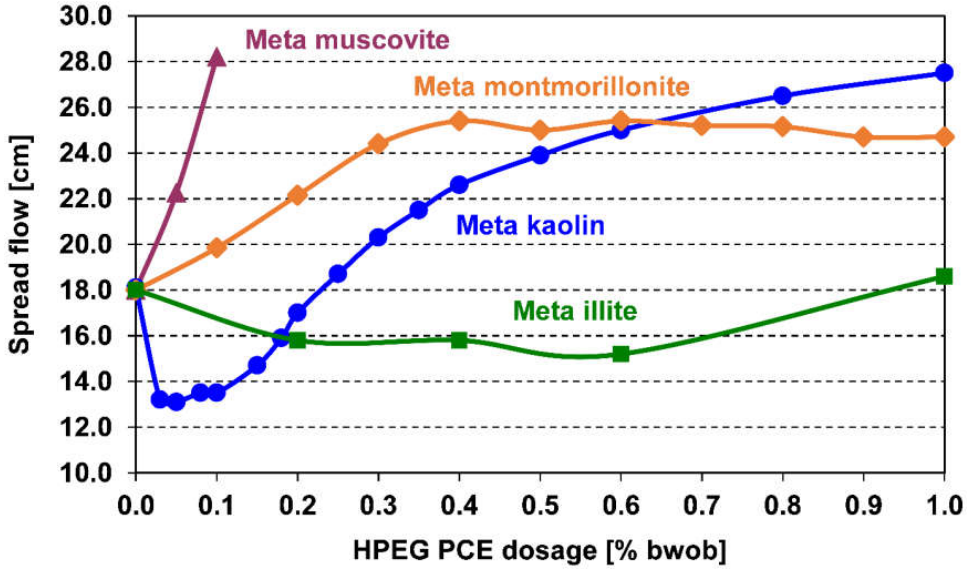

Figure 2 - Dispersing behavior of the pure calcined clay samples suspended in synthetic cement pore solution and admixed with increasing dosages of HPEG PCE; w/solids ratios: Mmu = 2.70; Mmo = 0.78; Mka = 0.94; Mil = 1.56.

6

The data clearly suggest that the suspension of meta muscovite is very easy to disperse, i.e. a low dosage (0.1 % by weight of CC) of the HPEG PCE is sufficient to increase the spread diameter from 18 to 28 cm. In comparison, meta montmorillonite already requires a PCE addition of 0.4 % to reach only 26 cm spread flow which presents the maximum achievable value. Furthermore, meta kaolin first is thickened by dispersant addition, but then at dosages > 0.2 % strongly responds to the polycarboxylate and reaches high fluidity (~ 28 cm at a dosage of 1.0 %). Most surprising is the behavior of the meta illite paste which does not become fluid even at a dosage of 1.0 % of PCE. It can be assumed that its pronounced fineness and the concomitant high surface area necessitate extremely high dispersant additions to cover these surfaces *via* physical adsorption.

Calcined Mixed-Layer Clay Samples

As mentioned before, actual natural clay and marl deposits always contain a mixture of different clays, and the variations in composition can be enormous. For this reason, three samples of calcined mixed layer clays from Germany, India and China were probed for their behavior in cement, and an attempt was made to correlate their properties with the content of individual clay components such as the portion of meta kaolin, meta illite etc.

At first, the **particle size distribution** of the three samples was captured *via* laser granulometry. The results are displayed in **Figure 3**.

There, it is observed that the German CC exhibits a larger particle size (d_{50} value = 13.2 µm) than the Chinese CC (d_{50} value = 10.4 µm). The Indian CC differs significantly from them in that it contains at the same time relatively high fractions of fine and of coarse particles. All three CC samples exhibit higher fineness than the OPC sample which is used to formulate the composite cements. Thus, it becomes evident that in such CC blended cements, the water demand will increase.

Furthermore, the phase composition of the calcined mixed layer clays was assessed *via* XRD. It was found that the **amorphous content** increased from 60.8 % for the German CC to 62.2 % for the Chinese CC and to 78.9 % for the Indian CC (see **Table 1**). Moreover, analysis of the raw clays utilized in the manufacture of these CCs produced kaolinite contents of 25 % (German clay), 45 % (Indian clay) and 51 % (Chinese clay). This signifies that the Indian and the Chinese calcined clays are particularly rich in meta kaolin.

7

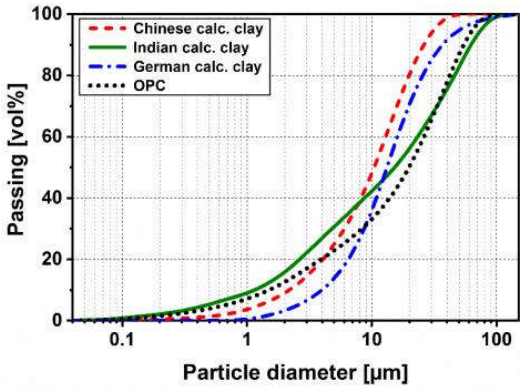

Sample	Particle size [µm]		
	d10	*d50*	*d90*
Chinese CC	2.2	10.4	26.2
Indian CC	1.1	15.0	62.5
German CC	4.0	13.2	37.0
OPC	1.5	19.8	54.6

Figure 3 - Particle size analysis of the three calcined mixed layer clay samples prepared from German, Indian and Chinese natural clay deposits.

The **dispersing effectiveness** of the HPEG PCE sample on the composite cements holding 20, 30 or 40 wt. % of the mixed layer CCs was probed next. **Figure 4** shows the results. It was found that the binder holding the German CC required the lowest dosages to achieve the target spread flow value of 26 cm. The Indian mixed layer CC demands significantly higher dosages than the German CC and behaves more similar to the cement holding the Chinese CC which prompts exceptionally high PCE dosages. To summarize, for the composite cement holding 40 wt. % of the German CC, the PCE dosage increases by 60 % whereas it rises by 280 % for the Indian CC and by a staggering 420 % for the Chinese CC.

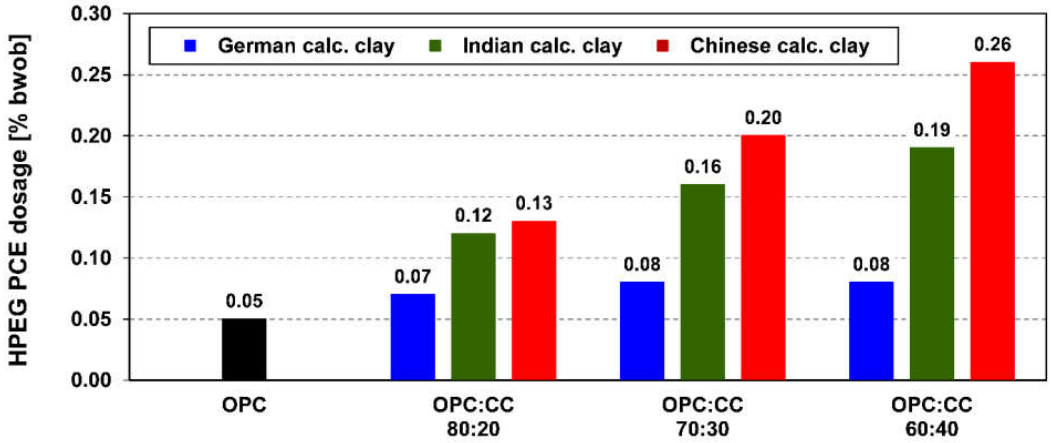

Figure 4 - Dosages of the HPEG PCE superplasticizer required in OPC and OPC/CC composite cements to increase the spread flow of the pastes from 18 to 26 cm.

8

4 Conclusion

This study first elaborates on the behavior of pure calcined kaolin, montmorillonite, illite and muscovite. It is shown that in comparison to an ordinary Portland cement, all calcined clays prompt a higher water demand and thus higher superplasticizer dosages to achieve the same workability as in neat Portland cement. This behavior is explained by their higher fineness (resp. surface area) in comparison to OPC. Moreover, it was found that the presence of meta muscovite and meta illite in composite cements (70:30) increases the dosage of HPEG PCE by as much as 14 times (Mmu) or 10 times (Mil) while meta kaolin prompts only a slight increase (5 times) and meta montmorillonite no increase at all. The results signify that when the calcined clay samples contain certain meta clays, then the selection of a high performance PCE presents the key for its applicability in cement.

Second, composite cements were prepared, and their water demand, response to superplasticizer addition and early strength were investigated. It was confirmed that the content of specific meta clay phases controls their behavior. For example, a high content of meta kaolin provides high early strength, but is very unfavorable with respect to workability and necessitates high addition rates of superplasticizer. As such, depending on the requirements for workability or strength development, either clay deposits which are rich in kaolin content or those which are low on this mineral should be selected.

The study also reveals that while calcined clays significantly reduce the CO_2 footprint of cement and offer the potential of a more eco-friendly binder, they partially compromise this advantage because of higher superplasticizer dosages required. However, considering the very minor amount of CO_2 associated with PCE production, still a significant savings can be realized from the use of calcined clay blended cements. This way, the cement industry can move into an era of more eco-friendly production.

References

1. The Cement Sustainable Initiative (CSI). 2016. Getting the Numbers Right, Project Emissions Report 2014.
2. Scrivener K, Martirena F, Bishnoi S, Maity S. 2018. Calcined clay limestone cements (LC3). In: Cement and Concrete Research. Volume 114. p. 49-56.
3. Scrivener K, Avet F, Maraghechi H, Zunino F, Ston J, Hanpongpun W, Favier A. 2019. Impacting factors and properties of limestone calcined clay cements (LC3). In: Green Mater. Volume 77. p. 3-14.
4. Hollanders S, Adriaens R, Skibsted J, Cizer Ö, Elsen J. 2016. Pozzolanic reactivity of pure calcined clays. In: Applied Clay Science. Volume 132-133. p. 552-560.

Section 5.6

Publication # 6

Effect of calcined clay types on the performance of polycarboxylate superplasticizers

R. Li, L. Lei, J. Plank

8th National Conference on Polycarboxylate Superplasticizer and Application Technology

Nov. 21 - 23, 2022, Xiamen (China)

Proceedings, 70 - 74.

This **publication # 6** (a conference paper), discussed the influence of calcined clays from different sources on the dispersing performance of PCE superplasticizers in a composite cement containing those calcined clays. **Three calcined common clay samples** were selected from different countries: Germany, India and China respectively. The workability of the composite cement admixed with PCEs and prepared from these clays with a clinker substitution ratio of 70:30 was compared with that of OPC. It is found that the **PCE dosages** required for those calcined clay blended cements significantly **depend** on the **types of calcined clay**. Interestingly, the higher the meta kaolin content in the calcined clay, the more PCE dosage is required. On the other hand, high meta kaolin content in the calcined clay promotes the early strength development of those composite cements.

In worldwide clay deposits the mineral composition of the clays varies considerably which leads to inconsistent calcined clay composite cements. Therefore, it is necessary to understand the impact of different clay minerals and their calcined phases on the workability of concrete.

煅烧黏土种类对聚羧酸高性能减水剂工作性能的影响研究

李冉，雷蕾，Johann Plank
（慕尼黑工业大学无机化学系，德国慕尼黑）

摘要：掺煅烧黏土的复合水泥作为新型低碳水泥引起了业内学者的广泛关注。但是通常来讲煅烧黏土需水量高，可大幅度降低 PCE 对水泥基材料的分散能力。而不同类型的煅烧黏土对 PCE 的作用影响差异较大。本文主要探究了煅烧黏土的类型对复合水泥流动性能的影响。首先通过 XRD 对来自不同地域的煅烧黏土进行表征。然后测试了商用 HPEG PCE 在不同煅烧黏土复合水泥中的工作性能（内掺煅烧黏土量为 20%、30% 和 40%）。最后比较了由不同煅烧黏土制备的水泥砂浆的早期抗压强度。试验结果表明，偏高岭土的含量是影响煅烧黏土复合水泥流动性的关键因素，虽然较高的偏高岭土含量会提高水泥砂浆的早期强度，但会大大降低施工和易性。

关键词：低碳水泥；煅烧黏土；聚羧酸系高性能减水剂；流动度；早期强度

1 引言

水泥熟料生产的过程伴随着大量 CO_2 产生，据调查，每生产 1 吨水泥伴随有 850 kg 二氧化碳排放，给环境带来了极大的负担。解决水泥熟料生产中碳排放量大的问题迫在眉睫。煅烧黏土由于其原材料分布广、烧结温度低、碳排放量低、具有火山灰活性等特点，可作为新型低碳辅助性胶凝材料而受到业内的广泛关注。其中，高岭土的含量是选择黏土原材料的重要指标。与其他黏土矿相比较，偏高岭土具有最高的火山灰活性。研究表明，偏高岭土含量会提高复合水泥砂浆的早期强度。然而，由于煅烧黏土材料通常颗粒细度小于传统硅酸盐水泥熟料，煅烧黏土通常具有较高的比表面积，使得大量聚羧酸减水剂吸附在其表面，从而大大降低了聚羧酸减水剂对水泥基材料的分散能力。本研究中，从不同地域得到三种具有不同偏高岭土含量的煅烧黏土，分别来自中国、德国、印度。将这些煅烧黏土分别与普通硅酸盐水泥熟料按照不同质量比例混合，探讨了偏高岭土的含量对聚羧酸高性能减水剂工作性能的影响。

李冉，女，1993 年 8 月，博士研究生，Technical University of Munich，Lichtenbergstr. 4，Garching bei München，85747，Tel.：+49（089）28913151。

2　试验

2.1　试验材料

（1）水泥。采用标号为 42.5R 的普通硅酸盐水泥（Schwenk Zement KG，Allmendingen plant，Germany）。水泥密度为 3.15 g/cm^3，平均粒径（d_{50}）为 19.8 μm。

（2）煅烧黏土。三种不同的煅烧黏土分别从德国、印度、中国获得。其中，德国煅烧黏土（以下表示为 CCG，即 Calcined Clay from Germany）的煅烧温度为 750 ℃，偏高岭土含量为 23 %。印度和中国的煅烧黏土的煅烧温度均为 800 ℃，偏高岭土含量分别为 45% 和 51% （以下分别表示为 CCI 和 CCC，即 Calcined Clay from India 和 Calcined Clay from China）。

（3）高效减水剂。本文中采用的 HPEG 聚羧酸高性能减水剂由吉林众鑫化工集团有限公司提供，这是一种由 HPEG 大单体以及丙烯酸制备而来，通常用于预拌混凝土的高效减水剂。

2.2　试验方法

2.2.1　煅烧黏土 XRD 表征

煅烧后的样品通过 X 射线衍射仪表征煅烧黏土的矿相。表征条件为：步长 0.15 s/step，2θ 扫描范围为 5°～70°。各煅烧黏土样品的 XRD 图谱如图 1 所示。

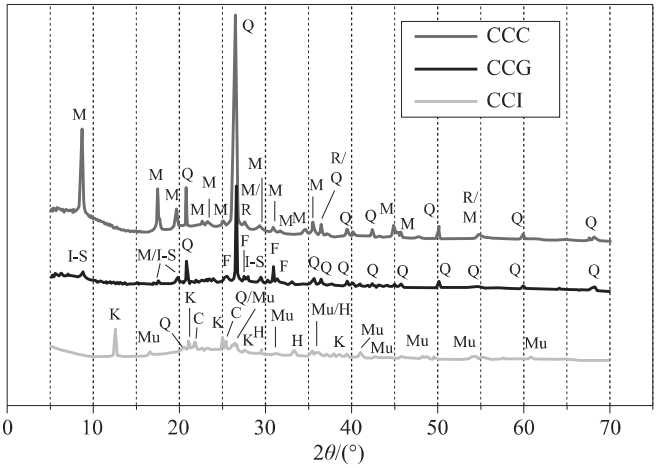

M=Muscovite（白云母），Q=Quartz（石英），R=Rutile（金红石），I-S=Illite-Smectite（伊利石–蒙脱石），F=Feldspar（长石），K=Kaolinite（高岭土），Mu=Mullite（莫来石），C=Cristobalite（方石英），H=Hematite（赤铁矿）

图 1　各煅烧黏土样品的 XRD 图谱

2.2.2　水泥需水量测试

首先，将普通硅酸盐水泥熟料与各煅烧黏土样品按照 80∶20、70∶30 和 60∶40 的质量比混合。然后，采用“微型坍落度试验”测量复合水泥浆体的流动度。调整各复合水泥的水灰比，并记录使水泥浆体的摊铺直径达到（18 ± 0.5）cm 的水灰比。

2.2.3 净浆流动度

同样采取“微型坍落度试验”测量复合水泥浆体的流动度，以此评价 HPEG 聚羧酸减水剂的作用效果。根据 DIN EN 1015 中规定的试验方法，首先确定水泥浆体的水灰比。在水泥、拌合水、无减水剂掺入的系统中，测得水泥浆体的摊铺直径为（18 ± 0.5）cm 时的水灰比为 0.5。在其他煅烧黏土复合水泥中使用同一水灰比。在这一水灰比下，测定水泥浆体摊铺直径为（26 ± 0.5）cm 时的减水剂的掺量。

2.2.4 抗压强度

根据 DIN EN 196 – 1，以 0.58 的水灰比和 3.0 的胶砂比制备砂浆样品。复合水泥选用 70∶30 比例。模具尺寸为 40 mm × 40 mm × 160 mm。在温度为（20 ± 1）℃和湿度为 90% 的条件下进行养护。养护 24 h 后拆模并进行力学测试。

3 结果与讨论

3.1 煅烧黏土复合水泥的需水量

普通硅酸盐水泥与煅烧黏土复合水泥的需水量结果如图 2 所示。从图 2 可以看出，所有复合水泥的需水量都高于普通硅酸盐水泥。此外，随着煅烧黏土掺量的增加，需水量也随之增加。这是由于煅烧黏土比普通硅酸盐水泥的颗粒更细。值得注意的是，德国煅烧黏土与印度煅烧黏土的表现相似，而中国煅烧黏土复合水泥的需水量远高于另外两种，并且需水量随掺量的增加而急剧增加。这是因为中国煅烧黏土具有更高的细度（d_{50} 为 10.4 μm）和较高的偏高岭土含量（51%）。

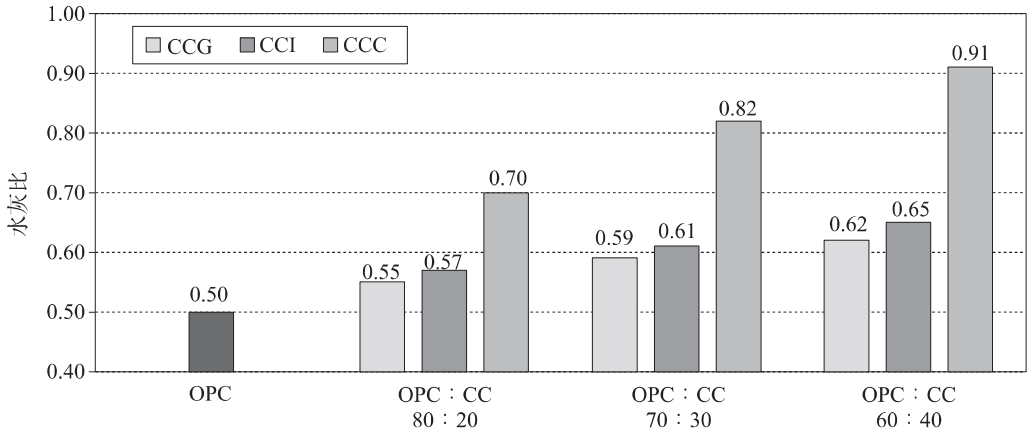

图 2 复合水泥净浆流动度达到 18 cm 的需水量

3.2 PCE 在煅烧黏土复合水泥中的饱和掺量

固定水灰比为 0.5，在该水灰比下，普通硅酸盐水泥净浆流动度为 18 cm，测定普通硅酸盐水泥及煅烧黏土复合水泥浆体摊铺直径为（26 ± 0.5）cm 时的聚羧酸高效减水剂的掺量。HPEG 聚羧酸高效减水剂在 20% 、30% 和 40% 质量分数的煅烧黏土复合水泥中的分散

效率如图 3 所示。发现与需水量结果一致，煅烧黏土复合水泥需要更高剂量的减水剂才能达到目标摊铺直径 26 cm。值得注意的是，尽管在需水量结果中，印度煅烧黏土与德国煅烧黏土的表现相近，但是在掺 PCE 情况下，印度煅烧黏土复合水泥所需的减水剂剂量远高于德国煅烧黏土复合水泥样品。此发现可以与煅烧黏土中偏高岭土的含量相联系。印度煅烧黏土的偏高岭土含量为 45%，与中国煅烧黏土接近（约 51%），同时，所需减水剂的量相近。因此，我们认为煅烧黏土中的偏高岭土含量是影响 PCE 在复合水泥中工作效率的重要因素。

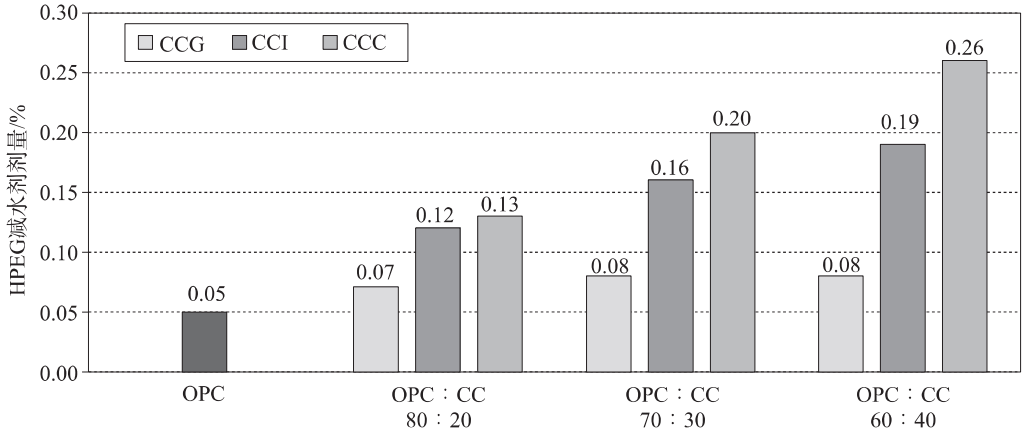

图 3　HPEG 聚羧酸高效减水剂在各水泥中的饱和掺量（W/C = 0.5）

3.3　煅烧黏土复合水泥的抗压强度

研究表明，偏高岭土的含量是影响煅烧黏土复合水泥砂浆早期强度的重要因素之一，因此，在接下来的试验中，我们采用几种不同偏高岭土含量的煅烧黏土与普通硅酸盐水泥以 30∶70 的质量比混合，在水灰比 W/C = 0.58 的条件下制备复合水泥砂浆，并与普通硅酸盐水泥砂浆强度进行比较。结果如图 4 所示。

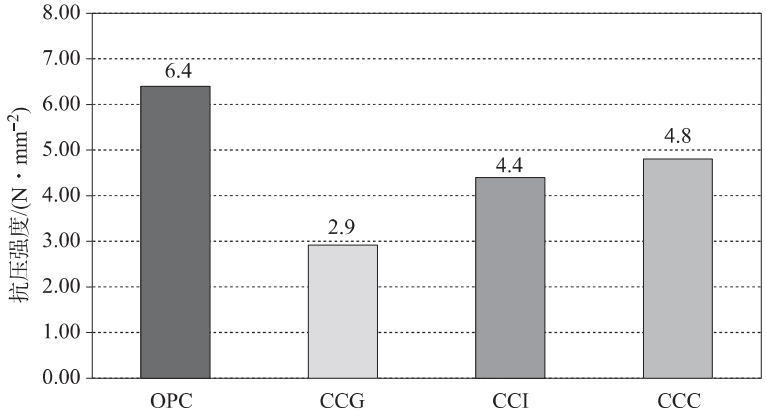

图 4　水泥砂浆的 1 d 强度（W/C = 0.58）

结果表明，与传统硅酸盐水泥相比，复合水泥的早期强度发展缓慢，1 d 抗压强度远低

于普通水泥砂浆。在复合水泥中，掺有中国煅烧水泥的样品 1 d 强度最高，这是因为这种煅烧黏土具有较高的偏高岭土含量，从而加速水泥中的火山灰反应。此外，印度煅烧黏土复合水泥的早期强度比德国煅烧黏土水泥的早期强度高得多，这是由于德国煅烧黏土具有更低的偏高岭土含量。

4 结论

本研究采用三种不同的煅烧黏土制备了复合水泥，并研究了它们的需水量，以及对聚羧酸高性能减水剂分散性能和早期强度的影响。结果表明，煅烧黏土中的偏高岭土含量是影响这种新型低碳水泥性能的关键因素。具体来讲，高含量的偏高岭土为砂浆提供了较高的早期强度，然而极大地降低了减水剂的工作效率，往往需要更高掺量的聚羧酸高性能减水剂来达到一定的分散性能。因此，在选择煅烧黏土时，应根据具体要求，将偏高岭土含量作为重要参考指标。

另外，值得注意的是，煅烧黏土复合水泥作为新型低碳水泥在减少 CO_2 排放量的同时，也需要更高掺量的外加剂。这无疑从另一方面增加了温室气体排放量。因此，需要进一步开展有关新型外加剂的相关研究，从而促进低碳水泥的进一步推广。

参考文献

[1] Sharma M, Bishnoi S, Martirena F, Scrivener K. Limestone calcined clay cement and concrete: A state - of - the - art review [J]. Cement and Concrete Research, 2021 (149): 106564.

[2] Scrivener K, Martirena F, Bishnoi S, Maity S. Calcined clay limestone cements (LC3) [J]. Cement and Concrete Research, 2018 (114): 49 - 56.

[3] Fernandez R, Martirena F, Scrivener K. The origin of the pozzolanic activity of calcined clay minerals: A comparison between kaolinite, illite and montmorillonite [J]. Cement and Concrete Research, 2011 (41): 113 - 122.

[4] Tironi A, Trezza M A, Scian A N, Irassar E F. Potential use of Argentine kaolinitic clays as pozzolanic material [J]. Applied Clay Science, 2014 (101): 468 - 476.

[5] Li R, Lei L, Sui T, Plank J. Effectiveness of PCE superplasticizers in calcined clay blended cements [J]. Cement and Concrete Research, 2021 (141): 106334.

[6] DIN EN. Methods of test for mortar for masonry - Part 3: Determination of consistence of fresh mortar (by flow table) [S]. 1015 - 3: 2007 - 5.

[7] DIN EN. Methods of testing cement - Part 1: Determination of strength [S]. 196 - 1: 2016.

Section 5.7

Publication # 7

Characterization data of reference industrial polycarboxylate superplasticizer VP 2020/15.2 used for Priority Program DFG SPP 2005 “Opus Fluidum Futurum-Rheology of reactive, multiscale, multiphase construction materials”

L. Zhang, **R. Li**, L. Lei and J. Plank.

Data in Brief

2021 Vol. 39 Pages 107657

DOI: 10.1016/j.dib.2021.107657

This work (**publication # 7**) was carried out under the Priority Program DFG SPP 2005 “Opus Fluidum Futurum - Rheology of reactive, multiscale, multiphase construction materials”.

Within the frame of this SPP program, an **industrial polycarboxylate superplasticizer** is being used by many researchers in both OPC and limestone calcined clay cement (LCC cement). Our task was to **char`acterize the PCE sample** with respect to its molecular properties, dispersing effectiveness and interaction with LCC cement and OPC via adsorption and zeta potential measurements. The data were made available to all research partners within the DFG SPP 2005 Priority Program and other researchers who use the same PCE in their investigations. The overall purpose of this work was to provide researchers with more insight into the **interactions occurring between binder systems** and **PCE superplasticizers**.

Data in Brief 39 (2021) 107657

Contents lists available at ScienceDirect

Data in Brief

journal homepage: www.elsevier.com/locate/dib

Data Article

Characterization data of reference industrial polycarboxylate superplasticizer VP 2020/15.2 used for Priority Program DFG SPP 2005 “Opus Fluidum Futurum - Rheology of reactive, multiscale, multiphase construction materials”

Lin Zhang, Ran Li, Lei Lei*, Johann Plank

Technische Universität München, Chair for Construction Chemistry, 85747 Garching, Lichtenbergstraße 4, Germany

ARTICLE INFO

Article history:
Received 5 November 2021
Accepted 26 November 2021
Available online 30 November 2021

Keywords:
Polycarboxylate
Characterization
Molecular properties
Dispersing effectiveness
Fluidity
DFG SPP 2005

ABSTRACT

An industrial polycarboxylate superplasticizer sample has been chosen in the Priority Program 2005 of the German Research Foundation (DFG SPP 2005). The molecular properties of this superplasticizer sample, such as molecular weight (M_w, M_n), the polydispersity index (PDI) and the macromononmer conversion rate were determined using Size Exclusion Chromatography (SEC), and the sample’s specific anionic charge amount was obtained via charge titration. Furthermore, the dispersing effectiveness of this superplasticizer sample was assessed through ‘mini-slump’ tests in pure OPC (CEM I 42.5 R) and in a limestone-calcined clay (LCC) cement. Moreover, the adsorption of the superplasticizer on both cements, and the dosage-dependent development of the zeta potential of both cement suspensions were captured. The data shall be used for the ongoing research within the Priority Program.

* Corresponding author.
E-mail address: lei.lei@bauchemie.ch.tum.de (L. Lei).

https://doi.org/10.1016/j.dib.2021.107657

Specifications Table

Subject	Polymers and Plastics
Specific subject area	Admixture for concrete; Dispersant; Polyethylene glycol derivatives
Type of data	Table; Image; Figure
How data were acquired	PCD 03 pH particle charge detector; Size exclusion chromatography (SEC); High TOC II Instrument; DT 1200 Electroacoustic Spectrometer; Infrared balance; pH meter; DIN EN 1015
Data format	Raw; Analyzed
Parameters for data collection	Molecular weight (M_w, M_n); Polydispersity index; Conversion; Solid content; Density; Specific anionic charge amount; Zeta potential; Adsorbed amount; Spread flow, Slump retention
Description of data collection	The data were obtained at the Chair for Construction Chemistry, Prof. Dr. J. Plank, Technische Universität München.
Data source location	Technische Universität München, Chair for Construction Chemistry, 85747 Garching, Lichtenbergstraße 4, Germany
Data accessibility	Repository name: mediaTUM Data identification number: https://doi.org/10.14459/2021mp1632413 Direct URL to data: https://mediatum.ub.tum.de/1632413

Value of the Data

- The chemical and physical properties, as well as application performance, of a polycarboxylate (PCE) superplasticizer used in the Priority Program 2005 of the German Research Foundation (DFG SPP 2005) were characterized in detail and are recorded in this dataset.
- This data is available to all research partners within the DFG SPP 2005 Priority Program and other researchers who use the same material in their research.
- The research groups involved in the SPP 2005 employ the polymer as a slump retainer for cement suspensions, including the LCC binder, and other colloidal systems to produce rheological data.
- The structural parameters, such as molecular weights and anionic charge, of this polymer should be helpful for researchers to compare this superplasticizer with other superplasticizers to determine the optimal structures for their specific application.
- The data should help the researchers in the SPP project gain more insight into the interactions that occur between particles and the polycarboxylate polymer.

1. Data Description

A thorough characterization of two superplasticizers was published in [1]. The data presented here relate to a new superplasticizer, VP2020/15.2, provided by MBCC group (Mannheim / Germany); this superplasticizer was tested in a CEM I 42.5 R sample and LCC cement. Detailed information about the chemical composition, physical properties and molecular characteristics of this polycarboxylate superplasticizer are provided below. The dispersing effectiveness of this polycarboxylate polymer was evaluated using 'mini-slump' tests and its interaction with both cements was assessed by zeta potential and adsorption measurements.

1.1. Characterization data of physical and chemical properties

The physical properties, such as solid content, density, pH value, and chemical characteristics, including molecular weights (M_w, M_n), PDI, macromonomer conversion of this industrial PCE sample, are listed in Table 1. The chemical structure of this PCE is displayed in Fig. 1, and the

Table 1
Solid content, density, molecular weights, polydispersity index (PDI), macromonomer conversion and pH value of the industrial PCE sample VP 2020/15.2.

Product	Solid content [wt.%]	Density [kg/L]	M_w [g/mol]	M_n [g/mol]	PDI	Macromonomer Conversion [%]	pH
VP 2020/15.2 (ready-mix type PCE)	20.5	1.01	78,100	28,560	2.73	86.1	5.6

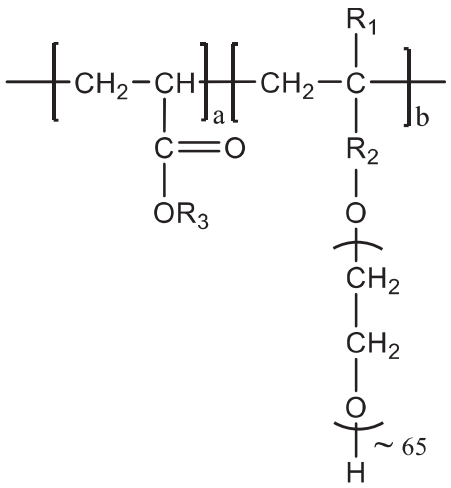

Fig. 1. Chemical structure of the industrial PCE sample VP 2020/15.2.

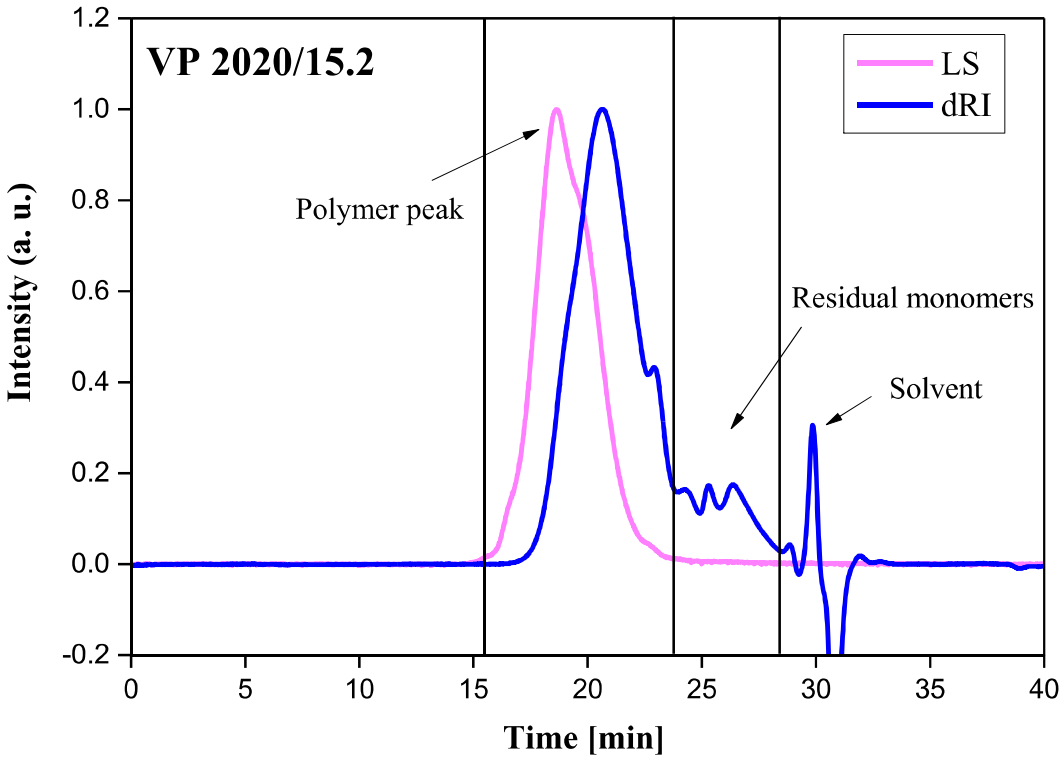

Fig. 2. SEC spectrum of PCE sample VP 2020/15.2; eluent: 0.1 M $NaNO_3$.

Table 2
Specific anionic charge amount of the industrial superplasticizer sample.

Product	Specific anionic charge amount [μeq/g]	
	in DI water	in 0.01 M NaOH, pH = 12
VP 2020/15.2 (ready-mix type PCE)	655	1,754

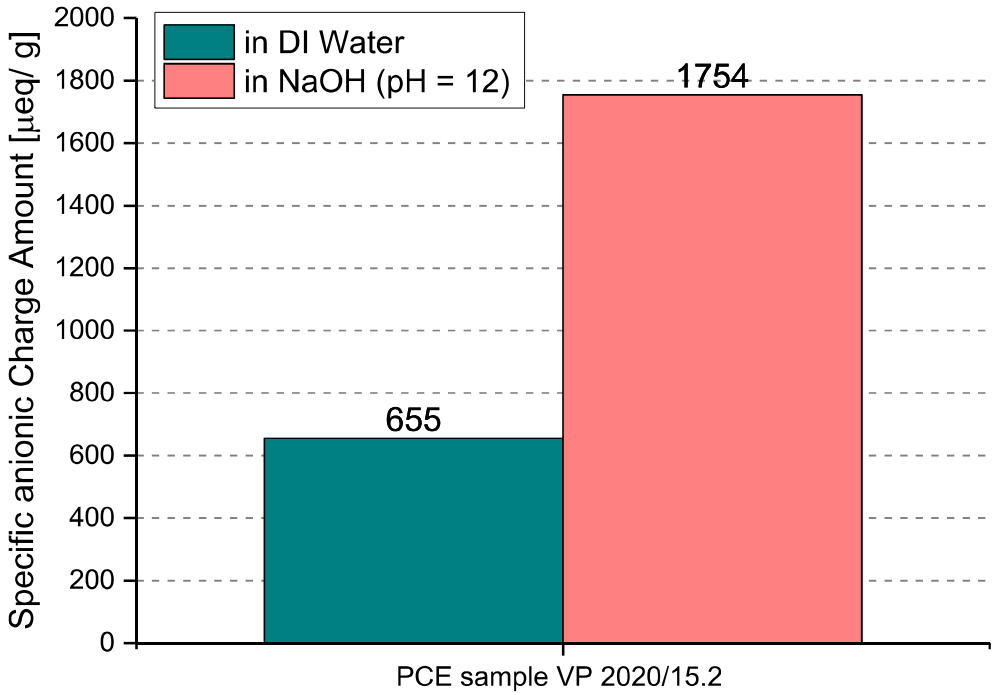

Fig. 3. Specific anionic charge amount of VP 2020/15.2.

SEC spectrum is presented in Fig. 2. VP 2020/15.2 is a polycarboxylate comb polymer, and the ethylene oxide unit number in the side chain is approximately 65.

1.2. Characterization data of anionic charge property

The PCD 03 pH particle charge detector (Mütek Analytic, Herrsching, Germany) was used to capture the specific anionic charge amount of this PCE. The PCE superplasticizer sample was dissolved in deionized water as well as in 0.01M NaOH solution (pH = 12) respectively. Polydiallyl dimethyl ammonium chloride (polyDADMAC) solution was employed to titrate PCE until the charge was neutralized. The results are shown in Table 2 and Fig. 3.

1.3. Dosage - dependent dispersing effect in cement pastes

The dispersing power as a function of dosage of this superplasticizer was investigated in cement paste via the 'mini slump' test at 20°C and 40% rel. humidity according to DIN EN 1015-3 [2]. The water-to-cement ratio was fixed at 0.4 for both the CEM I 42.5 R and the LCC cement, based on water demand [3,4].

The dispersing effectiveness of this superplasticizer at different dosages in two cements (CEM I 42.5 R and LCC cement) was assessed, and the results are shown in Fig. 4. The dosage required

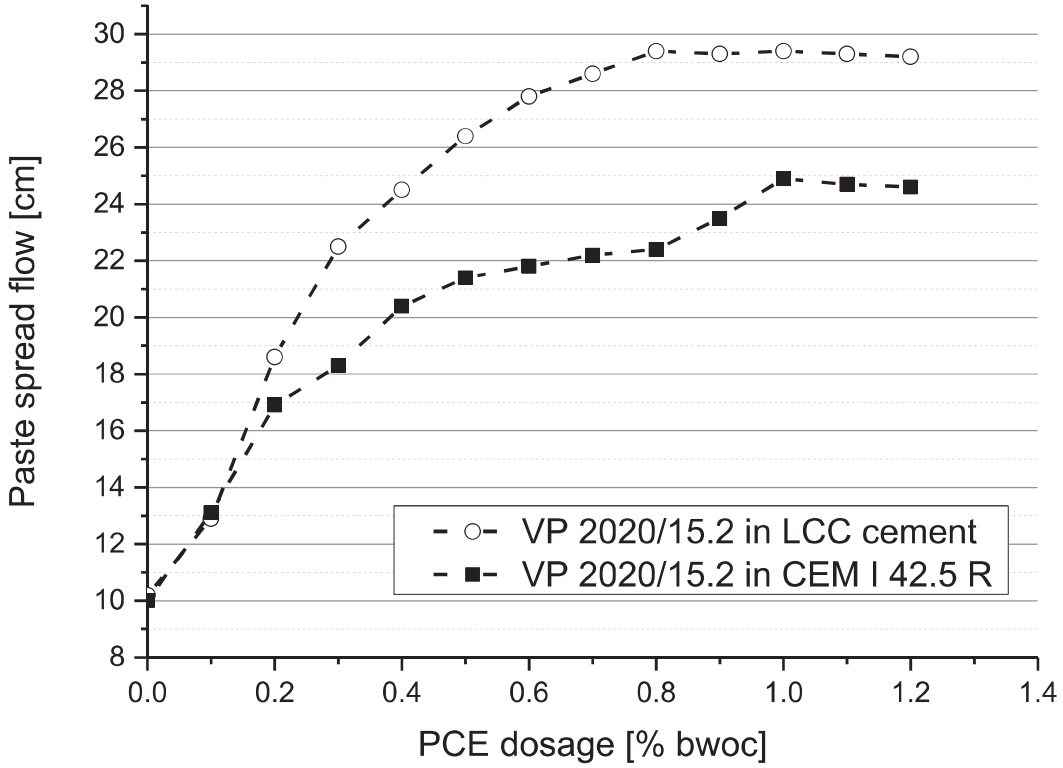

Fig. 4. Dosage - dependent spread flow of VP 2020/15.2 in CEM I 42.5 R and LCC cement paste (w/c ratio = 0.4).

for VP 2020/15.2 in CEM I 42.5 R to reach maximum fluidity was ~ 1.0% bwoc, while in the LCC cement the dosage required to reach maximum effect was ~ 0.8% bwoc (w/c ratio = 0.4).

1.4. Slump retention

The slump retention performance of the superplasticizer sample VP 2020/15.2 (ready-mix type PCE) in two cements (CEM I 42.5 R and LCC cement) was measured over a period of 6 hours. The w/c ratio was 0.4. The results are shown in Fig. 5.

The dosages of VP 2020/15.2 used in CEM I 42.5 R and LCC cement were 0.7% bwoc and 0.3% bwoc, respectively. In both cements, VP 2020/15.2 shows strong delayed plastification. This effect is weaker in the LCC cement.

1.5. Adsorption of the PCE sample on CEM I 42.5 R and LCC cement

The adsorbed amounts of VP 2020/15.2 on CEM I 42.5R and LCC cements were obtained via using the depletion method [5]. A Liquid TOC-II instrument (Elementar Analysen systeme GmbH, Hanau/ Germany) was employed to obtain the total organic carbon amount.

The adsorption isotherms for VP 2020/15.2 on CEM I 42.5 R and LCC cement are shown in Fig. 6.

1.6. Zeta potential of cement suspensions admixed with VP 2020/15.2

In order to further understand the interaction of the PCE and the cement particle surface, zeta potentials as a function of PCE dosage were characterized via a DT-310 instrument (Dispersion

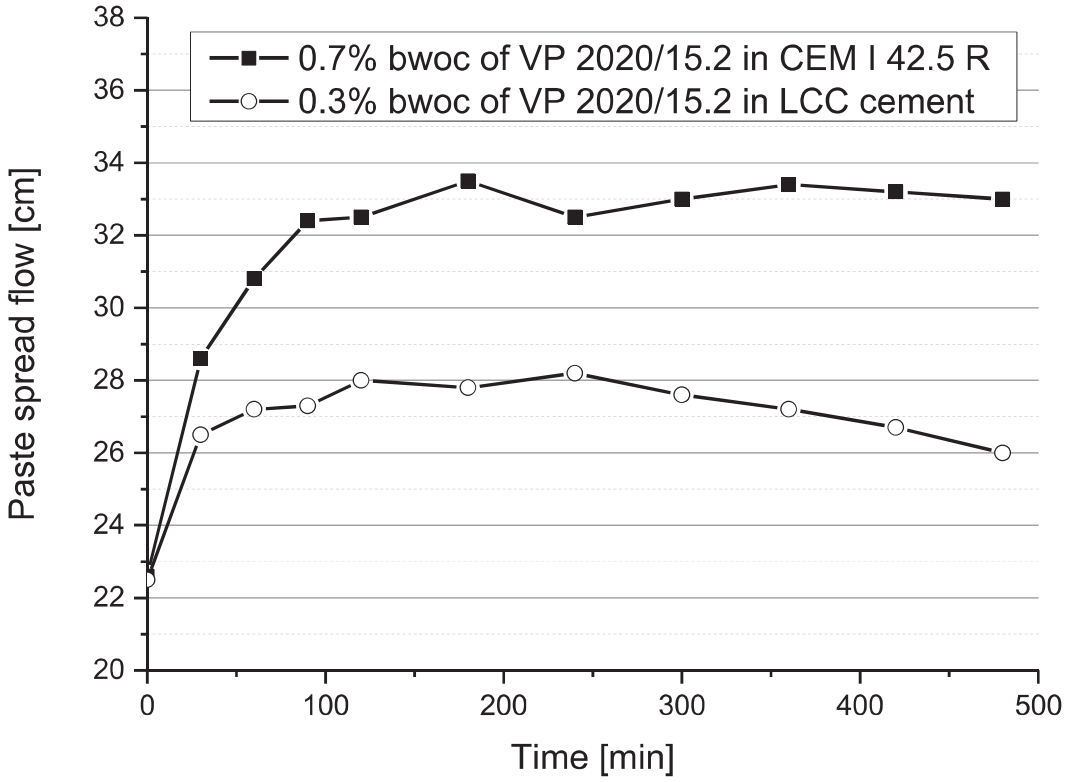

Fig. 5. Slump retention of VP 2020/15.2 in CEM I 42.5 R and LCC cement paste (w/c ratio = 0.4).

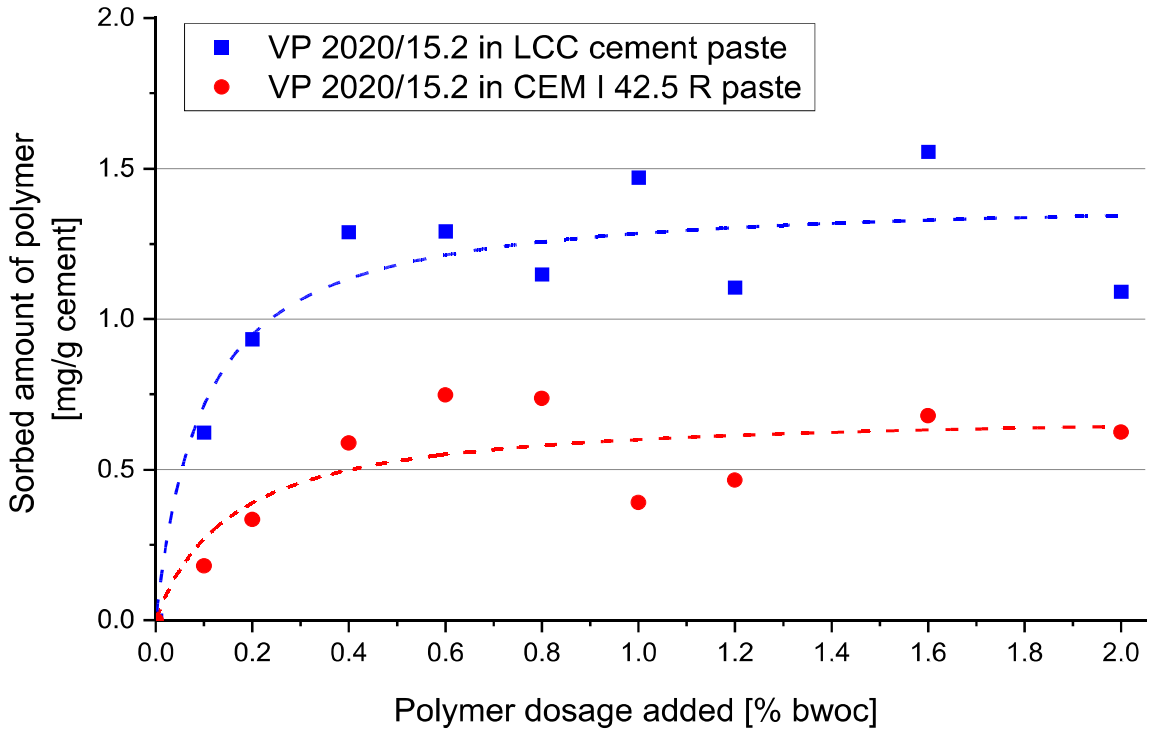

Fig. 6. Adsorption amount for VP 2020/15.2 on CEM I 42.5 R and LCC cement; w/c ratio = 0.5, cement paste.

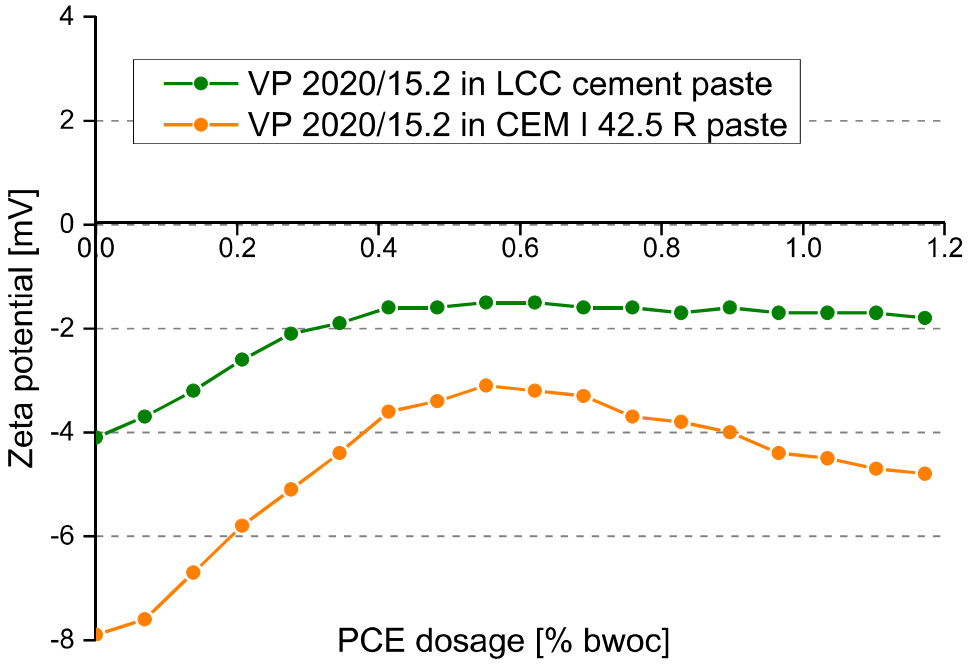

Fig. 7. Dosage-dependent zeta potentials of pastes prepared from CEM I 42.5 R and LCC cement, treated with VP 2020/15.2 (w/c ratio = 0.5).

Technology Inc., Bedford Hills, NY/USA). The zeta potential value was calculated by means of the colloidal vibration current (CVI) [6]. The w/c ratio was fixed at 0.5 to achieve a slump flow value of 18 cm in both the CEM I 42.5 R and the LCC cement. The dosage dependent zeta potential values were recorded and are shown in Fig. 7.

2. Experimental Design, Materials and Methods

The molecular characteristics of VP 2020/15.2 were determined utilizing size exclusion chromatography (SEC) to obtain the conversion of the macromonomers and the molecular properties (M_w, M_n and PDI). The instrument employed was a Waters Alliance 2695 (Waters, Eschborn, Germany) with a "mini Dawn" detector (Wyatt Technology Corp., Santa Barbara, CA). Three Ultrahydrogel columns (Waters, Eschborn, Germany) were used to separate the polymer and 0.1 N $NaNO_3$ at a flow rate of 1.0 mL*min^{-1} was used as the mobile phase [7].

The specific anionic charge amount of the PCE sample was obtained using a PCD 03 pH particle charge detector (Mütek Analytic, Herrsching, Germany). For this measurement, the PCE polymer (0.1 g/L) was dissolved in DI water and 0.01 M NaOH solution. Polydiallyl dimethyl ammonium chloride (polyDADMAC, 0.34 g/L) was used to titrate the PCE until the charge was neutralized. The negative charge amount of polymer (per gram) was calculated based on the polyDADMAC consumption to reach the zero potential [8].

Based on the norm DIN EN 1015-3, the dispersion and slump retention performance of the PCE polymer were investigated utilizing the "mini-slump" test. The cement (300 g) was added into a porcelain cup with pre-mixed PCE solution and kept still for 1 min, then manually stirred for 2 min. The cement paste was immediately poured into the Vicat cone (40 mm × 70 mm × 80 mm), filled to the brim, and then placed on a glass plate, thereafter the cone was removed vertically. The resulting paste diameter indicates the cement paste flow value. The paste diameter was measured twice, perpendicular to each other, and the average was then calculated. With respect to the slump retention performance, the similar fluidity test was conducted after 30, 60, 90, 120, 180, 240, 300, 360, 420 and 480 minutes after the first measurement.

The total organic carbon (TOC) content was used to characterize the PCE adsorption amounts on the cement surface. In this experiment, cement (16 g) and deionized water (8.0 g), containing the pre-dissolved VP 2020/15.2, were mixed (w/c ratio = 0.5), and the mixture was then shaken for two minutes at 2400 rpm (VWR International, Darmstadt / Germany), afterwards centrifuged for 10 minutes at 8,500 rpm. The supernatant was collected and filtered (0.2 µm), adding 0.1 M HCl to prevent carbonation and to remove inorganic carbonates. The instrument used to quantify the organic carbon amount was Liquid TOC-II (Elementar Analysensysteme GmbH, Hanau, Germany). The organic carbon amount was measured twice and the adsorbed amount of PCE was then calculated based on the initial PCE concentration and TOC content in the supernatant.

Zeta potential: The cement suspensions' electro - kinetic characteristics were determined with the DT 1200 instrument (Dispersion Technology, Inc, NY/ USA). In this experiment, cement (300 g) and DI water (150 g) were mixed in a porcelain cup and kept still for 1 min, then manually stirred for another 2 min. For the measurement, the paste was poured into a glass container, and the titrator, zeta potential electrode, pH meter, temperature probe were merged into the cement paste. During the test, the paste was continuously stirred at ambient temperature at 200 rpm. The ionic background was subtracted from the resulting zeta potential value to yield the values shown in Fig. 7.

Ethics Statement

The work did not involve the use of human subjects, animal experiments, or data collected from social media platforms.

CRediT Author Statement

Lin Zhang: Investigation, Methodology, Data curation, Validation, Writing - original draft; **Ran Li**: Investigation, Data curation; **Lei Lei**: Writing - Conceptualization, Reviewing and Editing; **Johann Plank**: Conceptualization, Resources, Supervision.

Declaration of Competing Interest

The authors declare that they have no known competing financial interests or personal relationships which have or could be perceived to have influenced the work reported in this article.

Acknowledgments

The authors wish to thank the German Research Foundation (DFG) for funding the Priority Program DFG SPP 2005 Priority Program "Opus Fluidum Futurum - Rheology of reactive, multiscale, multiphase construction materials" (project number 313773090) and MBCC for providing the sample of VP 2020/15.2.

References

[1] L. Lei, C. Chomyn, M. Schmid, J. Plank, Characterization data of reference industrial polycarboxylate superplasticizers used within Priority Program DFG SPP 2005 "Opus Fluidum Futurum - Rheology of reactive, multiscale, multiphase construction materials", Data Brief 31 (2020) 106026.

[2] European Norm DIN EN 1015-3: Methods of test for mortar for masonry – Part 3: Determination of consistence of fresh mortar (by flow table), DIN Deutsches Institut für Normung e. V, 1999.

[3] ZC. Lu, M. Haist, D. Ivanov, Characterization data of reference cement CEM III/A 42.5N used for priority program DFG SPP 2005 "Opus Fluidum Futurum – Rheology of reactive, multiscale, multiphase construction materials", Data Brief 30 (2020) 105524.

[4] L. Zhang, TU München, unpublished results 2021.
[5] C. Schröfl, M. Gruber, J. Plank, Preferential adsorption of polycarboxylate superplasticizers on cement and silica fume in ultra-high performance concrete (UHPC), Cem. Concr. Res. 42 (2012) 1401–1408.
[6] A.S. Dukhin, P.J. Goetz, Ultrasound for Characterizing Colloids: Particle Sizing, Zeta Potential, Rheology, Elsevier Science B. V., Amsterdam, 2002.
[7] M.T.R. Laguna, R. Medrano, M.P. Plana, M.P. Tarazona, Polymer characterization by size-exclusion chromatography with multiple detection, J. Chromatogr. A. 919 (2001) 13–19, doi: 10.1016/S0021-9673(01)00802-0.
[8] J. Plank, B. Sachsenhauser, Experimental determination of the effective anionic charge density of polycarboxylate superplasticizers in cement pore solution, Cem. Concr. Res. 39 (2009) 1–5, doi: 10.1016/j.cemconres.2008.09.001.

Section 5.8

Publication # 8

Low Carbon Alkali Activated Slag Binder and Its Interaction with Polycarboxylate Superplasticizers (PCE): Importance of Microstructural Design of the PCEs

R. Li, W. Eisenreich, L. Lei, J. Plank

ACS Sustainable Chemistry & Engineering (IF = 8.2)

Publication date 14.12.2022

DOI: 10.1021/acssuschemeng.2c05430

Alkali-activated slag (AAS) is attracting increasing attention as supplementary cementitious material due to its environmentally friendly property. However, AAS is also known to exhibit **inferior rheological properties** as **compared to OPC**. In order to identify potential solutions for this problem, the dispersing performance of different PCE superplasticizers was investigated in AAS composite cements. This topic was researched under the supervision of **Dr. Lei Lei**.

This **publication # 8** focused on the influence of the molecular structures of polycarboxylate superplasticizers on the AAS system. Using free-radical copolymerization, two series of APEG PCEs and HPEG PCEs exhibiting different anionicities were synthesized from acrylic acid (AA) and either α-allyl-ω-hydroxy poly (ethylene glycol) ether (APEG) or α-methallyl poly (ethylene glycol) ether (HPEG) macromonomer.

At first, the polymer structures were investigated using size exclusion chromatography (SEC), anionic charge titration and high-resolution ^{13}C NMR spectroscopy. Based on the ^{13}C NMR signals for the carbon in the carboxylic groups, specific motifs in the microstructures of the PCE copolymers could be assigned. By relating the results on the dispersing performance (“mini slump” tests) with adsorption measurements, it was revealed that the **dispersing power** and enhanced adsorption behavior on slag particles **of PCEs** correlates with their **anionicity** and **specific motifs in their microstructures** and, based upon their individual properties, HPEG PCEs performed superior in comparison to APEG PCEs.

ACS Sustainable Chemistry & Engineering

pubs.acs.org/journal/ascecg

Research Article

Low Carbon Alkali-Activated Slag Binder and Its Interaction with Polycarboxylate Superplasticizer: Importance of Microstructural Design of the PCEs

Ran Li, Wolfgang Eisenreich, Lei Lei,* and Johann Plank*

Cite This: https://doi.org/10.1021/acssuschemeng.2c05430

Read Online

ACCESS | Metrics & More | Article Recommendations

ABSTRACT: To investigate the role of polycarboxylate superplasticizers in a low carbon alkali-activated slag (AAS) system, two series of APEG and HPEG polycarboxylate ethers (PCEs) with different anionicities were designed and synthesized in this study. The resulting PCE samples were characterized via size exclusion chromatography, anionic charge titration, and high-resolution ^{13}C NMR spectroscopy. The paste and mortar spread flow tests suggest that in AAS, the synthesized HPEG PCEs exhibit superior dispersing performance over the APEG PCEs, especially at high anionicity. Based on the spread flow tests and adsorption measurements, it became apparent that the dispersing power of the PCEs increases with their anionicity as a result of stronger adsorption on slag. Furthermore, ^{13}C NMR spectroscopy was utilized to identify specific structural motifs in the architecture of the PCE copolymers. It was found that HPEG PCEs possessing AAA and AAE as dominant monomer sequences represent preferable molecular structures compared to APEG PCEs holding EAE as their main monomer sequence. The study confirms the pivotal role of specific molecular design for effective PCE superplasticizers.

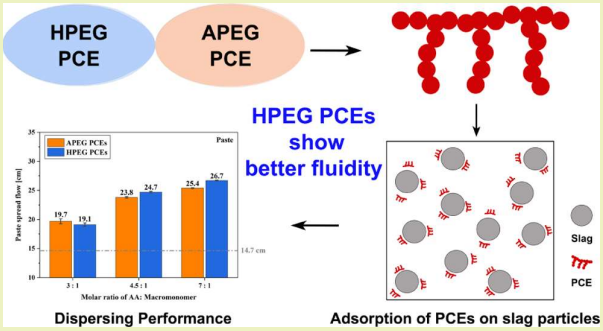

KEYWORDS: *low carbon binder, granulated blast-furnace slag, ^{13}C NMR spectroscopy, polycarboxylate superplasticizer, dispersion*

INTRODUCTION

Cement is, after water, the second most-consumed material on Earth, with over 4 billion tons manufactured per year.[1] Unfortunately, its production causes huge CO_2 emissions. As a result, a massive research effort is being made to reduce its CO_2 footprint, including reducing the clinker ratio of cement by using supplementary cementitious materials (SCMs), switching to high-efficiency fuels, or deploying advanced technologies including carbon capture and storage.[2]

In recent years, alkali-activated materials have become increasingly popular as SCM.[3−10] Ground granulated blast furnace slag is an alkali-activated material which, when used in concrete, can help to decrease the negative environmental impact of cement considerably.[11] Yang et al.[12] reported that by using alkali-activated slag (AAS) as a binder in concrete, the carbon footprint could be reduced by as much as 55−75%, depending on the chemical nature and dosage of the activator. Further advantages of using slag as an exclusive binder include conversing natural resources and enhancing the mechanical properties and durability of such concrete.[13−17] However, slag as a binder suffers from high shrinkage,[18,19] quick setting,[20−23] and, most undesirably, inferior rheological properties.[24] Poor workability prohibits the large-scale application of AAS. Therefore, superplasticizers present the key to achieving acceptable workability for AAS systems.[25]

Among all superplasticizer admixtures, polycarboxylates have emerged as the most promising candidate, due to their extraordinary dispersing power and high degree of molecular structural designability.[26] To improve the workability of the AAS, sophisticated molecular design of polycarboxylate ethers (PCE) polymers is urgently needed. Earlier Conte and Plank[27] identified an α-allyl-ω-hydroxy poly (ethylene glycol)-based PCE, which is highly effective in NaOH-activated slag systems. More recently, Lei and Chan[25] studied a series of α-methallyl poly(ethylene glycol)ether (HPEG)-based PCEs of specific molecular design and found that HPEG polymers possessing high anionicity, high molecular weight, and short side chains can induce superior workability in NaOH-activated slag pastes.

Received: September 10, 2022
Revised: December 4, 2022

ACS Sustainable Chemistry & Engineering pubs.acs.org/journal/ascecg Research Article

However, in both studies, no information was provided relative to the specific microstructure of PCE polymers, which should be suitable for AAS; hence, a correlation between the microstructure of PCE polymers and their interaction with AAS has not yet been established. Consequently, the purpose of this study is to establish an understanding about which structural motifs in the PCEs are the most efficient in terms of fluidizing AAS binder systems and to provide a guideline for the design of novel PCE geometries in the future.

EXPERIMENTAL SECTION

The slag sample used in this research was provided by Ecocem France (Fos-sur-Mer, France). Its fineness was characterized as meeting the requirements of the European standard EN 15167-1 (2006) and the concrete standard NF EN 206-1/CN (December 2012). The oxide composition of the slag is shown in Table 1. In addition, the particle size distribution of the slag sample was determined via laser granulometry (Cilas, Marseille/France), and the result is displayed in Figure 1. This slag exhibits the d_{10}, d_{50}, d_{90} values of 1.58, 14.53, and 41.20 μm, respectively.

Table 1. Oxide Composition of the Slag Used in This Paper

oxide composition	[wt %]
CaO	43.9
SiO_2	37.4
Al_2O_3	10.9
MgO	6.5
FeO	0.7
TiO_2	0.5
SO_3	0.1
Na_2O	0.3
K_2O	0.2
total	100

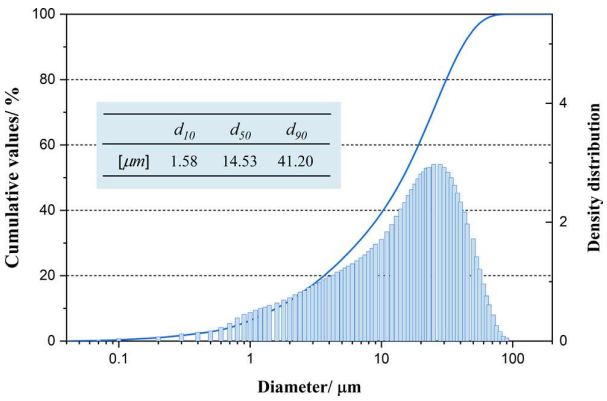

Figure 1. Particle size distribution and d_{10}, d_{50}, and d_{90} values of the slag sample used in this study.

Chemicals. Acrylic acid (AA) (>99% purity), ammonium persulfate (>99% purity), and sodium methallyl sulfonate (>99% purity) were purchased from Sigma-Aldrich (Germany). Sodium hydroxide (≥97.0% purity) was purchased from Merck KGaA (Germany), while α-allyl-ω-hydroxy poly(ethylene glycol)ether (APEG) (>98% purity) was obtained from the NOF Corporation (Japan). α-Methallyl-ω-hydroxy poly(ethylene glycol) ether (HPEG) was supplied by the Jilin Zhongxin Chemical Group Co., Ltd (China). All these chemicals were used without further purification.

PCE Preparation. In this study, two different series of ether-type PCEs (APEG type and HPEG type) were synthesized via aqueous-free radical copolymerization. The same synthesis procedure was applied to both PCE types. The detailed synthesis procedure of the 7HPEG7.0 polymer is described below (the components and their amounts for the synthesis of all PCEs are listed in Table 2):

37.45 g (0.107 mol) of HPEG macromonomer (M_w = 350 g/mol) was dissolved in 75 g of DI water and charged in a five-neck flask equipped with a stirrer (400 rpm stirring rate), reflux condenser, nitrogen inlet, and two separated feeding inlets. The flask was then heated to 60 °C and flushed with N_2 throughout the synthesis process. While flushing the flask, two feeding solutions were prepared separately. First, 5.08 g (0.032 mol) of sodium methallyl sulfonate (SMAS) and 53.97 g (0.75 mol) of AA were mixed with 50 g of DI water, designed as solution A. Second, 4.13 g (0.018 mmol) of ammonium persulfate (APS) was dissolved in 25 g of DI water, designated solution B.

Solutions A and B were then charged into a reaction vessel over 3 h by means of peristaltic pumps. Once this was completed, an additional 2 h stirring at 60 °C was required to finish the reaction. Finally, the resulting PCE solution was cooled to an ambient temperature. A neutral pH of about 7 was achieved via the addition of 30 wt % NaOH solution.

Test Methods. The specific anionic charge value of ether-based PCEs was determined using a particle charge detector PCD 03 pH (Mütek Analytic, Herrsching, Germany). Here, 10 mL of the 0.2 g/L PCE solution was titrated against a 0.34 g/L aqueous solution of polydiallyl dimethyl ammonium chloride (polyDADMAC) until charge neutralization appeared with zero potential. The anionic charge per gram of PCE was then calculated according to the amount of polyDADMAC titrated.

Size exclusion chromatography, also referred to as gel permeation chromatography, was utilized to determine the molecular properties (M_w, M_n, and PDI) of the synthesized ether-based PCEs on a Waters Alliance 2695 instrument (Waters, Eschborn, Germany) equipped with three Ultrahydrogel columns (120, 250, 500). An Ultrahydrogel Guard column, Waters RI 2414 detector was used as a concentration detector, while the combined Wyatt multiangle light scattering and quasielastic light scattering system allowed us to simultaneously determine the absolute molar mass, root mean square radius (r_g), and hydrodynamic radius (r_h). These detectors were calibrated in toluene (normalization with pullulan). For eluent, 0.1 N $NaNO_3$ (pH = 12) was used with a flow rate of 1.0 mL/min. To calculate M_w and M_n, a dn/dc value of 0.135 mL/g (value for PEO) was utilized.[28]

NMR spectroscopy was used to analyze the structure of the APEG macromonomer, HPEG macromonomer, and synthesized PCE samples. ^{1}H NMR spectra (16 scans, 5 s repetition period, 27 °C) were measured on an AVANCE-III 400 MHz NMR spectrometer equipped with a BBO probe head (Bruker BioSpin GmbH, Karlsruhe, Germany). Prior to measurement, the macromonomers were freeze-dried for 48 h at −50 °C at 0.37 mbar. The powdered samples (~0.1 g) were dissolved in 0.5 mL of D_2O (pH value of 13.0). The FIDs were multiplied with a mild Gaussian function prior to Fourier transformation. The chemical shifts were calibrated to external TSP at 0 ppm.

^{13}C NMR spectroscopy was deployed to detect the microstructure (monomer sequences) present in the PCE copolymers. ^{13}C NMR spectra (128−1024 scans, 5 s repetition delay, CPD ^{1}H-decoupling, 27 °C) were recorded at 125.8 MHz on an AVANCE-III 500 MHz NMR spectrometer equipped with a cryo-cooled probehead (QNP CryoProbe) (Bruker BioSpin GmbH). For sample preparation, all polymers were first purified by dialysis in water for 3 days and then freeze-dried for 48 h before they were dissolved in 0.5 mL D_2O (pH value of 13.0 adjusted with 30 wt % NaOH solution). The FIDs were multiplied with a mild Gaussian function prior to Fourier transformation. The chemical shifts were calibrated to external TSP at 0 ppm. For the ^{13}C NMR analysis of PCE samples, the spectra obtained were deconvolved for quantitative analysis of their motifs. For this purpose, the data sets were processed using the "Origin" software and deconvolved afterward, when a Gaussian−LorenCross function was applied. For APEG series PCEs, the initial locations of the peaks were

https://doi.org/10.1021/acssuschemeng.2c05430
ACS Sustainable Chem. Eng. XXXX, XXX, XXX−XXX

Table 2. Components and Their Amounts in the Synthesis of PCEs

	flask		solution A			solution B	
PCE samples	MM (g)	DI water (g)	SMAS (g)	AA (g)	DI water (g)	APS (g)	DI water (g)
7APEG3.0	37.45	75	5.08	23.13	50	4.13	25
7APEG4.5	37.45	75	5.08	34.70	50	4.13	25
7APEG7.0	37.45	75	5.08	53.97	50	4.13	25
7HPEG3.0	37.45	75	5.08	23.13	50	4.13	25
7HPEG4.5	37.45	75	5.08	34.70	50	4.13	25
7HPEG7.0	37.45	75	5.08	53.97	50	4.13	25

Table 3. Molecular Properties of the Synthesized PCE Polymers Based on Different Poly(ethylene glycol)ether Macromonomer

macromonomer type	ide chain length [n_{EO}]	PCE sample	PDI [M_w/M_n]	M_w [Da]	M_n [Da]	conversion (wt %)
APEG	7	7APEG3.0	2.2	28,780	12,890	87
		7APEG4.5	2.4	53,100	21,830	90
		7APEG7.0	2.2	61,450	27,090	93
HPEG	7	7HPEG3.0	2.4	35,000	15,000	96
		7HPEG4.5	2.6	66,430	25,690	94
		7HPEG7.0	2.4	65,330	27,430	96

manually selected, which was necessary due to the level of the ^{13}C NMR spectrum's congestion.

Based on the norm DIN EN 1015-3,[29] the spread flow of slag pastes containing different ether-based PCE polymers was assessed by performing a mini-slump test. The selected water to binder ratio was 0.5. In a typical experiment, 300 g of slag was added into a porcelain cup which contained an alkali activator (12 g of NaOH, 4% by weight of slag) and 150 g of water. After being manually agitated for 90 s, 0.05% of aqueous polymer sample (by weight of slag, bwos) was added into the mixture. After an additional 2.5 min of hand-mixing, a homogeneous suspension formed. Thereafter, the slag mixture was poured into a Vicat cone (height 40 mm, top diameter 70 mm, bottom diameter), filling it to the rim, and then it was lifted vertically. The spread flow was measured in horizontal and vertical directions once the paste stopped spreading further. The average value of both diameters was designated as the final result.

The dispersing ability of the PCE polymers was also determined via a mortar spread flow test following the DIN EN 196-1 standard. The water-to-slag ratio was fixed at 0.5, while the slag-to-sand ratio was set at 1:3. By applying the same PCE dosage (0.08% bwoc), a spread flow of mortar admixed with PCE polymers was assessed. First, the specified amount of PCE polymer and 18 g of NaOH were dissolved in 225 g mL of DI water placed in a steel vessel. After the vessel was attached to the mortar mixer (ToniMIX, Toni Technik, Berlin, Germany), 450 g of slag was added into the mixing bowl. Immediately afterward, the mortar mixer ran as follows: initially mix for 30 s at 140 rpm, then mix for another 30 s at 140 rpm, while the sand is automatically poured into the vessel, then pause for 90 s, and mix again for 60 s at 285 rpm. The resulting mortar was fed into a slump cone (60 mm height, 70 mm top diameter, 100 mm bottom diameter) and compacted using a tamper. The slump flow was measured on a shock table (Toni Technik, Berlin, Germany) which generated 15 strokes. The diameter of the mortar was measured twice, with the second measurement being at a 90° angle to the first and averaged to give the spread value.

The total organic carbon (TOC) content was used to characterize the PCE adsorption amounts on the slag surface. In a typical experiment, 16 g of slag, 0.64 g of NaOH (4% by weight of slag), and 8 g of water holding a certain amount of PCE were premixed in a 50 mL centrifuge tube. The mixture was then shaken for two min at 2400 rpm (VWR International, Darmstadt/Germany) and afterward centrifuged for 10 min at 8500 rpm. The supernatant was collected and filtered (0.2 μm syringe filter), adding DI water to dilute the filtrate and also 0.1 M HCl to prevent carbonation. The instrument used to quantify the organic carbon amount was Liquid TOC-II (Elementar Analysensysteme GmbH, Hanau, Germany).

RESULTS AND DISCUSSION

Synthesis of PCEs. Two series of APEG PCEs and HPEG PCEs, possessing different anionic charge densities, were synthesized via free-radical copolymerization from AA and either α-allyl-ω-hydroxy poly (ethylene glycol) ether (APEG) or α-methallyl poly (ethylene glycol) ether (HPEG) macromonomers. In order to synthesize APEG PCEs with a more diversified anionicity, AA was introduced as the backbone instead of traditional maleic anhydride (MA), thereby breaking the restriction of the regular alternation of maleic acid and APEG macromonomers.

The nomenclature system for the synthesized PCE samples was chosen as follows: first, the side chain length of the macromonomer (n_{EO}), then the abbreviation of the poly-(ethylene glycol) ether-based macromonomer (i.e., APEG and HPEG), and finally the feeding molar ratio of AA and the macromonomer. The molecular properties and composition of the different poly(ethylene glycol) ether-based PCEs possess the same side chain length (n_{EO} = 7), but different AA/Macromonomer molar ratios (3.0:1, 4.5:1, and 7.0:1) were successfully synthesized, as shown in Table 3. It is worth noting that the APEG PCEs used in this study were synthesized via aqueous-free radical copolymerization from AA and the APEG macromonomer, which is different from the conventional bulk polymerization method derived from MA and the APEG macromonomer. In this way, a broader molecular geometry of the APEG PCEs could be achieved, which promotes good workability of the AAS pastes.

Characteristic Properties of PCE Samples. All of the synthesized PCEs exhibited high macromonomer conversion, indicating a well-distributed molecular weight property (Table 3). The chemical structures of the two different ether-based PCEs are illustrated in Figure 2, while the size exclusion chromatography (SEC) chromatograms of the resulting 7APEG7.0 and 7HPEG7.0 polymers are displayed in Figure 3 as an example.

In addition, the structural analysis of the APEG and HPEG PCE polymers was carried out via ^1H NMR spectroscopy. Figure 4 displays the spectra of 7APEG3.0 and 7HPEG3.0 as examples. The actual molar ratios of AA to APEG (or HPEG) macromonomer were calculated based on their proton

https://doi.org/10.1021/acssuschemeng.2c05430
ACS Sustainable Chem. Eng. XXXX, XXX, XXX−XXX

ACS Sustainable Chemistry & Engineering pubs.acs.org/journal/ascecg Research Article

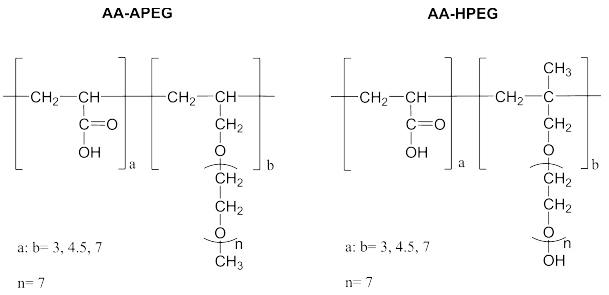

Figure 2. Molecular structure of the structurally different PCE polymers (AEPG and HPEG type).

intensities in the ^{1}H NMR spectrum, and the results are listed in Table 4. Note that, to calculate the composition of APEG PCE polymers from ^{1}H NMR analysis, the method described in ref 30 was applied. According to the results in Table 4, the actual compositions for both PCE types are relatively close to the feeding molar ratios.

Dispersing Effectiveness of PCEs in NaOH-Activated Slag. Figure 5 displays the results of the minislump tests for the two types of PCE polymers (APEG- and HPEG type), which possess different anionicity (=decreasing side chain density), but the same side chain length of 7 EO units when applied at a dosage of 0.05% bwos to the slag paste. According to our test results, the spread flow of the neat AAS paste without any superplasticizer registered at 14.7 cm. With the addition of the PCE polymers, the flowability of the AAS pastes subsequently increased. It can be summarized that all PCE polymers represent effective dispersants in AAS systems. Moreover, PCE polymers possessing higher anionicity exhibited slightly stronger dispersing power. According to Lei et al., in the AAS system, PCEs having high anionicity and a short side chain provide superior dispersing performance, which is driven by higher adsorption on the surface of the slag particles.[25,31] Dalas et al. studied the influence of the PCE anionic functionality on adsorption. They found that the positive effect of anionic functional modifications on the adsorption leads to enhanced flowability.[32] Our finding here is in good agreement with these studies. Most interestingly, we found that the dispersing effectiveness is closely related to the PCE kind. To be more specific, the HPEG-based PCEs were found to exhibit stronger dispersing effectiveness compared to the APEG-based PCEs, especially for the PCE polymers with higher anionicity. For example, the 7HPEG7.0 polymer sample (AA/HPEG = 7) achieved a paste spread flow of 26.7 cm, whereas the 7APEG7.0 polymer sample (AA/APEG = 7) achieved a spread flow of 25.4 cm.

In addition, the dispersing performance of these polymers was further investigated in AAS mortar at the w/b ratio of 0.5. As displayed in Figure 6, all the PCEs show high spread flow values in the mortar test, and the HPEG PCEs were slightly superior to the APEG PCEs. Furthermore, it is clear that the higher the anionicity of the PCEs, the higher the flowability that can be achieved.

Adsorption of PCEs on AAS. It is commonly acknowledged that superplasticizers derive their dispersion from adsorption on binder particles or early hydrates, such as ettringite, monosulfate, syngenite, portlandite, and gypsum.[33,34] As a general rule, as the number of PCE molecules adsorbed on the binder surface increases, so does the flowability, and maximum flowability is reached when the adsorption approaches the plateau (saturation).[35]

In order to gain more insights into the interaction between the PCE polymers and slag particles, TOC measurement was employed to determine the amount adsorbed for the two PCE series on AAS. Figure 7 presents the amount adsorbed for a series of 7HPEG polymers prepared with different anionic charge densities (molar ratio varied from 3.0:1 to 7.0:1); as expected, all PCE samples produced a typical Langmuir adsorption curve. Furthermore, we noticed that higher anionic charge density promoted the adsorption on AAS, and as a result, a more highly saturated amount of adsorbed polymers was achieved. Indeed, the improved adsorption induced by PCEs possessing a higher anionic charge character leads to better dispersion in AAS. A similar trend was also applied to the 7APEG series; a higher charge density substantially promoted the adsorption of polymers on slag particles, as shown in Figure 8. This phenomenon has also been reported for the OPC system in the literature. He et al.[36] reported that a higher carboxylate group content in the PCE polymer backbone causes the enhanced adsorption of PCE polymers on cement grains due to the greater binding capacity of Ca^{2+}. Han and Plank[37] compared the adsorption capacity of two MPEG-based PCE polymers. It transpired that the adsorbed amount is higher for highly anionic 45PC6 than for the less

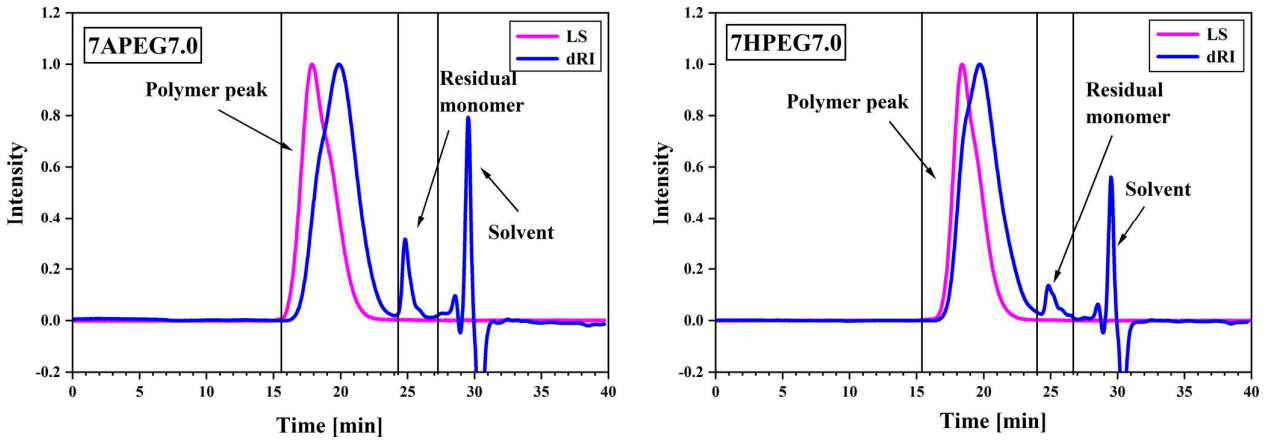

Figure 3. SEC chromatograms of 7APEG7.0 and 7HPEG7.0 samples.

https://doi.org/10.1021/acssuschemeng.2c05430
ACS Sustainable Chem. Eng. XXXX, XXX, XXX−XXX

ACS Sustainable Chemistry & Engineering pubs.acs.org/journal/ascecg Research Article

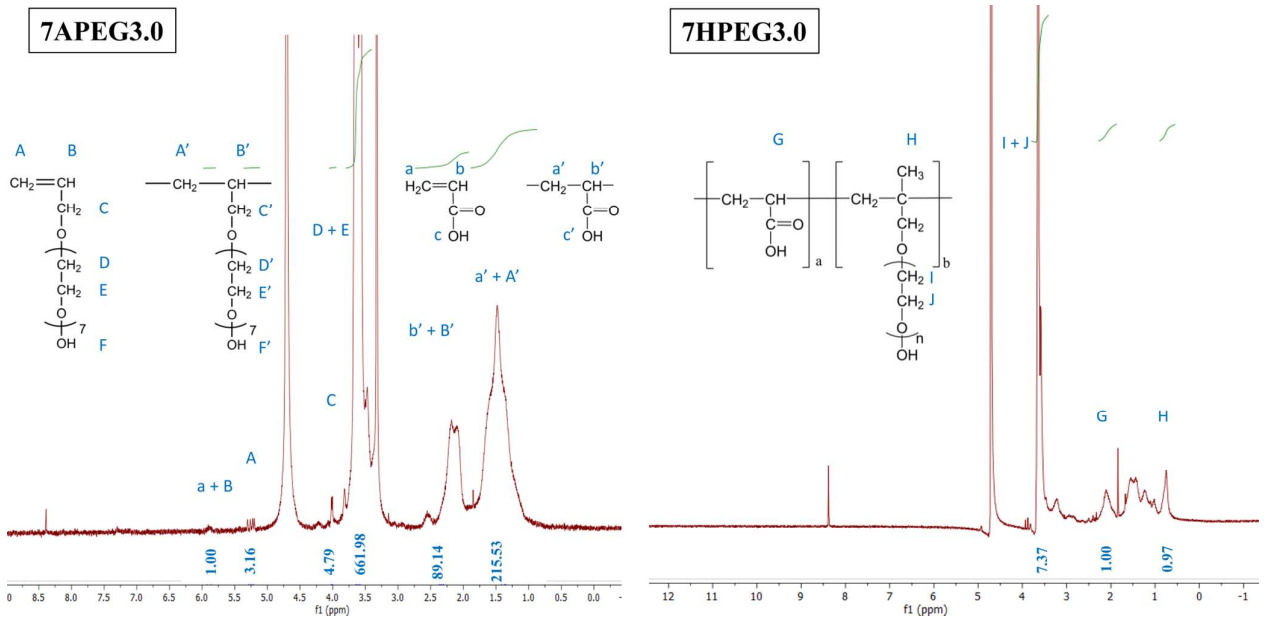

Figure 4. ^{1}H NMR spectra of 7APEG3.0 and 7HPEG3.0 PCE samples.

Table 4. Molar Ratios of Acrylic Acid to APEG or HPEG Macromonomer in the 7APEG and 7HPEG PCEs, Calculated via Quantitative ^{1}H NMR Spectroscopy

PCE sample	feeding ratio	actual ratio
7APEG3.0	3.0:1	3.4:1
7APEG4.5	4.5:1	4.8:1
7APEG7.0	7.0:1	7.8:1
7HPEG3.0	3.0:1	3.1:1
7HPEG4.5	4.5:1	4.3:1
7HPEG7.0	7.0:1	8.1:1

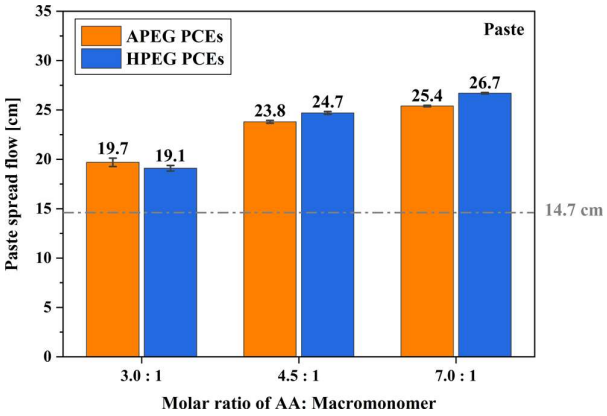

Figure 5. Spread flow of NaOH-activated slag pastes containing 0.05 wt % of two types of PCE polymers (APEG and HPEG) made from different AA/macromonomer molar ratios but the same side chain length (n_{EO} = 7).

anionic counterpart 45PC1.5 (3.5 mg/g for 45PC6 vs 1.8 mg/g for 45PC1.5).

Until now, some previous studies have attempted to establish a correlation between the adsorption behavior of specific PCE types (e.g., HPEG) possessing different geometry (e.g., anionicity, side chain length) and their dispersing

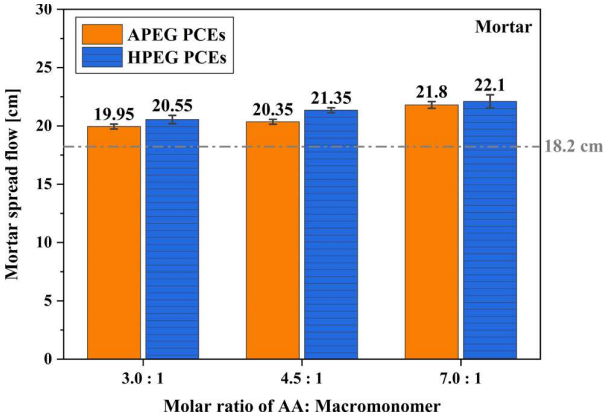

Figure 6. Spread flow of NaOH activated slag mortar containing 0.08 wt % of 7APEG and 7HPEG PCE series, w/b ratio = 0.5.

effectiveness in AAS. However, there has been no investigation to assess the impact of PCE type on dispersing performance. In this study, the amount adsorbed for these two types of PCE samples on AAS was determined and compared. According to the results, higher adsorbed amounts were recorded for the 7HPEG series compared to the 7APEG series at the same anionicity. To be specific, 7HPEG3.0, 7HPEG4.5, and 7HPEG7.0 reached the saturated adsorption at 1.25, 1.36, and 1.58 mg/g slag, respectively, whereas 7APEG3.0, 7APEG4.5, and 7APEG7.0 attained the plateau at 1.1, 1.25, and 1.45 mg/g slag. These findings indicate that the 7HPEG PCE series is more strongly anchored on the surface of slag particles than polymers of the 7APEG PCE series, which could be explained by their different microstructures. The enhanced adsorption of 7HPEG PCEs promotes the dispersion in AAS, as is shown in Figures 5 and 6. As shown in Table 5, the HPEG PCEs contain high amounts of polyacrylic acid (AAA) blocks, which are known to adsorb particularly well onto positively charged surfaces.

https://doi.org/10.1021/acssuschemeng.2c05430
ACS Sustainable Chem. Eng. XXXX, XXX, XXX−XXX

ACS Sustainable Chemistry & Engineering pubs.acs.org/journal/ascecg Research Article

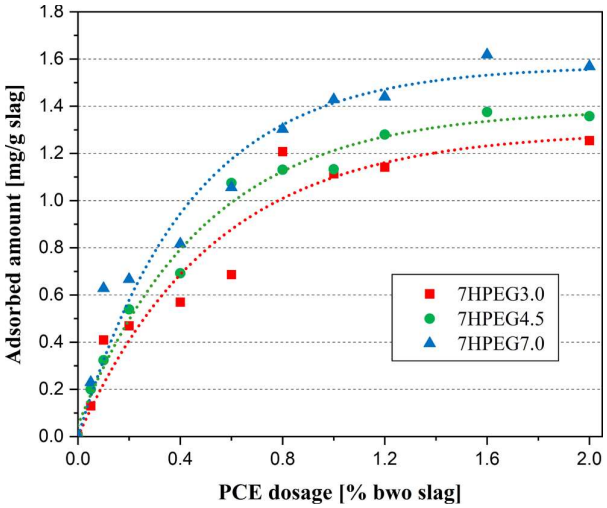

Figure 7. Adsorption isotherms of a series of HPEG PCEs (n_{EO} = 7) possessing different anionic charge densities in AAS paste (w/slag = 0.5).

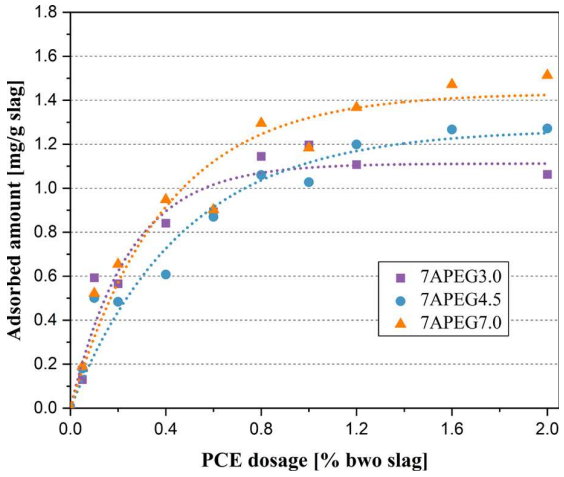

Figure 8. Adsorption isotherms of a series of APEG PCEs (n_{EO} = 7) possessing different anionic charge densities in AAS paste (w/slag = 0.5).

Table 5. Integrated Area Values (Percentage) of Peaks on EAE, AAE, and AAA Sequences for PAA and PCE Samples

samples	EAE %	AAE %	AAA %
PAA			100
7HPEG3.0	8.28	49.94	41.79
7HPEG4.5	4.81	46.63	48.57
7HPEG7.0	4.39	36.61	59.00
7APEG3.0	87.51	5.33	7.16
7APEG4.5	74.90	13.80	11.30
7APEG7.0	66.44	12.74	20.81

With respect to the sorption isotherms, all PCE polymers required high saturation dosages (>1.0%), which were much higher than the actual amounts (0.05%) used in the performance test. Therefore, in order to reflect the realistic dispersing power of different PCE polymers in AAS, the amount adsorbed at a specific dosage of 0.05% was determined. The results are illustrated in Figure 9. Here, at a dosage of 0.05% bwo slag, the 7HPEG series exhibited the same or a slightly higher adsorption amount than the APEG polymers. Again, the data clearly signify that 7HPEG PCEs exhibited stronger adsorption on slag, and this in turn results in superior dispersing ability. This trend is in line with previous investigations. According to the literature, Lange and Plank[38] compared the adsorption behavior of charged and uncharged PCE polymers and found that one MPEG PCE polymer (45PC6) exhibited strong interaction with cement, as evidenced by the high amount adsorbed. They also attributed the extraordinary dispersing power of the MPEG PCE polymer to the enhanced adsorption behavior. Vo and Plank[39] evaluated the dispersing performance of a novel phosphate PCE polymer in gypsum systems compared to the conventional MPEG PCE polymers. They attributed the superior dispersing as well as water reducing capability of the phosphate PCE polymer to the high amounts adsorbed in gypsum.

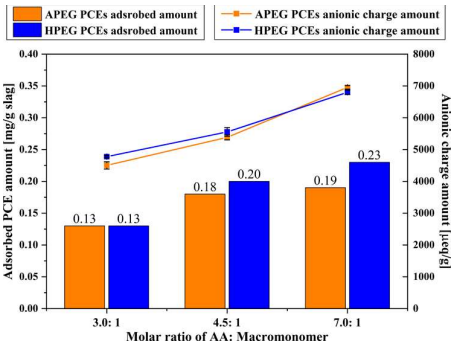

Figure 9. Adsorbed amount of APEG and HPEG PCE series (n_{EO} = 7) possessing different anionic charge densities at a dosage of 0.05% in AAS paste (left *Y*-axis) and anionic charge amounts of those APEG and HPEG PCEs measured in 0.1 M NaOH solution (right *Y*-axis).

One potential reason postulated for the discrepancy in the dispersing capacity of two types of PCE is related to their distinct anionic characteristics. In the next step, the anionic charge densities of all PCE polymers were determined in a 0.1 M NaOH solution. As is shown in Figure 9, the anionic charge amounts of different PCE kinds exhibiting the same acid to macromonomer ratio were quite comparable, which means the PCE polymers prepared from different macromonomers (e.g., APEG and HPEG) did not result in much difference in their charge characteristics. Given all this, we can eliminate the potential influence of the difference in charge characters.

There is no doubt that several parameters may influence the adsorption behavior of PCE polymers,[34] namely, chemical composition,[40] polymer conformation,[41] main chain/side chain length,[42] charge density,[43] flexibility and stiffness of the polymer chain,[44,45] synthesis method,[46] and microstructure.[47] Here, in this study, PCE polymers were prepared using the same technique, also their molecular weight, side chain length, and charge density were comparable. The specific microstructure of PCE polymers prepared from different macromonomers (APEG and HPEG) is worth investigating in depth. It should be mentioned that the additional $-CH_3$ in HPEG macromonomer enhanced the backbone stiffness and may have resulted in less shrinkage. Thus, more anchor groups could be exposed, which in turn promotes the adsorption.[44]

Microstructure of the Synthesized APEG and HPEG PCEs. To gain insights into the microstructural information of the synthesized APEG- and HPEG-based polymers, NMR

https://doi.org/10.1021/acssuschemeng.2c05430
ACS Sustainable Chem. Eng. XXXX, XXX, XXX−XXX

ACS Sustainable Chemistry & Engineering pubs.acs.org/journal/ascecg Research Article

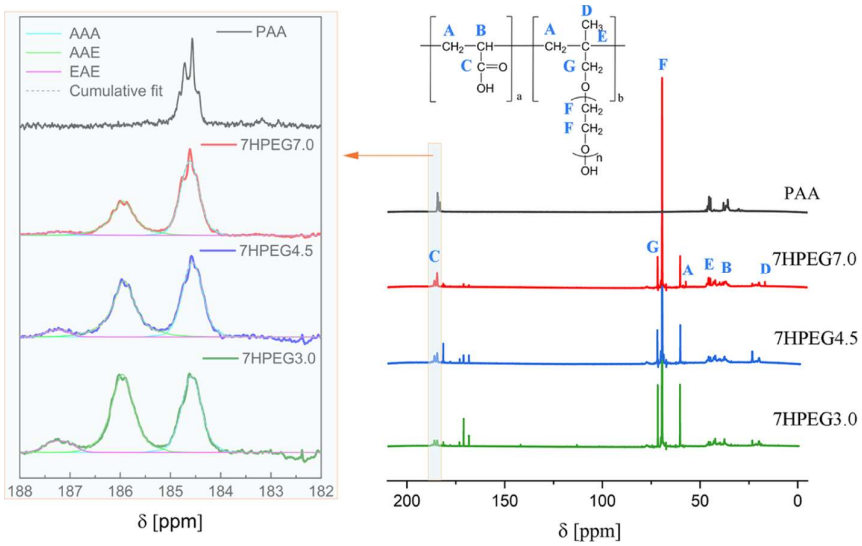

Figure 10. ^{13}C NMR spectra of HPEG PCE polymers and PAA measured in D_2O at pH = 13.

spectroscopy was employed to identify the actual monomer sequence of the PCEs. In ^{13}C NMR spectra, signals generally reflect the resonance of the ^{13}C nucleus to an external magnetic field, which is influenced by the nearby electron density. Thus, the resonance of the ^{13}C nucleus varies when linked to different neighboring monomers. This effect can be used to determine the sequence of monomers along polymer chains such as in methacrylate copolymers. In an earlier study, Plank et al.[47] studied the repartition of IPEG pendent chains along the polymer backbone via ^{13}C NMR spectroscopy. They claimed that variations in side chain repartition are closely related to the adsorption and dispersion behaviors of IPEG PCE polymers. Here, this technique was deployed to compare the microstructure of two kinds of PCE polymers. In the following investigation, the carboxyl carbon present in AA was taken as the marker atom, depending on the neighboring monomers, enabling potential triads of monomer sequences (EAE, AAE and AAA; E = ether, A = acid monomer) to be detected. Note that the structural motif EEE was not considered due to the steric hindrance and repulsion effect induced by the macromonomers exhibiting long polyethylene glycol side chains. As mentioned above, the chemical shift of the carboxyl carbon presented in poly(acrylic acid) was pH-dependent,[47] so all the experiments here were performed in D_2O at a consistent pH value of 13.0.

To determine the chemical shift of ^{13}C NMR spectra illustrating the carboxyl carbon in the series of 7HPEG PCEs exhibiting different anionic charge densities, the spectrum of AAA was recorded first. As is shown in Figure 10, the carboxyl carbon present in AAA exhibited a characteristic signal at a chemical shift δ of 184.4 ppm, which is identical to the value being reported before.[47] A ^{13}C NMR signal of PCEs at a chemical shift ~185 ppm can therefore be assigned to an AAA motif in the polymers. On the other hand, the downfield shifted ^{13}C NMR signals detected for HPEG PCEs (see below) can be assigned to AAE or EAE motifs due to the electronic effects of the E subunits.[48] Applying this method, three potential triads of monomer sequences (EAE, AAE, and AAA; E = ether, A = acid monomer) in the HPEG PCE polymer could be identified. It is worth noting that the chemical shifts between δ = 180−200 ppm represent the finger-print area needed to identify the monomer sequence in the PCE polymers.

The ^{13}C NMR spectra of HPEG PCE polymers are displayed in Figure 10. The spectra clearly indicated that the molar feeding ratio of the monomers (AA/HPEG macromonomer) exhibits a strong impact on the microstructure of the resulting comb copolymers. For example, in 7HPEG3.0, two peaks were observed in the ^{13}C NMR spectrum. One peak appearing at a chemical shift δ of 184.5 ppm can be assigned to the AAA motif, whereas another peak arising at a chemical shift δ of 186.0 ppm represents the AAE motif. Moreover, as listed in Table 5, the integral area for AAA and AAE sequences was found to be comparable, which indicates that these two triads are the dominating units. Furthermore, with the increasing molar feeding ratio of the monomers (AA/HPEG macromonomer), AAA triad intensity rose significantly, whereas AAE triad intensity weakened. In the ^{13}C NMR spectrum of the sample 7HPEG7.0, AAA became the dominant unit, while the AAE motif remained the second most frequently occurring unit. The data presented here agrees with the anionic charge amount measurements (see Figure 9). With the increasing molar feeding ratio of the monomers (AA/HPEG macromonomer), a higher amount of AA was incorporated into the PCE structures. Thereafter, more of the AAA motif was formed, as displayed in Table 5, which in turn increased the anionic charge density of the PCE polymers. Moreover, PCE polymers (e.g., 7HPEG7.0) exhibiting, such an architecture characterized by a substantially high AAA motif, could lead to stronger adsorption on slag particles (see Figure 7). As a result, enhanced dispersing power could be achieved (see Figures 5 and 6). It is worth noting that in the spectrum of the 7HPEG3.0 PCE sample, a very minor peak appeared at a chemical shift of 187.2 ppm, which can be assigned to the EAE triad. However, for the higher anionic HPEG PCE samples (7HPEG4.5 and 7HPEG7.0), the sequence representing EAE almost vanished from the spectra. Our finding is in good agreement with the previous study.[47] Combining the HPEG PCE microstructural information (having a different molar feeding ratio of AA to HPEG macromonomer) with the performance tests in AAS, we can conclude that PCE polymers possessing a higher amount of AAA and AAE motif

https://doi.org/10.1021/acssuschemeng.2c05430
ACS Sustainable Chem. Eng. XXXX, XXX, XXX−XXX

ACS Sustainable Chemistry & Engineering pubs.acs.org/journal/ascecg Research Article

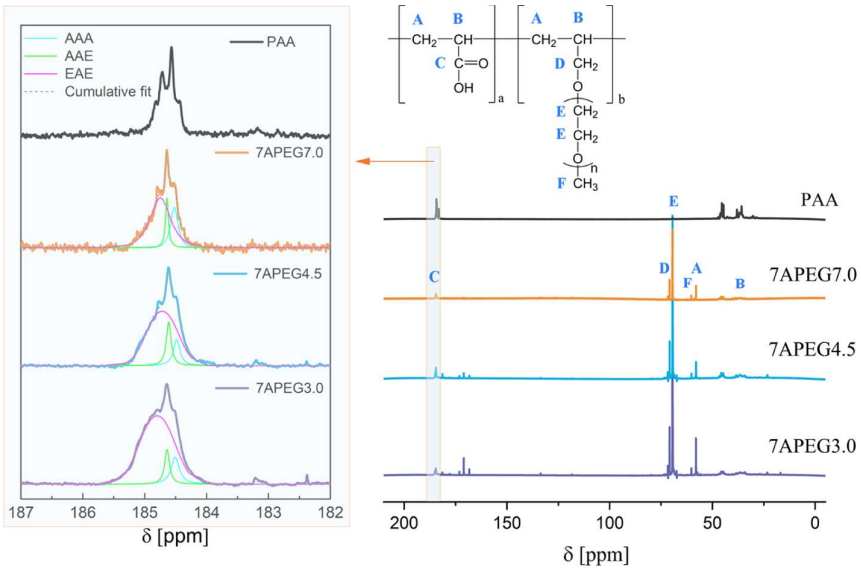

Figure 11. ^{13}C NMR spectra of APEG PCE polymers and PAA, measured in D_2O at pH = 13.

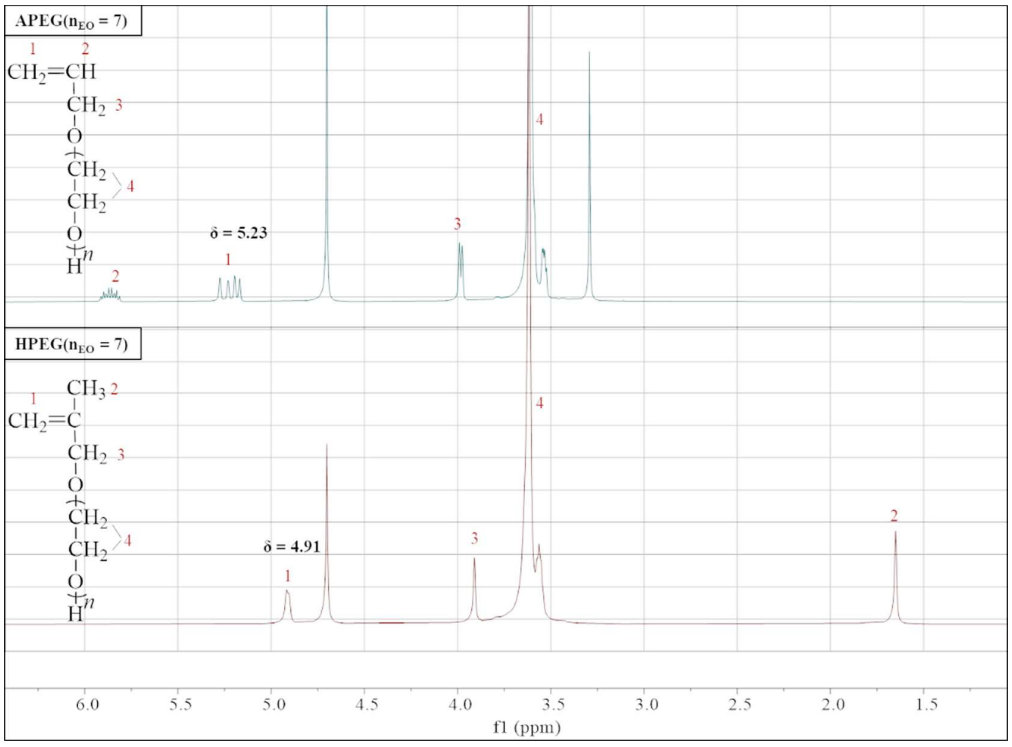

Figure 12. ^{1}H NMR spectra of APEG and HPEG macromonomers, measured in D_2O.

contributed to the enhanced dispersing capacity. Our finding here is consistent with the previous study carried out in the OPC system.[47]

In the following, the microstructural details of APEG PCEs were also analyzed. Figure 11 shows the ^{13}C NMR spectra of APEG series PCEs, which were deconvolved into three peaks, and the peak positions were kept constant for all three PCEs. The first peak at δ = 184.7 ppm is assigned to the EAE motif, while the peaks at δ = 184.6 and 184.4 ppm correspond to AAE and AAA, respectively. Furthermore, the integrated area of each fitting peak from APEG and HPEG series PCEs is listed in Table 5.

Comparing the ^{13}C NMR spectra of HPEG PCEs and APEG PCEs in Figures 10 and 11, it is obvious that PCE polymers prepared from different macromonomers exhibited distinct architectures. At first, the signal observed at δ = 184.4 ppm can be attributed to the carboxyl carbon presented in PAA. The two types of PCE polymers exhibited different spectrum shapes, in which HPEG PCEs typically contained three distinct peaks, whereas APEG PCEs possessed an

https://doi.org/10.1021/acssuschemeng.2c05430
ACS Sustainable Chem. Eng. XXXX, XXX, XXX−XXX

overlapping peak. The different spectrum shapes between two series PCEs can be attributed to the presence or the absence of the methyl group adjacent to the α carbon in HPEG and APEG macromonomers. For instance, 7HPEG PCEs exhibited three peaks arising at δ = 184.5 ppm, representing the AAA motif, and δ = 186.0 ppm δ = 187.3 ppm, standing for the AAE and EAE motifs, respectively. On the other hand, 7APEG4.5 possessed only one overlapping peak at δ = 184.5 ppm, which could be deconvolved into three peaks at δ = 184.7 ppm, 184.6 ppm, and 184.4 ppm, assigned to the EAE, AAE, and AAA motifs, respectively. As shown in Table 5, for both APEG and HPEG series PCEs, the proportion of AAA motif increases with the increasing AA to macromonomer ratio. The high percentage of AAA motif in the PCEs' microstructures enhanced their anchoring force, resulting in the high adsorption amounts of PCEs with a higher AA to macromonomer ratio. This result is in line with the dispersing performance of the PCE samples.

Interestingly, the proportion of EAE motifs in APEG PCEs was generally much higher than that in HPEG PCEs. This is because the allyl ether macromonomers exhibit an extremely low tendency to homopolymerize as a consequence of mesomeric stabilization.[26] Furthermore, the difference in the microstructure of PCE polymers can be attributed to the different reactivity ratios of the macromonomers (APEG and HPEG), which leads to an inhomogeneous repartition of the PEG side chains along the trunk chain. Factors such as the properties of the polymerizable groups, the compatibility between macromonomers and growing chains, the molecular weight of the macromonomers, and the polarity of the solvent, all have an impact on the macromonomer reactivity, thus, upon the polymer microstructures.

Next, the reactivity of C═C double bonds in APEG and HPEG macromonomers was estimated on the basis of ^{1}H NMR. The chemical shifts of the β-hydrogen atoms bonded to the C═C double bonds in these macromonomers were compared and are shown in Figure 12. The signal representing the β-hydrogen atom (marked as no. 1) in APEG macromonomer (n_{EO} = 7) appeared at a chemical shift of 5.2 ppm. The HPEG macromonomer (n_{EO} = 7) exhibited a signal at a chemical shift of 4.9 ppm, which can be assigned to the β-hydrogen atom (marked as no. 1) bonded to the C═C double bond. This difference in the chemical shifts is caused by the extra methyl group (marked as no. 2), which is directly connected to the C═C double bond in the HPEG macromonomer structure. The electron-donating methyl substituent led to an increased electron density of the β-hydrogen atom and the upfield shift observed caused an increase of the shielding effect. On this basis, ^{1}H NMR spectroscopic analysis confirmed the expected higher reactivity of the HPEG macromonomer compared to the APEG macromonomer.

According to the performance tests (Figures 5 and 6), HPEG PCEs generally exhibited superior dispersing capability over the APEG series. Apparently, the microstructure of PCE polymers—the repartition of the polyethylene glycol pendant chains along the mainchain—played a vital role in their dispersing effectiveness in the AAS system. This statement is supported by previous investigations.[49−51] Pourchet et al.[49] demonstrated that the repartition of the charged anchor groups (MAA) and polyethylene glycol side chains along the mainchain exert a strong impact on the adsorption behavior of PCE polymers on cement particles as well as their subsequent dispersing power. In their work, intrachain composition modification of PCE polymers was achieved via a living/controlled radical polymerization technique (RAFT). It was found that the PCE polymer exhibiting the gradient microstructure overperformed the counterpart polymer with the random microstructure in the performance tests.

Similarly, Pickelmann et al.[51] compared the different adsorption conformation of two MPEG PCEs prepared using two distinct methods. The results revealed that the copolymerized PCE sample exhibiting a gradient-like side chain distribution showed a stronger adsorption tendency on cement particles resulting from the blocks of $-COO^-$ in the structure. Nevertheless, the grafted PCE polymer characterized by a statistical side chain distribution adsorbed less on cement grains. As a consequence, the difference in microstructural composition could translate into a different interaction with cement.

In fact, when comparing different ether-type PCEs, multiple factors have an influence on the dispersing performance of polycarboxylate copolymers, such as their chain composition and polydispersity index as well as their adsorption conformations. In the present work, we mainly focus on monomer sequences in copolymers. When connecting the dispersing capability with the microstructural information of PCE, one can conclude that HPEG PCE polymers exhibiting two monomer sequences (AAA and AAE) represent more optimal molecular structures compared to APEG PCE polymers, where EAE is the dominant unit. We attribute this phenomenon to the enhanced adsorption which is in good agreement with previous studies.[25,27,30]

CONCLUSIONS

Based on our experience, there are several factors which determine the dispersing efficacy of PCE superplasticizers in AAS systems, among which the most important are solubility, specific anionic amount, specific molecular weight, and the tailored synthesis method. First, the PCE polymers need to be soluble in a high alkaline environment; second, the PCE polymers need to interact strongly via adsorption on AAS. As such, it has been demonstrated that PCE polymers with higher anionicity exhibit higher adsorption, and similar observations have been made for PCE polymers possessing higher molecular weight. Distinct polymer conformation which can be achieved via tailored synthesis methods, such as gradient polymers prepared from free radical copolymerization, typically exhibit stronger dispersion.

Here, we investigate the influence of the architecture and the PEG side chain's repartition along the trunk chain of two PCE copolymer types on the AAS system's dispersing behavior. Paste and mortar flowability results revealed that HPEG-based PCEs exhibited stronger dispersing effectiveness compared to APEG-based PCEs, especially for the PCE polymers with higher anionicity. The increased adsorption of HPEG PCEs on slag particles was demonstrated to contribute significantly to their extraordinary dispersion performance. In addition, the architecture of PCE polymers also plays a vital role relative to the dispersing capability in the AAS systems. ^{13}C Nuclear magnetic resonance (NMR) spectroscopy clearly indicated that the molar feeding ratio of the monomers (AA/HPEG macromonomer) strongly impacts the architecture of the resulting comb copolymers. PCE polymers with higher molar ratios typically possessed higher amounts of the AAE and AAA motif, which in turn resulted in the enhanced dispersing

https://doi.org/10.1021/acssuschemeng.2c05430
ACS Sustainable Chem. Eng. XXXX, XXX, XXX−XXX

capacity. When the two kinds of PCEs were compared, it was found that HPEG PCE exhibiting two dominating monomer sequences (AAA and AAE) represent an optimized molecular structure as compared to APEG PCEs with EAE as the main monomer sequence. Our findings suggest that the individual microstructure of a PCE polymer plays a pivotal role with respect to its dispersing capacity in such low carbon eco-friendly binders.

AUTHOR INFORMATION

Corresponding Authors

Lei Lei − *Chair for Construction Chemistry, Technische Universität München, 85747 Garching, Germany;* orcid.org/0000-0003-1177-6966; Phone: +49 (0)89 289 13161; Email: lei.lei@tum.de; Fax: +49 (0)89 289 13152

Johann Plank − *Chair for Construction Chemistry, Technische Universität München, 85747 Garching, Germany;* orcid.org/0000-0002-4129-4784; Email: sekretariat@bauchemie.ch.tum.de

Authors

Ran Li − *Chair for Construction Chemistry, Technische Universität München, 85747 Garching, Germany*

Wolfgang Eisenreich − *Bavarian NMR Center—Structural Membrane Biochemistry, Technische Universität München, 85747 Garching, Germany*

Complete contact information is available at: https://pubs.acs.org/10.1021/acssuschemeng.2c05430

Notes

The authors declare no competing financial interest.

ACKNOWLEDGMENTS

The authors wish to thank Jilin Zhongxin for generously providing HPEG macromonomer and Ecocem France for providing the slag for this research. R.L. would like to thank the China Scholarship Council (CSC) for generous funding of her PhD studies at the TU München. The authors also would like to thank M. Sc. Hsien-Keng Chan and M. Sc. Yuheng Deng for their support in the laboratory experiments. Appreciation goes to Frau Tina Schrier from TUM Language Center for proofreading this article several times.

REFERENCES

(1) Mittelman, E. *The Cement Industry, One of the World's Largest CO_2 Emitters, Pledges to Cut Greenhouse Gases*, 2019.

(2) IEA (2021), France 2021, IEA, Paris, License: CC BY 4.0, https://www.iea.org/reports/france-2021 (retrieved on November, 2021).

(3) Pacheco-Torgal, F.; Castro-Gomes, J.; Jalali, S. Alkali-activated binders: A review. *Construct. Build. Mater.* **2008**, *22*, 1305−1314.

(4) Bougara, A.; Lynsdale, C.; Milestone, N. B. Reactivity and performance of blastfurnace slags of differing origin. *Cem. Concr. Compos.* **2010**, *32*, 319−324.

(5) Ben Haha, M.; Le Saout, G.; Winnefeld, F.; Lothenbach, B. Influence of activator type on hydration kinetics, hydrate assemblage and microstructural development of alkali activated blast-furnace slags. *Cem. Concr. Res.* **2011**, *41*, 301−310.

(6) Deng, G.; He, Y.; Lu, L.; Wang, F.; Hu, S. Comparison between Fly Ash and Slag Slurry in Various Alkaline Environments: Dissolution, Migration, and Coordination State of Aluminum. *ACS Sustainable Chem. Eng.* **2021**, *9*, 12109−12119.

(7) Provis, J. L.; Palomo, A.; Shi, C. Advances in understanding alkali-activated materials. *Cem. Concr. Res.* **2015**, *78*, 110−125.

(8) Huang, Z.; Wang, Q.; Lu, J. The effects of cations and concentration on reaction mechanism of alkali-activated blast furnace ferronickel slag. *Compos. B Eng.* **2022**, *236*, 109825.

(9) Baalamurugan, J.; Kumar, V. G.; Chandrasekaran, S.; Balasundar, S.; Venkatraman, B.; Padmapriya, R.; Raja, V. K. B. Recycling of steel slag aggregates for the development of high density concrete: Alternative & environment-friendly radiation shielding composite. *Compos. B Eng.* **2021**, *216*, 108885.

(10) Ke, X.; Criado, M.; Provis, J. L.; Bernal, S. A. Slag-Based Cements That Resist Damage Induced by Carbon Dioxide. *ACS Sustainable Chem. Eng.* **2018**, *6*, 5067−5075.

(11) Shi, C.; Jiménez, A. F.; Palomo, A. New cements for the 21st century: The pursuit of an alternative to Portland cement. *Cem. Concr. Res.* **2011**, *41*, 750−763.

(12) Yang, K.-H.; Song, J.-K.; Song, K.-I. Assessment of CO_2 reduction of alkali-activated concrete. *J. Clean. Prod.* **2013**, *39*, 265−272.

(13) Favier, A.; De Wolf, C.; Scrivener, K. L.; Habert, G. A sustainable future for the European Cement and Concrete Industry. *Technology Assessment for Full Decarbonisation of the Industry by 2050*; ETH Zurich, 2018.

(14) Burris, L. E.; Alapati, P.; Moser, R. D.; Ley, M. T.; Berke, N.; Kurtis, K. E. Alternative cementitious materials: Challenges and opportunities, *International Workshop on Durability and Sustainability of Concrete Structures*: Bologna, Italy, 2015.

(15) Torres-Carrasco, M.; Tognonvi, M.; Tagnit-Hamou, A.; Puertas, F. Durability of Alkali-Activated Slag Concretes Prepared Using Waste Glass as Alternative Activator. *ACI Mater. J.* **2015**, *112*, 791−800.

(16) Tang, Z.; Li, W.; Tam, V. W. Y.; Luo, Z. Investigation on dynamic mechanical properties of fly ash/slag-based geopolymeric recycled aggregate concrete. *Compos. B Eng.* **2020**, *185*, 107776.

(17) Zhu, Y.; Longhi, M. A.; Wang, A.; Hou, D.; Wang, H.; Zhang, Z. Alkali leaching features of 3-year-old alkali activated fly ash-slag-silica fume: For a better understanding of stability. *Compos. B Eng.* **2022**, *230*, 109469.

(18) Ye, H.; Radlińska, A. Shrinkage mechanisms of alkali-activated slag. *Cem. Concr. Res.* **2016**, *88*, 126−135.

(19) Duran Atiş, C.; Bilim, C.; Çelik, Ö.; Karahan, O. Influence of activator on the strength and drying shrinkage of alkali-activated slag mortar. *Construct. Build. Mater.* **2009**, *23*, 548−555.

(20) Palacios, M.; Puertas, F. Effectiveness of Mixing Time on Hardened Properties of Waterglass-Activated Slag Pastes and Mortars. *ACI Mater. J.* **2011**, *108*, 73−78.

(21) Palacios, M.; Banfill, P. F. G.; Puertas, F. Rheology and setting of alkali-activated slag pastes and mortars: Effect of organic admixture. *ACI Mater. J.* **2008**, *105*, 140.

(22) Wang, D.; Wang, Q.; Huang, Z. New insights into the early reaction of NaOH-activated slag in the presence of $CaSO_4$. *Compos. B Eng.* **2020**, *198*, 108207.

(23) Liang, G.; Liu, T.; Li, H.; Wu, K. Shrinkage mitigation, strength enhancement and microstructure improvement of alkali-activated slag/fly ash binders by ultrafine waste concrete powder. *Compos. B Eng.* **2022**, *231*, 109570.

(24) Puertas, F.; González-Fonteboa, B.; González-Taboada, I.; Alonso, M. M.; Torres-Carrasco, M.; Rojo, G.; Martínez-Abella, F. Alkali-activated slag concrete: Fresh and hardened behaviour. *Cem. Concr. Compos.* **2018**, *85*, 22−31.

(25) Lei, L.; Chan, H.-K. Investigation into the molecular design and plasticizing effectiveness of HPEG-based polycarboxylate superplasticizers in alkali-activated slag. *Cem. Concr. Res.* **2020**, *136*, 106150.

(26) Plank, J.; Sakai, E.; Miao, C. W.; Yu, C.; Hong, J. X. Chemical admixtures — Chemistry, applications and their impact on concrete microstructure and durability. *Cem. Concr. Res.* **2015**, *78*, 81−99.

https://doi.org/10.1021/acssuschemeng.2c05430
ACS Sustainable Chem. Eng. XXXX, XXX, XXX−XXX

(27) Conte, T.; Plank, J. Impact of molecular structure and composition of polycarboxylate comb polymers on the flow properties of alkali-activated slag. *Cem. Concr. Res.* **2019**, *116*, 95−101.
(28) Laguna, M. T. R.; Medrano, R.; Plana, M. P.; Tarazona, M. P. Polymer characterization by size-exclusion chromatography with multiple detection. *J. Chromatogr., A* **2001**, *919*, 13−19.
(29) DIN EN 1015-3: 2007-5. *Methods of Test for Mortar for Masonry—Part 3: Determination of Consistence of Fresh Mortar (By Flow Table)*.
(30) Lei, L.; Zhang, Y.; Li, R. Specific molecular design of polycarboxylate polymers exhibiting optimal compatibility with clay contaminants in concrete. *Cem. Concr. Res.* **2021**, *147*, 106504.
(31) Lei, L.; Zhang, Y. Preparation of isoprenol ether-based polycarboxylate superplasticizers with exceptional dispersing power in alkali-activated slag: Comparison with ordinary Portland cement. *Compos. B Eng.* **2021**, *223*, 109077.
(32) Dalas, F.; Nonat, A.; Pourchet, S.; Mosquet, M.; Rinaldi, D.; Sabio, S. Tailoring the anionic function and the side chains of comb-like superplasticizers to improve their adsorption. *Cem. Concr. Res.* **2015**, *67*, 21−30.
(33) Plank, J.; Hirsch, C. Impact of zeta potential of early cement hydration phases on superplasticizer adsorption. *Cem. Concr. Res.* **2007**, *37*, 537−542.
(34) Ma, Y.; Sha, S.; Zhou, B.; Lei, F.; Liu, Y.; Xiao, Y.; Shi, C. Adsorption and dispersion capability of polycarboxylate-based superplasticizers: a review. *J. Sustain. Cem.-Based Mater.* **2022**, *11*, 319−344.
(35) Karakuzu, K.; Kobya, V.; Mardani-Aghabaglou, A.; Felekoğlu, B.; Ramyar, K. Adsorption properties of polycarboxylate ether-based high range water reducing admixture on cementitious systems: A review. *Construct. Build. Mater.* **2021**, *312*, 125366.
(36) He, Y.; Zhang, X.; Shui, L.; Wang, Y.; Gu, M.; Wang, X.; Wang, H.; Peng, L. Effects of PCEs with various carboxylic densities and functional groups on the fluidity and hydration performances of cement paste. *Construct. Build. Mater.* **2019**, *202*, 656−668.
(37) Han, S.; Plank, J. Mechanistic study on the effect of sulfate ions on polycarboxylate superplasticisers in cement. *Adv. Cem. Res.* **2013**, *25*, 200−207.
(38) Lange, A.; Plank, J. Contribution of non-adsorbing polymers to cement dispersion. *Cem. Concr. Res.* **2016**, *79*, 131−136.
(39) Vo, M. L.; Plank, J. Dispersing effectiveness of a polycarboxylate in α-and β-calcium sulfate hemihydrate systems. *Construct. Build. Mater.* **2020**, *237*, 117731.
(40) Yang, Z.; Yu, M.; Liu, Y.; Chen, X.; Zhao, Y. Synthesis and performance of an environmentally friendly polycarboxylate superplasticizer based on modified poly (aspartic acid). *Construct. Build. Mater.* **2019**, *202*, 154−161.
(41) Flatt, R. J.; Schober, I.; Raphael, E.; Plassard, C.; Lesniewska, E. Conformation of Adsorbed Comb Copolymer Dispersants. *Langmuir* **2009**, *25*, 845−855.
(42) Plank, J.; Sachsenhauser, B. Impact of Molecular Structure on Zeta Potential and Adsorbed Conformation of α-Allyl-ω- Glycol - Maleic Anhydride Superplasticizers. *J. Adv. Concr. Technol.* **2006**, *4*, 233−239.
(43) Tian, H.; Kong, X.; Su, T.; Wang, D. Comparative study of two PCE superplasticizers with varied charge density in Portland cement and sulfoaluminate cement systems. *Cem. Concr. Res.* **2019**, *115*, 43−58.
(44) Shu, X.; Ran, Q.; Liu, J.; Zhao, H.; Zhang, Q.; Wang, X.; Yang, Y.; Liu, J. Tailoring the solution conformation of polycarboxylate superplasticizer toward the improvement of dispersing performance in cement paste. *Construct. Build. Mater.* **2016**, *116*, 289−298.
(45) Shu, X.; Wang, Y.; Yang, Y.; Wang, X.; Zhang, Q.; Zhao, H.; Ran, Q.; Liu, J. Rheological properties of cement pastes with polycarboxylate superplasticizers of varied backbone stiffness. *J. Mater. Civ. Eng.* **2019**, *31*, 04019092.
(46) Chomyn, C.; Plank, J. Impact of different synthesis methods on the dispersing effectiveness of isoprenol ether-based zwitterionic and anionic polycarboxylate (PCE) superplasticizers. *Cem. Concr. Res.* **2019**, *119*, 113−125.
(47) Plank, J.; Li, H.; Ilg, M.; Pickelmann, J.; Eisenreich, W.; Yao, Y.; Wang, Z. A microstructural analysis of isoprenol ether-based polycarboxylates and the impact of structural motifs on the dispersing effectiveness. *Cem. Concr. Res.* **2016**, *84*, 20−29.
(48) Rozzoni, A.; Bellotto, M. Configurational NMR Study of Sodium Polymethacrilate-g-PEO Comb Polymers, *14th International Congress on the Chemistry of Cement*: Madrid, 2011.
(49) Pourchet, S.; Liautaud, S.; Rinaldi, D.; Pochard, I. Effect of the repartition of the PEG side chains on the adsorption and dispersion behaviors of PCP in presence of sulfate. *Cem. Concr. Res.* **2012**, *42*, 431−439.
(50) Emaldi, I.; Hamzehlou, S.; Sanchez-Dolado, J.; Leiza, J. R. Kinetics of the Aqueous-Phase Copolymerization of MAA and PEGMA Macromonomer: Influence of Monomer Concentration and Side Chain Length of PEGMA. *Processes* **2017**, *5*, 19.
(51) Pickelmann, J.; Li, H.; Baumann, R.; Plank, J. A 13C NMR Spectroscopic Study on the Reparation of Acid and Ester Groups in MPEG Type PCEs Prepared via Radical Copolymerization and Grafting Techniques. *SP-302: Eleventh International Conference on Superplasticizers and Other Chemical Admixtures in Concrete*, 2015.

https://doi.org/10.1021/acssuschemeng.2c05430
ACS Sustainable Chem. Eng. XXXX, XXX, XXX−XXX

6. Summary and outlook

The focus of this thesis was to investigate the effectiveness and interaction of PCE superplasticizers with with low-carbon composite cements containing calcined clay or alkali-activated slag. Two main topics were addressed in this thesis: (1) effectiveness and interaction of PCEs with calcined clay blended cements; (2) impact of PCEs on the fluidity of AAS composite cements. For this purpose, severial series of PCE superplasticizers with defined molecular structures were synthesized, and their dispersing effectiveness in both paste and mortars of those low carbon cements was assessed. Moreover, mechanistic studies relating to the surface charge of the binders, the adsorption of PCEs on calcined clay, OPC and slag and the microstructural properties of specific PCE molecules were conducted.

For the calcined clay composite cement, the study targeted three main aspects: the **initial fluidity** of the composite cement containing a calcined clay rich in meta kaolin; approaches to achieve **slump retention** in those calcined clay blended composite cements; and the **impact of meta kaolin** content and fineness on the dispersing force of different PCE superplasticizers.

Based on this analysis, it can be concluded that the addition of a calcined clay holding a high content of meta kaolin to OPC clinker makes it extremely difficult to achieve proper initial fluidity as well as slump retention. Due to the high specific surface area and the highly negative surface charge of pristine calcined clay, a large amount of PCE is taken up. This high sorption of PCE on calcined

clay is facilitated by a layer of adsorbed Ca^{2+} ions onto the negatively charged calcined clay surface. In both, neat calcined clay and calcined clay blended cements, the methallyl ether (HPEG) PCE polymers were found to provide superior dispersing performance over MPEG based superplasticizers. In addition, a comparison between an anionic and an amphoteric MPEG PCE reveals that the presence of a positively charged functionality in the backbone of the zwitterionic positively influences its performance in such cements. Generally, the water demand of the pure meta clays is determined by their fineness, particle size and internal porosity and was found to follow this order: meta muscovite ≫ meta illite ≫ meta kaolin > meta montmorillonite. Relative to PCE dosage requirements, the order as follows was established: meta kaolinite > meta montmorillonite > meta muscovite. Surprisingly, no PCE polymer was identified which could disperse meta illite.

Moreover, in order to achieve long slump retention from such cements, a novel PCE-LDH admixture which allows to achieve extended slump retention times was invented, while only short slump retaining times were obtained from conventional hydrolyzing esters based PCEs (e.g. HPEG ready-mix) and its combination with a retarder (sodium gluconate). The high effectiveness of the PCE-LDH nanocomposite is attributed to the gradual release of superplasticizer from the nanocomposite via progressive anion exchange with sulfate anions present in the cement pore solution.

In addition, by comparing calcined clays of different meta kaolin contents, it was

found that increased meta kaolin contents in a calcined clay improves its pozzolanic reactivity and early strength development; however, it also increases the water demand and unfortunately prompts high superplasticizer dosages for those composite cements. Furthermore, water demand and PCE dosage of such composite cements are also closely related to the particle fineness. The fineness mainly affects the water demand, while the meta kaolin content plays a dominant role with respect to PCE dosage requirement. This behavior was confirmed for several commercial meta kaolin samples obtained from different sources.

In AAS composite cements, the influence of PCEs possessing different microstructures on their dispersing effectiveness was investigated. It was found that anionicity and molecular weight of the PCEs present the most critical parameters for their dispersing effctiveness in AAS. Moreover, HPEG-based PCEs exhibited superior dispersing performance as compared to APEG-based PCEs. A mechanistic study via ^{13}C Nuclear magnetic resonance (NMR) spectroscopy revealed that enhanced dispersing capacity of those PCE polymers is observed when the structural motif of AAE (A= acrylic acid, E= macromonomer ether) becomes dominant. Furthermore, results from measuring their dissolved hydrodynamic radii signify that the dispersing performance of these PCEs also can be correlated to their adsorbed conformation.

Low-carbon cements present highly attractive OPC alternatives due to their

lower CO_2 footprint. Yet multiple factors, such as early strength development and workability issues need to be taken into account when applying such cements. Unfortunately, both low-carbon binders represented by calcined clay and AAS composite cements exhibit the distinct disadvantage of poor flowability (workability).

This thesis provides a basic understanding of the effectiveness and interaction between common PCE superplasticizers and calcined clay or AAS composite cements. In the future, it will be necessary for the admixture industry to develop new technologies to ensure improved workability while at the same time achieving sufficiently high early strength from those binders.

7. Zusammenfassung und Ausblick

Der Schwerpunkt dieser Arbeit lag auf der Untersuchung der Wirksamkeit und Wechselwirkung von PCE-Fließmitteln mit CO_2-reduzierten Kompositzementen, die kalzinierten Ton oder alkalisch aktivierte Schlacke enthalten. Zwei Hauptthemen wurden in dieser Arbeit behandelt: (1) Wirksamkeit und Wechselwirkung von PCEs mit Kompositzementen mit kalzinierten Tonen; (2) Einfluss von PCEs auf die Fließfähigkeit von AAS-Kompositzementen. Zu diesem Zweck wurden mehrere Serien von PCE-Fließmitteln mit definierten Molekülstrukturen synthetisiert und ihre Dispergierwirkung sowohl im Zementleim als auch im Mörtel dieser CO_2-reduzierten Zemente untersucht. Darüber hinaus wurden mechanistische Studien zur Oberflächenladung der Bindemittel, zur Sorption der PCEs auf kalziniertem Ton, OPC und Schlacke sowie zu den mikrostrukturellen Eigenschaften bestimmter PCE-Moleküle durchgeführt.

Für den Zement mit kalziniertem Ton zielte die Studie auf drei Hauptaspekte ab: die anfängliche Fließfähigkeit des Kompositzements, der einen kalzinierten Ton enthält, der reich an Meta-Kaolin ist; Ansätze zum Erreichen der Aufrechterhaltung der Fließfähigkeit über Zeit in diesen mit kalziniertem Ton gemischten Kompositzementen; und die Auswirkungen des Meta-Kaolingehalts und der Feinheit auf die Dispergierwirkung verschiedener PCE-Fließmittel.

Aus dieser Analyse lässt sich schließen, dass die Zugabe von kalziniertem Ton

mit einem hohen Anteil an Meta-Kaolin zum OPC-Klinker das Erreichen einer angemessenen anfänglichen Fließfähigkeit sowie die Aufrechterhaltung des Fließmaßes über die Zeit extrem erschwert. Aufgrund der hohen spezifischen Oberfläche und der stark negativen Oberflächenladung des reinen kalzinierten Tons wird eine große Menge an PCE sorbiert. Diese hohe Adsorption von PCE auf kalziniertem Ton wird durch eine Schicht adsorbierter Ca^{2+}-Ionen auf der negativ geladenen Oberfläche des kalzinierten Tons ermöglicht. Sowohl im reinen kalzinierten Ton als auch in Kompositzementen mit kalziniertem Ton ergaben die PCE-Polymere auf Methallyletherbasis (HPEG) eine bessere Dispergierleistung als MPEG-basierte Fließmittel. Darüber hinaus zeigt ein Vergleich zwischen einem anionischen und einem amphoteren MPEG-PCE, dass das Vorhandensein einer positiven Ladung in der Hauptkette des zwitterionischen Polymers seine Wirkung in solchen Zementen positiv beeinflusst. Im Allgemeinen wird der Wasserbedarf der reinen Meta-Tone durch ihre Feinheit, Partikelgröße und innere Porosität bestimmt und folgende Reihenfolge wurde ermittelt: Meta-Muskovit ≫ Meta-Illit ≫ Meta-Kaolin > Meta-Montmorillonit. Bezogen auf den Bedarf an PCE-Dosierung wurde folgende Reihung festgestellt: Meta-Muskovit < Meta-Montmorillonit < Meta-Kaolinit. Überraschenderweise wurde kein PCE-Polymer identifiziert, das Meta-Illit dispergieren konnte.

Um eine langanhaltende Aufrechterhaltung des Fließmaßes solcher Zemente zu erreichen, wurde ein neuartiges PCE-LDH-Zusatzmittel erfunden, mit dem

eine lang anhaltende Verarbeitbarkeit erreicht werden konnte, während mit herkömmlichen PCEs auf Basis hydrolysierender Ester (z. B. Transportbeton HPEG-PCE) und deren Kombination mit einem Verzögerer (Natriumgluconat) nur kurze zeitliche Aufrechterhaltung des Fließmaßes erzielt wurde. Die hohe Wirksamkeit des PCE-LDH-Nanokomposits wird auf die allmähliche Freisetzung des Fließmittels aus dem Nanokomposit durch fortschreitenden Anionenaustausch mit in der Zementporenlösung vorhandenen Sulfatanionen zurückgeführt.

Darüber hinaus wurde durch den Vergleich von kalzinierten Tonen mit unterschiedlichem Meta-Kaolingehalt festgestellt, dass ein höherer Meta-Kaolingehalt in einem kalzinierten Ton die puzzolanische Reaktivität und die frühe Festigkeitsentwicklung verbessert, jedoch auch den Wasserbedarf erhöht und ungünstigerweise zu einer hohen Fließmitteldosierung für diese Kompositzemente führt. Darüber hinaus sind Wasserbedarf und Fließmitteldosierung solcher Kompositzemente auch eng mit der Kornfeinheit verbunden. Die Feinheit wirkt sich hauptsächlich auf den Wasserbedarf aus, während der Meta-Kaolin-Gehalt im Hinblick auf die erforderliche PCE-Dosierung eine dominierende Rolle spielt. Dieses Verhalten wurde für mehrere kommerzielle Meta-Kaolinproben aus verschiedenen Quellen bestätigt.

In AAS-Kompositzementen wurde der Einfluss von PCEs mit unterschiedlichen Mikrostrukturen auf ihre Dispergierwirkung untersucht. Es wurde festgestellt, dass die Anionizität und das Molekulargewicht der PCEs die wichtigsten

Parameter für die Dispergierwirkung in AAS darstellen. Darüber hinaus zeigten HPEG-basierte PCEs im Vergleich zu APEG-basierten PCEs eine bessere Dispergierleistung. Eine mechanistische Studie mittels ^{13}C-Kernresonanzspektroskopie (NMR) ergab, dass die verbesserte Dispergierfähigkeit dieser PCE-Polymere auf das strukturelle Motiv AAE (A= Acrylsäure, E= Makromonomerether) zurückzuführen ist, während die Ergebnisse der Messung des hydrodynamischen Radius in Lösung zeigten, dass die Dispergierleistung auch mit ihrer adsorbierten Konformation korreliert werden kann.

CO_2-reduzierte Zemente sind aufgrund ihres geringeren CO_2-Fußabdrucks äußerst attraktive OPC-Alternativen. Allerdings müssen bei der Anwendung solcher Zemente mehrere Faktoren wie die Entwicklung der Frühfestigkeit und die Verarbeitbarkeit berücksichtigt werden. Leider haben sowohl derartige Zemente mit kalziniertem Ton oder AAS-Kompositzemente den entscheidenden Nachteil einer schlechten Fließfähigkeit (Verarbeitbarkeit).

Diese Arbeit vermittelt ein grundlegendes Verständnis der Wirksamkeit und der Wechselwirkung zwischen gängigen PCE-Fließmitteln und Kompositzementen mit kalziniertem Ton oder AAS. In Zukunft wird es für die Zusatzmittelindustrie notwendig sein, neue Technologien zu entwickeln, um eine verbesserte Fließfähigkeit dieser umweltfreundlichen Zemente zu gewährleisten und gleichzeitig eine ausreichend hohe Frühfestigkeit aus diesen Bindemitteln zu erzielen.

8. References

[1] "German Cabinet approves landmark climate bill". DW.COM. 2021-05-12. , Archived from the original on 2021-05-20. Retrieved 2021-05-22.

[2] Darby, Megan (2019-06-14). "Which countries have a net zero carbon goal?", Climate Home News, Archived from the original on 2021-04-09. Retrieved 2019-06-16.

[3] "China Pledges Carbon Neutrality by 2060 and Tighter Climate Goal". news.bloomberglaw.com., Archived from the original on 2021-01-22. Retrieved 2020-09-22.

[4] R.M. Andrew, Global CO_2 emissions from cement production, Earth System Science Data, 10 (2018) 195-217.

[5] International Energy Agency and The Cement Sustainability Initiative, Technology Roadmap: Low-Carbon Transition in the Cement Industry, Paris, 2018, pp. 61.

[6] E. Gartner, T. Sui, Alternative cement clinkers, Cement and Concrete Research, 114 (2018) 27-39.

[7] M.H. Samarakoon, P.G. Ranjith, T.D. Rathnaweera, M.S.A. Perera, Recent advances in alkaline cement binders: A review, Journal of Cleaner Production, 227 (2019) 70-87.

[8] C. Shi, B. Qu, J.L. Provis, Recent progress in low-carbon binders, Cement and Concrete Research, 122 (2019) 227-250.

[9] S. Hollanders, R. Adriaens, J. Skibsted, Ö. Cizer, J. Elsen, Pozzolanic reactivity of pure calcined clays, Applied Clay Science, 132-133 (2016) 552-560.

[10] M. Izadifar, P. Thissen, A. Steudel, R. Kleeberg, S. Kaufhold, J. Kaltenbach, R. Schuhmann, F. Dehn, K. Emmerich, Comprehensive Examination of Dehydroxylation of Kaolinite, Disordered Kaolinite, and Dickite: Experimental Studies and Density Functional Theory, Clays and Clay Minerals, 68 (2020) 319-333.

[11] K. Scrivener, F. Martirena, S. Bishnoi, S. Maity, Calcined clay limestone cements (LC^3), Cement and Concrete Research, 114 (2018) 49-56.

[12] R. Fernandez, F. Martirena, K. Scrivener, The origin of the pozzolanic activity of calcined clay minerals: A comparison between kaolinite, illite and montmorillonite, Cement and Concrete Research, 41 (2011) 113-122.

[13] S. Krishnan, A.C. Emmanuel, S. Bishnoi, Hydration and phase assemblage of ternary cements with calcined clay and limestone, Construction and Building Materials, 222 (2019) 64-72.

[14] P. Awoyera, A. Adesina, A critical review on application of alkali activated

slag as a sustainable composite binder, Case Studies in Construction Materials, 11 (2019) e00268.

[15] A. Favier, C. De Wolf, K. Scrivener, G. Habert, A sustainable future for the European Cement and Concrete Industry. Technology assessment for full decarbonisation of the industry by 2050, ETH Zurich, 2018.

[16] L.E. Burris, P. Alapati, R.D. Moser, M.T. Ley, N. Berke, K.E. Kurtis, Alternative cementitious materials: Challenges and opportunities, International Workshop on Durability and Sustainability of Concrete Structures, Bologna, Italy, 2015.

[17] J. Plank, E. Sakai, C.W. Miao, C. Yu, J.X. Hong, Chemical admixtures — Chemistry, applications and their impact on concrete microstructure and durability, Cement and Concrete Research, 78 (2015) 81-99.

[18] P.C. Nkinamubanzi, S. Mantellato, R.J. Flatt, 16 - Superplasticizers in practice, in: P.-C. Aïtcin, R.J. Flatt (Eds.) Science and Technology of Concrete Admixtures, Woodhead Publishing2016, pp. 353-377.

[19] P.-C. Aïtcin, R.J. Flatt, Science and technology of concrete admixtures, Woodhead Publishing2015.

[20] K. Yamada, T. Takahashi, S. Hanehara, M. Matsuhisa, Effects of the chemical structure on the properties of polycarboxylate-type superplasticizer, Cement and Concrete Research, 30 (2000) 197-207.

[21] T.M. Vickers, S.A. Farrington, J.R. Bury, L.E. Brower, Influence of dispersant structure and mixing speed on concrete slump retention, Cement and Concrete Research, 35 (2005) 1882-1890.

[22] J. Plank, B. Sachsenhauser, Impact of Molecular Structure on Zeta Potential and Adsorbed Conformation of α-Allyl-ω-Methoxypolyethylene Glycol - Maleic Anhydride Superplasticizers, Journal of Advanced Concrete Technology, 4 (2006) 233-239.

[23] F. Winnefeld, S. Becker, J. Pakusch, T. Götz, Effects of the molecular architecture of comb-shaped superplasticizers on their performance in cementitious systems, Cement and Concrete Composites, 29 (2007) 251-262.

[24] J. Plank, K. Pöllmann, N. Zouaoui, P.R. Andres, C. Schaefer, Synthesis and performance of methacrylic ester based polycarboxylate superplasticizers possessing hydroxy terminated poly(ethylene glycol) side chains, Cement and Concrete Research, 38 (2008) 1210-1216.

[25] T. Hirata, T. Nawa, The effect of polycarboxylate-type superplasticizer controlled its adsorption rate onto the cement particles by changing the polymer structur, Nihon Kenchiku Gakkai Kozokei Ronbunshu, 74 (2009) 765-773.

[26] C. Miao, Q. Ran, J. Liu, Y. Mao, Y. Shang, J. Sha, New Generation

Amphoteric Comb-like Copolymer Superplasticizer and Its Properties, Polymers and Polymer Composites, 19 (2011) 1-8.

[27] L. Lei, J. Plank, Synthesis, working mechanism and effectiveness of a novel cycloaliphatic superplasticizer for concrete, Cement and Concrete Research, 42 (2012) 118-123.

[28] M. Ilg, J. Plank, Synthesis and Properties of a Polycarboxylate Superplasticizer with a Jellyfish-Like Structure Comprising Hyperbranched Polyglycerols, Industrial & Engineering Chemistry Research, 58 (2019) 12913-12926.

[29] C. Schröfl, M. Gruber, J. Plank, Preferential adsorption of polycarboxylate superplasticizers on cement and silica fume in ultra-high performance concrete (UHPC), Cement and Concrete Research, 42 (2012) 1401-1408.

[30] P.P. Li, Q.L. Yu, H.J.H. Brouwers, Effect of PCE-type superplasticizer on early-age behaviour of ultra-high performance concrete (UHPC), Construction and Building Materials, 153 (2017) 740-750.

[31] J. Du, W. Meng, K.H. Khayat, Y. Bao, P. Guo, Z. Lyu, A. Abu-obeidah, H. Nassif, H. Wang, New development of ultra-high-performance concrete (UHPC), Composites Part B: Engineering, 224 (2021).

[32] Y. Chen, S. He, Y. Zhang, Z. Wan, O. Çopuroğlu, E. Schlangen, 3D printing of calcined clay-limestone-based cementitious materials, Cement and Concrete Research, 149 (2021).

[33] H. Kloft, H.-W. Krauss, N. Hack, E. Herrmann, S. Neudecker, P.A. Varady, D. Lowke, Influence of process parameters on the interlayer bond strength of concrete elements additive manufactured by Shotcrete 3D Printing (SC3DP), Cement and Concrete Research, 134 (2020).

[34] L. Lei, H.-K. Chan, Investigation into the molecular design and plasticizing effectiveness of HPEG-based polycarboxylate superplasticizers in alkali-activated slag, Cement and Concrete Research, 136 (2020) 106150.

[35] L. Lei, Y. Zhang, Preparation of isoprenol ether-based polycarboxylate superplasticizers with exceptional dispersing power in alkali-activated slag: Comparison with ordinary Portland cement, Composites Part B: Engineering, 223 (2021).

[36] S.Y. Oderji, B. Chen, C. Shakya, M.R. Ahmad, S.F.A. Shah, Influence of superplasticizers and retarders on the workability and strength of one-part alkali-activated fly ash/slag binders cured at room temperature, Construction and Building Materials, 229 (2019) 11.

[37] T. Conte, J. Plank, Impact of molecular structure and composition of polycarboxylate comb polymers on the flow properties of alkali-activated slag, Cement and Concrete Research, 116 (2019) 95-101.

[38] R. Sposito , N. Beuntner, K.-C. Thienel, Rheology, setting and hydration

of calcined clay blended cements in interaction with PCE-based superplasticisers, Magazine of Concrete Research, 73 (2021) 785-797.

[39] M. Schmid, J. Plank, Dispersing performance of different kinds of polycarboxylate (PCE) superplasticizers in cement blended with a calcined clay, Construction and Building Materials, 258 (2020).

[40] R. Sposito, N. Beuntner, K.-C. Thienel, Characteristics of components in calcined clays and their influence on the efficiency of superplasticizers, Cement and Concrete Composites, 110 (2020).

[41] R. Sposito, M. Maier, N. Beuntner, K.-C. Thienel, Evaluation of zeta potential of calcined clays and time-dependent flowability of blended cements with customized polycarboxylate-based superplasticizers, Construction and Building Materials, 308 (2021) 125061.

[42] K. Yoshioka, E. Sakai, M. Daimon, A. Kitahara, Role of Steric Hindrance in the Performance of Superplasticizers for Concrete, Journal of the American Ceramic Society, 80 (1997) 2667-2671.

[43] M. Schmid, R. Sposito, K. Thienel, J. Plank, Novel zwitterionic PCE superplasticizers for calcined clays and their application in calcined clay blended cements, 15th International Congress on the Chemistry of Cement, Prague, Czech Republic Research Institute of Binding Materials Prague, 2019, pp. 8.

[44] C. Chomyn, J. Plank, Impact of different synthesis methods on the dispersing effectiveness of isoprenol ether-based zwitterionic and anionic polycarboxylate (PCE) superplasticizers, Cement and Concrete Research, 119 (2019) 113-125.

[45] L. Jiang, X. Kong, Z. Lu, S. Hou, Preparation of amphoteric polycarboxylate superplasticizers and their performances in cementitious system, Journal of Applied Polymer Science, 132 (2015).

[46] L. Lei, A Comprehensive Study of Interactions Occurring Between Superplasticizers and Clays, and Superplasticizers and Cement, Dissertation: Lehrstuhl für Bauchemie, Technische Universität München, 2016.

[47] L. Lei, M. Palacios, J. Plank, A.A. Jeknavorian, Interaction between polycarboxylate superplasticizers and non-calcined clays and calcined clays: A review, Cement and Concrete Research, 154 (2022) 106717.

[48] T. Hirata, Dispersant, JP patent, 842022 (S59-018338), 1981.

[49] A. Lange, T. Hirata, J. Plank, Influence of the HLB value of polycarboxylate superplasticizers on the flow behavior of mortar and concrete, Cement and Concrete Research, 60 (2014) 45-50.

[50] S.-I. Akimoto, S. Honda, T. Yasukohchi, Additives for cement, EP 0291073, 1987.

[51] Z. Sun, L.L. Shui, H. Yang, Polycarboxylic water reducer with strong cement adaptability and good slump retention and synthetic method of polycarboxylic water reducer, CN102887664B, 2012.

[52] G. Albrecht, J. Weichmann, J. Penkner, A. Kern, Copolymers based on oxyalkyleneglycol alkenyl ethers and derivatives of unsaturated dicarboxylic acids, EP0736553, (1996).

[53] G. Liu, X. Qin, X. Wei, Z. Wang, J. Ren, Study on the monomer reactivity ratio and performance of EPEG-AA (ethylene-glycol monovinyl polyethylene glycol–acrylic acid) copolymerization system, Journal of Macromolecular Science, Part A, 57 (2020) 646-653.

[54] J. Dong, Q. Luo, C. Hu, J. Ji, H. Liu, L. Zhai, Polyether macromonomer, the preparation of polycarboxylate superplasticizer and application methods thereof, assigned to Shanghai Dongda Chemical Co. Ltd., CN Patent 108102085A, 2018.

[55] Z. Wang, Y. Xu, H. Wu, X. Liu, F. Zheng, H. Li, S. Cui, M. Lan, Y. Wang, A room temperature synthesis method for polycarboxylate superplasticizer, CN103897119, (2013).

[56] M. Yamamoto, T. Uno, Y. Onda, H. Tanaka, A. Yamashita, T. Hirata, N. Hirano, Copolymer for cement admixtures and its production process and use, US 6727315, 2004.

[57] S. Li, H. Pang, J. Zhang, Y. Meng, J. Huang, X. Lin, B. Liao, Synthesis and performance of a novel amphoteric polycarboxylate superplasticizer with hydrolysable ester group, Colloids and Surfaces A: Physicochemical and Engineering Aspects, 564 (2019) 78-88.

[58] X. Tang, C. Zhao, Y. Yang, F. Dong, X. Lu, Amphoteric polycarboxylate superplasticizers with enhanced clay tolerance: Preparation, performance and mechanism, Construction and Building Materials, 252 (2020) 119052.

[59] M. Schmid, N. Beuntner, K.-C. Thienel, J. Plank, Colloid-Chemical Investigation of the Interaction Between PCE Superplasticizers and a Calcined Mixed Layer Clay, Springer Netherlands, Dordrecht, 2018, pp. 434-439.

[60] M. Schmid, N. Beuntner, K.-C. Thienel, J. Plank, Amphoteric superplasticizers for cements blended with a calcined clay, Special Publication, 329 (2018) 41-54.

[61] M. Schmid, R. Sposito, K.-C. Thienel, J. Plank, Effectiveness of Amphoteric PCE Superplasticizers in Calcined Clay Blended Cements, Calcined Clays for Sustainable Concrete: Proceedings of the 3rd International Conference on Calcined Clays for Sustainable Concrete, Springer Nature, 2020, pp. 201- 209.

[62] M. Schmid, R. Sposito, K.-C. Thienel, J. Plank, Novel zwitterionic

superplasticizers for cements blended with calcined clays, Proc., 15th Int. Cong. on the Chemistry of Cement, edited by L. Peřka and J. Gemrich, 8 (2019).

[63] J. Plank, D. Zhimin, H. Keller, F.v. Hössle, W. Seidl, Fundamental mechanisms for polycarboxylate intercalation into C_3A hydrate phases and the role of sulfate present in cement, Cement and Concrete Research, 40 (2010) 45-57.

[64] A. Zingg, F. Winnefeld, L. Holzer, J. Pakusch, S. Becker, R. Figi, L. Gauckler, Interaction of polycarboxylate-based superplasticizers with cements containing different C_3A amounts, Cement and Concrete Composites, 31 (2009) 153-162.

[65] M.L. Vo, J. Plank, Dispersing effectiveness of a phosphated polycarboxylate in α- and β-calcium sulfate hemihydrate systems, Construction and Building Materials, 237 (2020).

[66] A. Lange, J. Plank, Contribution of non-adsorbing polymers to cement dispersion, Cement and Concrete Research, 79 (2016) 131-136.

[67] C. Chomyn, Synthesis, Characterization and Dispersing Properties of Anionic and Zwitterionic Polycarboxylate Superplasticizers Prepared Via Different Synthetic Methods, Dissertation: Lehrstuhl für Bauchemie, Technische Universität München, 2020.

[68] A. Meunier, Clays, Springer Science & Business Media2005.

[69] M. Brigatti, E. Galan, B. Theng, Structures and mineralogy of clay minerals, Hand book of clay science, Elsevier, Amsterdam, 2006, pp. 19-86.

[70] C.E. Weaver, L.D. Pollard, The chemistry of clay minerals, Elsevier, Amsterdam, 1973.

[71] S.M.R. Shaikh, M.S. Nasser, I. Hussein, A. Benamor, S.A. Onaizi, H. Qiblawey, Influence of polyelectrolytes and other polymer complexes on the flocculation and rheological behaviors of clay minerals: A comprehensive review, Separation and Purification Technology, 187 (2017) 137-161.

[72] D. Tunega, A. Zaoui, Mechanical and bonding behaviors behind the bending mechanism of kaolinite clay layers, The Journal of Physical Chemistry C, 124 (2020) 7432-7440.

[73] R.E. Grim, Clay mineralogy, McGraw-Hill series in the geological sciences, McGraw-Hill, New York, 1953.

[74] A.A. Lewinsky, Hazardous materials and wastewater: treatment, removal and analysis, Nova Publishers2007.

[75] R.E. Grim, Clay mineralogy 2 nd ed, McGraw-Hill Book Company1968.

[76] A. Meunier, B. Velde, The Mineralogy of Illite—What is Illite?, Illite,

Springer2004, pp. 3-62.

[77] S. Kakuta, T. Okayama, M. Kato, A. Oda, T. Abe, Clarification of photocatalysis induced by iron ion species naturally contained in a clay compound, Catalysis Science & Technology, 1 (2011) 1671-1676.

[78] F. Bergaya, G. Lagaly, Handbook of clay science, Newnes, 2013.

[79] F. Avet, K. Scrivener, Simple and reliable quantification of kaolinite in clay using an oven and a balance, Calcined Clays for Sustainable Concrete, RILEM Bookseries; Springer: Dordrecht, The Netherlands, 15 (2020) 147-156.

[80] M. Canut, S. Miller, M. Jolnæs, Calcined Clay: Process Impact on the Reactivity and Color, Calcined Clays for Sustainable Concrete: Proceedings of the 3rd International Conference on Calcined Clays for Sustainable Concrete, Springer Nature, 2020, pp. 163- 167.

[81] ASTM C618. Standard specification for fly ash and raw or calcined natural pozzolan for use as a mineral admixture in Portland cement concrete, ASTM International, West Conshohocken (PA, USA), 2003.

[82] DIN EN 197-1:2011-11, Cement - Part 1: Composition, specifications and conformity criteria for common cements.

[83] B. Samet, T. Mnif, M. Chaabouni, Use of a kaolinitic clay as a pozzolanic material for cements: Formulation of blended cement, Cement and Concrete Composites, 29 (2007) 741-749.

[84] R. Fernández, B. Nebreda, R.V. de la Villa, R. García, M. Frías, Mineralogical and chemical evolution of hydrated phases in the pozzolanic reaction of calcined paper sludge, Cement and Concrete Composites, 32 (2010) 775-782.

[85] A. Tironi, M.A. Trezza, A.N. Scian, E.F. Irassar, Assessment of pozzolanic activity of different calcined clays, Cement and Concrete Composites, 37 (2013) 319-327.

[86] J. Rocha, J. Klinowski, ^{29}Si and ^{27}Al magic-angle-spinning NMR studies of the thermal transformation of kaolinite, Physics and Chemistry of Minerals, 17 (1990) 179-186.

[87] J. Rocha, J. Klinowski, Solid‐state NMR studies of the structure and reactivity of metakaolinite, Angewandte Chemie International Edition in English, 29 (1990) 553-554.

[88] D.L. Carroll, T.F. Kemp, T.J. Bastow, M.E. Smith, Solid-state NMR characterisation of the thermal transformation of a Hungarian white illite, Solid State Nuclear Magnetic Resonance, 28 (2005) 31-43.

[89] I.W.M. Brown, K.J.D. MacKenzie, R.H. Meinhold, The thermal reactions of montmorillonite studied by high-resolution solid-state29Si and27Al NMR, Journal of Materials Science, 22 (1987) 3265-3275.

[90] G. Habert, N. Choupay, G. Escadeillas, D. Guillaume, J.M. Montel, Clay content of argillites: Influence on cement based mortars, Applied Clay Science, 43 (2009) 322-330.

[91] A. Tironi, F. Cravero, A.N. Scian, E.F. Irassar, Pozzolanic activity of calcined halloysite-rich kaolinitic clays, Applied Clay Science, 147 (2017) 11-18.

[92] C. He, B. Osbaeck, E. Makovicky, Pozzolanic reactions of six principal clay minerals: Activation, reactivity assessments and technological effects, Cement and Concrete Research, 25 (1995) 1691-1702.

[93] G. Kakali, T. Perraki, S. Tsivilis, E. Badogiannis, Thermal treatment of kaolin: the effect of mineralogy on the pozzolanic activity, Applied Clay Science, 20 (2001) 73-80.

[94] J. Kostuch, G. Walters, T. Jones, High performance concretes incorporating metakaolin: a review, Concrete, 2 (2000) 1799-1811.

[95] A. Alujas, R. Fernández, R. Quintana, K.L. Scrivener, F. Martirena, Pozzolanic reactivity of low grade kaolinitic clays: Influence of calcination temperature and impact of calcination products on OPC hydration, Applied Clay Science, 108 (2015) 94-101.

[96] A. Shvarzman, K. Kovler, G.S. Grader, G.E. Shter, The effect of dehydroxylation/amorphization degree on pozzolanic activity of kaolinite, Cement and Concrete Research, 33 (2003) 405-416.

[97] J. Ambroise, S. Martin-Calle, J. Pera, Pozzolanic behavior of thermally activated kaolin, Special Publication, 132 (1992) 731-748.

[98] S. Ferreiro, M.M.C. Canut, J. Lund, D. Herfort, Influence of fineness of raw clay and calcination temperature on the performance of calcined clay-limestone blended cements, Applied Clay Science, 169 (2019) 81-90.

[99] B.B. Sabir, S. Wild, J. Bai, Metakaolin and calcined clays as pozzolans for concrete: a review, Cement and Concrete Composites, 23 (2001) 441-454.

[100] S. Salvador, Pozzolanic properties of flash-calcined kaolinite: a comparative study with soak-calcined products, Cement and Concrete Research, 25 (1995) 102-112.

[101] J. Harder, OneStone Consulting Ltd., Varna/ Bulgaria, Latest trends in clay activation, ZKG, 2021/6, https://www.zkg.de/en/artikel/zkg_Latest_trends_in_clay_activation_3683572.html.

[102] FL Smidth Clay Calciner, Calciner system for clay activation- Improve your productivity and reduce CO_2 emissions, 2021, https://flsmidth-prod-cdn.azureedge.net/.

[103] S. Wild, J.M. Khatib, Portlandite consumption in metakaolin cement pastes and mortars, Cement and Concrete Research, 27 (1997) 137-146.

[104] M. Kaloumenou, E. Badogiannis, S. Tsivilis, G. Kakali, Effect of the kaolin particle size on the pozzolanic behaviour of the metakaolinite produced, Journal of Thermal Analysis and Calorimetry, 56 (1999) 901-907.

[105] M. Antoni, J. Rossen, F. Martirena, K. Scrivener, Cement substitution by a combination of metakaolin and limestone, Cement and Concrete Research, 42 (2012) 1579-1589.

[106] A. Tironi, C.C. Castellano, V.L. Bonavetti, M.A. Trezza, A.N. Scian, E.F. Irassar, Kaolinitic calcined clays – Portland cement system: Hydration and properties, Construction and Building Materials, 64 (2014) 215-221.

[107] S. Krishnan, S. Bishnoi, Understanding the hydration of dolomite in cementitious systems with reactive aluminosilicates such as calcined clay, Cement and Concrete Research, 108 (2018) 116-128.

[108] Y. Dhandapani, T. Sakthivel, M. Santhanam, R. Gettu, R.G. Pillai, Mechanical properties and durability performance of concretes with Limestone Calcined Clay Cement (LC3), Cement and Concrete Research, 107 (2018) 136-151.

[109] T. Danner, G. Norden, H. Justnes, Characterisation of calcined raw clays suitable as supplementary cementitious materials, Applied Clay Science, 162 (2018) 391-402.

[110] F. Avet, K. Scrivener, Investigation of the calcined kaolinite content on the hydration of Limestone Calcined Clay Cement (LC^3), Cement and Concrete Research, 107 (2018) 124-135.

[111] M. Sharma, S. Bishnoi, F. Martirena, K. Scrivener, Limestone calcined clay cement and concrete: A state-of-the-art review, Cement and Concrete Research, 149 (2021).

[112] F. Avet, E. Boehm-Courjault, K. Scrivener, Investigation of C-A-S-H composition, morphology and density in Limestone Calcined Clay Cement (LC^3), Cement and Concrete Research, 115 (2019) 70-79.

[113] F. Avet, K. Scrivener, Effect of temperature on the water content of C-A-S-H in plain Portland and blended cements, Cement and Concrete Research, 136 (2020).

[114] R. Li, L. Lei, T. Sui, J. Plank, Effectiveness of PCE superplasticizers in calcined clay blended cements, Cement and Concrete Research, (2020) accepted on 09.12.2020.

[115] I.P. Sfikas, E.G. Badogiannis, K.G. Trezos, Rheology and mechanical characteristics of self-compacting concrete mixtures containing metakaolin, Construction and Building Materials, 64 (2014) 121-129.

[116] O. Akhlaghi, T. Aytas, B. Tatli, D. Sezer, A. Hodaei, A. Favier, K. Scrivener, Y.Z. Menceloglu, O. Akbulut, Modified poly(carboxylate ether)-based superplasticizer for enhanced flowability of calcined clay-

limestone-gypsum blended Portland cement, Cement and Concrete Research, 101 (2017) 114-122.

[117] M. Schmid, N. Beuntner, K.-C. Thienel, J. Plank, Amphoteric superplasticizers for cements blended with a calcined clay, ACI Symposium Publication 12th International Conference on Superplasticizers and Other Chemical Admixtures in Concrete, American Concrete Institute, Beijing, China, 2018, pp. 41-54.

[118] R. Sposito, M. Schmid, N. Beuntner, S. Scherb, J. Plank, K.-C. Thienel, Early hydration behavior of blended cementitious systems containing calcined clays and superplasticizer, 15th International Congress on the Chemistry of Cement (ICCC), Prague (Czech Republic), 2019.

[119] T.R. Muzenda, P. Hou, S. Kawashima, T. Sui, X. Cheng, The role of limestone and calcined clay on the rheological properties of LC^3, Cement and Concrete Composites, 107 (2020) 103516.

[120] R. Li, L. Lei, T. Sui, J. Plank, Approaches to achieve fluidity retention in low-carbon calcined clay blended cements, Journal of Cleaner Production, 311 (2021).

[121] R. Li, L. Lei, T. Sui, J. Plank, Effectiveness of PCE superplasticizers in calcined clay blended cements, Cement and Concrete Research, 141 (2021) 106334.

[122] M. Schmid, J. Plank, Interaction of individual meta clays with polycarboxylate (PCE) superplasticizers in cement investigated via dispersion, zeta potential and sorption measurements, Applied Clay Science, 207 (2021).

[123] L. Gebbard, B. Feneuil, M. Palacios, N. Roussel, Rheology of Limestone Calcined Clays Cement Pastes. A Comparative Approach with Pure Portland Cement Pastes, in: K. Scrivener, A. Favier (Eds.) Calcined Clays for Sustainable Concrete, Springer Netherlands, Dordrecht, 2015, pp. 595-595.

[124] S. Ng, H. Justnes, Influence of dispersing agents on the rheology and early heat of hydration of blended cements with high loading of calcined marl, Cement and Concrete Composites, 60 (2015) 123-134.

[125] M. Bishop, A.R. Barron, Cement Hydration Inhibition with Sucrose, Tartaric Acid, and Lignosulfonate: Analytical and Spectroscopic Study, Industrial & Engineering Chemistry Research, 45 (2006) 7042-7049.

[126] G. Huang, D. Pudasainee, R. Gupta, W.V. Liu, Utilization and performance evaluation of molasses as a retarder and plasticizer for calcium sulfoaluminate cement-based mortar, Construction and Building Materials, 243 (2020).

[127] M.C.G. Juenger, H.M. Jennings, New insights into the effects of sugar on

the hydration and microstructure of cement pastes, Cement and Concrete Research, 32 (2002) 393-399.

[128] C. Nalet, A. Nonat, Ionic complexation and adsorption of small organic molecules on calcium silicate hydrate: Relation with their retarding effect on the hydration of C3S, Cement and Concrete Research, 89 (2016) 97-108.

[129] R. Rixom, N. Mailvaganam, D.P. Manson, C. Gonzales, Chemical Admixtures for Concrete, 3rd ed., CRC Press, London, 1999.

[130] A. Kleinlogel, Influences on Concrete, Frederick Ungar Publishing, New York (1950) 222– 223.

[131] G. Li, T. He, D. Hu, R. Huang, C. Shi, Effects of retarders on the fluidity of pastes containing β-naphthalenesulfonic acid-based superplasticiser, Advances in Cement Research, 24 (2012) 203-210.

[132] J. Cheung, A. Jeknavorian, L. Roberts, D. Silva, Impact of admixtures on the hydration kinetics of Portland cement, Cement and Concrete Research, 41 (2011) 1289-1309.

[133] M.-C. Han, C.-G. Han, Use of maturity methods to estimate the setting time of concrete containing super retarding agents, Cement and Concrete Composites, 32 (2010) 164-172.

[134] L. Lei, R. Li, A. Fuddin, Influence of maltodextrin retarder on the hydration kinetics and mechanical properties of Portland cement, Cement and Concrete Composites, 114 (2020) 103774.

[135] A. Mardani-Aghabaglou, M. Tuyan, G. Yılmaz, Ö. Arıöz, K. Ramyar, Effect of different types of superplasticizer on fresh, rheological and strength properties of self-consolidating concrete, Construction and Building Materials, 47 (2013) 1020-1025.

[136] L. Zhang, X. Kong, F. Xing, B. Dong, F. Wang, Working mechanism of post-acting polycarboxylate superplasticizers containing acrylate segments, Journal of Applied Polymer Science, 135 (2018) 45753.

[137] S. Qian, H. Jiang, B. Ding, Y. Wang, C. Zheng, Z. Guo, Synthesis and performances of polycarboxylate superplaticizer with clay-inerting and high slump retention capability, IOP Conference Series: Materials Science and Engineering, 182 (2017) 012033.

[138] X.H. Yang, Research on the Effect of Different Esters on the Synthesis of Polycarboxylate Superplasticizer at Low Content, IOP Conference Series: Earth and Environmental Science, IOP Publishing, 2020, pp. 012155.

[139] J. Ren, X. Wang, S. Xu, Y. Fang, W. Liu, Q. Luo, N. Han, F. Xing, Effect of polycarboxylate superplasticisers on the fresh properties of cementitious materials mixed with seawater, Construction and Building

Materials, 289 (2021).
[140] L. Lei, J. Plank, A concept for a polycarboxylate superplasticizer possessing enhanced clay tolerance, Cement and Concrete Research, 42 (2012) 1299-1306.
[141] L. Lei, J. Plank, Synthesis and Properties of a Vinyl Ether-Based Polycarboxylate Superplasticizer for Concrete Possessing Clay Tolerance, Industrial & Engineering Chemistry Research, 53 (2014) 1048-1055.
[142] S. Chen, S. Sun, X. Chen, K. Zhong, Q. Shao, H. Xu, J. Wei, Effects of core-shell polycarboxylate superplasticizer on the fluidity and hydration behavior of cement paste, Colloids and Surfaces A: Physicochemical and Engineering Aspects, 590 (2020) 124464.
[143] H. Tahara, H. Ito, Y. Mori, M. Mizushima, Cement additive, method for producing the same, and cement composition, assigned to Nippon Shokubai Co., Ltd., US patent 5476885, 1995.
[144] Y. Tanaka, A. Ohta, T. Hirata, T. Uno, T. Yuasa, H. Tahara, Cement composition using the dispersant of (meth)acrylic esters, (meth)acrylic acids polymers, US Patent 6187841B1, 2001.
[145] A. Lange, L. Lei, J. Plank, Cement Compatibility of PCE Superplasticizers, in: C. Shi, Y. Yao (Eds.) 14th International Congress on the Chemistry of Cement, Section 4: AdmixturesBeijing, China, 2015, pp. 380.
[146] Y. Cai, T. Yang, Q. Ren, M. Liang, S. Zhou, Enhanced slump retention using polycarboxylate superplasticizers obtained by micro-crosslinking reaction, Materials Express, 9 (2019) 587-595.
[147] S.B. Laramay, J.J. Lavene, Encapsulated compositions, assigned to Fritz Industries, INC., US patent 8273426B1, application granted in 2012.
[148] P.C. Hewlett, Lea’s Chemistry of Cement and Concrete, John Wiley and Sons Inc, 605 (2005) 10158-10012.
[149] F. Leroux, P. Aranda, J.P. Besse, E. Ruiz-Hitzky, Intercalation of Poly(Ethylene Oxide) Derivatives into Layered Double Hydroxides, European Journal of Inorganic Chemistry, 2003 (2003) 1242-1251.
[150] C.O. Oriakhi, I.V. Farr, M.M. Lerner, Incorporation of poly (acrylic acid), poly (vinylsulfonate) and poly (styrenesulfonate) within layered double hydroxides, Journal of Materials Chemistry, 6 (1996) 103-107.
[151] H.N. Tran, C.-C. Lin, H.-P. Chao, Amino acids-intercalated Mg/Al layered double hydroxides as dual-electronic adsorbent for effective removal of cationic and oxyanionic metal ions, Separation and Purification Technology, 192 (2018) 36-45.
[152] J. Plank, Z. Dai, Novel hybrid materials obtained by intercalation of organic comb polymers into Ca–Al–LDH, Journal of Physics and

Chemistry of Solids, 69 (2008) 1048-1051.
[153] J.L. Provis, A. Palomo, C. Shi, Advances in understanding alkali-activated materials, Cement and Concrete Research, 78 (2015) 110-125.
[154] M.M.A. Elahi, M.M. Hossain, M.R. Karim, M.F.M. Zain, C. Shearer, A review on alkali-activated binders: Materials composition and fresh properties of concrete, Construction and Building Materials, 260 (2020) 18.
[155] Q. Zhang, T. Ji, Z. Yang, C. Wang, H.-c. Wu, Influence of different activators on microstructure and strength of alkali-activated nickel slag cementitious materials, Construction and Building Materials, 235 (2020).
[156] F. Xie, Z. Liu, D. Zhang, J. Wang, D. Wang, J. Ni, The effect of NaOH content on rheological properties, microstructures and interfacial characteristic of alkali activated phosphorus slag fresh pastes, Construction and Building Materials, 252 (2020).
[157] G.N. Obuzor, J.M. Kinuthia, R.B. Robinson, Utilisation of lime activated GGBS to reduce the deleterious effect of flooding on stabilised road structural materials: A laboratory simulation, Engineering Geology, 122 (2011) 334-338.
[158] K.-H. Yang, J.-I. Sim, S.-H. Nam, Enhancement of reactivity of calcium hydroxide-activated slag mortars by the addition of barium hydroxide, Construction and Building Materials, 24 (2010) 241-251.
[159] Y. Yi, M. Liska, A. Al-Tabbaa, Properties and microstructure of GGBS–magnesia pastes, Advances in Cement Research, 26 (2014) 114-122.
[160] A. Fernández-Jiménez, J. Palomo, F. Puertas, Alkali-activated slag mortars: mechanical strength behaviour, Cement and Concrete Research, 29 (1999) 1313-1321.
[161] S.-D. Wang, K.L. Scrivener, P. Pratt, Factors affecting the strength of alkali-activated slag, Cement and Concrete Research, 24 (1994) 1033-1043.
[162] A. Fernández-Jiménez, A. Palomo, Composition and microstructure of alkali activated fly ash binder: Effect of the activator, Cement and Concrete Research, 35 (2005) 1984-1992.
[163] A. Fernández-Jiménez, A. Palomo, Characterisation of fly ashes. Potential reactivity as alkaline cements, Fuel, 82 (2003) 2259-2265.
[164] S. Wang, K. Scrivener, Hydration products of alkali activated slag cement, Cement and Concrete Research, 25 (1995) 561-571.
[165] D. Krizan, B. Zivanovic, Effects of dosage and modulus of water glass on early hydration of alkali–slag cements, Cement and Concrete Research, 32 (2002) 1181-1188.
[166] F. Pacheco-Torgal, J. Castro-Gomes, S. Jalali, Alkali-activated binders:

A review: Part 1. Historical background, terminology, reaction mechanisms and hydration products, Construction and Building Materials, 22 (2008) 1305-1314.

[167] C.K. Yip, G.C. Lukey, J.S.J. van Deventer, The coexistence of geopolymeric gel and calcium silicate hydrate at the early stage of alkaline activation, Cement and Concrete Research, 35 (2005) 1688-1697.

[168] V. Glukhovsky, G. Rostovskaja, G. Rumyna, High strength slag-alkaline cements, 7th International Congress on the Chemistry of Cement, 1980, pp. 164-168.

[169] P.V. Krivenko, Alkaline cements, Proceedings of the 1st International Conference on Alkaline Cements and Concretes, Kiev, Ukraine, 1994, Vipol Stock Company, 1994, pp. 11-129.

[170] M.L.G. Fernández, Activación alcalina de metacaolín desarrollo de nuevos materiales cementantes, Universidad Autónoma de Madrid, 1998.

[171] C. Shi, D. Roy, P. Krivenko, Alkali-activated cements and concretes, CRC press, 2003.

[172] T. Bakharev, J.G. Sanjayan, Y.B. Cheng, Sulfate attack on alkali-activated slag concrete, Cement and Concrete Research, 32 (2002) 211-216.

[173] T. Bakharev, J.G. Sanjayan, Y.B. Cheng, Resistance of alkali-activated slag concrete to acid attack, Cement and Concrete Research, 33 (2003) 1607-1611.

[174] S.A. Bernal, E.D. Rodríguez, R. Mejía de Gutiérrez, J.L. Provis, Performance of alkali-activated slag mortars exposed to acids, Journal of Sustainable Cement-Based Materials, 1 (2012) 138-151.

[175] T. Su, Y.Q. Zhou, Q. Wang, Recent advances in chemical admixtures for improving the workability of alkali-activated slag-based material systems, Construction and Building Materials, 272 (2021) 14.

[176] F. Puertas, C. Varga, M.M. Alonso, Rheology of alkali-activated slag pastes. Effect of the nature and concentration of the activating solution, Cement and Concrete Composites, 53 (2014) 279-288.

[177] F. Puertas, B. González-Fonteboa, I. González-Taboada, M. Alonso, M. Torres-Carrasco, G. Rojo, F. Martínez-Abella, Alkali-activated slag concrete: Fresh and hardened behaviour, Cement and Concrete Composites, 85 (2018) 22-31.

[178] V. Živica, Effects of type and dosage of alkaline activator and temperature on the properties of alkali-activated slag mixtures, Construction and Building Materials, 21 (2007) 1463-1469.

[179] M. Palacios, P.F. Banfill, F. Puertas, Rheology and setting of alkali-activated slag pastes and mortars: effect of organic admixture, ACI

Materials Journal, 105 (2008) 140.

[180]F. Pacheco-Torgal, Introduction to Handbook of Alkali-activated Cements, Mortars and Concretes, Handbook of Alkali-Activated Cements, Mortars and Concretes2015, pp. 1-16.

[181] C.D. Atiş, C. Bilim, Ö. Çelik, O. Karahan, Influence of activator on the strength and drying shrinkage of alkali-activated slag mortar, Construction and Building Materials, 23 (2009) 548-555.

[182] M. Palacios, Y.F. Houst, P. Bowen, F. Puertas, Adsorption of superplasticizer admixtures on alkali-activated slag pastes, Cement and Concrete Research, 39 (2009) 670-677.

[183] J.G. Jang, N.K. Lee, H.K. Lee, Fresh and hardened properties of alkali-activated fly ash/slag pastes with superplasticizers, Construction and Building Materials, 50 (2014) 169-176.

9. Appendix

Section 9.1

Publication # 10

Influence of maltodextrin retarder on the hydration kinetics and mechanical properties of Portland cement

L. Lei, **R. Li**, A. Fuddin.

Cement and Concrete Composites (IF = 9.9)

114 (2020) 103774

DOI: 10.1016/j.cemconcomp.2020.103774

Cement and Concrete Composites 114 (2020) 103774

Contents lists available at ScienceDirect

Cement and Concrete Composites

journal homepage: http://www.elsevier.com/locate/cemconcomp

Influence of maltodextrin retarder on the hydration kinetics and mechanical properties of Portland cement

Lei Lei *, Ran Li, Andriana Fuddin

Technische Universität München, Chair for Construction Chemistry, 85747, Garching, Lichtenbergstraße 4, Germany

ARTICLE INFO

Keywords:
Ordinary Portland cement
Retarder
Maltodextrin
Hydration kinetics
Adsorption

ABSTRACT

In this study, the effect of maltodextrin on the hydration kinetics of ordinary Portland cement was investigated. Additionally, the impact of maltodextrin on the physical and mechanical properties of cement is further studied via setting time, fluidity and mechanical strength tests which has been conducted with different curing times (16 h, 1 d, 3 d, 28 d). The results revealed the impact on the mechanical properties of OPC is dosage and time dependent. At the early curing time of 16 h, the addition of maltodextrin decreased the compressive strength of all mortar samples substantially; a higher dosage of maltodextrin resulted in even lower compressive strength. However, at extended curing times such as 1 d, 3 d or 28 d, the impact on the compressive strength of OPC is dependent on dosage: relatively low dosages (0.01–0.05%) of maltodextrin increased the compressive strength of mortar, whereas higher dosages (≥0.1%) of maltodextrin was found to decrease the compressive strength of mortar. Furthermore, the time – dependent development of hydration products was monitored via *in-situ* XRD at the different ages of cement hydration. The results showed that the addition of maltodextrin delays cement hydration which results in less hydration products like Portlandite and ettringite. Finally, the mode of interaction between maltodextrin and cement was assessed through adsorption and zeta potential measurements. The adsorption as well as zeta potential measurements confirm that the retarding mechanism of maltodextrin relies on adsorption on the surface of cement particles.

1. Introduction

Chemical admixtures are commonly applied in the construction industry to improve concrete properties [1,2]. As one of the most commonly used admixtures, retarders are mainly applied to increase the concrete's workability time (= slump retention), which is important in ready-mix concrete delivery and oil well cementing [3]. Retarders can be divided into two categories: organic and inorganic compounds. Inorganic retarders include salts such as borates [4,5], phosphates [6,7], zinc oxide [8], and calcium sulfates [5]. On the other hand, organic retarders mainly include sugars [9], polysaccharides [10], sodium gluconate [11,12], polycarboxylic acids [13–15], phenol derivatives [16], lignosulfonates [17], as well as tartaric [18] and citric acids [4,5,19,20]. There are significantly differences from the way they inhibit cement hydration. As outlined by Bishop and Barron [21,22], there are four predominant cement hydration retarding mechanisms: (1) calcium complexation functions through either removing calcium ions in cement pore solution by forming insoluble compounds or chelating calcium in solution to inhibit the formation of early cement hydrates, i.e. C–S–H gel; (2) surface adsorption of retarders on anhydrous surfaces or partially hydrated clinker phases to prevent further hydration; (3) nucleation and growth poisoning of hydrates such as C–S–H and Portlandite; and (4) formation of semipermeable layer on cement grains to slow down the water migration.

As is reported in previous literatures, many inorganic salts delay the cement hydration, their working mechanism mainly relies on precipitation with Ca^{2+} or on nucleation inhibition [23]. Recently, many studies are focusing on different kinds of sugar to be used as cement retarder, such as glucose [11,24], fructose [25], sucrose [8]. Ma et al. investigated the retarding effect of sodium gluconate on ordinary Portland cement and found that this admixture significantly delayed the hydration of C_3S as a result of sodium gluconate adsorption. Other studies presented sodium gluconate as a retarder for alkali activated slag (AAS) [24] and sulphoaluminate cement [4,13]. According to the study of Hou and Bao [9], also cellulosic sugar acids exhibit good retardation properties on cement.

Enormous amount of work on revealing the retarding mechanism of various sugars also has been carried out. Thomas and Birchall [26]

* Corresponding author.
E-mail address: lei.lei@bauchemie.ch.tum.de (L. Lei).

https://doi.org/10.1016/j.cemconcomp.2020.103774
Received 26 June 2020; Received in revised form 1 August 2020; Accepted 5 August 2020
Available online 13 August 2020

reported that retarding action of sugars is attributed to the adsorption and poisoning of hydrate phases. Juenger and Jennings [32] elucidated that sugar compounds not only promote the dissolution of ions but also poison the cement clinker phases and/or generated hydration products. The adsorption on hydration products shuts off further crystal growth. As one of the most effective cement retarders, the retarding action of sucrose was investigated in-depth by Smith et al. [27,28]. Results revealed that sucrose exhibits different adsorption selectivity and binding strength towards aluminate and silicate surfaces, preferably adsorbs at tricalcium silicate phases, resulting in larger surface coverages and formation of a metastable hydrate layer on the surface of C_3S to prevent further hydration [27,28].

To summarize, various forms of sugars were systematically studied as retarder for cementitious materials. However, maltodextrin, a rather common retarder admixed to concrete, has so far not been studied regarding its impact on the hydration and mechanical properties of hardened Portland cement. Furthermore, its retardation mechanism is not yet understood.

To supply this gap, the effect of maltodextrin on the hydration kinetics of ordinary Portland cement was investigated. Additionally, the influence of maltodextrin on workability and mechanical properties of mortars was also studied. Furthermore, the time-dependent development of hydration products was monitored via *in-situ* XRD at the early age of cement hydration. Finally, the mode of interaction between maltodextrin and cement was assessed through adsorption (total organic carbon) and zeta potential measurements. From the above it was hoped to gain a better understanding of the interaction between maltodextrin and cement and its mode of action.

2. Experimental

2.1. Materials

2.1.1. Cement sample

An ordinary Portland cement sample CEM I 42.5R from Schwenk cement company (Ulm, Germany) with a density of 3.13 g/cm^3 and d_{50} value of 18.73 μm was used. Table 1 displays the phase composition of the cement sample which was determined via Q-XRD including *Rietveld* refinement.

2.1.2. Chemicals

A commercial maltodextrin sample used in this study was supplied by Shandong Xiwang Group, China and exhibited > 99% purity. Its chemical structure is illustrated in Fig. 1.

Table 1
Phase composition of the cement sample CEM I 42.5 R, determined via Q-XRD analysis.

Phase	wt. %
C_3S, monoclinic	53.73
C_2S, monoclinic	18.63
C_3A, cubic	5.37
C_3A, orthorhombic	1.78
C_4AF, orthorhombic	10.03
Anhydrite ($CaSO_4$)	1.8
Dihydrate ($CaSO_4 \bullet 2H_2O$)	3.93
Hemihydrate ($CaSO_4 \bullet 0.5H_2O$)	0.2
Calcite ($CaCO_3$)	2.71
Dolomite ($CaMg(CO_3)_2$)	0.8
Quartz (SiO_2)	0.44
Periclase (MgO)	0.37
Free lime (*Franke*)	0.2
Total	100.00

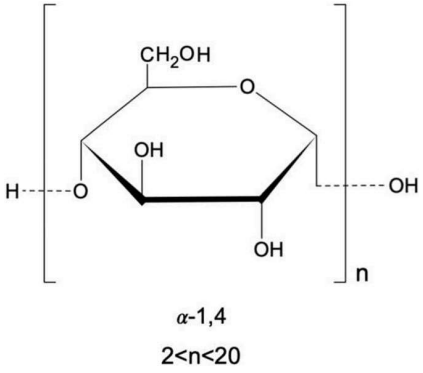

Fig. 1. Chemical structure of maltodextrin.

2.2. Experimental methods

2.2.1. Setting time

The water to cement ratio was set at 0.3 according to the DIN EN 196-3 standard. In this experiment, 500 g of cement were dry blended with maltodextrin with the dosage of 0.01, 0.02, 0.05, 0.1, 0.2, and 0.5% by weight of cement (bwoc) respectively. Then they were poured into 150 mL of deionized water which was placed in the mixing machine (Toni Technik, Berlin, Germany). The mixer was programmed to follow this procedure: mix for 90 s at a speed of 140 rpm, pause for 15 s for scraping, and mix again for another 90 s at 140 rpm. Thereafter, the cement paste was immediately poured into an oiled container. After levelling the surface of the cement paste with a scraper to achieve a smooth surface, the initial setting time was measured manually while the final setting time was tested every 15 min via the automatic Vicat apparatus (InfraTest, Prüftechnik GmbH) with the setting "BB" selected. Using the data, the initial and final setting time were calculated accordingly.

2.2.2. Mechanical properties of mortar

The compressive strengths of mortars admixed with different dosages of maltodextrin were measured at a water to cement ratio of 0.5 and binder to sand ratio of 1: 3 following DIN EN 196-1 standard. First, 450 g of cement was added in a mixing bowl containing 225 g of water and different dosages of maltodextrin. Immediately after the cement was added, the mixer was started with the mixing speed of 140 rpm for 30 s. Next the standard sand was added within the next 30 s at the same speed. After the addition, the mixer stirred at 285 rpm for another 30 s. During the 90 s pause, a spoon was used to scrape the mixture from the bowl edges to ensure a homogeneous mortar. Then the mixing was continued at 285 rpm for another 60 s. Finally, the mortar sample was placed in a mold with the scale of 40 × 40 × 160 mm. Samples were tested after curing times of 16 h and 1, 3 and 28 days, respectively. For the 16 h and 1 d samples which were kept on air at 20 ± 1 °C and 90% RH, the mechanical properties were tested immediately after demolding. However, the mortar samples were stored for 3 and 28 days and demolded after the first 1 d and then were submerged in water at 20 ± 1 °C for the remaining curing time. The Toni Technik (Berlin, Germany) instrument was used for the compressive strength tests.

2.2.3. Workability of cement paste

In order to determine the workability of cement pastes admixed with maltodextrin, 'mini slump' tests according to DIN EN 1015 standard were employed. A detailed description of this test can be found in a previous publication [29]. The water-to-cement ratio was set to 0.48, resulting in a spread flow of 18 ± 0.5 cm. Each spread flow was measured twice, the second being perpendicular to the first one. The average value was taken as the final spread flow value.

2.2.4. Isothermal heat flow calorimetry

In order to investigate the influence of maltodextrin on the hydration kinetics of the cement sample, the heat evolvement during cement hydration was monitored. In a typical experiment, 4 g of cement were first filled into 10 mL glass ampoules, then the designated dosage of maltodextrin (0.01–0.05, 0.10, and 0.50% by weight of cement, bwoc) was dissolved in the mixing water (water-to-cement ratio = 0.48) which was then discharged into the glass ampoules. The ampoules were sealed, homogenized for 120 s on a vortex mixer and then immediately transferred into an isothermal conduction calorimeter (TAM AIR, Thermometric, Järfälla, Sweden). Heat flow curves were recorded for 72–120 h until the heat release subsided.

2.2.5. In-situ X-Ray Diffraction (XRD)

The phase development in cement pastes admixed with different dosages of maltodextrin was observed over 16 h or 48 h using *in-situ* XRD on a BRUKER AXS D8 diffractometer (Karlsruhe, Germany) with Bragg - Brentano geometry operating between 3° and 60° 2θ at 30 kV and 35 mA with Cu Kα radiation. Cement pastes were prepared at a water-to-cement ratio of 0.48 from 4 g of cement and maltodextrin solutions containing 0.03, 0.05 or 0.10% bwoc of this polysaccharide and covered with a Kapton foil (7.6 μm thick polyimide) provided by VHG Labs (Manchester, USA) to avoid carbonation and dehydration during measurement.

2.2.6. Adsorption measurements via TOC

The adsorption of maltodextrin on cement was captured based on the depletion method. A High TOC II instrument (Elementar Analysensysteme, Hanau, Germany) was utilized to measure the non-adsorbed part of maltodextrin remaining in the cement pore solution. In a typical experiment, 16 g of cement and 7.68 mL of DI water corresponding to a w/c ratio of 0.48 and the amount of retarder to be tested were filled into a 50 mL centrifuge tube and homogenized with a wobbler (VWR International, Darmstadt, Germany) for 2 min at 2400 rpm and then centrifuged for 10 min at 8,500 rpm. Prior to TOC measurement, the supernatant was diluted with DI water to a suitable concentration and 10 drops of 1 M HCl were added to remove any inorganic carbon. The sorbed amount of maltodextrin was calculated from the TOC content of the supernatant. Each sample was measured twice, and average value was taken as the final result.

2.2.7. Zeta potential measurements

Zeta potentials of the cement suspensions were determined using a DT-1200 Electroacoustic Spectrometer (Dispersion Technology Inc., Bedford Hills, NY, USA). Cement pastes were prepared at a w/c ratio of 0.48, then 1% bwoc of maltodextrin was titrated to the cement paste in 60 steps. The resulting zeta potential of the paste was recorded as a function of the polymer dosage.

3. Results and discussion

3.1. Impact of maltodextrin on setting times

At first, the retarding effect of maltodextrin was assessed via setting time tests. The results are displayed in Fig. 2.

Generally, both the initial and final setting time are prolonged with maltodextrin dosages ascending from 0 to 0.2% bwoc, thus indicates that cement hydration is delayed by the addition of maltodextrin. When the maltodextrin dosage was less than 0.05% bwoc, the initial setting time remained unchanged as compared to the neat cement slurry while the final setting time slightly extended. At the maltodextrin dosages of 0.1% and 0.2%, however, both initial and final setting times increased significantly, with the effect on the final setting time being particularly pronounced, thus producing a large gap between initial and final setting time which signifies a longer workability time. Interestingly, from the above it can be concluded that at low to moderate dosages (≤0.2% bwoc) maltodextrin effectively prolongs the setting time of cement. At an even higher maltodextrin dosage of 0.5% bwoc, both initial and final setting times decreased sharply to values close or even below that of the neat cement paste. This indicates that excessive dosages of maltodextrin reverse its effect from being a retarder to accelerator, as is widely known also for carboxylic acids such as citric acid [30].

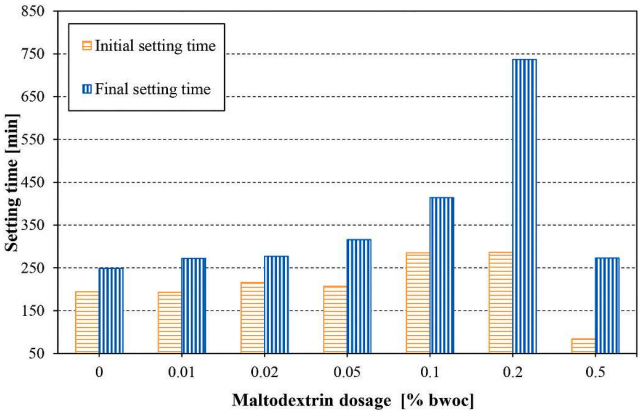

Fig. 2. Setting time of cement pastes admixed with different maltodextrin dosages, w/c ratio = 0.3.

3.2. Fluidity of cement pastes admixed with maltodextrin

The influence of maltodextrin on the workability of cement pastes was probed via "mini slump" tests, and the results are shown in Fig. 3. From there, it is obvious that the spread flow of cement pastes increases linearly with ascending maltodextrin dosages. Moreover, the enhancement of cement paste fluidity by maltodextrin is quite significant. For example, at 0.2% bwoc addition of maltodextrin, the spread flow of the cement paste increases from 18 cm to 22 cm (~22% increase), and at 0.5% dosage a spread flow at 26 cm is reached. From these results it can be concluded that the incorporation of maltodextrin can significantly enhance the fluidity of the cementitious system. A similar dispersing effect was also reported for sodium gluconate, but there the improvement was considerably less [11,31].

3.3. Mechanical properties

The effect of the maltodextrin on the mechanical properties of the OPC sample was probed via mortar tests. There, the mortar samples

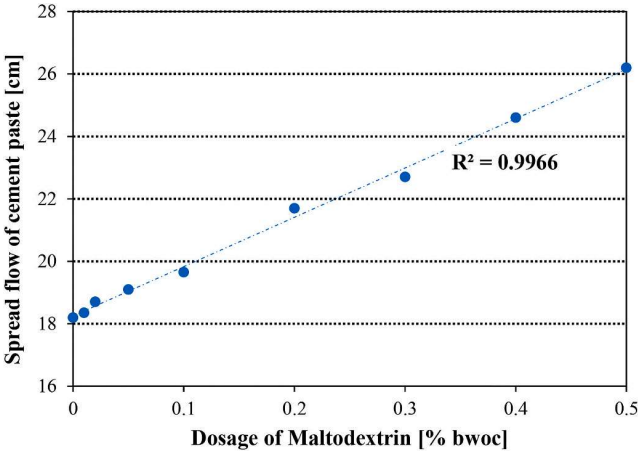

Fig. 3. The fluidity of cement pastes containing different dosages of maltodextrin; w/c ratio = 0.48.

admixed with different dosages of maltodextrin were prepared at a w/c ratio of 0.5, and the results are displayed in Fig. 4.

As is shown here, addition of maltodextrin decreases, the compressive strength of all mortar samples at the early curing age of 16 h. The decrease is nearly linear with the maltodextrin dosage. However, at extended curing times such as 1 d, 3 d or 28 d, the addition of maltodextrin in fact increases the compressive strength of the mortar samples by up to 12% following a parabolic curve with respect to maltodextrin dosage, i.e. at ~0.03% addition a maximum in strength increase is observed, and at higher dosages the gain in strength is gradually lost, at 0.1% dosage even falls below the value of the neat mortar. These results confirm that the effect of maltodextrin on strength development corresponds to a non-linear behavior, and this needs to be kept in mind when formulating concretes or mortars.

To summarize, at very early age (16 h) addition of a relatively low dosage of maltodextrin (≤0.05% bwoc) hinders the compressive strength development while it promotes these mechanical properties after extended aging periods of 1 d, 3 d and 28 d. At medium dosages (0.03–0.04%), maltodextrin even procures noticeable gains in strength whereas at higher additions (≥0.1% bwoc), strength values decrease and even fall bellows that of non-admixed reference mortar. The findings here reveal that maltodextrin acts as a hardening retarder, the effect however is dependent of time and dosage, which is similar to that of sodium gluconate and other sugar derivatives [11,32]. According to Juenger and Jennings [32], sugar compounds not only promotes the dissolution of ions but also poisons the cement clinker phases and/or generated hydration products. The adsorption on hydration products shuts off further crystal growth, and the enhanced initial dissolution of cement clinker leads to high concentrations of ions, more nuclei are formed. In the next step, the "retardation barrier'' is being overcome when the available nucleation sites exceed the sugar amount. Then the rate of hydration reaction increases rapidly, resulting in the substantial increased amount of hydration products, exhibiting delayed acceleration effect.

Peterson et al. [33] monitored the kinetics of the cement hydration reaction through the quasi elastic neutron scattering technique (QENS) coupled with hydration models and reported that the length of the nucleation and growth period increases with the addition of sucrose. Our findings can also be explained by the mechanism proposed by Juenger and Jennings.

3.4. Hydration kinetics of OPC

In order to gain a more profound understanding of the retarding effect on cement caused by maltodextrin, the heat evolvement during cement hydration was monitored via heat flow calorimetry at a water-to-cement ratio of 0.48.

Figs. 5 and 6 present the calorimetric results from cement pastes admixed with maltodextrin at varied dosages. As is evident from Fig. 5, all of the samples containing maltodextrin produced a peak signifying maximum heat release after that of the reference sample, and with increasing dosage of maltodextrin, the main hydration peak during the acceleration period was continuously shifted to longer times. This observation confirms the retarding effect of maltodextrin which is signified by an extension of the induction period from cement hydration. The calorimetric results are also in agreement with the observations for setting times as shown in Fig. 2. Besides, the total hydration heat of the cement samples admixed with 0.01%–0.05% of maltodextrin was increased, as is evident from Fig. 6. Most interestingly consistent with the compressive strength results is that high maltodextrin dosage of 0.1%, the total heat released over the first 20 h was significantly reduced which explains why there the compressive strength results were always

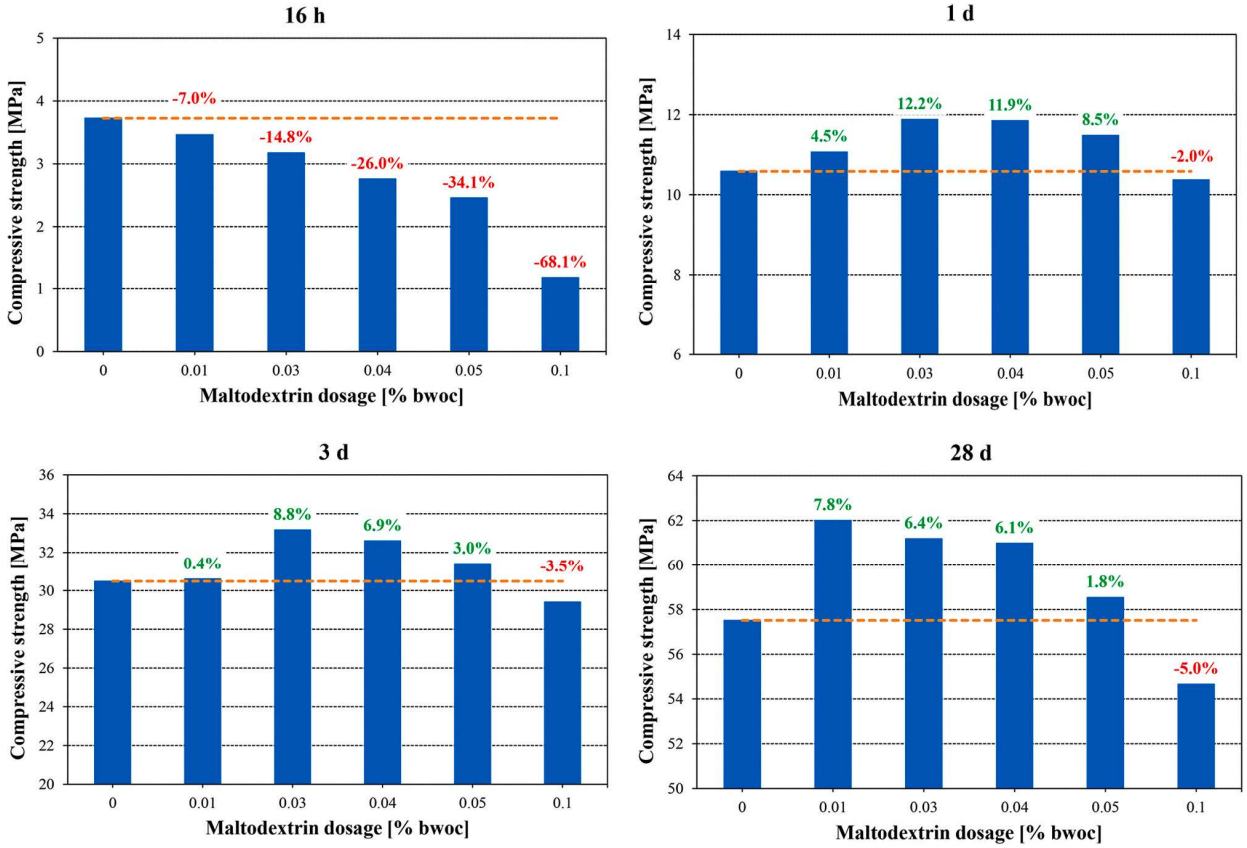

Fig. 4. Compressive strength of mortar samples admixed with different maltodextrin dosages; w/c ratio = 0.5.

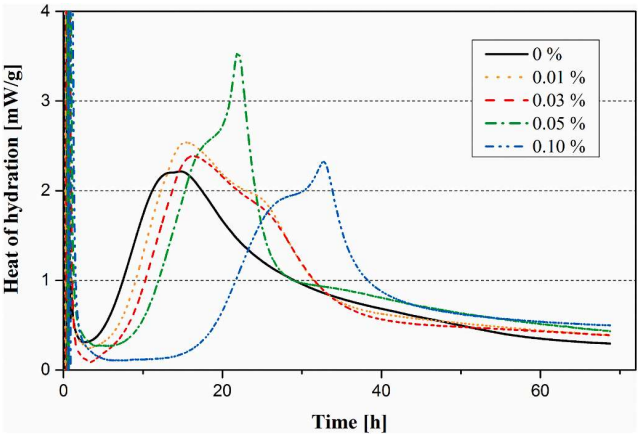

Fig. 5. Heat flow calorimetry of cement pastes admixed with 0–0.1% maltodextrin; w/c = 0.48.

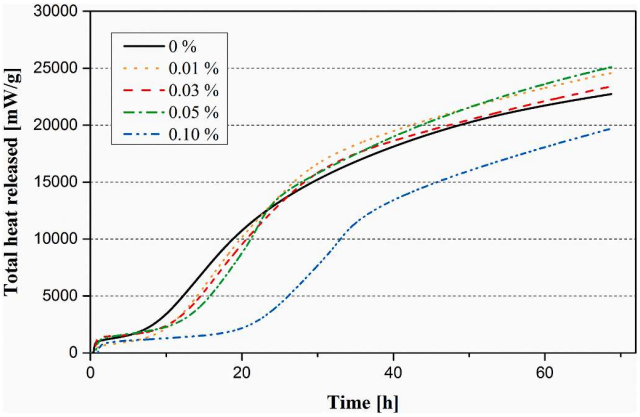

Fig. 6. Cumulative heat flow from the cement pastes admixed with 0–0.1% maltodextrin; w/c = 0.48.

lower than that of the reference sample.

3.5. Development of hydration products via in-situ XRD

It is well established that hydration time, temperature and the presence of chemical admixtures represent main factors that influence the development of cement hydration products. Thus, *in-situ* XRD was applied to investigate the progress of hydration over time. Here, cement pastes admixed with maltodextrin dosages of 0%, 0.03% or 0.05% bwoc were studied and the results are shown in Fig. 7.

There, a decrease in the signal intensity representing C_3S/C_2S and C_3A (reactants) was observed over time for the reference sample. At the same time, signals for cement hydration products including Portlandite (CH) and ettringite (AF_t) appeared and increased in intensity as hydration progressed. Whereas, upon addition of maltodextrin the intensity of the Portlandite peak was reduced significantly, indicating that the CH formation was delayed. Even more, at dosage of 0.05% the Portlandite signal even disappeared completely, indicating that the higher the dosage of maltodextrin, the more significant is its inhibiting effect on CH formation. As it is commonly known that initially CH is formed resulting from the C_3S hydration [31]. An inhibition of C_3S hydration by maltodextrin can be concluded. Furthermore, AF_t signals from the cement samples admixed with maltodextrin were also much less in intensity, signifying a delayed C_3A reaction.

The findings from *in-situ* XRD suggest that the addition of maltodextrin delays cement hydration which results in less hydration products like Portlandite and ettringite.

From the compressive strength results presented in section 3.3, it is obvious that appropriate dosing (≤0.05% bwoc) of maltodextrin increased the strength after 1 day. To elucidate the reason behind a cement paste holding 0.03% maltodextrin was monitored via *in-situ* XRD over the first 48 h. The results are displayed in Fig. 8.

There, after ~15 h rapid formation of Portlandite and at the same time a significant decrease in the reflections representing the silicate phases (C_3S/C_2S) was also noticed. These findings suggest that after 15 h C–S–H hydrate phases are formed which are responsible for the mechanical strength enhancement of the mortar observed after 1 d of curing.

3.6. Adsorption of maltodextrin on cement

The above results reveal that maltodextrin exercises a strong retarding effect on ordinary Portland cement. However, its interaction with cement is poorly understood. In comparison, a handful of work can be found to explain the retarding effect and mechanism of another commonly used retarder - sodium gluconate on cement. Generally, a few theories can be applied to explain the retardation behavior of sodium gluconate: the nucleation and/or growth of hydration products was inhibited by sodium gluconate [34]; the adsorption of gluconate or the complexation of Ca^{2+} on the surface of C_3A prevents the formation of early hydrates like Af_t; In a related manner, the adsorption of sodium gluconate on the surface of silicate phases hinders the further hydration [35]. However much less information on maltodextrin has been published so far. Thus, TOC and zeta potential measurements were utilized to probe into the retardation mechanism of maltodextrin.

As shown in Fig. 9, the adsorbed amount of maltodextrin on cement increases with ascending dosage signifying a *langmuir* isotherm until it reaches a plateau which represents the saturated adsorption at ~5.3 mg maltodextrin/g cement. The adsorption curve can be expressed by equation (1)

$$y = \frac{a*b*x^{1-c}}{1 + b*x^{1-c}} \quad (1)$$

where a stands for the saturated sorption amount, b represents a coefficient, c is the equilibrium adsorption constant, $R^2 = 0.97754$.

The results allow to conclude that maltodextrin achieves retardation as well as dispersion via an adsorptive interaction with cement. The adsorption mechanism of maltodextrin needs to be further investigated. Looking into literature, Steinour claimed that these organic retarders typically contain H–C–OH groups which adsorb on cement particles via hydrogen bonding [36]. Taplin argued that the active adsorbing group for various organic sugars is HO–C–C=O group [36]. All the reducing sugars either comprise HO–C–C=O group in the molecule or possess the ability to be converted to saccharinic acid containing this group by dilute alkali [36]. Nalet and Nonat reported that D-gluconate has a higher affinity with Portlandite as well as C–S–H, as it exhibits a higher saturated adsorbed amount as compared to D-glucitol [37]. Consequently, they attributed the much enhanced adsorbing property of D-gluconate to the presence of ending hydroxy-carboxylate group in the molecule. In more recent works, Smith et al. [27,28] monitored the structural changes of saccharide species such as glucose, sucrose, and maltodextrin in alkali environment via solution-state ^{13}C APT NMR. By comparing the solution-state ^{13}C APT NMR spectra of a glucose sample under neutral ambient conditions to a glucose sample being admixed in cement paste, it is obvious that the glucose sample under neutral ambient conditions does not produce any degradation products whereas the glucose sample being exposed in alkali environment undergoes substantial transformations to generate different kinds of carboxylic acids.

Maltodextrin is a polysaccharide which is composed of D-glucose units connected in chains via bridging oxygen atoms. In contrast to

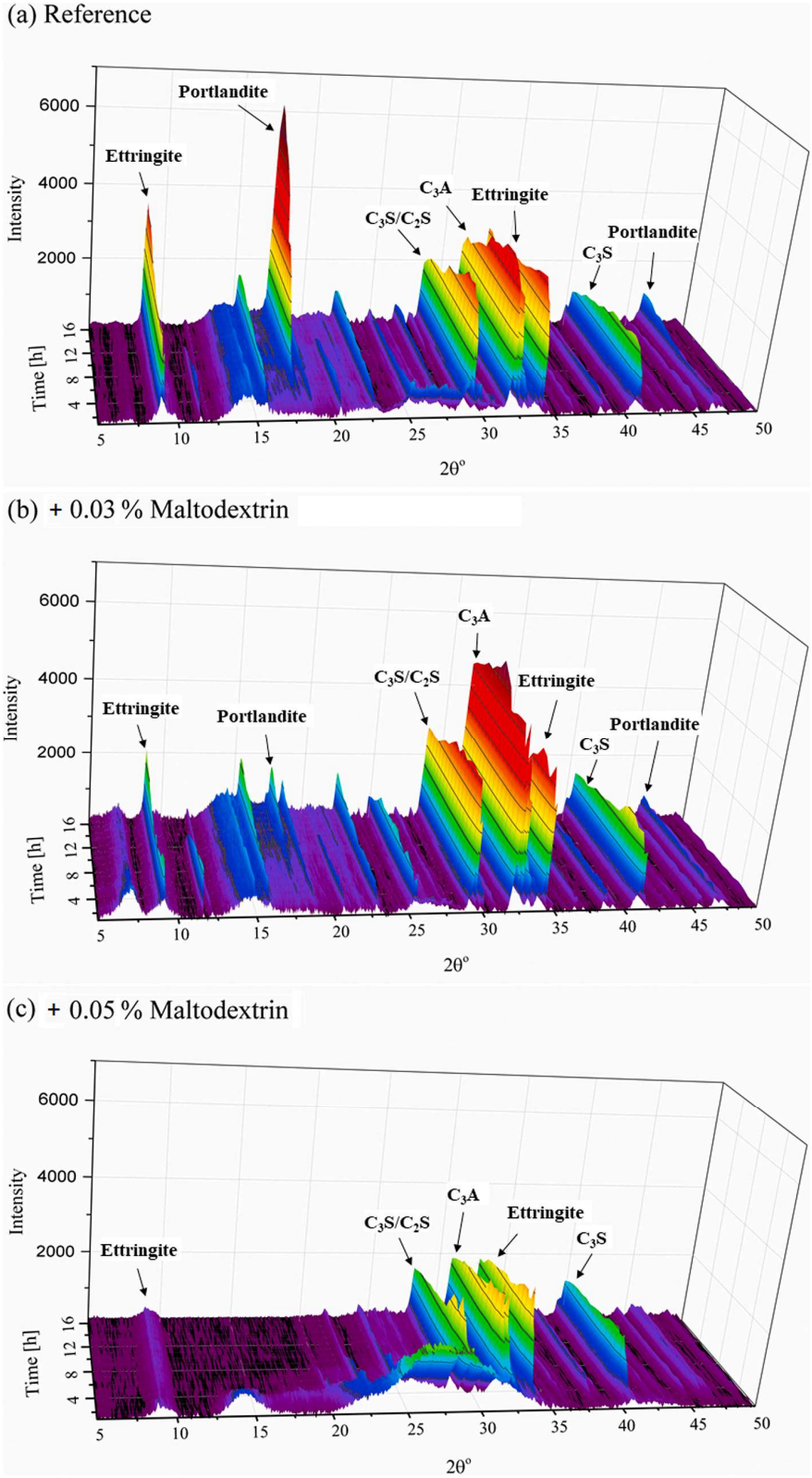

Fig. 7. *In-situ* XRD diagrams of cement pastes admixed with 0–0.05% maltodextrin captured during the first 16 h: (a) reference, (b) + 0.03% maltodextrin (c) + 0.05% maltodextrin; w/c = 0.48.

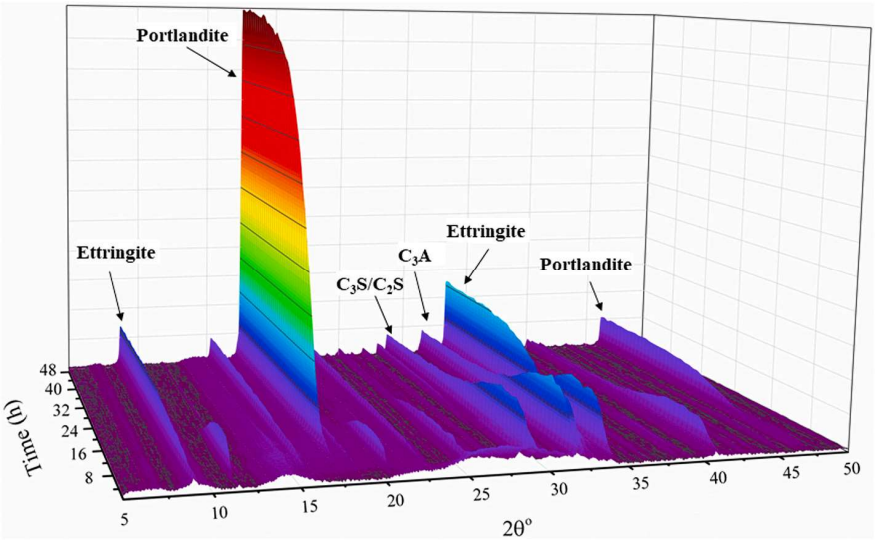

Fig. 8. Development of cement hydration products from cement paste admixed with 0.03% maltodextrin, observed via *in-situ* XRD over the first 48 h; w/c = 0.48.

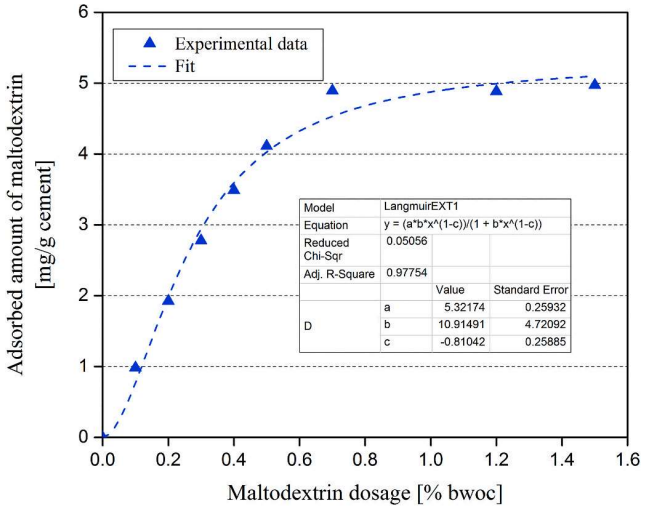

Fig. 9. Adsorption isotherm for maltodextrin admixed to cement paste; w/c = 0.48.

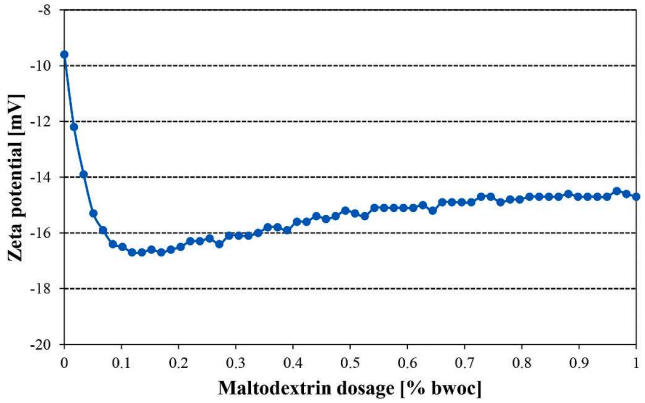

Fig. 10. Zeta potential of cement paste as a function of maltodextrin dosage; w/c = 0.48.

glucose which represents a typical monosaccharide, the structural transformation of maltodextrin is a more complex process, resulting in various degradation products, such as oligosaccharides, monosaccharides, and low M_W carboxylic acids [27,28,38]. It suggests that the adsorption of maltodextrin on cement clinker phases or hydrates could be achieved via being converted to saccharinic acid in alkaline environment, subsequently retarding effect is exercised.

In the next step, zeta potential measurements were performed to further verify the adsorptive mechanism of maltodextrin in cement.

Fig. 10 presents the zeta potential curve of a cement paste admixed with an increasing dosage of maltodextrin. As is obvious here, the cement paste initially carried a negative charge of around – 10 mV. With gradual addition of maltodextrin, a significant decline of the zeta potential from – 10 to – 17 mV was recorded followed by a slightly steady increment. This phenomenon is known for highly anionic polyelectrolytes and is presented in previous literatures [29,39]. This effect can be ascribed to counterion condensation or Manning condensation, this theory originated in the 1970s [40,41]. To be more specific, the small counterions in the cement pore solution can partially neutralize the polyelectrolyte charge, resulting in lower effective charge than the nominal charge of the polyelectrolyte [42]. This zeta potential curve confirms that maltodextrin adsorbs on cement.

To summarize, the adsorption as well as zeta potential measurements confirm that the retarding mechanism of maltodextrin relies on adsorption on cement. The retarding effect induced by adsorption of maltodextrin on cement can be explained by different concepts. When maltodextrin becomes adsorbed on the surface of cement particles, then a diffusion barrier around the cement particles is created which hinders the access of water [43]; The interaction between maltodextrin molecules or the corresponding degradation products and the silicate and aluminate phases at cement particle surfaces can also cause hydration inhibition effect [28,44]. Such adsorption of maltodextrin at active etch pits of tricalcium silicate surfaces leads to slower dissolution of various ions from anhydrate phases, in consequence blocks the further hydration. In a related manner, the direct adsorption of maltodextrin on hydration products poisons nucleation sites to shut off further crystal growth such as C–S–H and Portlandite [10,27,28]. Likewise, maltodextrin degradation products adsorb onto C_3A surface prevents the formation of early hydrates like Af_t [27]. A review of these concepts elucidates that one or more models may be apply to the retardation of cement hydration by maltodextrin.

4. Conclusions

This study demonstrates that maltodextrin presents a viable cement retarder and also possesses dispersing ability. Its impact on the setting time and mechanical properties of OPC was studied and the mechanism behind was investigated to gain more profound understanding of the interaction between maltodextrin and cement.

From the results obtained, the following conclusions can be drawn:

1. Maltodextrin acts as both a setting and hardening retarder, the effect however is dependent of dosage. Besides, maltodextrin also contributes to the fluidity of cement paste.
2. The impact of maltodextrin on the mechanical properties of OPC is much more dependent of dosage. Relatively low dosages (0.01–0.05%) increase compressive strength of mortar at the curing ages of 1, 3 or 28 days, but decrease strength values at higher dosages ($\geq$0.1%).
3. These results were confirmed via heat flow calorimetry. At dosages from 0.01% to 0.05% the total heat released after ~20 h was increased. Whereas, when the maltodextrin dosage increased to 0.1%, the total liberated heat was reduced.
4. *In-situ* XRD results suggest that in the presence of maltodextrin, hydration of C_3S and C_3A in particular is inhibited during the first 16 h, thus less hydration products (CH and AF_t) can be detected which explains the lower mechanical strength observed in the first 16 h. Thereafter cement hydration during 15–25 h is strongly progressing as is evidenced by abundant CH formation. As a consequence, cement admixed with maltodextrin develops its strength slower, but produces an overall higher strength in the long term.
5. Based on our findings: maltodextrin appears to have significant potential as a slump-retaining admixture for ready-mix concrete, especially when higher ambient temperature is encountered.
6. The mode of action of maltodextrin retarder is based on adsorption, as was confirmed via TOC and zeta potential measurements.

For the future it might be interesting to study the retarding mechanism of maltodextrin on individual cement clinker phases, i.e. C_3S and C_3A.

Declaration of competing interest

The authors declare that they have no known competing financial interests or personal relationships that could have appeared to influence the work reported in this paper.

Acknowledgement

The authors would like to thank China Academy of Building Research (CABR) for providing the maltodextrin sample used in this study. Moreover, the support of TUM International for establishing the contact to CABR via “TUM Global Incentive” Fund granted to the Chair for Construction Chemistry, Prof. Johann Plank, is greatly acknowledged. Ran Li would like to thank China Scholarship Council (CSC) for generous funding of her Ph.D. study at TU München.

References

[1] J. Plank, E. Sakai, C.W. Miao, C. Yu, J.X. Hong, Chemical admixtures - chemistry, applications and their impact on concrete microstructure and durability, Cement Concr. Res. 78 (2015) 81–99.
[2] J. Liu, C. Yu, X. Shu, Q. Ran, Y. Yang, Recent advance of chemical admixtures in concrete, Cement Concr. Res. 124 (2019) 105834.
[3] K. Kupwade-Patil, P.J. Boul, D.K. Rasner, S.M. Everett, T. Proffen, K. Page, D. Ma, D. Olds, C.J. Thaemlitz, O. Büyüköztürk, Retarder effect on hydrating oil well cements investigated using in situ neutron/X-ray pair distribution function analysis, Cement Concr. Res. 126 (2019).
[4] M. Zajac, J. Skocek, F. Bullerjahn, M. Ben Haha, Effect of retarders on the early hydration of calcium-sulpho-aluminate (CSA) type cements, Cement Concr. Res. 84 (2016) 62–75.
[5] L. Zhang, Y. Ji, J. Li, F. Gao, G. Huang, Effect of retarders on the early hydration and mechanical properties of reactivated cementitious material, Construct. Build. Mater. 212 (2019) 192–201.
[6] D.A. Hall, R. Stevens, B. El-Jazairi, The effect of retarders on the microstructure and mechanical properties of magnesia-phosphate cement mortar, Cement Concr. Res. 31 (2001) 455–465.
[7] H. Lahalle, C. Cau Dit Coumes, C. Mercier, D. Lambertin, C. Cannes, S. Delpech, S. Gauffinet, Influence of the w/c ratio on the hydration process of a magnesium phosphate cement and on its retardation by boric acid, Cement Concr. Res. 109 (2018) 159–174.
[8] F.F. Ataie, M.C.G. Juenger, S.C. Taylor-Lange, K.A. Riding, Comparison of the retarding mechanisms of zinc oxide and sucrose on cement hydration and interactions with supplementary cementitious materials, Cement Concr. Res. 72 (2015) 128–136.
[9] W. Hou, J. Bao, Evaluation of cement retarding performance of cellulosic sugar acids, Construct. Build. Mater. 202 (2019) 522–527.
[10] A. Peschard, A. Govin, J. Pourchez, E. Fredon, L. Bertrand, S. Maximilien, B. Guilhot, Effect of polysaccharides on the hydration of cement suspension, J. Eur. Ceram. Soc. 26 (2006) 1439–1445.
[11] S. Ma, W. Li, S. Zhang, D. Ge, J. Yu, X. Shen, Influence of sodium gluconate on the performance and hydration of Portland cement, Construct. Build. Mater. 91 (2015) 138–144.
[12] B. Mota, T. Matschei, K. Scrivener, Impact of sodium gluconate on white cement-slag systems with Na_2SO_4, Cement Concr. Res. 122 (2019) 59–71.
[13] G. Zhang, G. Li, Y. Li, Effects of superplasticizers and retarders on the fluidity and strength of sulphoaluminate cement, Construct. Build. Mater. 126 (2016) 44–54.
[14] D. Marchon, F. Boscaro, R.J. Flatt, First steps to the molecular structure optimization of polycarboxylate ether superplasticizers: mastering fluidity and retardation, Cement Concr. Res. 115 (2019) 116–123.
[15] L. Zhang, X. Miao, X. Kong, S. Zhou, Retardation effect of PCE superplasticizers with different architectures and their impacts on early strength of cement mortar, Cement Concr. Compos. 104 (2019) 103369.
[16] V.S. Ramachandran, 2 - Research techniques, standards and specifications, in: V. S. Ramachandran (Ed.), Concrete Admixtures Handbook, second ed., William Andrew Publishing, 1996, pp. 69–94.
[17] R. Flatt, I. Schober, Superplasticizers and the Rheology of Concrete, Understanding the Rheology of Concrete, 2012, pp. 144–208. Elsevier.
[18] X. Zhang, C. Lu, J. Shen, Influence of tartaric acid on early hydration and mortar performance of Portland cement-calcium aluminate cement-anhydrite binder, Construct. Build. Mater. 112 (2016) 877–884.
[19] Y. Zhang, J. Yang, X. Cao, Effects of several retarders on setting time and strength of building gypsum, Construct. Build. Mater. 240 (2020) 117927.
[20] G. Möschner, B. Lothenbach, R. Figi, R. Kretzschmar, Influence of citric acid on the hydration of Portland cement, Cement Concr. Res. 39 (2009) 275–282.
[21] M. Bishop, A.R. Barron, Cement hydration inhibition with sucrose, tartaric acid, and lignosulfonate: analytical and spectroscopic study, Ind. Eng. Chem. Res. 45 (2006) 7042–7049.
[22] M. Bishop, S.G. Bott, A.R. Barron, A new mechanism for cement hydration inhibition: solid-state chemistry of calcium nitrilotris (methylene) triphosphonate, Chem. Mater. 15 (2003) 3074–3088.
[23] V.S. Ramachandran, 3 - admixture interactions in concrete, in: V.S. Ramachandran (Ed.), Concrete Admixtures Handbook, second ed., William Andrew Publishing, 1996, pp. 95–136.
[24] N. Schneider, D. Stephan, The effect of d-gluconic acid as a retarder of ground granulated blast-furnace slag pastes, Construct. Build. Mater. 123 (2016) 99–105.
[25] R.O.A. Rahman, R.Z. Rakhimov, N.R. Rakhimova, M.I. Ojovan, Cementitious Materials for Nuclear Waste Immobilization, John Wiley & Sons, 2014.
[26] N.L. Thomas, J.D. Birchall, The Retarding Action of Sugars on Cement Hydration, 1983, pp. 830–842.
[27] B.J. Smith, A. Rawal, G.P. Funkhouser, L.R. Roberts, V. Gupta, J.N. Israelachvili, B. F. Chmelka, Origins of saccharide-dependent hydration at aluminate, silicate, and aluminosilicate surfaces, Proc. Natl. Acad. Sci. Unit. States Am. 108 (2011) 8949–8954.
[28] B.J. Smith, L.R. Roberts, G.P. Funkhouser, V. Gupta, B.F. Chmelka, Reactions and surface interactions of saccharides in cement slurries, Langmuir 28 (2012) 14202–14217.
[29] L. Lei, J. Plank, Synthesis, working mechanism and effectiveness of a novel cycloaliphatic superplasticizer for concrete, Cement Concr. Res. 42 (2012) 118–123.
[30] N.B. Singh, A.K. Singh, S. Prabha Singh, Effect of citric acid on the hydration of portland cement, Cement Concr. Res. 16 (1986) 911–920.
[31] X. Lv, J. Li, C. Lu, Z. Liu, Y. Tan, C. Liu, B. Li, R. Wang, The effect of sodium gluconate on pastes' performance and hydration behavior of ordinary portland cement, Adv. Mater. Sci. Eng. 2020 (2020) 9231504.
[32] M.C. Garci Juenger, H.M. Jennings, New insights into the effects of sugar on the hydration and microstructure of cement pastes, Cement Concr. Res. 32 (2002) 393–399.
[33] V.K. Peterson, M.C.G. Juenger, Time-resolved quasielastic neutron scattering study of the hydration of tricalcium silicate: effects of $CaCl_2$ and sucrose, Phys. B Condens. Matter 385 (2006) 222–224.
[34] N.B. Milestone, Hydration of tricalcium silicate in the presence of lignosulfonates, glucose, and sodium gluconate, J. Am. Ceram. Soc. 62 (1979) 321–324.

9. Appendix

[35] J.P. Perez, The mechanism of action of sodium gluconate on the fluidity and set of Portland cement, in: 12th International Congress on the Chemistry of Cement, 2007.
[36] G.M. Bruere, Set-retarding effects of sugars in portland cement pastes, Nature 212 (1966) 502–503.
[37] C. Nalet, A. Nonat, Ionic complexation and adsorption of small organic molecules on calcium silicate hydrate: relation with their retarding effect on the hydration of C_3S, Cement Concr. Res. 89 (2016) 97–108.
[38] M.T. Cancilla, S.G. Penn, C.B. Lebrilla, Alkaline degradation of oligosaccharides coupled with matrix-assisted laser desorption/ionization Fourier transform mass spectrometry: a method for sequencing oligosaccharides, Anal. Chem. 70 (1998) 663–672.
[39] K. Yamada, Basics of analytical methods used for the investigation of interaction mechanism between cements and superplasticizers, Cement Concr. Res. 41 (2011) 793–798.
[40] G.S. Manning, Limiting laws and counterion condensation in polyelectrolyte solutions I. Colligative properties, J. Chem. Phys. 51 (1969) 924–933.
[41] G.S. Manning, Limiting laws and counterion condensation in polyelectrolyte solutions: IV. The approach to the limit and the extraordinary stability of the charge fraction, Biophys. Chem. 7 (1977) 95–102.
[42] J. Duhamel, Advances in chemical physics, J. Am. Chem. Soc. 119 (1997) 3850–3851.
[43] J.F. Young, A review of the mechanisms of set-retardation in portland cement pastes containing organic admixtures, Cement Concr. Res. 2 (1972) 415–433.
[44] J. Cheung, A. Jeknavorian, L. Roberts, D. Silva, Impact of admixtures on the hydration kinetics of Portland cement, Cement Concr. Res. 41 (2011) 1289–1309.

Section 9.2

Publication # 11

Specific molecular design of polycarboxylate polymers exhibiting optimal compatibility with clay contaminants in concrete

L. Lei, Y. Zhang, **R. Li**

Cement and Concrete Research (IF = 12.0)

147 (2021) 106504

DOI: 10.1016/j.cemconres.2021.106504

Cement and Concrete Research 147 (2021) 106504

Contents lists available at ScienceDirect

Cement and Concrete Research

journal homepage: www.elsevier.com/locate/cemconres

Specific molecular design of polycarboxylate polymers exhibiting optimal compatibility with clay contaminants in concrete

L. Lei *, Y. Zhang, R. Li

Technische Universität München, Chair for Construction Chemistry, 85747 Garching, Lichtenbergstraße 4, Germany

ARTICLE INFO

Keywords:
Dispersion (A)
Cement (D)
Superplasticizer
Polycarboxylate (PCE)
Bentonite

ABSTRACT

It is widely recognized that the dispersing ability of polycarboxylate superplasticizers (PCEs) could be hindered due to the presence of clay contaminants in concrete. In this study, a series of allyl ether-based polycarboxylate superplasticizers possessing short polyethylene glycol side chains was successfully synthesized and probed for their clay tolerance. The resulting PCE polymers were characterized via Size Exclusion Chromatography (SEC) to obtain their molecular properties. Thereafter, their dispersing ability was probed in the absence and presence of sodium bentonite. Allyl ether-based polycarboxylate (APEG) polymers possessing short side chains were found to exhibit enhanced clay resistance as compared to that of conventional MPEG PCEs holding long pendant chains. The mode of interaction between APEG PCEs and bentonite was investigated via sorption and XRD measurements. The data revealed that APEG PCEs possessing a lower side chain density intercalate less into the interlayer space of bentonite than those exhibiting higher side chain density.

1. Introduction

Polycarboxylate superplasticizers (PCEs) have attracted increasing attention and have been extensively studied in the recent decades [1–3]. Due to the great variability of the polycarboxylate structure, PCEs allow for significant modification of the molecular architecture in order to meet the specific needs of the various applications by the concrete industry [4,5].

From the use of various materials for the manufacture of concrete, PCEs have been found to be very sensitive towards clay contaminants occurring in concrete aggregates [6–10]. This is evidenced by extremely high PCE dosages required to achieve the same fluidity as for the clay-free system. In some cases, even with triple or quadruple dosage of the PCE product, desirable concrete workability cannot be achieved. Obviously, depending on the type of clay which can vary with respect to its composition and physicochemical properties, PCEs can be affected in different ways by such minerals [11]. More specifically, PCE polymers can interact with clay minerals via surface adsorption and/or chemical intercalation. In the case of sodium bentonite, both effects will occur, with intercalation being vastly dominant. The mechanism appears to involve partially polarized polyethylene glycol pendant chains anchoring on the silanol groups present on the surface of the aluminosilicate layers via H-bonding mediated by water molecules [12]. The specific interaction between superplasticizers and clay minerals is typically evidenced by powder X-ray diffraction analysis [13]. Typically, a change in the *d*-spacing from initial 1.23 nm (sodium montmorillonite without superplasticizer) to 1.72 nm can be detected when polycarboxylate superplasticizers with polyethylene side chains are present, which confirms the intercalation mechanism [13]. In a very recent study, Borralleras et al. tested the fresh clay samples admixed with various dosages of PCE polymer via in situ XRD measurements and proposed a multiple intercalation model of polyethylene glycol (PEG) side chains, which offers a more robust methodology [14,15]. Moreover, it has been reported that the sorbed amounts of PCE superplasticizers on swelling clay are ~100 times higher than on Portland cement [16]. Consequently, PCE performance is severely hindered in the presence of clay, and developing PCE polymers exhibiting high resistance to the negative effect of clay contaminants in aggregates remains as a research priority [17].

Looking into the literature, a handful of studies have attempted to establish mitigation strategies for the clay problem [8,11,13,16,18–23]. For instance, several reports [18] have indicated that addition of polyethylene glycol (PEG) as a sacrificial agent to the clay contaminated cement pastes can hinder the intercalation of PCE completely, and the dispersion capability and workability retention could be maintained. However, the dosage of the sacrificial agent required is extremely high

* Corresponding author.
E-mail address: lei.lei@bauchemie.ch.tum.de (L. Lei).

https://doi.org/10.1016/j.cemconres.2021.106504
Received 3 June 2020; Received in revised form 26 May 2021; Accepted 2 June 2021
Available online 22 June 2021

which renders this approach economically unfeasible. Another approach is to admix a clay tolerant PCE having a modified structure. For example, Lei et al. [13] synthesized novel PCE superplasticizers possessing HAMA (hydroxyl alkyl methacrylate) side chains instead of PEG pendants for enhanced robustness towards clay. This new structure was found to provide good dispersing ability in cement pastes in the presence of clay and was much less affected by montmorillonite as compared to conventional PCEs with polyethylene oxide (PEO) side chains. Unfortunately, due to its extremely short pendant chains, its addition rate required in a clay-free system was relatively high. For another case of modifying the PCE side chains, Xu et al. [24] incorporated a three dimensional β-cyclodextrin into the structure of an HPEG (α-methallyl-ω-hydroxy poly(ethylene glycol)) PCE. Because of this modification, the PCE structure exhibiting bulky side chains could not enter the interlayer structure of montmorillonite. Consequently, the clay robustness of such PCE structure is much enhanced. However, the process of cement hydration was inevitably delayed and a lower hydration heat value was monitored when such bulky groups are incorporated [25].

It is widely accepted that certain clays expand when in contact with water and this accounts for the loss in dispersing efficiency of PCE polymers. A completely new concept to mitigate the clay problem is to prohibit the swelling of clay, in consequence, the intercalation of PCE would be hindered. Jacquet et al. [26] presented that various organic cations, i.e. quaternary amine [27], exhibited a strong affinity for cationic exchange with clay and can be used as clay-activity-modifying agents. In a similar manner, Lawrence et al. [28,29] reported to use cationic copolymers for inerting clays in sand aggregates which are used in concrete. It was found that the cationic polymers would shield the detrimental effects of swelling clays in the concrete and consequently enhance properties, such as workability and fluidity in the cementitious compositions.

Admittedly, a great need exists for suitable PCE polymers with high dispersion ability which are not affected by the presence of clay. In this study, we have synthesized allyl ether-based PCEs with particularly short PEO side chains and further studied their clay tolerance through a series of performance tests. The mode of interaction between allyl ether-based polycarboxylate superplasticizers and montmorillonite was further investigated via sorption and XRD experiments. The sorption behavior of these newly prepared allyl ether-based PCEs was compared with that of β-naphthalene sulfonate (BNS) and a typical MPEG-based PCE superplasticizer with long PEO side chains. The overall goal of this investigation is to identify a specific polycarboxylate molecular design that exhibits tolerance with montmorillonite clay.

2. Experimental

2.1. Materials

2.1.1. Chemicals

Acrylic acid (AA) (>99% purity, Sigma-Aldrich, Germany), α-allyl-ω-hydroxy poly (ethylene glycol) ether (APEG macromonomer, $n_{EO} = 7$) (>98%, NOF Corporation, Japan), ω-methoxy poly (ethylene oxide) methacrylate ester (MPEG macromonomer, $n_{EO} = 45$) (>98%, Clariant, Germany), ammonium persulfate (≥98%, Sigma-Aldrich, Germany), sodium methallyl sulfonate (>98%, Sigma-Aldrich, Germany), 3-mercaptopropionic acid (≥99%, Sigma-Aldrich, Germany), and sodium hydroxide (≥97%, Merck KGaA, Germany) were all used without further purification.

In addition, one MPEG-based PCE and one β-naphthalene sulfonate formaldehyde polycondensate (BNS) were tested and used as reference admixture in this study. The self-synthesized MPEG-PCE, identified as 45PC6 was obtained through aqueous free radical copolymerization of acrylic acid and ω-methoxy poly (ethylene oxide) methacrylate ester with methallyl sulfonic acid added as a chain transfer agent. The molar ratio between acrylic acid and MPEG macromonomer was 6:1, and the side chain consisted of 45 ethylene oxide units. A detailed description of the preparation can be found in reference [30]. In our study, methacrylic acid was substituted by acrylic acid. The BNS polymer is an industrial product commercialized under the trade name FLUBE CA 40 and was obtained from Bozzetto Group, Italy.

Table 1
Phase composition of the OPC sample CEM I 42.5 R by Q-XRD using *Rietveld* refinement.

Phase	wt%
C_3S, monoclinic	54.52
C_2S, monoclinic	18.41
C_4AF, orthorhombic	10.85
C_3A, cubic	5.23
C_3A, orthorhombic	0.88
Anhydrite ($CaSO_4$)	0.94
Dihydrate ($CaSO_4{\cdot}2H_2O$)	3.61
Hemihydrate ($CaSO_4{\cdot}0.5H_2O$)	0.33
Calcite ($CaCO_3$)	3.04
Dolomite ($CaMg(CO_3)_2$)	1.13
Quartz (SiO_2)	0.91
Free lime (*Franke*)	0.14
Total	100.00

Table 2
Oxide composition of the bentonite sample as determined by XRF.

Oxide	wt%
SiO_2	55.7
Al_2O_3	16.2
Fe_2O_3	3.5
CaO	3.0
Na_2O	2.0
MgO	1.4
K_2O	0.9
TiO_2	0.3
BaO	0.1
P_2O_5	0.1
MnO	0.1
SrO	0.1
SO_3	0.1
LOI	16.5
Total	100.00

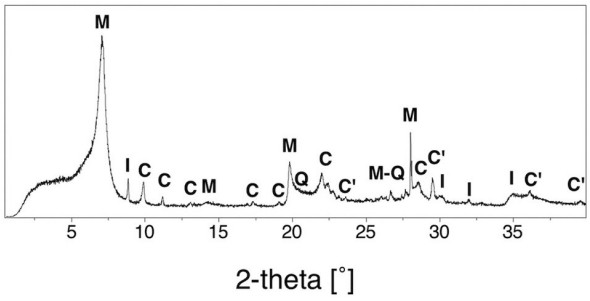

Fig. 1. XRD pattern of the raw clay (M: montmorillonite; C: clinoptilolite-Ca; I: illite; Q: quartz; C′: calcite).

2.1.2. Cement

The cement used in this study was an ordinary Portland cement (OPC) sample CEM I 42.5 R. The phase composition as shown in Table 1 was determined by quantitative XRD analysis with *Rietveld* refinement. The average particle size (d_{50} value), obtained by laser granulometry, was 18.83 μm. The density was determined to be 3.13 g/cm^3 (by Helium pycnometry).

Table 3
Mineralogical composition of the clay sample via Q-XRD.

Compositions	Montmorillonite	Clinoptilolite-Ca	Illite	Quartz	Calcite
Proportion (%)	80.56	11.21	2.62	4.45	1.15

2.1.3. Clay

An artificial sodium bentonite sample (BYK, Wesel, Germany), which represents a common contaminant in aggregate sources, was selected for this investigation. The oxide composition was determined by X-ray fluorescence and is shown in Table 2. The mineralogical composition was determined by Q-XRD via *Rietveld* refinement as shown in Fig. 1 and Table 3. The particle size distribution of the raw clay is illustrated in Fig. 2, with its d_{50} value of 23.55 μm.

2.2. Synthesis of AA-APEG polycarboxylate polymers

For this study, a series of AA-APEG PCEs possessing the same side chain length but different AA:APEG macromonomer ratios was synthesized according to the molar ratio of AA to APEG. As an example, the detailed synthesis procedure for AA-7APEG4.5 (molar ratio AA: APEG = 4.5:1, $n_{EO} = 7$) is as follows.

At first, 25 g (0.066 mol) of APEG macromonomer ($M_w = 350$ g/mol) and 45 mL of deionized (DI) water were placed in a five-neck flask, which was connected to a reflux condenser, a mechanical stirrer, a nitrogen inlet and two separated feeding inlets. The reaction vessel containing the macromonomer solution was heated to 80 °C and flushed with N_2 for 30 min. Next, two feeding solutions (Solution A and Solution B) were prepared. 21.334 g (0.30 mol) of acrylic acid and 0.225 g (0.002 mol) of 3-mercaptopropionic acid (chain transfer agent) were dissolved in 25 mL of DI water. This solution mixture was named as Solution A. Solution B was prepared by dissolving 5.629 g (0.025 mol) of ammonium persulfate in 30 mL of DI water. Solutions A and B were added dropwise into the reaction vessel using two peristaltic pumps via inlet A over 2.5 h and via inlet B over 3 h respectively. When the addition of solution B had finished, the mixture continued to sit for another hour. Finally, the reaction solution was cooled to ambient temperature and the pH was adjusted to 6.5–7 with 30 wt% sodium hydroxide solution. The solids content of the final solution was 35 wt%, and was used without further purification.

AA-7APEG2 as well as AA-7APEG15 were synthesized in a similar manner as described above, including the molar ratios of 3-mercaptopropionic acid (chain transfer agent) and ammonium persulfate (initiator). Only the molar ratio of AA:APEG macromonomer varied depending on the designed structure.

2.3. Characterization of AA-APEG polycarboxylate polymers

2.3.1. Size exclusion chromatography (SEC)

Molar mass (M_w and M_n), the polydispersity index (PDI) and macromonomer conversion of the synthesized ether-based PCEs were determined by size exclusion chromatography, also referred to as gel permeation chromatography (GPC). The measurements were performed with a Waters Alliance 2695 instrument (Waters, Eschborn, Germany) equipped with three Ultrahydrogel™ columns (120, 250, 500) and an Ultrahydrogel™ Guard column. The eluent was a 0.1 N $NaNO_3$ (pH = 12) with a flow rate of 1.0 mL/min. For the calculation of M_w and M_n, a *dn/dc* value of 0.135 mL/g (value for PEO) was utilized [31].

2.3.2. ^1H NMR spectroscopy for structural analysis

^{1}H NMR spectroscopy was used to analyze the structure of the synthesized PCEs. ^{1}H NMR (16 scans, 1 s relaxation delay) were measured on an AVANCE-III 400 MHz NMR spectrometer (Bruker BioSpin GmbH, Karlsruhe, Germany). Prior to measurement, APEG macromonomers and PCE samples were freeze dried overnight at −50 °C at 0.37 mbar. The powdered samples (~0.1 g) were dissolved in 0.4 mL D_2O.

2.3.3. Anionic charge amount measurement

The specific anionic charge amount of the synthesized PCEs was determined using a particle charge detector PCD 03 pH (Mütek Analytic, Herrsching, Germany). Here, 10 mL of the 0.2 g/L PCE solution were titrated with a 0.34 g/L aqueous solution of cationic poly-diallyl dimethyl ammonium chloride (polyDADMAC) until charge neutralization (zero potential) was reached. Then the anionic charge per gram of PCE polymer was derived from the consumption of the cationic polyelectrolyte polyDADMAC [32].

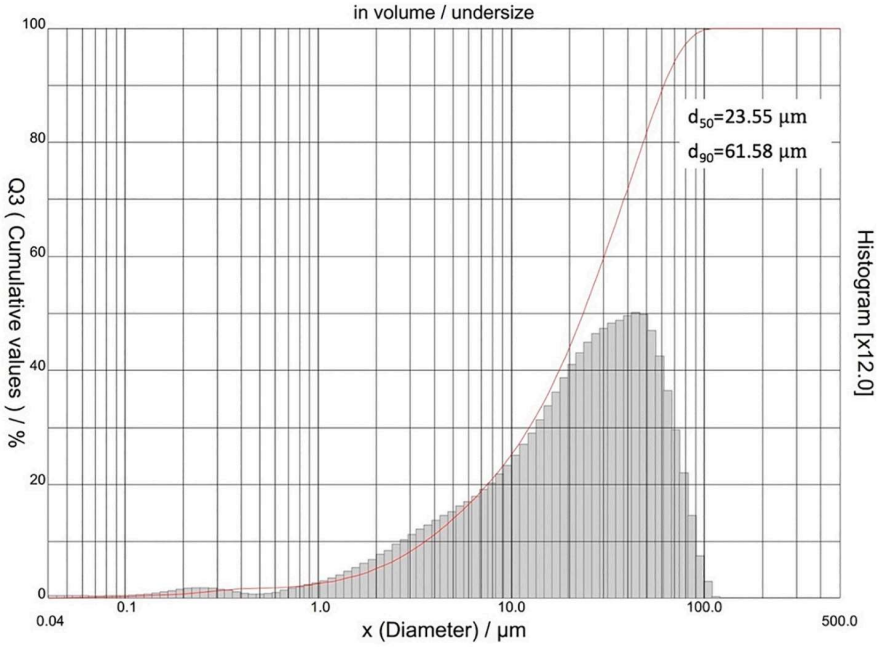

Fig. 2. The particle size distribution of the raw clay determined by laser granulometry.

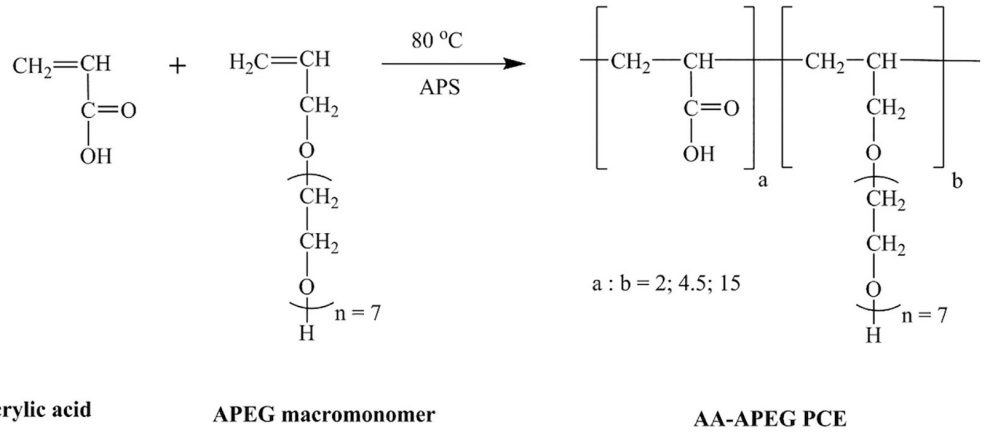

Fig. 3. Synthesis route for the preparation of the AA-APEG PCEs.

2.4. Dispersing performance in cement pastes with/without bentonite clay

For the evaluation of the dispersing effectiveness of the PCEs in cement, a 'mini slump' test was employed, which is described in DIN EN 1015 standard. At first, the water-to-cement (w/c) ratio of the paste without polymer to achieve a spread of 18 ± 0.5 cm was determined. At this w/c ratio, the dosage for each PCE sample to reach a spread flow of 26 ± 0.5 cm was determined.

The test was carried out as follows: The polymer was firstly mixed with DI water in a porcelain cup, whereby the water contained in the polymer solution was subtracted from the amount of mixing water. Then 300 g cement were added to the mixing water within 1 min, the mixture remained at rest for 1 min followed by 2 min of manual stirring. Thereafter, the cement paste was poured into a Vicat cone (height 40 mm, top diameter 70 mm, bottom diameter 80 mm) placed on a glass plate and the cone was quickly lifted vertically. Once the cement paste had stopped flowing, the spread flow was measured twice at two angles perpendicular to each other. Finally, the averaged spread flow of these two values was recorded as the spread flow value.

When the clay tolerance tests were performed, a similar procedure was followed and 1 wt% or 3 wt% of the cement was replaced by sodium bentonite.

2.5. PCE sorption on clay

The sorption of PCEs by sodium bentonite was determined in synthetic cement pore solution (SCPS, pH = 13.06) [13] and 0.1 M NaOH solution by means of total organic carbon (TOC) based on the depletion method. In principle, the amount of non-adsorbed portion of PCEs present in the solution in the equilibrium state was quantified by TOC. The sorbed portion can then be calculated by subtracting the quantity remaining in the supernatant from the amount added.

To further differentiate between physical surface adsorption and chemical intercalation, two fluid systems were chosen, namely a synthetic cement pore solution (SCPS) and 0.1 M sodium hydroxide (NaOH) solution to perform the sorption measurements.

In a typical experiment, 0.25 g of bentonite, 12 g of synthetic cement pore solution or 0.1 M NaOH solution (w/clay ratio = 48) and the different amounts of designated polymers were transferred into a 50 mL centrifuge tube and shaken in a wobbler (VWR International, Darmstadt, Germany) for 2 min at 2400 rpm, then centrifuged for 10 min at 8500 rpm. The resulting supernatant was then removed using a syringe, filtered through a 0.2 μm polyethersulfone syringe filter (Model FPS250020, Graphic Controls, New York, USA) and diluted 20–30 times with DI water. The TOC measurement was conducted on a High TOC II instrument (Elementar Analysensysteme, Hanau, Germany) at the temperature of 890 °C. The average of the sorbed amount at each concentration was calculated from at least two duplicate measurements.

2.6. XRD analysis

To verify whether the polycarboxylates had chemically incorporated in between the aluminosilicate layers of sodium bentonite, XRD analysis was performed. In a typical test, 0.5 g of clay and 24.25 g of 1.03 wt% PCE solution were added into a 50 mL centrifuge tube, shaken in a wobbler (VWR International, Darmstadt, Germany) for 2 min at 2400 rpm and then centrifuged for 10 min at 8500 rpm. The solid substance at the bottom was dried overnight at 50 °C in an oven, followed by being ground into powder as required for the measurement. The instrument for these XRD measurements was a D8 Advance, Bruker AXS instrument (Bruker, Karlsruhe/Germany) based on Bragg-Brentano geometry. Each sample to be scanned was placed on a mounted round plastic holder. The parameters for the scanning procedure were set as follows: step size of 0.15 s/step, scan spin at a revolution time of 4 s, 0.3° of aperture slit, scan ranging from 0.6° to 20° 2θ, using CuKα, λ = 1.5418 Å.

2.7. Zeta potential measurement

Measurements of initial zeta potential were performed on a "DT 1200 Electroacoustic Spectrometer" manufactured by Dispersion Technology, Inc., Bedford Hills, NY, USA. The solution-to-clay ratio was set to 48:1, same as in the TOC tests. A clay slurry containing 6 of clay and 288 mL of 0.1 M NaOH (pH = 13) or 288 mL of SCPS (pH = 13) was prepared. The mixture was manually stirred for 4 min and then transferred into the container of the zeta potential instrument with stirring rate of 200 rpm.

2.8. Adsorbed layer thickness of polycarboxylate polymers

To investigate the effect of Ca^{2+} cations on the sorption of polycarboxylate polymers on negatively charged substrates, i.e. clay, the adsorbed layer thickness (ALT) of a PCE polymer was determined in Ca^{2+} and Ca^{2+} free medium. 1% wt. PCE polymer (AA-7APEG 4.5) was dissolved in 0.1 M aqueous NaOH and mixed with their charge equivalent amounts of Ca^{2+} added as $CaCl_2{\cdot}2H_2O$ [33]. In a separate solution, 1 wt% PCE polymer (AA-7APEG 4.5) was dissolved in 0.1 M aqueous NaOH without any Ca^{2+} addition. Both stock solutions were then diluted to prepare a series of PCE concentrations from 0.1–1.5 g/L in a volume of 50 mL. Thereafter, 50 μL of polystyrene nanoparticle were added into the PCE solutions with various concentrations. The polystyrene nanoparticle was prepared according to the literature [33]. The opaque dispersions were subjected to ultrasonication for 15 min and remained at rest for 15 min before the diameter determination with dynamic light

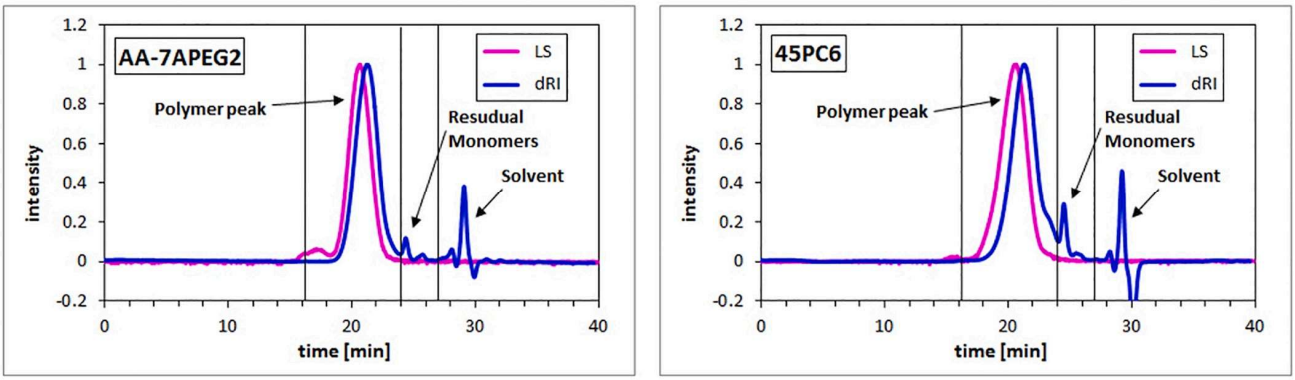

Fig. 4. Size exclusion chromatograms of PCE samples AA-7APEG2 and 45PC6 (MPEG type PCE).

Table 4
Characteristic molecular parameters of the synthesized PCE polymers.

Polymer sample	M_w [Da]	M_n [Da]	PDI	Macromonomer conversion
AA-7APEG2	6700	4000	1.7	91%
AA-7APEG4.5	12,000	6800	1.7	93%
AA-7APEG15	18,000	9900	1.8	97%
45PC6	16,920	8295	2.0	93%

scattering on the ZetaSizer Nano ZS instrument. The corresponding diameters of polymer free polystyrene nanoparticles were measured before each sample measurement. The adsorbed layer thickness of PCE was calculated according to the following equation:

$$ALT = (D_1 - D_0)/2,$$

where D_1 was defined as the particle diameter with adsorbed PCE, and D_0 was noted for the pristine particle diameter.

3. Results and discussion

3.1. Molecular properties of the synthesized AA-APEG PCE polymers and the reference samples

A series of AA-APEG copolymers exhibiting different anionicity was synthesized via aqueous free radical copolymerization of acrylic acid and α-allyl-ω-hydroxy poly (ethylene glycol) ether (APEG, $M_w = 350$ g/mol). The synthetic route is displayed in Fig. 3.

The molecular characteristics of the resulting APEG PCE polymers were determined via Size Exclusion Chromatography (SEC). In Fig. 4, as examples, the SEC spectra of one APEG PCE polymer (AA-7APEG2) and the comparative PCE sample 45PC6 are displayed.

The molar masses (M_n, M_w), polydispersity index (PDI) and conversion rate of the macromonomer are summarized in Table 4. The three synthesized anionic AA-APEG PCE polymers differ with respect to their AA:APEG ratio, thus possess different anionic charge amounts.

According to the SEC data in Table 4, all synthesized PCE polymers exhibited properties that are characteristic for high-quality PCE polymers, namely relatively low PDIs (≤2), and high macromonomer conversions (>90%). Additionally, the molecular weights (M_w) of all synthesized PCE polymers lie in the range up to 20,000 Da which is comparable to the reference copolymer 45PC6. The molecular weight of PCEs is understood to significantly impact their dispersing effectiveness [34,35].

In order to further characterize the structure of the synthesized APEG polymers, ^{1}H NMR measurements were performed, the spectra are illustrated in Fig. 5 and the calculated parameters are summarized in Table 5.

As shown in the ^{1}H NMR spectrum of APEG macromonomer, the δ (chemical shift) for group C (—CH_2O—) and group D [—(CH_2CH_2O)—] are at 4.0 ppm and 3.4–3.8 ppm, respectively. Here, we assume the integral intensity of D is 1, the intensity of C is calculated as 0.07. Hence, the number of EO units approximately equals to 7. Next, to determine the conversion rate of APEG macromonomer for the three synthesized APEG PCE polymers, the integral intensity of D is set to 1 since [—($CH_2CH_2O)_7$—] remains unchanged during the polymerization process. The integral intensity of C varies before and after the copolymerization process. The corresponding conversion ratio of APEG macromonomer for each APEG PCE polymer was calculated according to the formula: $\frac{C(\text{APEG MM}) - C(\text{PCE copolymer})}{C(\text{APEG MM})}$.

The calculated values for all three APEG PCE polymers are listed in Table 5.

Furthermore, the conversion rate of AA could also be obtained from ^{1}H NMR spectroscopy. Similarly, the integral intensity of D is set to 1. Group a (CH_2═) in AA is selected as the trigger group to calculate the conversion. In the AA-APEG PCE copolymer, the residual AA is detected since a signal at 6.0 ppm appears which can be assigned to CH_2═ group (a). And the reacted group a′ (CH_2—) in the PCE copolymer shows a signal at 1.5 ppm. However, group B (—CH═) in unreacted APEG macromonomer also appears at 6.0 ppm. The group A′ (—CH_2—) from the reacted APEG macromonomer shows a signal at 1.5 ppm. In combination with the conversion rate of APEG macromonomer, the conversion rate of AA for the AA-7APEG PCE polymers can be calculated accordingly (see Table 5).

Based on the conversion rates of AA as well as APEG macromonomer, the actual molar ratios of AA:APEG macromonomer for three AA-APEG PCE copolymers were calculated accordingly. As can be seen in Fig. 5, the actual composition of the synthesized PCE polymers are very close to the designed polymer structure.

3.2. Anionic charge characteristics of synthesized PCE polymers

Anionic charge amount measurements were conducted in 0.01 M NaOH (pH = 12) [32]. The ability of a PCE to adsorb onto the surfaces of cement hydrates has a direct influence on their dispersing effectiveness in concrete. In this study, a correlation between the charge characteristics of the PCE polymer and their sorption behavior on sodium bentonite was evaluated.

As is presented in Fig. 6, the charge amount of the synthesized APEG PCEs increases with increasing AA: APEG molar ratio stemming from the higher number of carboxylic groups in the PCE polymer.

3.3. Dispersing ability of PCEs in neat cement paste (w/o clay)

The dispersing power of the newly synthesized AA-APEG copolymers was evaluated by a 'mini slump' test according to DIN EN 1015. The

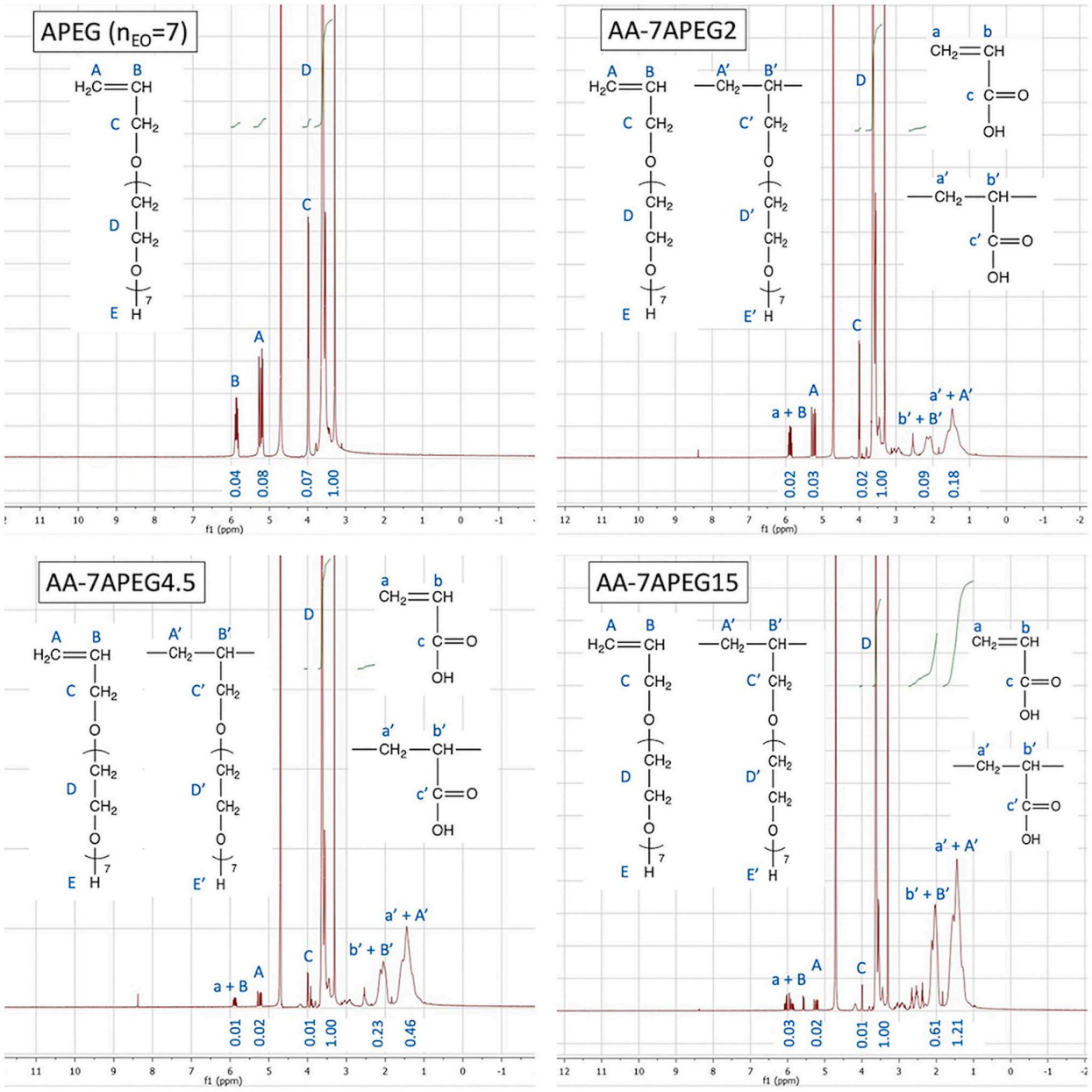

Fig. 5. The ^{1}H NMR spectra of APEG macromonomer and the synthesized AA-APEG PCE copolymers.

Table 5
Structural analysis of the AA-APEG PCE polymers and the monomer conversion rates determined via ^{1}H NMR spectroscopy.

PCE samples	Feeding molar ratio	Actual molar ratio	EO units	APEG conversion [%]	AA conversion [%]
AA-7APEG2	2:1	2.6:1	7	71	93
AA-7APEG4.5	4.5:1	4.6:1	7	86	99
AA-7APEG15	15:1	17:1	7	86	98

reference dispersants 45PC6 and BNS were chosen as the comparative samples for the fact that 45PC6 represents a highly effective PCE polymer which is commonly used in cement and concrete whereas BNS is a widely used polycondensate which is far more tolerant with clay contaminants.

In the following tests, the dosages required for various cement dispersants to achieve a cement paste spread of 26 ± 0.5 cm were determined (Fig. 7). Among them, polymer 45PC6 required the lowest dosage (appr. 0.07% bwoc (by weight of cement)) to obtain the required target, while the dosage increased to 0.26% bwoc in the case of BNS. Compared with these two reference samples, the AA-APEG series required higher dosages than that for 45PC6. The required dosages for AA-7APEG2 and AA-7APEG4.5 were 0.15% bwoc and 0.12% bwoc, respectively. 45PC6 polymer was expected to outperform the short side

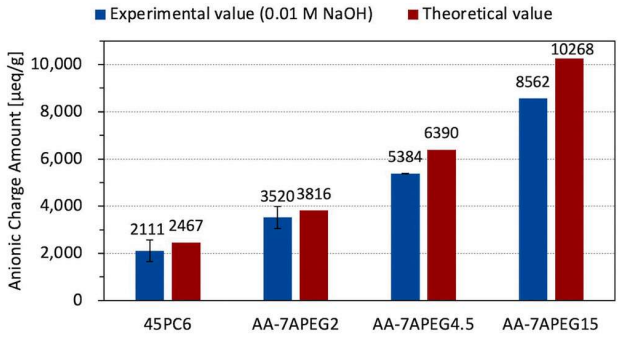

Fig. 6. Anionic charge amounts of the synthesized PCE polymers.

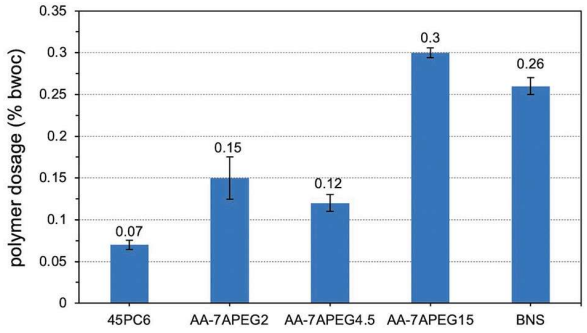

Fig. 7. Dosages of the synthesized AA-APEG copolymers, 45PC6 and BNS samples required to achieve a cement paste spread of 26 ± 0.5 cm (w/c = 0.48).

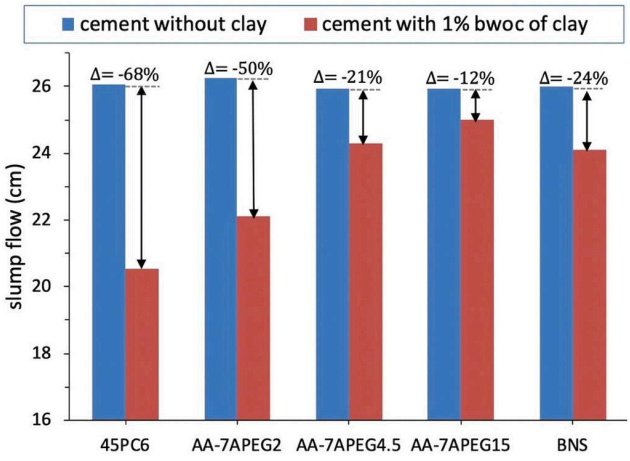

Fig. 8. Spread flow of cement pastes (w/c = 0.48) containing different superplasticizers, measured in the absence and presence of 1% bwoc of clay.

chain AA-APEG PCE polymers because of the relatively long pendant chains (n_{EO} = 45 for 45PC6 vs. n_{EO} = 7 for AA-APEG series). The highest dosage was recorded for the AA-7APEG15 polymer which required 0.3% bwoc to achieve the required spread flow. This can be ascribed to a very low side chain density producing a relatively weak steric hindrance effect on cement, the primary dispersion mechanism associated with polycarboxylates [4].

3.4. Dispersing effectiveness of superplasticizers in the presence of 1 or 3 wt% bentonite

For the cement pastes, the dispersing effectiveness of

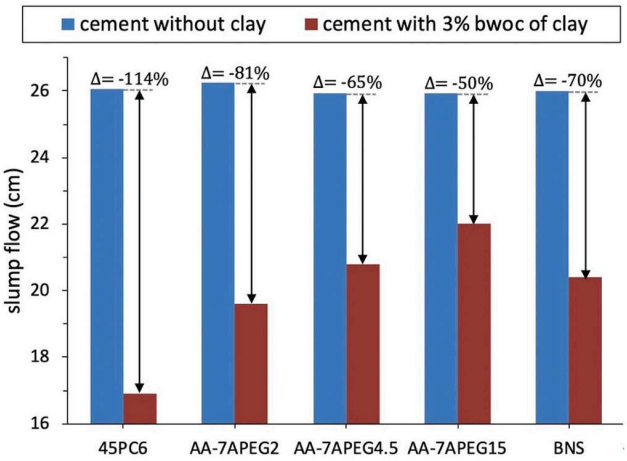

Fig. 9. Spread flow of cement pastes (w/c = 0.48) containing different superplasticizers, measured in the absence and presence of 3% bwoc of clay.

polycarboxylates and BNS were evaluated with dosages determined from the 'mini slump' tests in neat cement pastes. As expected, each cement dispersing polymer exhibits a different degree of tolerance to bentonite which is presented in Figs. 8 and 9.

Polymer 45PC6 among all tested samples was affected the strongest by sodium bentonite, in which case the slump flow dropped from 26 cm to 20.6 cm (68% decrease in its dispersing efficiency). Furthermore, in the presence of 3 wt% of bentonite, the spread flow of cement paste prepared with 45PC6 decreased to 16.8 cm, a 114% loss in its effectiveness. As expected, in comparison to 45PC6, BNS was much more resistant to the bentonite, whose spread flow only decreased to 20.6 cm even in the presence of 3 wt% of bentonite.

The aforementioned difference of these two polymers in the dispersing power in the presence of bentonite could be ascribed to their different interaction modes with bentonite. As for the PCE sample 45PC6, its polyethylene glycol side chains can easily incorporate into the interlayer structure of bentonite, hence less PCE polymer is available to provide adequate dispersing force between hydrating cement grains. Whereas, the dispersing power of BNS is hindered only via adsorption onto the surface of bentonite, and is not negatively impacted by intercalation.

All AA-APEG PCE samples exhibited better clay resistance than the MPEG PCE sample 45PC6, although they all contain polyethylene glycol side chains. Especially the more anionic polymers AA-7APEG4.5 and AA-7APEG15 exhibited excellent clay tolerance, even better than that of BNS. In the presence of 1 wt% of sodium bentonite, the efficiency loss ratio for AA-7APEG4.5 and AA-7APEG15 is 21% and 12% respectively, in comparison to that of BNS which had a 24% loss. A similar trend can be observed in the presence of 3 wt% of sodium bentonite. Furthermore, a clear correlation between the anionic character and clay tolerance is observed. Apparently, AA-APEG PCEs possessing higher anionic charge exhibit enhanced clay tolerance.

Furthermore, to detect whether the absolute quantity of PCE itself would exert the influence on the fluidity of cement in the presence of clay, the normalized PCE dosage of 0.15% bwoc was selected to probe its dispersing capacity as well as clay tolerance. As shown in Fig. 10, different superplasticizers exhibited various dispersing capacity in cement pastes in the presence of 1% and 3% bwoc of clay. The cement pastes in the presence of 1% bwoc clay exhibited a spread flow of 16 cm without any polymer. When the same dosage of polymers were applied, 45PC6 reached a spread flow as high as 28 cm. However, it was worth noting that its dispersing power declined the most (−73%) among all the polymers, when another 2% bwoc of clay were added to the system. In

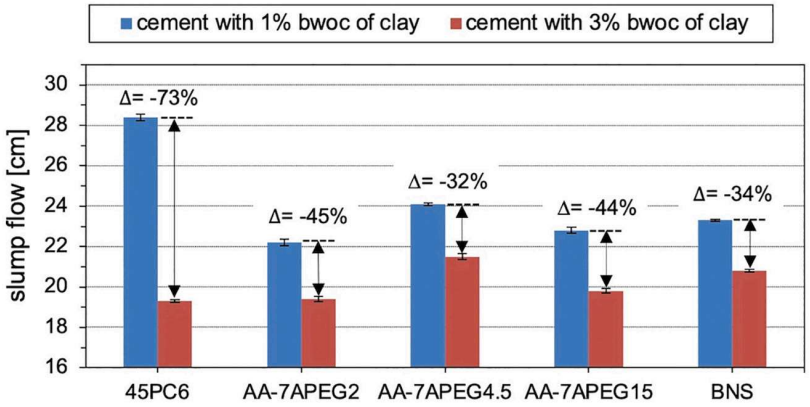

Fig. 10. Spread flow of cement pastes (w/c = 0.48) at the same dosage (0.15% bwoc) of various polymer samples, measured in the presence of 1% and 3% bwoc of clay.

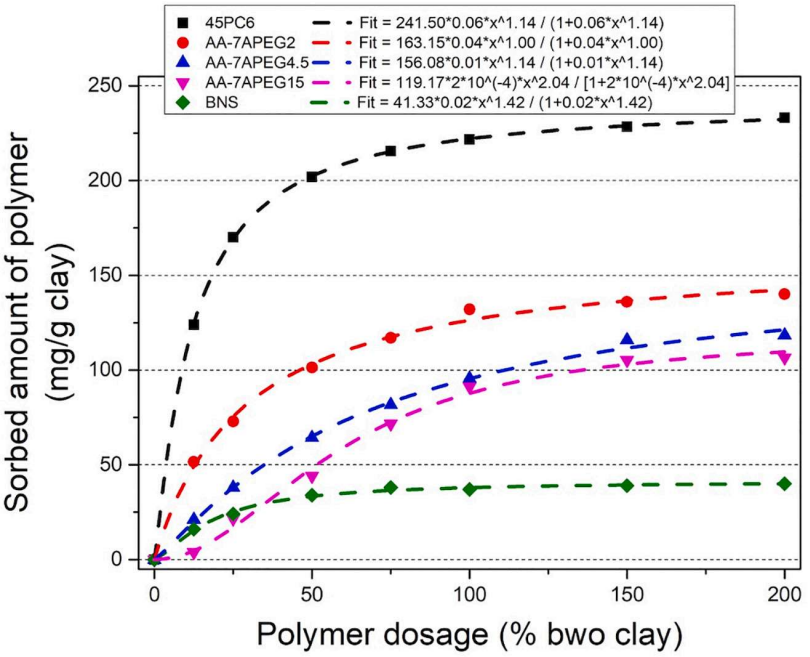

Fig. 11. Sorption isotherms for various polymer samples with sodium bentonite dispersed in synthetic cement pore solution (pH = 13, solution/clay ratio = 48). The Langmuir isotherm here is plotted with the specified solid-liquid ratio on the x-axis for the explicit interpretation of sorption behaviors of polymer on clay. The Langmuir plots normalized with solution concentration on the x-axis and corresponding equations are presented in the supplementary material.

comparison, the three synthesized AA-APEG copolymers showed better resistance against the further addition of clay than that of 45PC6. Furthermore, among all AA-APEG PCE polymers, AA-7APEG4.5 showed the lowest decrease in the dispersing power (−32%) which is even better than that of the BNS sample (−34%). Although AA-7APEG15 possessed lower side chain density than AA-7APEG4.5, but it exhibited higher loss in spread flow (−44%) than the latter polymer at the same dosage. Based on the results here, AA-7APEG4.5 exhibited better clay tolerance than AA-7APEG15 at the same dosed amount.

To summarize, AA-APEG PCEs with shorter side chains exhibit higher tolerance to sodium bentonite as compared to an MPEG PCE with longer side chains. Furthermore, among these AA-APEG PCEs with short PEO side chains, PCEs with lower side chain density generally possessed improved clay resistance. However, when the clay robustness of AA-APEG PCE polymers were compared at the same dosed amount, PCEs with medium side chain density exhibited the best performance.

3.5. Sorption on clay

To investigate the interaction between the individual superplasticizers and bentonite quantitatively, Langmuir sorption isotherms in synthetic cement pore solution were conducted as shown in Fig. 11.

According to the sorption isotherms, sodium bentonite exhibited an extremely high affinity for the MPEG PCE 45PC6, which was adsorbed at an extremely high amount ~241.5 mg/g at equilibrium. The high affinity for PCE 45PC6 can be attributed to two effects: (1) chemisorption of the relatively long PEO side chain into the layered structure of bentonite, and (2) surface adsorption onto the bentonite. In contrast, BNS exhibits the lowest sorbed amount at equilibrium which lies at ~41 mg/g of clay. As for the AA-APEG PCE series, their saturated sorbed amount varies between 110 and 170 mg/g clay which is nearly half of the sorbed value as compared to PCE sample 45PC6. This result indicates a weak interaction between the AA-APEG PCEs and sodium bentonite.

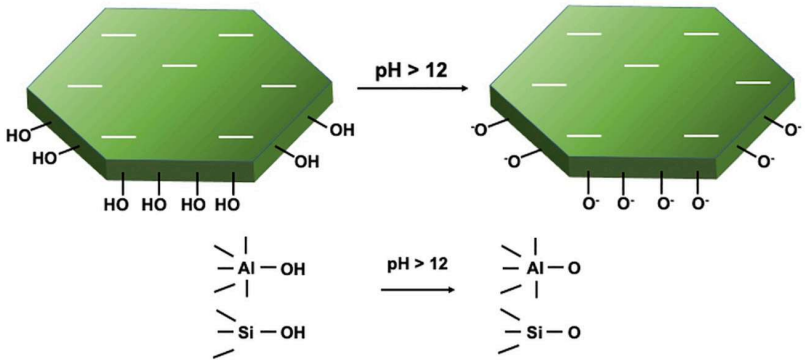

Fig. 12. Schematic illustration of charge distribution of a montmorillonite particle. The basal planes carry permanent negative charge, whereas edge faces exhibit pH-dependent behavior. Reproduced with permission from [16].

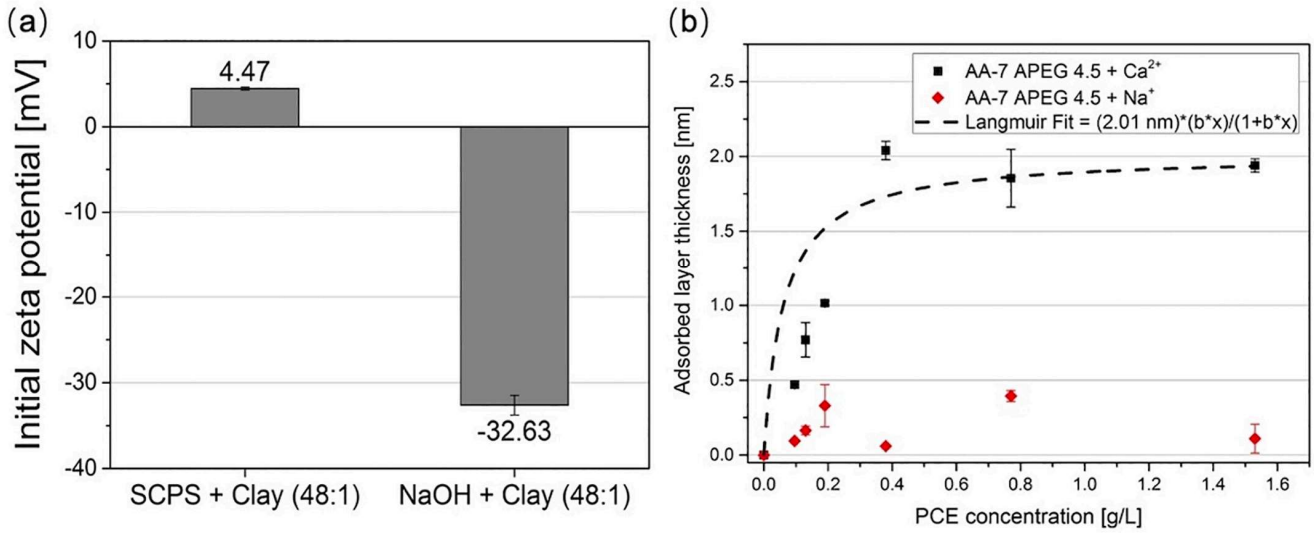

Fig. 13. (a) Initial Zeta potential of bentonite sample dispersed in SCPS and NaOH solution; (b) Adsorbed layer thickness of AA-7APEG4.5 determined in 0.1 M NaOH solution (pH = 13) with or without Ca^{2+} [33].

Furthermore, the lower side chain density of the AA-APEG PCEs leads to a lower amount sorbed on bentonite which is in line with the clay tolerance tests. There, we found that AA-APEG PCEs possessing lower side chain density generally exhibited increased clay tolerance (Figs. 8 and 9).

In above we have intensely discussed the interaction between the various superplasticizer polymers and the bentonite sample, however for the individual mineralogical components including montmorillonite, clinoptilolite-Ca, illite etc. they would exhibit different mode of interaction with the PCE polymers. For example, montmorillonite represents a typical expandable 2:1 clay mineral, and interacts with PCEs in two different manners, namely, surface adsorption and chemisorption. In contrast, illite which belongs to a typical non-swelling 2:1 dioctahedral clay, can only interact with PCE polymers via surface adsorption [11].

3.6. Chemisorption of PCE polymers on bentonite

In order to quantify the portion of PCE being intercalated into the layered structure of bentonite, the amount adsorbed from a 0.1 M NaOH solution instead of in synthetic cement pore solution was measured.

The unique charge heterogeneity of bentonite platelets has been well known for decades [36]. The basal surfaces of the clay minerals (i.e. montmorillonite, kaolinite, mica) often carry permanent negative charges resulting from the isomorphic substitution within the particles, whereas edge surfaces show pH-dependent colloidal behavior [36]. Under high pH conditions, the deprotonation of the terminal hydroxyl groups at the amphoteric clay edge surfaces leads to a negative charge [37,38]. The charge distribution of montmorillonite platelets (the main component of bentonite) is illustrated in Fig. 12.

The generally accepted viewpoint is that Ca^{2+} plays a critical role for anionic polymers to be adsorbed onto the negatively charged cement or clay particles [16,39]. In 0.1 M NaOH solution, without Ca^{2+} cations, anionic PCE polymers cannot adsorb onto the surfaces of bentonite platelets (basal and edge surfaces) which are negatively charged. Hence, the sorbed amounts of PCEs found in the tests here are solely attributed to chemisorption into the interlayer gallery of sodium bentonite [40].

To prove the validity of this methodology, surface potential of clay sample as well as adsorbed layer thickness of PCE polymers have been determined, and the results are shown in Fig. 13. According to Fig. 13 (a) the surface potential of bentonite turned out to be 4.47 mV in SCPS while −32.63 mV in NaOH solution. Therefore, anionic PCE polymers can only adsorb onto the surface of bentonite which are positively charged in SCPS solution, not in NaOH medium.

The adsorbed layer thickness of AA-7APEG4.5 (for example) on polystyrene nanoparticles – a model substrate – was determined in Ca^{2+} and Ca^{2+} free medium. According to the results in Fig. 13 (b), in the

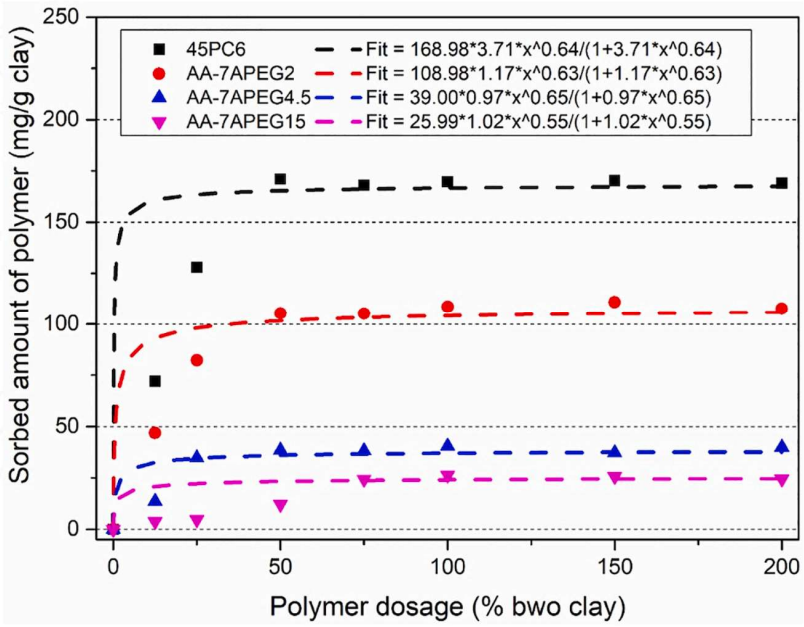

Fig. 14. Sorption isotherms for various superplasticizer samples on bentonite dispersed in 0.1 M sodium hydroxide solution (pH = 13, w/clay ratio = 48). The proper Langmuir plots of adsorption isotherms with solution concentration on the x-axis are provided in the supplementary material.

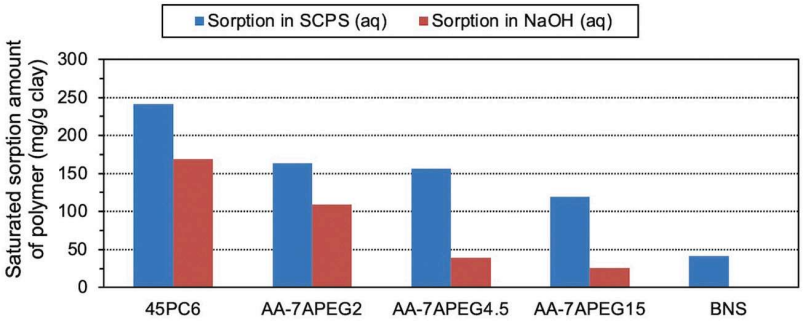

Fig. 15. Saturated sorbed amount of various superplasticizers at equilibrium in SCPS or 0.1 M NaOH as obtained from Figs. 11 and 14.

presence of Ca^{2+}, AA-7APEG4.5 polymer reached the adsorbed layer thickness of ~2 nm indicating the successful adsorption on the surface of the model substrate. Whereas, in the absence of Ca^{2+}, basically no adsorbed layer thickness value can be obtained which confirms that AA-7APEG4.5 polymer cannot adsorb on the surface of model substrate.

To summarize, as proven by zeta potential and adsorbed layer thickness measurements, in 0.1 M NaOH solution, without Ca^{2+} cations, anionic PCE polymers cannot adsorb onto the surfaces of bentonite platelets, therefore, the sorbed amounts of PCEs determined here are solely attributed to chemisorption into the interlayer gallery of sodium bentonite.

As depicted in Fig. 14, in 0.1 M NaOH solution without Ca^{2+}, the sorbed amounts of all PCE polymers are lower as compared to those in synthetic cement pore solution (Fig. 11). Again, PCE sample 45PC6 exhibits the highest sorbed amount (~170 mg/g at equilibrium), followed by AA-APEG2, AA-APEG4.5 and AA-APEG15. All AA-APEG PCE samples exhibit relatively low saturated sorbed amounts (≤110 mg/g), especially for AA-APEG15 only ~25 mg/g. This experiment clearly reveals that intercalation of the PCEs into bentonite is dependent on the side chain density of the polymer. PCE polymers possessing lower side chain density intercalate less than those with higher side chain density.

The difference between PCE polymers becomes even more evident when plotting the saturated sorbed amount in synthetic cement pore solution, in 0.1 M NaOH solution, and the intercalated portion of polymer, as is shown in Fig. 15. It was found that polymers from the AA-APEG PCE series exhibit lower sorbed amounts in both fluid systems (SCPS and 0.1 M NaOH) in comparison to polymer 45PC6 which indicates weaker interaction between the AA-APEG PCEs and bentonite. This finding corresponds to their better clay robustness as evidenced in the 'mini slump' tests (Figs. 8 and 9).

Next, the intercalated portion of various PCE polymers was calculated and compared. The saturated sorbed amount in SCPS results from the sum of surface adsorbed and intercalated polymer, whereas the saturated sorbed amount in 0.1 M NaOH only accounts for the part of intercalated polymer. The intercalated portion was calculated by dividing the intercalated amount of the polymer by the total sorbed amount. The intercalated portion shown in Fig. 15 demonstrate that AA-7APEG15 possesses the lowest proportion of intercalated polymer which indicates the lowest affinity to the interlayer of bentonite. Thus PCE polymer predominantly sorbs onto the surface of bentonite. PCE sample AA-7APEG4.5 behaves similar to AA-7APEG15, the amount of 7APEG4.5 sorbed by bentonite decreases from 156 mg/g clay (in SCPS) to ~39 mg/g clay (in 0.1 M NaOH), suggesting that only 25% of this PCE polymer is consumed by intercalation while the rest is taken up via electrostatically induced surface adsorption. The intercalated portion for polymer 45PC6 is 70%, which explains the poor dispersing

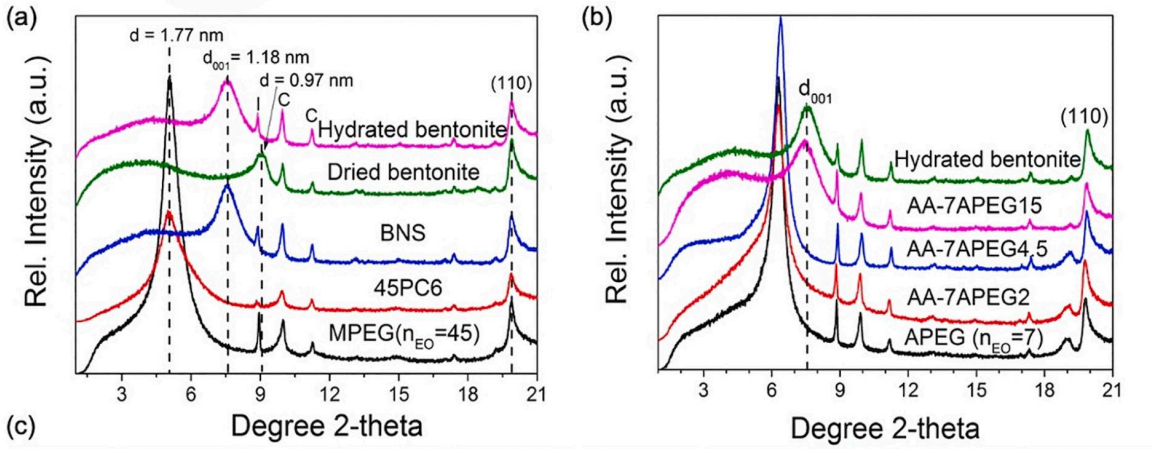

(c)

Sample	MPEG (n_{EO}=45)	45PC6	APEG (n_{EO}=7)	7APEG2	7APEG4.5	7APEG15	BNS	Hydrated bentonite	Dried bentonite
d-value /nm	1.77	1.77	1.42	1.41	1.39	1.19	1.18	1.18	0.97

Fig. 16. XRD patterns of bentonite dispersed in synthetic cement pore solution containing 50% by weight of (bwo) clay of AA-APEG copolymers, α-allyl-ω-hydroxy poly (ethylene glycol) ether macromonomer (n_{EO} = 7), ω-methoxy poly (ethylene oxide) methacrylate ester macromonomer (n_{EO} = 45), conventional MEPG PCE (45PC6) as well as BNS, after drying at 50 °C (solution/clay ratio = 48) (C: clinoptilolite-Ca; I: illite).

performance in the presence of bentonite. Surprisingly, also sample AA-7APEG2 exhibits a very high intercalated portion (67%), but still provides better clay robustness than polymer 45PC6 which can be attributed to its overall lower sorbed amount on bentonite, thus more PCE samples remain available to disperse cement particles.

3.7. XRD study of PCE/clay interaction

To further investigate the mode of interaction between AA-APEG PCEs and bentonite, XRD analysis was performed. From the interlayer spacing as evidenced in the XRD results (Fig. 16), the extent of intercalation of the AA-APEG PCEs can be deduced.

In the absence of PCE, the pure sodium bentonite shows a *d*-spacing of 1.18 nm, while it decreased to the 0.97 nm when dried at 50 °C for 24 h. Based on the PCE intercalation model in bentonite clay proposed by P. Borralleras, the reported thickness of H_2O monolayer is 2.81 Å [14]. The *d*-spacing was detected decreasing from 1.18 nm to 0.97 nm after drying here, it can be calculated that the hydrated bentonite incorporated H_2O monolayer in the gallery structure. When ω-methoxy polyethylene glycol methacrylate (MPEG, M_w = 2000 Da) and 45PC6 are present (Fig. 16 (a)), a shift in the *d*-spacing from 1.18 nm to 1.77 nm is detected. These results are in accord with recent studies indicating that the PEO side chains of PCEs exhibit a similar tendency as polyglycols to intercalate in between the aluminosilicate layers [16,41,42]. For BNS (Fig. 16 (a)), no shift in the *d*-spacing is found indicating the absence of intercalation. Moreover, XRD patterns of bentonite dispersed in synthetic cement pore solution containing α-allyl-ω-hydroxy poly (ethylene glycol) ether macromonomer (APEG, n_{EO} = 7) and the synthesized AA-APEG PCEs are compared in Fig. 16 (b), and the observed *d* values are listed in Fig. 16 (c). When α-allyl-ω-hydroxy poly (ethylene glycol) ether macromonomer is added to bentonite, the basal spacing expands from 1.18 nm to 1.42 nm. This interlayer spacing at 1.42 nm differs from that of methoxy polyethylene glycol methacrylate macromonomer (MPEG, n_{EO} = 45) (1.77 nm), and this difference between the two macromonomers can be attributed to their difference in the number of EO units presented, which is consistent with previous reports [18]. Furthermore, the basal spacings of bentonite containing the AA-APEG PCEs exhibit very different values for *d*-spacing. For example, 7APEG2 with the

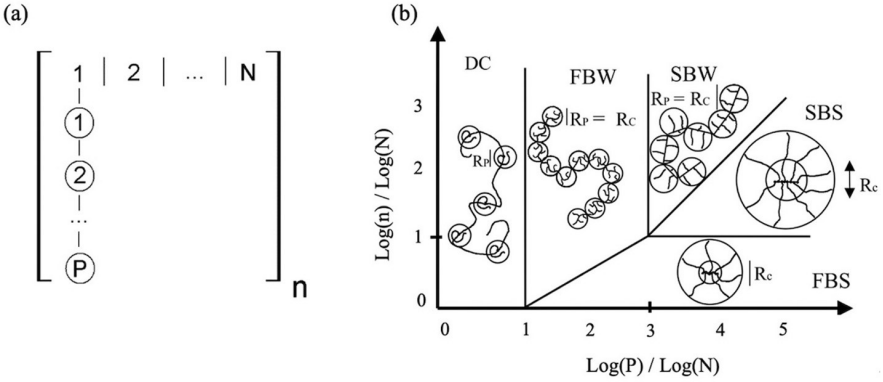

Fig. 17. Schematic conformation diagram for the comb polymers [43]. (a) The polymer backbone is defined as the assemblage of **n** repeating structure units with Mw, each containing **N** backbone monomers and one side chain of **P** units of EO; (b) Different conformation types are then defined in five regimes: decorated chain (DC), flexible backbone worm (FBW), stretched backbone worm (SBW), stretched backbone star (SBS), and flexible backbone star (FBS).

Table 6
Modeling parameters of PCEs and the resulting quantities derived from a classic Flory free energy approach.

PCE samples	Configuration	P	N	n	R/nm	R_P/nm
AA-7APEG2	FBW	7	3	13	3.16	1.26
AA-7APEG4.5	FBW	7	5.5	17	4.19	1.18
AA-7APEG15	DC	7	16	12	5.86	1.16

lowest anionic charge exhibits a similar *d*-spacing value to that of the APEG macromonomer. 7APEG4.5 and 7APEG15 exhibit a lower *d*-spacing value, namely 1.39 nm and 1.19 nm respectively, which again confirms that PCE polymers possessing lower side chain density intercalate less than those with high side chain density.

Here, a parameterized model is introduced to quantitatively determine the molecular conformation, from which a clear correlation between the *d*-value and the molecular size is provided.

As depicted in Fig. 17, the conformation type of APEG PCEs has been defined, AA-7APEG2 and AA-7APEG4.5 belong to the flexible backbone worm while the "best polymer" AA-7APEG15 belongs to the decorated chain conformation. A few parameters for further calculation are defined as follows: R is the radius of gyration of overall conformation of comb molecules, R_{nN} and R_p stand for the radius of gyration of main chain and side chain, respectively [44]. The relevant parameters a_N and a_P indicate the size of monomer anchored in the backbone and side chains. For the polymers used in this study, a_P is 0,36 nm and a_N is 0.25 nm [43]. For DC regime, $R = R_{nN} = a_N(nN)^{3/5}$, $R_p = a_P P^{3/5}$, while in the domain of FBW, $R = R_{nN} = a_N n^{3/5} P^{2/5} N^{1/5}$, $R_p = a_P P^{7/10} N^{-1/10}$ [44].

The calculated values for each PCE are presented in Table 6. It can be seen clearly that with decrease of the side chain density, R increases gradually from AA-7APEG2 (3.16 nm) to AA-7APEG15 (5.86 nm), while R_p decreases accordingly, whereby AA-7APEG15 shows the minimum value of 1.16 nm. We could therefore conclude that AA-7APEG15 with the highest R would encounters the strongest steric effect, thus possesses the least intercalation tendency. Moreover, the lowest R_p from AA-7APEG15 indicates that the polymer possesses the smallest size of side chains, which corresponds to its lowest *d*-value (see Fig. 16).

To further establish a correlation between the intercalated amount of polyethylene glycol within the layers of the sodium bentonite, the clay was mixed with different dosages of α-allyl-ω-hydroxy poly (ethylene glycol) ether macromonomer ($n_{EO} = 7$), from 5% to 50% bwo clay. From the dry substances, XRD diagrams were taken.

As is shown in Fig. 18, the peak indicating the layer distance shifts towards lower 2θ degrees with higher amounts of polyethylene glycol used, indicating that increased interlayer *d* values signify a higher intercalation degree. For example, when bentonite is mixed with 50% bwo clay of the APEG macromonomer, a *d*-value of 1.42 nm is observed, whereas when only 5% bwo clay of APEG macromonomer are present, a *d*-spacing of 1.28 nm is recorded. Therefore, we can now demonstrate that there is a clear correlation between the intercalated amount of polyethylene glycol (intercalation degree) and the characteristic adsorption by the sodium bentonite.

4. Conclusion

In this study, a series of allyl ether-based PCEs exhibiting short side PEO chains ($n_{EO} = 7$) was synthesized via free radical copolymerization. The resulting APEG PCEs possessed comparable M_w and high macromonomer conversion was achieved. Among these AA-APEG PCEs with short PEO side chains, PCEs with lower side chain density generally possessed improved clay resistance. However, when the clay robustness of AA-APEG PCE polymers were compared at the same dosed amount, PCEs with medium side chain density exhibited the best performance. Furthermore, through a series of performance tests it was found that these AA-APEG PCE samples possessing short side chains exhibited superior clay resistance compared to a conventional PCE polymer such as 45PC6 with long PEO pendant chains. Although the optimum PCE for clay resistance (AA-7APEG4.5) requires 1.7× greater dose versus the standard 45PC6 PCE without clay, it actually offers a more economically advantaged means to use PCEs when clay-bearing aggregates are used in concrete production versus more standard PCEs with typical 2000 Mw PEO side chains.

According to total organic carbon analysis of the supernatant, the sodium bentonite exhibited an extremely high affinity for reference polymer 45PC6 which possesses long PEO side chains. Whereas, in the case of the AA-APEG PCE series, their saturated sorbed amounts were almost half as compared to that of 45PC6, indicating much less affinity of the AA-APEG PCE polymers to clay. In all prior literature, the sorbed

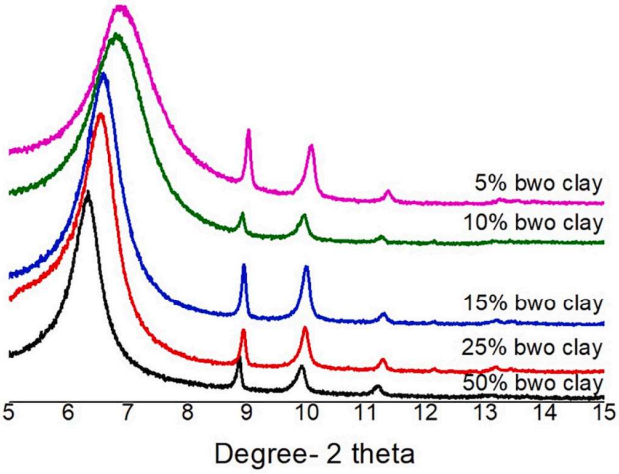

Dosage of APEG (n_{EO}=7) (% bwo clay)	50%	25%	15%	10%	5%
d-value (nm)	1.42	1.35	1.34	1.30	1.28

Fig. 18. Bentonite dispersed in synthetic cement pore solution holding different dosages of α-allyl-ω-hydroxy poly (ethylene glycol) ether macromonomer ($n_{EO} = 7$) varying from 5% to 50% bwo clay.

amounts of PCE polymers comprising of both surface adsorbed and intercalated amount on sodium bentonite were reported. In this study, for the first time, the portion of PCE being intercalated into the layered structure of bentonite was quantified. Sorption measurements of the AA-APEG PCEs in 0.1 M NaOH solution revealed that from the AA-APEG PCEs featuring lower side chain density only a small portion intercalated into the bentonite interlayer space. The validity of this methodology was proven by zeta potential and adsorbed layer thickness measurements, in 0.1 M NaOH solution, without Ca cations. Anionic PCE polymers cannot adsorb onto the surfaces of bentonite platelets, therefore, the sorbed amounts of PCEs determined here are solely attributed to chemisorption into the interlayer gallery of sodium bentonite. Furthermore, an XRD analysis of clay/PCE samples confirmed again that AA-APEG PCEs possessing short side chains intercalated less than the conventional PCE sample with long PEO side chains. Among AA-APEG PCEs, it was also theoretically demonstrated that the PCEs with lower side chain density would exhibit lower side chain size (R_P) and thus lower d-values are recorded in the XRD analysis. Due to the weak interaction between the AA-APEG PCEs and bentonite, more PCE polymers are available to disperse cement and achieve high fluidity.

CRediT authorship contribution statement

Lei Lei: Conceptualization, Resources, Investigation, Supervision, Writing - Review & Editing.

Yue Zhang: Methodology, Data Curation, Software, Writing - Original draft preparation.

Ran Li: Methodology, Formal analysis, Visualization.

Declaration of competing interest

The authors declare that they have no known competing financial interests or personal relationships that could have appeared to influence the work reported in this paper.

Acknowledgment

The authors would like to thank Dr. Möller from BYK-Chemie GmbH (Moosburg/Germany) for supplying the sodium bentonite sample, and Dr. Parsa from Clariant Produkte (Deutschland) GmbH for providing ω-methoxy poly (ethylene oxide) methacrylate ester (MPEG macromonomer) and Mr. Fujii from NOF Corporation, Japan for providing α-allyl-ω-hydroxy poly (ethylene glycol) ether (APEG macromonomer) for this study. Also, Ran Li would like to thank China Scholarship Council (CSC) for generous funding of her Ph.D. study at TU München.

Appendix A. Supplementary data

Supplementary data to this article can be found online at https://doi.org/10.1016/j.cemconres.2021.106504.

References

[1] K. Yamada, T. Takahashi, S. Hanehara, M. Matsuhisa, Effects of the chemical structure on the properties of polycarboxylate-type superplasticizer, Cem. Concr. Res. 30 (2000) 197–207.
[2] J. Plank, E. Sakai, C. Miao, C. Yu, J. Hong, Chemical admixtures—chemistry, applications and their impact on concrete microstructure and durability, Cem. Concr. Res. 78 (2015) 81–99.
[3] R.J. Flatt, Y.F. Houst, A simplified view on chemical effects perturbing the action of superplasticizers, Cem. Concr. Res. 31 (2001) 1169–1176.
[4] G. Gelardi, S. Mantellato, D. Marchon, M. Palacios, A. Eberhardt, R. Flatt, Chemistry of Chemical Admixtures, Science and Technology of Concrete Admixtures, Elsevier, 2016, pp. 149–218.
[5] Y.F. Houst, P. Bowen, F. Perche, A. Kauppi, P. Borget, L. Galmiche, J.-F. Le Meins, F. Lafuma, R.J. Flatt, I. Schober, Design and function of novel superplasticizers for more durable high performance concrete (superplast project), Cem. Concr. Res. 38 (2008) 1197–1209.
[6] P.-C. Aïtcin, High Performance Concrete, E & FN SPON, London, UK, 2011.
[7] K. Yoshioka, E.-i. Tazawa, K. Kawai, T. Enohata, Adsorption characteristics of superplasticizers on cement component minerals, Cem. Concr. Res. 32 (2002) 1507–1513.
[8] M.L. Nehdi, Clay in cement-based materials: critical overview of state-of-the-art, Constr. Build. Mater. 51 (2014) 372–382.
[9] E. Sakai, D. Atarashi, M. Daimon, Interaction between superplasticizers and clay minerals, in: Proceedings of the 6th International Symposium on Cement & Concrete, 2006, pp. 1560–1566.
[10] A.A. Jeknavorian, L. Jardine, C.C. Ou, H. Koyata, K. Folliard, Interaction of Superplasticizers With Clay-bearing Aggregates, Canmet/aci International Conference on Superplasticizers & Other Chemical Admixtures in Concrete, 2003.
[11] L. Lei, J. Plank, A study on the impact of different clay minerals on the dispersing force of conventional and modified vinyl ether based polycarboxylate superplasticizers, Cem. Concr. Res. 60 (2014) 1–10.
[12] S. Burchill, P. Hall, R. Harrison, M. Hayes, J. Langford, W. Livingston, R. Smedley, D. Ross, J. Tuck, Smectite-polymer interactions in aqueous systems, Clay Miner. 18 (1983) 373–397.
[13] L. Lei, J. Plank, A concept for a polycarboxylate superplasticizer possessing enhanced clay tolerance, Cem. Concr. Res. 42 (2012) 1299–1306.
[14] P. Borralleras, I. Segura, M.A. Aranda, A. Aguado, Influence of experimental procedure on d-spacing measurement by XRD of montmorillonite clay pastes containing PCE-based superplasticizer, Cem. Concr. Res. 116 (2019) 266–272.
[15] P. Borralleras, I. Segura, M.A. Aranda, A. Aguado, Absorption conformations in the intercalation process of polycarboxylate ether based superplasticizers into montmorillonite clay, Constr. Build. Mater. 236 (2020) 116657.
[16] S. Ng, J. Plank, Interaction mechanisms between Na montmorillonite clay and MPEG-based polycarboxylate superplasticizers, Cem. Concr. Res. 42 (2012) 847–854.
[17] J. Cheung, L. Roberts, J. Liu, Admixtures and sustainability, Cem. Concr. Res. 114 (2018) 79–89.
[18] H. Tan, B. Gu, S. Jian, B. Ma, Y. Guo, Z. Zhi, Improvement of polyethylene glycol in compatibility with polycarboxylate superplasticizer and poor-quality aggregates containing montmorillonite, J. Mater. Civ. Eng. 29 (2017), 04017131.
[19] G. Xing, W. Wang, G. Fang, Cement dispersion performance of superplasticisers in the presence of clay and interaction between superplasticisers and clay, Adv. Cem. Res. 29 (2017) 194–205.
[20] Y.-G. Li, Y. Li, Y. Wan, C. Deng, Z. Wang, J.-S. Qian, Effects of clay on the dispersibility of cement paste mixed with polycarboxylate superplasticizer, Chongqing Daxue Xuebao (Ziran Kexue Ban) 35 (2012) 86–92.
[21] S. Ng, J. Plank, Study on the Interaction of Na-montmorillonite Clay With Polycarboxylates 288, ACI Special Publication, 2012.
[22] Y. Ma, C. Shi, L. Lei, S. Sha, B. Zhou, Y. Liu, Y. Xiao, Research progress on polycarboxylate based superplasticizers with tolerance to clays-a review, Constr. Build. Mater. 255 (2020) 119386.
[23] L. Lei, J. Plank, Synthesis and properties of a vinyl ether-based polycarboxylate superplasticizer for concrete possessing clay tolerance, Ind. Eng. Chem. Res. 53 (2014) 1048–1055.
[24] H. Xu, S. Sun, J. Wei, Q. Yu, Q. Shao, C. Lin, β-Cyclodextrin as pendant groups of a polycarboxylate superplasticizer for enhancing clay tolerance, Ind. Eng. Chem. Res. 54 (2015) 9081–9088.
[25] X. Liu, Z. Wang, Y. Zheng, S. Cui, M. Lan, H. Li, J. Zhu, X. Liang, Preparation, characterization and performances of powdered polycarboxylate superplasticizer with bulk polymerization, Materials (Basel) 7 (2014) 6169–6183.
[26] J. Alain, V. Emmanuel, W. Olivier, Method for inerting impurities, US Patent US 0,287,794 A1 (2007).
[27] L.A. Jardine, H. Koyata, K.J. Folliard, C.-C. Ou, F. Jachimowicz, B.-W. Chun, A.A. Jeknavorian, C.L. Hill, Admixture and method for optimizing addition of EO/PO superplasticizer to concrete containing smectite clay-containing aggregates, US Patent US 6, 352, 952 B1, (2002).
[28] L.L. Kuo, Y. Chen, H. Koyata, Cationic polymers for treating construction aggregates, US Patent US 9,034,968 B2 (2015).
[29] L.L. Kuo, Y. Chen, H. Koyata, Hydrophobic, cationic polymers for treating construction aggregates, US Patent US 9,828,500 B2, (2017).
[30] S. Pourchet, S. Liautaud, D. Rinaldi, I. Pochard, Effect of the repartition of the PEG side chains on the adsorption and dispersion behaviors of PCP in presence of sulfate, Cem. Concr. Res. 42 (2012) 431–439.
[31] M.T.R. Laguna, R. Medrano, M.P. Plana, M.P. Tarazona, Polymer characterization by size-exclusion chromatography with multiple detection, J. Chromatogr. A 919 (2001) 13–19.
[32] J. Plank, B. Sachsenhauser, Experimental determination of the effective anionic charge density of polycarboxylate superplasticizers in cement pore solution, Cem. Concr. Res. 39 (2009) 1–5.
[33] J. Stecher, J. Plank, Adsorbed layer thickness of polycarboxylate and polyphosphate superplasticizers on polystyrene nanoparticles measured via dynamic light scattering, J. Colloid Interface Sci. 562 (2020) 204–212.
[34] Q. Ran, J. Liu, Y. Yang, X. Shu, J. Zhang, Y. Mao, Effect of molecular weight of polycarboxylate superplasticizer on its dispersion, adsorption, and hydration of a cementitious system, J. Mater. Civ. Eng. 28 (2016), 04015184.
[35] F. Winnefeld, S. Becker, J. Pakusch, T. Götz, Effects of the molecular architecture of comb-shaped superplasticizers on their performance in cementitious systems, Cem. Concr. Compos. 29 (2007) 251–262.
[36] E. Tombacz, M. Szekeres, Colloidal behavior of aqueous montmorillonite suspensions: the specific role of pH in the presence of indifferent electrolytes, Appl. Clay Sci. 27 (2004) 75–94.

9. Appendix

[37] E. Tombácz, M. Szekeres, Surface charge heterogeneity of kaolinite in aqueous suspension in comparison with montmorillonite, Appl. Clay Sci. 34 (2006) 105–124.
[38] T. Preocanin, A. Abdelmonem, G. Montavon, J. Luetzenkirchen, Charging behavior of clays and clay minerals in aqueous electrolyte solutions - experimental methods for measuring the charge and interpreting the results, in: Clays, Clay Minerals and Ceramic Materials Based on Clay Minerals, 2016, pp. 51–88.
[39] E. Sakai, K. Yamada, A. Ohta, Molecular structure and dispersion-adsorption mechanisms of comb-type superplasticizers used in Japan, J. Adv. Concr. Technol. 1 (2003) 16–25.
[40] G.B.S. Ng, Interactions of Polycarboxylate Based Superplasticizers with Montmorillonite Clay in Portland Cement and With Calcium Aluminate Cement, Technische Universität München, 2013.
[41] P.D. Svensson, S. Hansen, Intercalation of smectite with liquid ethylene glycol—resolved in time and space by synchrotron X-ray diffraction, Appl. Clay Sci. 48 (2010) 358–367.
[42] J.L. Suter, P.V. Coveney, Computer simulation study of the materials properties of intercalated and exfoliated poly (ethylene) glycol clay nanocomposites, Soft Matter 5 (2009) 2239–2251.
[43] R.J. Flatt, I. Schober, E. Raphael, C. Plassard, E. Lesniewska, Conformation of adsorbed comb copolymer dispersants, Langmuir 25 (2009) 845–855.
[44] C. Gay, E. Raphaël, Comb-like polymers inside nanoscale pores, Adv. Colloid Interface Sci. 94 (2001) 229–236.